



# **Development and Characterisation of a Cytokine Supplemented Serum Free Medium Formulation for Bone Marrow Derived Mesenchymal Stromal Cells**

**Steven Wilkinson, MSc**

This thesis is submitted as partial fulfilment of the requirements for the degree of Doctor of  
Engineering

Newcastle University

School of Chemical Engineering

Biopharmaceutical Bioprocess Technology Centre

October 2018



## Abstract

**Background:** The discovery and subsequent characterisation of adult human-derived stem cells appears poised to help revolutionise the fields of regenerative medicine and tissue engineering, offering clinicians the opportunity to develop fully functional replacement tissues, alongside holding significant promise as next generation gene or protein delivery vehicles. Despite their apparent potential however, current stem cell-based therapeutics typically rely on delivering massive doses of cells to sites of injury in order to help ensure adequate cell survival in the highly detrimental microenvironments presented by damaged and degrading biological material. In order to produce the cell numbers required for these types of treatments, relatively modest donor cell populations are subjected to extended periods of *in vitro* expansion, within highly regulated GMP culture conditions. One crucially important aspect of this manufacturing framework is the requirement for xeno-free expansion systems, including the use of serum-free culture medium. Unfortunately, whilst a number of functional serum-free media formulations are commercially available at the present time, their proprietary nature makes them both highly expensive and wholly unsuitable for use in academic research.

**Aims:** The goal of this project is to begin development of a characterised cytokine-supplemented serum-free medium formulation using a design of experiments-based methodology.

**Methods:** Primary bone marrow-derived mesenchymal stromal cells (BM-MSCs) were isolated, characterised and used to screen a series of selected cytokines and growth supplements for their ability to successfully support cell proliferation and continued survival in the absence of serum. Cells cultured in the resultant serum-free formulation were then compared to those grown in conventional medium in regard to genetic, metabolic and morphological factors. In addition, the impact of batch-to-batch variability on BM-MSC growth and metabolic activity was assessed as a means of determining the potential impact of raw material variation on cell quality and any related manufacturing processes. Finally, a number of different extracellular matrix proteins were also screened for the purpose of mediating cell-surface interactions in serum-free conditions.

Results: We successfully identified a cytokine supplemented medium preparation capable of supporting the proliferation of BM-MSCs during serum-free culture. Evaluation of cells expanded in this medium provided evidence of altered secretory and genetic characteristics leading to shifted therapeutic potential. Furthermore, the identification of a combination of different extracellular matrix proteins able to enhance cell adhesion in the absence of serum served to provide the beginnings of a complete serum-free formulation. In addition, FBS batch variability was shown to have significant effects on cell proliferation and gene expression, including a number of genetic markers linked to differentiation potential and lineage specificity.

Conclusions: We offer a new serum-free medium formulation for use in the expansion of primary BM-MSCs, alongside providing evidence of the impact of raw material variability on the therapeutically relevant characteristics of these cells.

## Acknowledgments

I would like to take this opportunity to express my sincere gratitude to a number of the individuals and groups that have helped make this thesis possible.

Firstly, I would like to thank my supervisors Professor Kenny Dalgarno and Dr Xiao Wang for their help and guidance throughout this process.

Secondly, I wish to thank Professor Elaine Martin, Dr Mark Birch, Dr Lucy Foley and Dr Andrew McCaskie for sharing their time and knowledge with me on numerous occasions during the course of this project

Finally, I would like to take some time to acknowledge the help and support of the many staff and students working at the Newcastle University School of Chemical Engineering and Advanced Materials, Institute of Cellular Medicine and the School of Mechanical Engineering, in particular Dr Simon Partridge and Dr Sotiria Toumpaniari for sharing with me their time and support over the past four years.



# Table of Contents

Abstract.....	i
Acknowledgments.....	iii
List of figures.....	ix
List of tables.....	xiii
List of key abbreviations.....	xv
1 Chapter 1: Introduction and Literature review.....	1
1.1 Regenerative medicine.....	1
1.1.1 A strategy of regeneration and repair.....	1
1.1.2 The current state of the sector.....	1
1.1.3 Product development and regulatory approval.....	2
1.2 Stem Cells.....	4
1.2.1 Embryonic stem cells.....	4
1.2.2 Induced pluripotent stem cells.....	7
1.2.3 Foetal stem cells.....	9
1.2.4 Adult stem cells.....	11
1.2.5 Mesenchymal stromal cells.....	16
1.3 Stem cell expansion processes.....	20
1.3.1 Small scale cell culture processes.....	20
1.3.2 Large scale cell processes.....	22
1.4 Stem cell culture medium.....	26
1.4.1 The importance of culture medium.....	26
1.4.2 Foetal bovine serum.....	27
1.4.3 Non-defined alternatives to foetal bovine serum.....	29
1.4.4 Chemically defined serum-free medium.....	32
1.5 Methods of media development and supplement screening.....	34
1.5.1 One-factor-at-a-time screening methods.....	34
1.5.2 Design or experiments and multifactorial approaches.....	35
1.5.3 Computational systems and random global searching.....	36
1.6 Project overview and aims.....	36
2 Chapter 2: Materials and methods.....	38
2.1 Cell culture.....	38
2.1.1 Tissue collection and informed consent.....	38
2.1.2 Cell culture standards.....	38
2.1.3 Primary cell isolation.....	39
2.1.4 Primary cell expansion.....	40

2.1.5	Primary cell cryopreservation and recovery .....	41
2.1.6	Cell line donation and culture .....	42
2.2	Quantification of cell number and metabolic activity .....	43
2.2.1	Haemocytometer-based cell counting.....	43
2.2.2	MTT assay.....	43
2.2.3	PrestoBlue assay .....	44
2.2.4	PicoGreen assay .....	44
2.2.5	Alkaline phosphatase activity assay.....	45
2.3	Directed tri-lineage differentiation.....	46
2.3.1	Osteogenic differentiation .....	46
2.3.2	Chondrogenic differentiation.....	47
2.3.3	Adipogenic differentiation .....	47
2.4	Flow cytometry .....	48
2.4.1	Cell staining and cytometric analysis .....	48
2.4.2	Assessing the impact of FGF-2 supplementation on surface marker expression .....	51
2.4.3	Identifying endothelial marker expression .....	52
2.5	Cell staining procedures.....	52
2.5.1	Cytoskeletal staining .....	52
2.5.2	Acetylated low density lipoprotein uptake assay .....	53
2.5.3	Staining for osteogenic differentiation .....	53
2.5.4	Staining for chondrogenic differentiation.....	54
2.5.5	Staining for adipogenic differentiation .....	55
2.5.6	Automated image analysis.....	55
2.6	RNA extraction and gene expression analysis .....	55
2.6.1	RNA extraction .....	55
2.6.2	RNA quality assessment.....	56
2.6.3	NanoString nCounter gene expression analysis.....	57
2.7	Identifying and characterising cellular protein secretions .....	58
2.7.1	Cell culture medium sample collection.....	58
2.7.2	Meso Scale Discovery immunoassay .....	59
2.8	Preparing aminosilane functionalised glass surfaces .....	60
2.8.1	Pre-preparation of glass surfaces .....	60
2.8.2	Silanization of glass surfaces.....	60
2.8.3	Measuring water contact angle .....	61
2.8.4	Measuring surface amine content .....	61
2.8.5	Surfaces characterisation via x-ray photoelectron spectroscopy.....	62

2.8.6	Assessing aminosilane layer stability in aqueous conditions.....	62
2.9	Screening selected extracellular matrix proteins in regard to cell adhesion and morphology	63
2.9.1	Surface preparation .....	63
2.9.2	Experimental set-up and cell seeding .....	63
2.10	Design of experiments and statistical analyses .....	65
2.10.1	Fractional factorial supplement screening .....	65
2.10.2	Full factorial formulation assessment.....	66
2.10.3	Data handling and statistical analyses .....	68
3	Chapter 3: Primary mesenchymal stromal cell and cell line characterisation.....	70
3.1	Introduction .....	70
3.2	Aims.....	70
3.3	Results.....	71
3.3.1	Morphological characterisation .....	71
3.3.2	Tri-lineage differentiation potential .....	71
3.3.3	Surface marker expression.....	75
3.3.4	Assessing the impact of fibroblast growth factor-2 supplementation on surface marker expression.....	76
3.4	Discussion.....	78
4	Chapter 4: Assessing the variability of foetal bovine serum as a cell culture supplement .....	80
4.1	Introduction .....	80
4.2	Aims.....	80
4.3	Results.....	81
4.3.1	Cell growth and metabolic activity .....	81
4.3.2	Cell morphology .....	87
4.3.3	Alkaline phosphatase activity .....	92
4.3.4	Surface marker expression.....	95
4.3.5	Gene expression analysis .....	96
4.4	Discussion.....	98
5	Chapter 5: Supplementing medium for improved cell growth and survivability in nutrient- deprived conditions .....	103
5.1	Introduction .....	103
5.2	Aims.....	103
5.3	Results.....	104
5.3.1	Supplement screening .....	104
5.3.2	Full factorial formulation assessment.....	106

5.4	Discussion.....	113
6	Chapter 6: Investigating the characteristics of cells following expansion in supplemented serum-free medium.....	115
6.1	Introduction .....	115
6.2	Aims.....	115
6.3	Results.....	116
6.3.1	Morphological characterisation .....	116
6.3.2	Tri-lineage differentiation potential .....	117
6.3.3	Cellular ac-LDL uptake.....	120
6.3.4	Surface marker expression.....	120
6.3.5	Gene expression analysis .....	121
6.3.6	Identifying and characterising cell protein secretions.....	125
6.4	Discussion.....	130
7	Chapter 7: Screening extracellular matrix proteins for enhanced cellular adhesion and viability	133
7.1	Introduction .....	133
7.2	Aims.....	133
7.3	Results.....	134
7.3.1	Surface cleaning and pre-functionalisation .....	134
7.3.2	Characterisation of aminosilane functionalised surfaces .....	135
7.3.3	Screening of extracellular matrix proteins.....	142
7.4	Discussion.....	149
8	Chapter 8: Discussion and conclusions .....	151
8.1	Summary of Results .....	151
8.2	Discussion.....	152
8.2.1	Cell Characterisation .....	152
8.2.2	Foetal bovine serum batch variability.....	153
8.2.3	Supplement screening for serum-free medium development .....	153
8.2.4	Screening of ECM Proteins for enhanced cell adhesion in serum free conditions .....	156
8.3	Conclusions .....	157
8.4	Future Directions .....	157
	References .....	158
	Appendices.....	182

## List of figures

Figure 1.1 The human pre-implantation blastocyst.....	5
Figure 1.2 The differentiation hierarchy of human hematopoietic stem cells.....	19
Figure 1.3 A typical stirred tank bioreactor system.....	29
Figure 1.4 A typical wave bioreactor system.....	29
Figure 2.1 The hBM-MSC isolation process.....	47
Figure 2.2 Culture process used in assessing the impact of FGF-2 supplementation on surface marker profile.....	62
Figure 2.3 An AO-7 standard curve plated into 96-well plate format.....	74
Figure 3.1 Representative phase contrast micrographs of cell belonging to the Y201 line together with primary hBM-MSCs.....	83
Figure 3.2 Phase contrast images of tri-lineage differentiated BM-MSCs.....	85
Figure 3.3 Phase contract images of tri-lineage differentiated Y201s.....	86
Figure 3.4 Example dot plots and histograms representative of the typical gating strategy used to characterise BM-MSCs.....	87
Figure 3.4 Example dot plots and histograms representative of the typical gating strategy used to characterise cells belonging to the Y201 cell line.....	88
Figure 3.5 Representative dot plots showing the expression of HLA-DR in BM-MSCs following expansion in bFGF supplemented and un-supplemented media across three subsequent subcultures.....	89
Figure 3.6 Mean percentages of living BM-MSCs remaining prior to and following selection based on lack of expression of HLA-DR.....	90
Figure 4.1 Mean hBM-MSC numbers across a 5 day culture period for each of the tested FBS and human serum types.....	95
Figure 4.2 Mean Y201 cell numbers across a 5 day culture period for each of the tested FBS and human serum types.....	96
Figure 4.3 Mean BM-MSC metabolic activity normalised to cell number across a 5 day culture period for each of the tested FBS and human serum types.....	97
Figure 4.4 Mean Y201 cell metabolic activity normalised to cell number across a 5 day culture period for each of the tested FBS and human serum types.....	98
Figure 4.5 Mean hBM-MSC doubling times during the exponential growth phase of a 5 day culture period for each of the tested FBS and human serum types.....	99
Figure 4.6 Mean Y201 cell doubling times during the exponential growth phase of a 5 day culture period for each of the tested FBS and human serum types.....	99

Figure 4.7 Fluorescent microscopy images of Phalloidin and DAPI stained hBM-MSCs following culture in a series of different FBS and human serum batches.....	101
Figure 4.8 Fluorescent microscopy images of Phalloidin and DAPI stained Y201s following culture in a series of different FBS and human serum batches.....	102
Figure 4.9 Fluorescent microscopy image of Phalloidin and DAPI stained Y201s alongside the same image overlaid with an analysis mask used to quantify cell number and area.....	103
Figure 4.10 Mean total hBM-MSC numbers on the final day of culture (day 5) for each of the tested FBS and human serum batches.....	103
Figure 4.11 Mean total Y201 cell numbers on the final day of culture (day 4) for each of the tested FBS and human serum batches.....	104
Figure 4.12 Mean hBM-MSC area per cell on the final day of culture (day 5) for each of the tested FBS and human serum batches.....	104
Figure 4.13 Mean Y201 area per cell on the final day of culture (day 4) for each of the tested FBS and human serum batches.....	105
Figure 4.14 Mean alkaline phosphatase activity as indicated by fluorescence per $10^5$ hBM-MSCs on day 3 of culture for each of the tested FBS and human serum batches.....	106
Figure 4.15 Mean alkaline phosphatase activity as indicated by fluorescence per $10^5$ hBM-MSCs on day 4 of culture for each of the tested FBS and human serum batches.....	107
Figure 4.16 Mean alkaline phosphatase activity as indicated by fluorescence per $10^5$ hBM-MSCs on the final day of culture (day 5) for each of the tested FBS and human serum batches.....	107
Figure 4.17 Mean alkaline phosphatase activity as indicated by fluorescence per $10^5$ Y201s on day 3 of culture for each of the tested FBS and human serum batches.....	108
Figure 4.18 Mean alkaline phosphatase activity as indicated by fluorescence per $10^5$ Y201s on the final of culture (day 4) for each of the tested FBS and human serum batches.....	108
Figure 4.19 Mean expression levels for BM-MSC-derived gene transcripts showing a minimum of 2-fold change following culture in high-growth rate FBS (FBS 4) when compared to low-growth rate FBS (FBS 3) presented in the form of log <sub>2</sub> transformed count data.....	110
Figure 4.20 Mean expression levels for Y201-derived gene transcripts showing a minimum of 2-fold change following culture in high-growth rate FBS (FBS 1) when compared to low-growth rate FBS (FBS 3) presented in the form of log <sub>2</sub> transformed count data.....	112
Figure 5.1 Mean 570nm absorbance values for each of the three fractional factorial investigations used to screen potential serum-free medium supplements.....	119
Figure 5.2 Mean BM-MSC numbers for each of the supplement combinations included within the full-factorial formulation assessment.....	121
Figure 5.3 Mean Y201 cell number for each of the supplement combinations included within the full-factorial formulation assessment.....	123

Figure 5.4 Mean BM-MSc metabolic activity normalised to total cell number for each of the supplement combinations included within the full-factorial formulation assessment.....	124
Figure 5.5 Mean Y201 metabolic activity normalised to total cell number for each of the supplement combinations included within the full-factorial formulation assessment.....	126
Figure 6.1 Phase contrast images of hBM-MSCs grown in serum-free conditions alongside those grown in standard serum-supplemented medium.....	130
Figure 6.2 Phase contrast images of Y201s grown in serum-free conditions alongside those grown in standard serum-supplemented medium.....	131
Figure 6.3 Phase contrast images of tri-lineage differentiated hBM-MSCs following culture in serum-free conditions.....	132
Figure 6.4 Phase contract images of tri-lineage differentiated Y201s following culture in serum-free conditions.....	133
Figure 6.5 Representative dot plots indicative of BM-MSc CD105 and HLA-DR expression following expansion in serum-supplemented and serum-free conditions.....	134
Figure 6.6 Representative dot plots indicative of Y201 CD105 and HLA-DR expression following expansion in serum-supplemented and serum-free conditions.....	135
Figure 6.7 Mean expression levels for all hBM-MSc-derived gene transcripts showing a minimum of 2-fold change following expansion in serum-free media when compared to standard serum-supplemented conditions presented in the form of log <sub>2</sub> transformed count data.....	136
Figure 6.8 Mean expression levels for all Y201-derived gene transcripts showing a minimum of 2-fold change following expansion in serum-free media when compared to standard serum-supplemented conditions presented in the form of log <sub>2</sub> transformed count data.....	138
Figure 6.9 Overview of the V-PLEX Human biomarker panel.....	140
Figure 6.10 Scree plot corresponding to the analysis of the combined serum-free, serum-supplemented and TNF-treated data sets.....	141
Figure 6.11 Score plot for the first two identified principle components.....	142
Figure 6.12 Log <sub>10</sub> transformed normalised expression data for LPS treated hBM-MSCs...	143
Figure 7.1 Representative images of static water contact angles taken on each of the cleaned surfaces along with uncleaned controls.....	148
Figure 7.2 Mean contact angle values for each of the cleaning methods used and associated controls.....	149
Figure 7.3 Representative images of static water contact angles taken on each of the aminosilane functionalised surfaces alongside appropriate controls.....	151
Figure 7.4 Mean contact angle values for each of the aminosilane functionalisation methods used and associated controls.....	152
Figure 7.5 Mean 482nm absorbance values for alkaline washes taken for each of the assessed aminosilane functionalisation methods and associated controls following treatment with Acid Orange-7.....	152

Figure 7.6 Representative XPS survey spectra showing increased carbon and nitrogen presence on aminosilane functionalised glass surfaces versus controls.....	153
Figure 7.7 Mean percentage surface nitrogen (N1s) content for each of the aminosilane functionalisation methods used and associated controls.....	153
Figure 7.8 Mean percentage surface oxygen (O1s) content for each of the aminosilane functionalisation methods used and associated controls.....	154
Figure 7.9 Mean percentage surface carbon (C1s) content for each of the aminosilane functionalisation methods used and associated controls.....	154
Figure 7.10 Mean percentage surface silicon (Si 2p) content for each of the aminosilane functionalisation methods used and associated controls.....	155
Figure 7.11 Mean contact angles of aminosilane functionalised surfaces following water-mediated degradation for 0, 15, 30 and 60 minutes.....	155
Figure 7.12 Mean 482nm absorbance values for each of the tested aminosilane functionalisation methods following water-mediated degradation for 0, 15, 30 and 60 minutes.....	156
Figure 7.13 Fluorescent microscopy images of Phalloidin and DAPI stained hBM-MSCs following 8 hours of culture on aminosilane coated glass functionalised with different combinations of extracellular matrix proteins.....	158
Figure 7.14 Fluorescent microscopy images of Phalloidin and DAPI stained hBM-MSCs following 8 hours of culture on aminosilane coated glass functionalised with different combinations of extracellular matrix proteins.....	159
Figure 7.15 Fluorescent microscopy images of Phalloidin and DAPI stained Y201s following 8 hours of culture on aminosilane coated glass functionalised with different combinations of extracellular matrix proteins.....	160
Figure 7.16 Fluorescent microscopy images of Phalloidin and DAPI stained Y201s following 8 hours of culture on aminosilane coated glass functionalised with different combinations of extracellular matrix proteins.....	161
Figure 7.17 Mean BM-MSC numbers retained on surfaces coated with each of the extracellular matrix protein combinations included within the full-factorial functionalisation assessment.....	162
Figure 7.18 Mean Y201 cell numbers retained on surfaces coated with each of the extracellular matrix protein combinations included within the full-factorial functionalisation assessment.....	163

## List of tables

Table 2.1 Standard MSC culture medium composition.....	49
Table 2.2 Osteogenic medium composition.....	56
Table 2.3 Chondrogenic medium composition.....	56
Table 2.4 Adipogenic medium composition.....	57
Table 2.5 Isotype control antibody list.....	59
Table 2.6 Test condition antibody list.....	59
Table 2.7 Fluorochrome excitation and emission filter wavelength values.....	59
Table 2.8 Compensation control and voltage calibration antibody list.....	60
Table 2.9 Protein secretion culture details.....	70
Table 2.10 Overview of the 2 <sup>3</sup> factorial design used for ECM protein screening.....	76
Table 2.11 Overview of the cytokines and culture supplements assessed over the course of three separate screening experiments.....	78
Table 2.12 Overview of the 2 <sup>4-1</sup> fractional factorial experimental design used in supplement screening.....	78
Table 2.13 Overview of the cytokines and culture supplements used in the assessed serum-free medium formulation.....	79
Table 2.14 Overview of the 2 <sup>4</sup> full factorial experimental design used in formulation assessment.....	80
Table 4.1 P-values and t-statistics associated with all genes seen to display a minimum of 2-fold change in expression in BM-MSCs following culture in high-growth rate FBS (FBS 4) when compared to low-growth rate FBS (FBS 3).....	111
Table 4.2 P-values and t-statistics associated with all genes seen to display a minimum of 2-fold change in expression in Y201s following culture in high-growth rate FBS (FBS 1) when compared to low-growth rate FBS (FBS 3).....	112
Table 4.3 The directionality of change and general functions of genes showing a statistically significant 2-fold or greater change in expression following BM-MSC culture in high-growth rate FBS (FBS 4) when compared to low-growth rate FBS (FBS 3).....	115
Table 4.4 The directionality of change and general functions of genes showing a statistically significant 2-fold or greater change in expression following Y201 culture in high-growth rate FBS (FBS 1) when compared to low-growth rate FBS (FBS 3).....	116
Table 5.1 Coded designations used for the supplements investigated in each of the three rounds of fractional factorial screening experiments.....	119
Table 5.2 Main effects and interactions table for hBM-MSC total cell number data.....	122

Table 5.3 Main effects and interactions table for Y201 total cell number data.....	123
Table 5.4 Main effects and interactions table for hBM-MSC normalised-metabolic activity data.....	125
Table 5.5 Main effects and interactions table for Y201 normalised-metabolic activity data.....	126
Table 6.1 P-values and t-statistics associated with all genes seen to display a minimum of 2-fold change in expression in hBM-MSCs following culture in serum-free medium when compared to a standard serum-supplemented formulation.....	137
Table 6.2 P-values and t-statistics associated with all genes seen to display a minimum of 2-fold change in expression in Y201s following culture in serum-free medium when compared to a standard serum-supplemented formulation.....	139
Table 6.3 Overview of the first 10 principle components identified for the combined serum-free, serum-supplemented and TNF-treated data sets.....	141
Table 6.4 Experimental factors seen to contribute to Principle Component 1.....	142
Table 6.5 Experimental factors seen to contribute to Principle Component 2.....	143
Table 6.6 The directionality of change and general functions of genes showing a statistically significant 2-fold or greater change in expression following BM-MSC culture in serum-free medium when compared to serum-supplemented conditions.....	145
Table 6.7 The directionality of change and general functions of genes showing a statistically significant 2-fold or greater change in expression following Y201 culture in serum-free medium when compared to serum-supplemented conditions.....	145

## List of key abbreviations

AD-MSC: Adipose derived Mesenchymal Stem Cell

BMP-3: Bone Morphogenetic Protein-3

BM-MSC: Bone Marrow derived Mesenchymal Stem Cell

ESC: Embryonic Stem Cell

FGF-2: Fibroblast Growth Factor-2

HB-EGF: Heparin Binding-Epidermal Growth Factor-like growth factor

HSC: Haematopoietic Stromal Cell

IL-6: Interleukin-6

IPSC: Induced Pluripotent Stem Cell

MSC: Mesenchymal Stem Cell

PDGF-BB: Platelet derived Growth Factor- BB

ROCK: Rho-associated protein Kinase-inhibitor Y-27632

SDF-1 $\alpha$ : Stromal cell Derived Factor-1 $\alpha$

SITE: Selenium Insulin Transferrin Ethanolamine

Thy- $\beta$ 4: Thymosin- $\beta$ 4

TGF- $\beta$ 1: Transforming Growth Factor-  $\beta$ 1

UCB-MSC: Umbilical Cord Blood derived Mesenchymal Stem Cell

VEGF: Vascular Endothelial Growth Factor



# 1 Chapter 1: Introduction and Literature review

## 1.1 Regenerative medicine

### 1.1.1 A strategy of regeneration and repair

Regenerative medicine is a multidisciplinary field combining together aspects of cell biology, genetics, engineering and biomaterials research in order to help repair and replace damaged and degrading tissues and organs. Unlike more conventional approaches, treatments utilising this type of strategy often seek to regenerate defective tissues through the application of novel biological or composite bio-synthetic constructs. Of all the various medicinal approaches typically encompassed under the banner of regenerative medicine, stem cell biotechnology represents one of the most highly publicised and potentially most promising. Stem cells are undifferentiated precursor cells which have the ability to transform into any one of a number of specific lineages, as defined by both their tissue of origin and genetic plasticity. Three primary sub-types of stem cell are commonly discussed in the relevant scientific literature; namely embryonic, foetal and adult, each of which is known to have its own specific set of therapeutically pertinent characteristics, as discussed further in section 1.2. Together with stem cells themselves, many regenerative approaches also utilise biomaterial scaffolds in the form of bio-synthetic constructs in order to provide enhanced therapeutic activity and mechanical stability, particularly within the dynamic environments presented by the human body. Such therapeutic strategies are not limited to use in regard to stem cells alone however, with various terminally differentiated somatic cell types such as fibroblasts, keratinocytes and a range of different immune cells, having also been utilised in order to treat damaged and degraded tissues in a regenerative manner (1, 2).

### 1.1.2 The current state of the sector

Since the early 1990s the tissue engineering and regenerative medicine sector has seen considerable growth, particularly following the advent of modern stem cell-based technologies (3). As of 2007 approximately 50 individual firms were recognised as supplying commercial regenerative products and services, generating an estimated 1.3 billion US dollars' worth of sales annually (4). More recent figures have suggested that the top 20 regenerative medicine

companies around the world saw 40% growth in 2010 (5). Unfortunately, not all the associated statistics appear to be so positive, with annual sales of three of the highest profile regenerative treatments; namely Apligraf, Dermagraft, and Carticel, barely breaking even since their approval (4). Despite this, growth in the sector is predicted to continue, with the global market value of the industry projected to reach approximately 30 billion US dollars by 2022 (6). Between 2016 and 2022 the North American, European and Asian-Pacific regions are forecasted to see compound annual growth rates (CAGRs) of 32.5%, 31.2% and 39.9%, respectively (6). In terms of investment within the sector, the primary sources of funding appear to be almost exclusively derived from public and charitable organisations, which were estimated to have donated approximately £38 million and £200 million respectively in the UK alone between the years of 2003 and 2009 (7). Overall these figures seem to suggest that there is currently significant support for the regenerative medicine sector and that commercial investment within the industry could potentially lead to healthy returns in the not-to-distant future.

### 1.1.3 Product development and regulatory approval

Medicinal product development is a highly complex process, being made up of a series of distinct sub-stages, including initial research, pre-clinical studies, clinical trials, marketing approval and finally post-marketing follow-up. Underlying this process are a series of region-specific regulatory bodies, who seek to ensure that products marketed within the scope of their influence maintain the highest possible production and safety standards, through the enforcement of specific sets of accompanying legislation. Whilst a large range of such regulatory agencies exist throughout the world, here we will concentrate solely on two of the most sizable; namely the United States Food and Drug Administration (FDA) and the European Medicines Agency (EMA).

The FDA is responsible for the ensuring the safety and efficacy of all medicinal products entering the US marketplace, including potential regenerative therapies. Companies intending to apply for marketing approval for an advanced therapy medicinal product (ATMP) must first apply for classification of their invention, before continuing on through a strictly regulated process of pre-clinical and clinical testing. In order to begin clinical studies, the companies involved are required to file an investigational new drug (IND) application, detailing the specifics of their proposed trials together with the results of their work so far; commonly

including the findings of studies involving the use of animal-models. Following the multi-stage clinical trial process; generally made-up of three distinct phases (safety, efficacy and comparative performance), the parties involved may file for a license to market the product. As previously alluded to, the nature of this license is decided upon during product classification, with most stem cell-based products requiring a biologics license application (BLA) to be submitted prior to release. It should be noted, that the primary mechanism involved in the therapeutic activity of a given product is typically used as the deciding factor during its regulatory classification. Furthermore, those therapies that involve the use of cellular materials are always deemed to be primarily biological in nature, regardless of the importance of any additional elements.

In Europe, the process of regulatory approval can appear somewhat more complex. Whilst the EMA is the primary agency responsible for this jurisdiction, each individual member state within the union has its own National Competent Authority (NCA); such as the Medicines and Healthcare Products Regulatory Agency (MHRA) in the United Kingdom for example. In addition, there are three separate methods through which products may be submitted for European-wide approval, namely the centralised, decentralised and mutual recognition procedures. ATMPs, including stem cell-based products, must be submitted for evaluation via the centralised procedure alone, potentially resulting in them being granted a single marketing authorisation which is valid in all EU member states; alongside a number of additional countries. Despite these differences however, the basic developmental process remains the same in both the US and the EU, with those companies wishing to enter a product into clinical testing requiring regulatory approval from the NCA under which the studies will be carried out.

Finally, it should be noted that the process of regulatory approval is an extremely costly one, with marketing license applications alone costing anywhere upwards of £250,000 depending upon the region for which they are sort. Additionally, both pre-clinical and clinical trials can be considered prohibitively expensive to undertake, with an estimated twenty-five billion US dollars having been spent on clinical trials in the US alone during 2006 (8). As a result, a great deal of planning and forethought is required before any such studies can be undertaken, stressing the need for early contact between manufacturing companies and the appropriate regulatory bodies.

## 1.2 Stem Cells

### 1.2.1 Embryonic stem cells

Embryonic stem cell or ESC is a term used to describe a group of cells derived from the inner cell mass (ICM) of the mammalian pre-implantation blastocyst, as shown below in figure 1.1 (9). If allowed to implant into the uterine wall this structure would eventually develop into the foetus, with the surrounding trophoblast becoming the placenta (10). Consequently, ESCs consistently display pluripotent behaviour, meaning that they are able to be differentiated into any non-placental cell type (11). In addition, the embryonic origins of these cells afford them seemingly unlimited proliferative potential due to their high telomerase activity maintaining telomere length and allowing them to remain essentially refractory to the effects of replicative senescence (12).

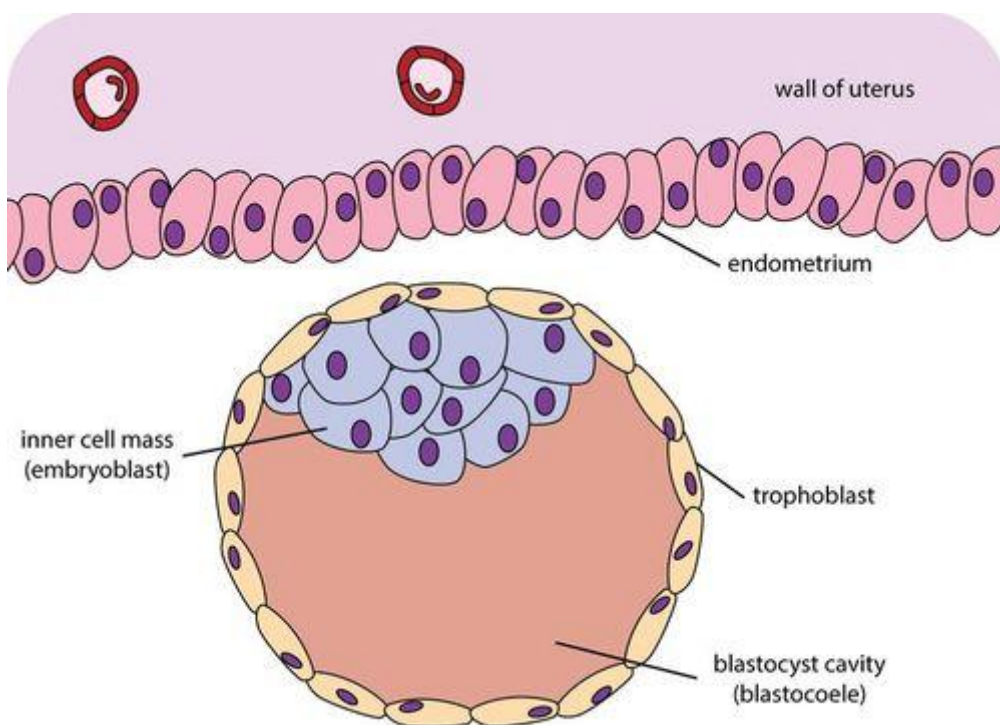


**Figure 1.1 The human pre-implantation blastocyst (206)**

ESCs are derived from the inner cell mass, a structure that would typically go on to form all of the non-placental tissues constituting a human foetus following endometrial implantation. The surrounding trophoblast would then go on to form the majority of the placenta.

As a result of their unique characteristics, ESCs have garnered considerable interest within the field of regenerative medicine, where a seemingly limitless supply of pluripotent material could be effectively utilised to treat a whole host of diseases by means of tissue replacement. To date ESCs have been utilised in clinical trials related to a broad range of indications, including Type-1 diabetes, spinal cord injuries, macular degeneration and Stargardt's macular dystrophy (13, 14, 15) with promising early-stage safety and efficacy data having been reported. Furthermore, it has been shown that the therapeutic potential of these cells isn't limited to the production of populations made up of a single cell type or the regeneration of only the most basic tissues. Recently, groups such as Sharon *et al* (2011) and Spence *et al* (2011) have demonstrated that ESCs can both differentiate into dedicated organizer cells and possess inherent self-organization potential enabling the manufacture of complex three-dimensional structures (16, 17). Given the findings of Jukes *et al* (2008) who reported bone formation via endochondral ossification following chondrogenic differentiation, such complex tissues could seemingly be produced using a single ESC line in a manner mechanistically equivalent to their generation during the natural developmental process (18).

Despite these reassuring results, one of the most prominent concerns when utilising ESCs in the aforementioned manner stems from their two most attractive properties and the inherent similarity to cancer stem cells these characteristics confer. Due to the combination of their proliferative potential and pluripotency, teratomas are known to arise following the *in vivo* application of undifferentiated ESCs (19). Whilst these tumours are typically benign in nature, the potential for them to interfere with normal biological functionality is acutely apparent. Unfortunately, despite researchers and clinicians utilising differentiated cells derived from ESCs rather than the parent cells themselves, small populations of undifferentiated cells are known to persist within these manufactured tissues. In order to combat this issue, a number of different strategies have been proposed, chief among them being the application of fluorescence-assisted cell sorting (FACS) technologies or chemical selection, either individually or in combination with other methods. For example, Kahan *et al* (2010) developed a multi-stage protocol for the removal of tumorigenic cells from ESCs differentiated towards endodermal lineages (20). Initially, undifferentiated and partially converted cells were removed using a magnetic bead-based sorting system, before the population was enriched for definitive endodermal cells on the basis of positive epithelial cell adhesion molecule expression (20). On the other hand, Ben-David *et al* (2013), screened 52000 different small molecules, eventually identifying 15 pluripotent cell-specific inhibitors labelled as PluriSIns, one of which was shown

to be capable of preventing teratoma formation following subcutaneous implantation of cells into mouse models (21). Despite the apparent success of both of these strategies, their incorporation into existing manufacturing processes raises specific questions relating to increased production times, cell manipulation requirements and chemical safety, alongside more general concerns regarding method validation specifications.

In addition to their tumorigenicity, ESCs also suffer from the problem of being inherently immunogenic. Early *in vitro* investigations into the impact of allogeneic ESCs on recipient immune activation demonstrated a level of immune privilege, with ESCs unable to induce the proliferation of human peripheral blood lymphocytes (22). However, it appears that this apparent privilege does not hold true *in vivo*, where inflammation-mediated interferon-gamma (IFN- $\gamma$ ) release is thought to increase surface expression of major histocompatibility complex-1 (MHC-1) molecules leading to immune activation (23). Whilst it has been proposed that transient immune suppression could be utilised to alleviate these issues, experiments using conventional immune suppressants in animal models have been unable to demonstrate grafted cell survival past 28 days (24). Furthermore, this type of approach could potentially result in significant increases in the risk of tumour formation, as cells are able to evade immune surveillance during this time and migrate to new regions in an unchecked manner (25). Whilst more complex methods of preventing ESC immune activation have been suggested, including the use of genetically modified hypoinmunogenic ESC lines capable of overexpressing a variety of immunomodulatory proteins, the aforementioned interaction with cell tumorigenicity remains a significant concern (26).

Regardless of the myriad of issues affecting the direct therapeutic application of these cells, human ESCs still hold significant promise in the realms of drug screening and developmental modelling. Interestingly, the similarities between ESCs and cancer cell progenitors provides researchers with a unique opportunity to accurately model a variety of different cancer types and screen potential therapeutic agents in a safe and reproducible manner. Avior *et al* (2017) utilised human ESCs to develop a platform with which to study the impact of the Retinoblastoma-1 (RB1) molecule on intraocular tumour formation (27). Intriguingly, teratomas formed by RB1-null ESCs displayed neural expansions potentially linked to the neural tumour formation commonly seen to accompany retinoblastoma development *in vivo* (27). In much the same manner, the biological origin of ESCs and their ability to form embryoid bodies, which precisely mimic early developmental processes, makes them an invaluable tool

in the study of mammalian development, alongside screening for teratogenic compounds which could negatively impact embryogenesis in humans (28).

Finally, it is impossible to discuss ESCs without drawing attention to the ethical debate surrounding their isolation and use. The moral and ethical aspects of utilising embryonic tissues are far too wide reaching to be properly examined here but typically include discussions regarding subjects such as the sanctity of life and the moral status of the human embryo (29). Rather than ignore the therapeutic and diagnostic potential of ESCs, many experts have turned their attention to the generation of artificial pluripotent cell populations, through methods such as somatic cell nuclear transfer (SCNT), cell fusion or targeted genetic reprogramming (30). Fortunately, whilst SCNT and fusion-based methods are plagued by efficacy and chromosomal number issues respectively, the genetic reprogramming of somatic cells to produce so called induced pluripotent stem cell (IPSC) populations has seen significant success in recent years.

### 1.2.2 Induced pluripotent stem cells

First produced by members of Shinya Yamanaka's Kyoto research group in 2006, IPSCs are considered by many to represent an ethically and intellectually sound alternative to the use of ESCs in regenerative medicine and related fields (31). Initially, IPSCs were formed by introducing over 20 different specially selected genes into murine skin fibroblasts using retroviral vectors (32). In the years since, this procedure has been repeated using cells derived from a myriad of different organisms, including humans and refined to require the insertion of only four fundamental transcription factors; namely Oct4, Sox2, Klf4 and c-Myc (33).

Much like their biologically-derived cousins, IPSCs are functionally pluripotent and able to divide almost indefinitely. As a direct result, many research groups have sought to utilise these cells as a means of replacing damaged or degrading tissues following *in vitro* differentiation, with significant overall success. For example, Cai *et al* (2017) reported the generation of functional regulatory dendritic cells from murine IPSCs, capable of inhibiting T-cell mediated immune activation through the secretion of transforming growth factor- $\beta$ 1 (TGF- $\beta$ 1), providing a promising method of creating a patient-specific immunosuppressant therapy for use alongside allograft transplantation procedures (34). This is far from the only such example however, with groups having demonstrated activities as varied as the production of functional hepatocytes

able to alleviate signs of liver damage in animal models to HSC generation for use in bone marrow reconstitution following diagnosis with Fanconi anaemia (35, 36).

Since the creation of human-IPSCs, one question has continued to plague the field: just how similar to ESCs are these cells? Unfortunately, many of the issues associated with the therapeutic application of embryonic cells are relevant here also. Of utmost importance is the tumorigenic nature of IPSCs, which are capable to teratoma formation *in vivo* when undifferentiated cells are transferred alongside differentiated material (37). In addition, IPSC-derived tissues have been shown to be highly immunogenic when utilised in an allogeneic manner. It has been suggested that the targeted knock-out of MHC class-2 related genes could be used to remedy this problem, as this modification would be inherited by any material generated from the undifferentiated cells (38). Regrettably, this solution would almost certainly exacerbate concerns regarding the aforementioned tumour-generating characteristics of these cells, allowing them to effectively evade immune destruction and migrate throughout the body unchecked.

Interestingly, despite unwanted similarities to the cells on which they are modelled, IPSCs are surprisingly different from ESCs as a result of their origins. Kim *et al* (2010) showed that IPSCs retain an epigenetic memory of their somatic origins which acts, not only to restrict their differentiation potential but also to preferentially differentiate them towards specific lineages (39). This is not the only aspect of these cells carried over from their ancestries however, with evidence suggesting that characteristics such as donor gender can impact upon cell behaviour (40). One possible explanation for these observations is that current IPSC production methods result in only incomplete or partial reprogramming of somatic cells. Surprisingly it appears that time in subculture may alleviate some of the genetic instability inherent to these cells, with cells appearing to take on a more fully realised ESC-like pluripotent state following longer periods in culture (41). Unfortunately, even this aspect of IPSCs seems to encounter inconsistency issues and is heavily influenced by donor-related characteristics (41).

Much like ESCs before them, the real potential of IPSCs may reside in the area of disease modelling and drug screening. Unlike embryonic cells however, these cells can be created from the tissues of adult individuals enabling clinicians to create bespoke screening platforms specific to an individual's own cellular or metabolic idiosyncrasies. This could be of particular value when applied to diseases for which there are no representative animal models, such as certain mitochondrial conditions which can have very different genetic underpinnings when

compared to their human counterparts (42). These facts have not been lost by the industry, with iPSCs having been used to manufacture models for close to 70 different diseases between the years of 2007 and 2014 (43). For example, iPSCs have been used to generate complex models of indications such as Parkinson's disease (PD), which is known to occur in individuals with no known family history as a result of one of a number of inherited or de novo mutations (44, 45). One such model produced by Su and Qi (2013), helped uncover a hereto unknown link between leucine-rich repeat kinase 2 mutations (LRRK2), aberrant autophagy mechanisms and PD onset in later life (46).

One important criticism that has been levelled at the use of iPSCs in disease modelling is their genetic immaturity, which could impact on the accuracy of any resultant models. Despite this, it has been suggested that this characteristic of the cells could actually be of benefit when investigating neonatal conditions or developmental defects. Rett syndrome for example, is an autism spectrum disease which manifests in infants at between 6 and 18 months of age (47). It has been shown that human iPSC-derived neurons can be utilised to develop representative *in vitro* models of the condition, displaying many characteristics consistent with cells seen in the brains of affected individuals, including reduced spine density (48).

### 1.2.3 Foetal stem cells

Before discussing the characteristics of foetal stem cells, it is first important that we address their similarities to stem cells isolated from the tissues of adult individuals. In fact, the specific types of cells and their respective tissues of origin can be seen to accurately mirror those observed in adults. Of particular interest however are MSCs, a class of multipotent progenitor capable of differentiating into any cell type of mesodermal origin and which have been isolated from a multitude of different foetal and adult tissues (49). In order to prevent repetition and despite their relevance to the discussion at hand, a more detailed examination of the specific properties of these cells can be found in section 1.2.5, of which they are the sole focus.

As previously mentioned, in spite of the vast potential offered by both ESCs and iPSCs their primitive nature and lack of genetic stability has led to serious concerns over the safety of their use, particularly in relation to their potent tumorigenic properties. As a middle ground between the use of embryonic cells and cells of adult origin, many groups have examined the possibility of utilising stem cells isolated from foetal tissues due to their relative immaturity and the

enhanced proliferative and differentiation-related potential this might offer. To date, foetal stem cells have been isolated from a wide variety of different tissues, including but not limited to; amniotic fluid, amniotic membrane, umbilical cord blood, the umbilical cord itself and even the placenta (50). In addition, human first-trimester bone marrow, liver, and blood and second-trimester bone marrow, liver, lung, spleen, pancreas, and kidney have all been shown to be rich sources of MSCs (51). Of all the sources presented here however, the umbilical cord and the blood contained within it represent the most extensively researched, likely due to the non-invasive nature of the associated cell isolation practices and the fact that these materials are commonly discarded following childbirth. Not only have UCB-MSCs seen extensive testing in animals as discussed by Yadav *et al* (2012), they have also been involved in over one hundred different registered clinical trials in the UK alone between 2007 and 2016 (52). The variety of different indications for which they have been investigated is vast, ranging from neurodegenerative disorders such as Parkinson's disease, to autoimmune conditions including type-1 diabetes and rheumatoid arthritis (53, 54). What makes these particular cells so attractive to researchers and clinicians alike, aside from the straightforward isolation procedures associated with them, are their enhanced therapeutic characteristics when compared to adult-derived MSCs. For instance, Lu *et al* (1996) demonstrated that whilst the total number of UCB-MSCs following long-term culture was lower than that of adult bone marrow-derived MSCs, umbilical cord cells were significantly more proliferative during the early stages of growth (55). Intriguingly this could mean that UCB-MSCs are perfect for use in small scale applications or as a component of so-called 'minimally manipulated' cell-based therapeutics.

Given the apparent popularity of UCB-MSCs within the medical field, one could be forgiven for thinking that foetal stem cells derived from other tissues are in some way less important or of lower quality. This could not be further from the truth however, with recent research suggesting that a distinct subpopulation of placental MSCs seen to express elevated CD200 and HGF secretion promote significantly improved angiogenesis together with increased immunosuppressive function *in vivo* when compared to maternal MSCs (56). In fact, a study done by Loukogeorgakis *et al* (2017) uncovered a population of CD117(c-kit)<sup>1</sup> positive cells within amniotic fluid that was capable of generating functional cells from all three developmental germ layers, much like ESCs but with no apparent indications of tumorigenicity (57). Interestingly, the differentiation-related properties of these cells were linked back to the stage at which they were isolated, with early trimester cells displaying a more primitive phenotype and related lineage potential (57).

It is important to remember that MSCs are not the only foetal stem cell type currently of interest to researchers and clinicians. Foetal HSCs, a type of multipotent progenitor capable of differentiating towards any haematopoietic lineage, may also represent a potent new tool for use in treating human disease. This is made even more likely given the greater repopulating ability demonstrated by these cells when used to help reconstitute bone marrow, a characteristic attributed to the relative immaturity of the cells when compared to their adult counterparts (58).

Given the apparent therapeutic potential of stem cells derived from foetal tissues, it would appear that research into the clinical application of adult human-derived stem cells would be unwarranted, unfortunately this is not the case. Of primary concern, is the poor isolation efficiency connected to many of the types of foetal stem cell described here. Many groups have reported that the maximum achievable isolation efficiency for MSCs from umbilical cord blood is only 65% and that this is only achievable through extensive manipulation, such as with the addition of various cytokines following targeted lymphocyte depletion (59). Some research groups have even reported that MSCs are as rare as to be undetectable in umbilical cord blood, seriously limiting the scope of their potential (60, 61). In addition, whilst the therapeutic application of these cells is not as controversial as is the use of ESCs, their utilisation is not free from ethical scrutiny, particularly when dealing with material that is directly foetal in nature and not part of the supportive structures necessary only during the developmental process.

#### 1.2.4 Adult stem cells

As previously alluded to in section 1.2.3, foetal tissues are not the only available source of non-embryonic human stem cells. In fact, an emerging body of evidence suggests that distinct populations of stem cells can be located in the vast majority of mature mammalian tissues and are likely associated with both homeostatic maintenance and repair of the surrounding material when damaged (62). As in section 1.2.3, it is important to note from the outset that the topic of MSCs will not be covered in this particular section and as a result of its relative importance and the vast quantity of literature available in regard to the subject, it will be discussed subsequently within its own self-contained section.

Typically, adult stem cell populations differ from their foetal and embryonic counterparts in a number of ways, primarily in relation to their proliferative potential, abundance and lineage

specificity. For instance, HSCs derived from foetal tissues have been shown to survive and proliferate more effectively following transplantation than comparable adult cells, producing larger numbers and more varied types of progeny after engraftment (63). One potential reason for this improved survival rate could be the inherent differences in regard to the immunogenicity between foetal and adult cells, with the expression of both MHC class 1 and class 2 molecules seemingly negative in foetal HSCs and increasing to high levels in adult cells (64). In addition, while researchers are generally divided over the relative levels of expression of MHC class 1 in foetal and adult MSCs, this same distinction is readily observed in relation to MHC class 2 expression in bone-marrow derived MSCs (65). In fact, MSCs represent an excellent example of abundance differences between adult and foetal stem cell populations, with one study having found that one in ten-thousand mid-trimester fetal bone marrow cells displayed MSC-like characteristics, compared to only one in every two-hundred and fifty-thousand in adult tissue (65).

Even in the face of these critical distinctions, one fact remains that highlights the importance of adult stem cells in modern tissue engineering; their accessibility. Being able to source populations of progenitor cells from almost any given adult tissue, each of which having lineage-specificity relevant to the tissue from which it was isolated opens up a surprisingly straight-forward avenue of targeted tissue repair in the form of autologous stem cell treatments. The concept is simple, identify and isolate a specific type of stem cell from a given patient, culture those cells *in vitro* in order to bolster their number and therapeutic efficacy, before finally transferring them back into the individual from which they were taken, at the site of injury (66). Importantly, this method circumvents concerns over immunogenicity and human leukocyte antigen (HLA) matching for readily apparent reasons. One example of this type of strategy in action, is the use of limbal stem cells (LSCs) for the treatment of limbal stem cell deficiency (LSCD) resulting from trauma, immunological issues or genetic disease, which inevitably leads to opacification of the corneal surface and subsequent loss of vision (67). LSCs represent a type of specialised epithelial stem cell located in the corneal limbus, an area found between the border of the cornea and sclera, known to be responsible for maintaining and regenerating the ocular surface (68). On this subject, Dua and Azuara-Blanco (2000) reported stable corneal autograft incorporation alongside substantial improvements in vision following the treatment of six patients presenting with unilateral LSCD as a result of a variety of different root causes including alkali burns and intraocular neoplasia (69). One aspect of autologous limbal stem cell transplantation that must be discussed is the problem posed by bilateral LSCD,

for which this treatment cannot be applied due to a lack of suitable material (70). While it is not a commonly encountered issue for other forms of autologous stem cell therapy, it should be recognised that similar issues can inhibit the use of such strategies particularly when stem cell loss or dysfunction is the root cause of the associated indication, such as in cases of Duchenne muscular dystrophy or during instances of widespread bone marrow destruction (71).

Alongside the use of LSCs, adult-derived neural stem cells (NSCs) have also seen success when utilised autologously. NSCs are generally characterised as multipotent progenitors located in the subventricular (SVZ) and subgranular zones (SGZ) of the central nervous system (CNS) and are capable of differentiating into any cell type belonging to the CNS (72,73). Whilst some groups have located NSCs outside of these regions, a consensus cannot be reached in regard to whether they permanently reside within these areas providing a source of localised neurogenic potential or had simply migrated there under specific physiological pressure (72). Regardless of this, autologous NSCs derived from the adult CNS have been shown on multiple occasions to help promote improved neurological function upon transplantation following *in vitro* differentiation or culture conditioning. For example, Levesque *et al* (2009) transplanted autologous NSC-derived dopaminergic and GABAergic neurons into the putamen of a symptomatic Parkinson's disease (PD) patient via microinjection after a nine-month period of *in vitro* expansion (74). In their five-year post-operative follow-up study the group went on to describe significant increases in dopamine uptake within the engrafted regions at three-months post transplantation, leading to substantially improved motor function (74).

One prospective issue that must be addressed concerning the autologous use of both LSCs and NSCs, is donor site morbidity. When sampling tissue for the purpose of cell isolation it is necessary to remove material from the donor-area, causing localised damage and leading to the need for subsequent activation of endogenous repair mechanisms. While this issue affects all manner of autologous cell therapies; whether utilising stem cell or non-stem cell populations, it is especially relevant here due to the sensitivity and biological importance of the donor sites in question. One method of alleviating this concern is to utilise cells isolated from an entirely different tissue in order to treat damage or degradation, as the autologous use of adult stem cells is not restricted to the tissues from which they were sourced. An example of this comes in the form of stem cells derived from dental pulp matter (DPSCs), which due to the ectodermal origin of dental tissues, are capable of neurogenic differentiation as well as having access to mesenchymal lineages (75, 76). As a result, these cells have been proposed for use in the

treatment of a variety of both orthopaedic and neurological conditions, such as the non-union fracture of long bones and Alzheimer disease, respectively (77, 78).

The use of adult stem cells outside of their *in vivo* niche has been shown to have therapeutic benefits, as well as the aforementioned safety advantages. Together with neurogenerative conditions such as PD and Alzheimer's disease, autologous NSC therapies have also been used to begin addressing the symptoms of Type-1 and Type-2 Diabetes, which are now known to be associated with impaired hippocampal learning and reduced cognitive function (79). The precise mechanisms underlying this relationship remain elusive but the discovery of an interplay between insulin activity and NSC neuronal differentiation resulted in the idea of using these cells to treat the primary symptoms of diabetes. In relation to this, Kuwabara *et al* (2011) transplanted autologous olfactory bulb NSCs into the pancreatic tissues of diabetic rodents following conditioning with a combination of Wnt3a ligand and an anti-IGFBP-4 antibody in order to promote increased cellular insulin secretion (80). Promisingly, the grafted NSCs were shown to have survived up to 10 weeks after transplantation and to have generated neurons capable of bioactive insulin secretion, resulting in reduced blood glucose levels (80).

As previously alluded to, autologous strategies can be utilised to treat conditions only when a suitable source of cells is available. Unfortunately, differences in donor-related factors such as age, gender, medical status and genetic make-up can seriously impact upon the proliferative and differentiation potential of various stem cell populations. As a direct result, many researchers and clinicians along with the vast majority of commercial enterprises are now focussing on allogeneic stem cell therapies, in which cells taken from a single donor are used to treat large numbers of recipients following extensive *in vitro* expansion processes.

The earliest example of such a strategy can be seen in the therapeutic use of HSCs, which were the first tissue-specific stem cells to be isolated and have been in clinical use since the early 1980s (81). These cells are readily isolated from bone marrow and are characterised as multipotent progenitors capable of differentiating into any known myeloid or lymphoid cell type, including all associated oligopotent precursors as seen below in figure 1.2 (82). Since their discovery, HSCs have been commonly used in the treatment of a wide range of blood cell related disorders, including leukaemia. In fact, the ability of engrafted HSCs to entirely reconstitute destroyed bone marrow, has enabled clinicians to utilise radiotherapy and chemotherapy doses at myeloablative levels in their quest to eradicate cancer, without permanently impacting upon the health of their patients (83). In addition, the use of HSCs to

produce cancer targeting immunotherapies has also generated promising results, suggesting that these cells may potentially have a more diverse use than first thought (84, 85).

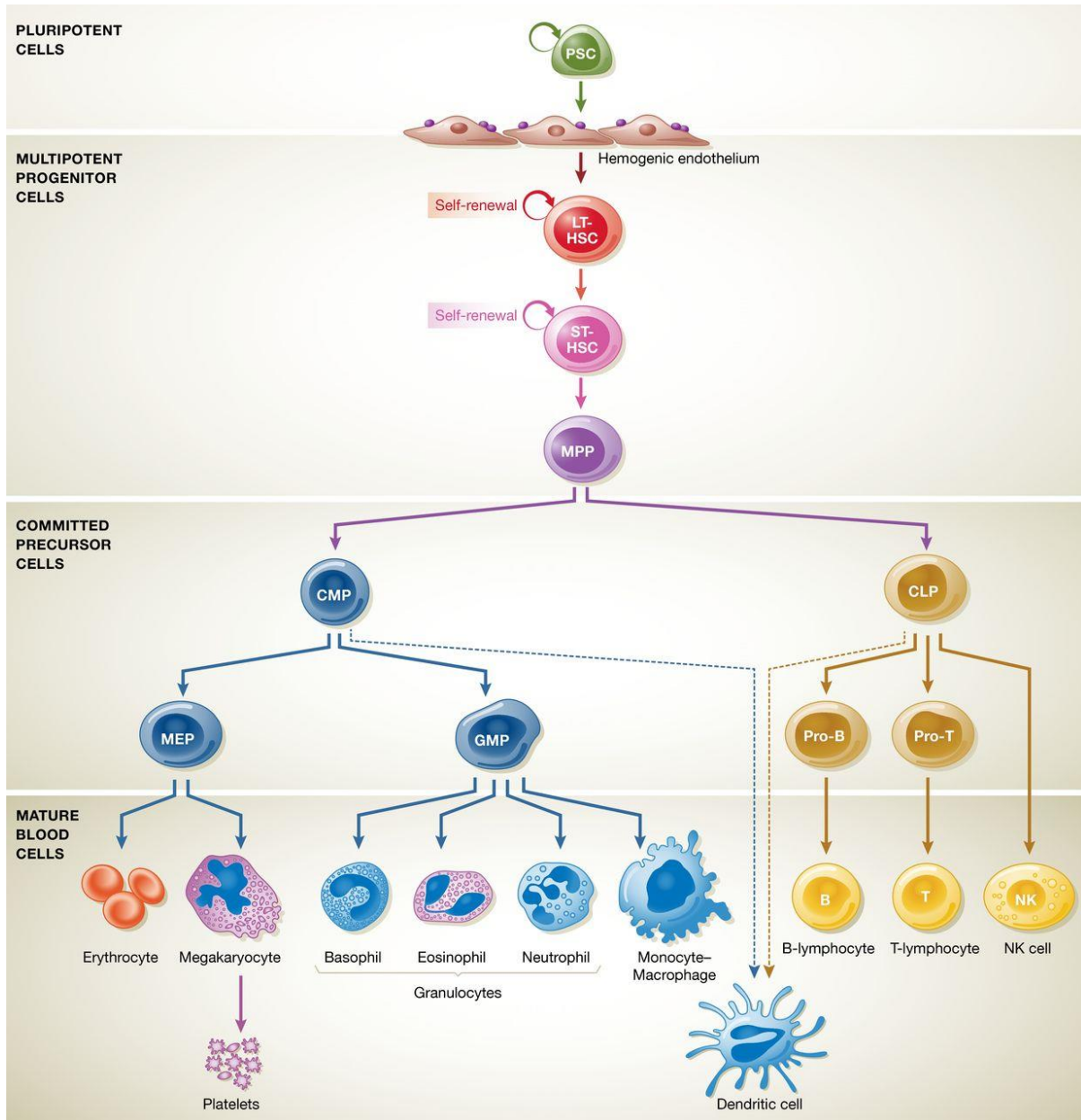


**Figure 1.2 The differentiation hierarchy of human hematopoietic stem cells (207)**

Human HSCs are capable of differentiating into all known myeloid or lymphoid cell types, via the production of oligopotent common myeloid progenitors (CLPs) and common lymphoid progenitors (CLPs), respectively. Intermediate megakaryocyte–erythroid progenitors (MEPs) and granulocyte–macrophage progenitors (GMPs) are also generated during this process.

### 1.2.5 Mesenchymal stromal cells

MSCs were first isolated almost fifty years ago by Friedenstein *et al* from the bone marrow of guinea-pigs and were described as non-phagocytic mononuclear cells with fibroblastic morphology, capable of adhering to culture surfaces to form a monolayer (86, 87). In regard to their characteristics, MSCs are best described as multipotent progenitors with limited *in vitro* proliferative potential and the ability to differentiate into any known mesenchymal cell type (88, 89). As has been previously mentioned, accessibility is one of the primary benefits of utilising stem cells derived from mature tissues. MSCs exemplify this quality, being readily isolated from trabecular bone, synovial fluid, synovial membrane, adipose tissue, skeletal muscle, the lungs, the heart and the peripheral circulation (90, 91, 92, 93, 94, 95, 96). As a result of the diverse range of tissues that are known to harbour these cells, the International Society for Cellular Therapy (ISCT) outlined a set of minimal criteria for the positive identification of MSCs (97). Three fundamental characteristics are described in these guidelines; namely fibroblastic morphology and plastic adherence, surface marker expression and tri-lineage differentiation potential, with this final point referring to the cell's ability to undergo directed osteogenic, chondrogenic and adipogenic differentiation *in vitro* (97, 98).

Following their initial characterisation, it became clear that MSCs could potentially be used to help generate replacement musculoskeletal tissues for use in reconstructive or regenerative procedures. Of particular interest was the idea of replacing damaged articular cartilage, which lines the internal surfaces of synovial joints creating a smooth low friction surface over which the bones can move (99). This material tends to become damaged over time as a result of trauma, life-style associated problems and inflammatory conditions such as osteoarthritis but due to its avascular nature has very limited endogenous healing potential (100). In order to circumvent this issue, groups such as Ghezzi *et al* (2015), Hofmann *et al* (2006) and Huang *et al* (2004) have generated cartilage or cartilage-like tissues using MSCs seeded onto collagen, silk and agarose scaffolds respectively (101, 102, 103). These studies highlight a trend typical of orthopaedic stem cell application but also true within other areas of regenerative medicine, namely the use of cells in combination with biomaterial scaffolds. It is important to note that cells are exposed to a variety of biomechanical and chemical stresses when transplanted into sites of injury. The use of specially formulated biomaterial constructs in situations such as those mentioned above can act to protect sensitive biological material, whilst at the same physically stabilising the injury site and even enhancing cell proliferation or differentiation. One area in

which this type of complex Advanced Therapy Medicinal Product (ATMP) is necessary, is bone restoration following non-union fracture. To this end, Quarto *et al* (2001) were able to demonstrate successful repair of five-centimetre bone defects using hBM-MSCs seeded onto ceramic scaffolds (104). Similarly, Maiti *et al* (2016) reported the production of well-mineralised woven bone following the use cytokine-impregnated silica-coated calcium hydroxyapatite (HASi) scaffolds seeded with BM-MSCs in a rabbit model of super-critical sized radial defects (105).

Intriguingly, despite their mesenchymal origins, a large number of independent sources have demonstrated the ectodermal and endodermal trans-differentiation of MSCs. For instance, Tondreau *et al* (2008) together with Zeng *et al* (2011) reported that MSCs have the ability to produce functional neurones capable of generating ion currents when exposed to specific neurogenic agents, such as nerve growth factor (NFG) and insulin (106, 107). In terms of endodermal lineage commitment, MSC have been shown to be able to develop into type-2 alveolar epithelial cells, hepatocytes and pancreocytes when exposed to properly conditioned media together with a variety of different growth supplements (108, 109).

The therapeutic potential of MSCs isn't limited to the generation of replacement tissues. In addition to their differentiation potential, these cells also secrete a vast array of different cytokines, chemokines, growth factors and regulatory agents (110). This secretome/sheddome, as it's known, acts as a multifunctional system utilising a combination of paracrine, exosomal and microvesicle-mediated systems for agent release (111). In regard to the specifics of its activity, the MSC secretome is known to include proliferative and regenerative factors such as HGF, VEGF, SDF-1, bFGF and MCP-1 alongside immunomodulatory cytokines such as IL-10, IL-1a, IL-6, IL-17, GM-CSF and TSG-6 (112,113). This means that when utilised in an undifferentiated state, MSCs have the potential to initiate endogenous repair mechanisms whilst also reducing inflammatory responses and modulating immune activation.

One of the earliest examples of MSCs being utilised in this manner is in the treatment of ischemic cardiac tissues following myocardial infarction, for which the application of undifferentiated MSCs was shown to activate revascularisation through the secretion of factors such as VEGF and bFGF (114). Interestingly, this may not be the only mechanism through which these cells act to restore cardiac function *in vivo*. For instance, MSCs have demonstrated the ability to produce HGF, TGF- $\beta$ , IGF-1, and stanniocalcin 1, all of which are known to be potent anti-apoptotic molecules capable of promoting cell survival in harmful ischemic

microenvironments (115,116). As well as their use restoring cardiac function, MSCs have also been suggested as a method of treating auto-immune diseases such as aplastic anaemia, which is characterised by the cytotoxic T cell-mediated destruction of haematopoietic precursors from the patient's bone marrow (117). Pang *et al* (2017) conducted a phase two clinical trial assessing the efficacy of utilising BM-MSCs to help support HSC recovery through microenvironmental reconstitution and immune modulation (118). Seventy-four patients presenting with aplastic anaemia refractory to immunosuppressive therapy were treated with four weekly doses of allogenic BM-MSCs, resulting in an overall response rate of 28.4% and over 85% of the recipients still alive at the 17-month follow-up point (118). While these results are not startlingly positive, they do appear promising in regard to both the efficacy and safety of this method of treatment.

In addition to the characteristics detailed above, MSCs also exhibit two further therapeutically relevant features; namely their ability to home-in on sites of injury and disease, and their anti-bacterial properties. The homing abilities of MSCs are mediated by conventional chemotactic principles, with factors such as MCP-1 and Chemokine C-C motif ligand-5 (CCL5) regulating MSC tumour-tropic behaviour (119). When combined with their trans-differentiation potential and secretory abilities, this property makes MSCs an attractive prospect when treating spinal cord injuries, where localised transplantation may cause additional damage. In a proof of concept study, Ohta *et al* (2017) utilised intravenously applied AD-MSCs in a rat model and reported functional recovery as indicated by improved hind-limb motor function (121). These findings were determined to be the result of localised cytokine-induced neutrophil chemoattractant-1 (CINC-1) release following gradual accumulation of the AD-MSCs at the injury site (120). As with their regulation of the mammalian immune system and endogenous healing mechanisms, the anti-bacterial properties of MSCs result from their complex secretory profile. In a study using equine cells, Harman *et al* (2017) identified four distinct anti-microbial peptides capable of damaging the cell walls of both gram-negative and gram-positive bacterial species, the production of which could reveal an additional means through which these cells are capable of contributing to wound healing and tissue repair (121).

In the face of all the evidence listed above it could appear that MSCs represent a 'magic-bullet'-type therapeutic, capable of helping to treat numerous distinct conditions without any associated efficacy or safety concerns. Unfortunately, this is not the case, with issues regarding cell heterogeneity and donor/tissue-related inconsistencies seriously affecting their use. For example, Amable *et al* (2014) described different functional profiles of protein secretion from

MSCs isolated from Warton's jelly (WJ-MSCs) as compared to adipose-derived cells (122). Specifically, AD-MSCs showed increased production of pro-angiogenic factors, whilst WJ-MSCs were seen to produce higher concentrations of chemokines, pro-inflammatory agents and growth factors, suggesting the need to tailor the origin of a given cell population to the condition it is being used to treat. Further research has suggested that metrics such as donor age, gender and health status can significantly impact on MSC behaviour (123). One method of addressing this concern is to utilise allogenic cell populations in therapeutic applications rather than providing autologous routes of stem cell delivery. In this way, cells selected from healthy donors can be utilised to treat a vast number of individuals without the need to worry about the aforementioned inconsistencies or donor site morbidity concerns discussed in the previous section. In fact, MSCs lend themselves well to use as part of allogenic strategies due to their lack of MHC class-2 expression and immunomodulatory secretions (124). In addition, the use of model stem cell populations would potentially enable clinicians to culture specific sub-populations of cells derived directly from heterogeneous primary isolates. One such cell type; multipotent adult progenitor cells (MASCs), have demonstrated mesodermal, ectodermal and endodermal differentiation similar to that of MSCs but with enhanced proliferative potential, being capable of expansion for over 100 population doublings without observable telomere shortening or karyotypic instability (125).

As a direct result of the therapeutic potential displayed by adult MSCs, their use has been the focus of a vast number of clinical trials in the past decade. According to Trounson and McDonald (2016) the National Institute of Health (NIH) database listed 374 registered trials involving MSCs in 2015, a three-fold expansion over the number listed in 2011 (126). Interestingly, the relative composition of these studies marks a shift towards to the use of allogeneic strategies within the industry, with ClinicalTrials.gov listing 56 ongoing trials utilising allogeneic MSCs in 2016 alone, whilst only 32 included autologous cells (127). Regardless of the preferred cell source however, one factor which continues to affect the clinical application of MSCs is the need to supply very large numbers of cells in order to guarantee survival following *in vivo* transplantation, a fact illustrated by the one-hundred million cells currently required to produce an effective therapeutic dose (128). In the next chapter, we will explore clinical and commercial cell culture strategies alongside the issues currently impacting upon their success.

### 1.3 Stem cell expansion processes

As of 2015, only four stem cell-based advanced therapy medicinal products were recognised as having been approved across the globe (within their respective jurisdictions), with this small list including both autologous and allogeneic examples (129). Holoclar® for instance, involves the treatment of moderate to severe limbal stem-cell deficiency through the use of autologous LSCs and represents the first approved example of an ATMP within the European Union (EU) (130). Prochymal® on the other hand, utilises allogeneic BM-MSCs to treat Graft versus Host Disease (GvHD) in paediatric patients and was itself Canada's first approved ATMP (131).

Irrespective of the associated indication or cell source, one common problem encountered during the development of each of these examples was the requirement for extremely large doses of cells. This is particularly true of products such as Prochymal® which rely on systemic delivery, following which large quantities of cells have been shown to become trapped in the lungs (132). There are currently two distinct methods of tackling this problem, namely; the use of high-frequency small-scale cell culture technologies or the application of low-frequency large-scale culture systems. The respective advantages and disadvantage associated with each of these methods will be explored in more detail within the following sections, with an explicit focus on their application to the expansion of adherent MSC populations.

#### 1.3.1 Small scale cell culture processes

Tissue culture flasks represent the single most widespread method of expanding cells for both academic and medical purposes. Manufactured from polystyrene due to its optical clarity and the ease with which it can be accurately moulded and sterilised, these flasks provide a simple and readily available means with which to culture cells (133). Originally, the hydrophobic nature of the polymer used to produce the flasks resulted in highly restricted cell growth, even when compared to glass, which had seen heavy use during the early-to-mid 20<sup>th</sup> century (133). By the mid-1970s however, it had been discovered that treating the flask's growth surface under vacuum with a gas-plasma could oxidise the material (134). As a direct consequence, functional carboxyl groups were deposited onto the surface, helping bind extracellular matrix proteins; either produced by the cells or available in the culture medium, facilitating enhanced cell adhesion and making the use of glass near obsolete (135).

Unfortunately, despite their prevalence, expansion within conventional monolayered flasks is far from ideal. One of the most problematic aspects of this particular culture method is the limited growth space available within each flask. With regard to MSCs specifically, it has been shown that confluence is reached at around  $5 \times 10^3$  cells per  $\text{cm}^2$  and that whilst seeding the cells at lower starting densities can significantly improve productivity, the use of large numbers of flasks is seemingly unavoidable (136). In order to address this concern, companies such as Nunc® and Corning® developed multi-layered culture vessels providing significant increases in the surface area available for cell growth, without substantial increases in complexity or flask footprint. In fact, recent advances by Corning® have seen the introduction of 120-layer HYPERstack™ vessels made from a gas permeable polymer and capable of providing growth surfaces up to two and a half times larger than conventional multi-level flasks of comparable volume (137). Since their inception, these types of technologies have seen extensive use throughout the regenerative medicine field, from routine cell culture during research activities, to use as a primary expansion method when manufacturing for clinical trials (138). Interestingly, it appears likely that the mechanistic similarities between monolayered flask culture and multi-layered flask culture are the prime rationale for their use during clinical trials, as very limited optimisation work would need to be performed prior to scale-up and the resultant cell populations would likely remain consistent with those utilised during pre-clinical testing.

Regrettably, despite technological advances, a number of the fundamental characteristics of this type of approach still limit its overall appeal and applicability. Firstly, the use of culture flasks typically requires extensive manual handling, making it necessary to train and employ appropriately skilled personal in order to undertake frequent subculture and media change activities. As such, this introduces an increased level of expenditure beyond that of the basic cost of goods associated with the process and also provides an additional avenue for culture contamination or product loss, as a direct result of human error. In response, a number of companies and research groups have explored the use of automation as a means of circumventing these concerns. Thomas *et al* (2007) for example, demonstrated the successful expansion of hBM-MSCs through the use of an automated cell culture platform and despite differences in cell number when compared to comparative manual methods, cells were seen to retain their ISCT-defined characteristics following automation (139). It should be noted however, that the capital costs involved in purchasing such systems may represent too greater investment for the majority of SMEs, academic institutions and medical service providers,

whilst also potentially introducing a major new source of variability within an expansion process that would have otherwise remained consistent. In addition to manual handling concerns, lack of process control is also a significant issue when dealing with flask-based culture strategies. Whilst the relative simplicity of expansion within static flasks does offer some notable advantages, the inability to accurately regulate the conditions to which cells are exposed seriously limits the adaptability of such processes and makes it almost impossible to accommodate unforeseen variability, including changes in raw material composition. Additionally, this problem also restricts efforts to optimise the process, severely limiting its long-term potential.

Finally, it should be mentioned that as an alternative to the previously discussed strategies, many groups have investigated the use of micro-carriers during suspension culture in small volume spinner flasks (140, 141, 142). In much the same way as for the use of static flask-based methods before them, these processes suffer from issues regarding manual handling requirements and lack of process control. Despite this, the application of microcarriers is an important concept when considering the large-scale expansion of adherent cell populations and as such will be explored in more detail within the following section.

### 1.3.2 Large scale cell processes

In order to discuss the manufacture of stem cells at large scale it is first necessary to explore the use of bioreactor technologies, which have seen widespread use throughout the mainstream biopharmaceutical industry. In this context, a bioreactor can be described as any device capable of providing a highly controlled non-static growth environment for the expansion of either eukaryotic or prokaryotic cells. Interestingly, the vast majority of antibody production processes utilise suspension-adapted cell types, such as Chinese Hamster Ovary (CHO) or murine myeloma (NS0), cultured in bioreactor systems in a fed-batch manner. Unfortunately, most types of adult-derived stem cell are adhesion-dependent and would be unable to survive in such conditions for even a relatively short length of time. MSCs for example have been shown to undergo anoikis, a form of programmed cell death resulting from lack of integrin-mediated substrate attachment, due to down-regulated extracellular signal-regulated kinase-1/2 (Erk1/2) and c-Jun N-terminal kinase (JNK) activity (143). The most common means of addressing this issue is the application of microcarriers within suspension culture, which were first utilised commercially by van Wezel in the manufacture of inactivated polio vaccine (IPV)

(144, 145). These fifty to hundred-micron sized beads are made from a variety of different materials, including synthetic and natural polymers together with bio-compatible ceramics and provide very large growth areas per unit volume due to their relative abundance (146). Schirmaier *et al* (2014) for example, successfully utilised microcarriers for the expansion of AD-MSCs within stirred tank bioreactors, reporting total cell numbers as high as  $1 \times 10^{10}$  following culture at thirty-five litre scale (147). Similarly, Timmins *et al* (2012) demonstrated expansion of placental MSCs in two litre wave bags using commercially available microcarriers over four successive subcultures, without loss of tri-lineage differentiation potential or characteristic surface marker expression (148). Intriguingly, stirred tank vessels and disposable wave-bag systems represent the two most popular methods of large scale stem cell culture, likely due to their relative simplicity and accessibility.

Stirred tank reactors, as the name suggests, are an evolution of the classic spinner-flask and typically consist of a single rigid glass or plastic tank into which sits an impeller that acts to facilitate nutrient transport and mixing within the media. In addition, these vessels are connected to computerised control systems, which regulate pH, oxygen supply and temperature via a set of feedback loops. Wave reactors function in a very similar manner, with the exception that disposable polymer bags are used to house the culture and that mixing is performed through the action of a rocking platform, rather than direct contact-based agitation. Figures 1.3 and 1.4 provide images of typical stirred tank and wave bioreactor set-ups for mammalian cell culture.



**Figure 1.3 A typical stirred tank bioreactor system (208)**

Stirred tank reactors are generally made up of a large transparent vessel, into which a set of monitoring devices measuring pH, temperature and dissolved oxygen are placed. Alongside these are an impeller and a sparger, which ensure proper nutrient and gas dispersal throughout the culture. Computerised control systems regulate gas addition, pH and temperature based on a series of feedback loops linked to the aforementioned sensors.



**Figure 1.4 A typical wave bioreactor system (209)**

Wave bioreactors function in much the same way as stirred tank systems, with the exceptions that the culture is contained within a single-use polymer bag and that mixing is achieved through the action of a rocking platform rather than an impeller.

Despite the popularity of stirred vessels and wave bags, these systems both suffer from issues regarding shear stress and the impact this can have on stem cell viability. Due to their relatively large size when compared to microbial cells; together with their lack of a cell wall, eukaryotic cells remain vulnerable to the forces generated as a result of culture agitation, which is necessary in order to guarantee homogenous nutrient and gas dispersal during the process (149). The precise results of exposure to shear stresses have been shown to vary according to both cell type and the magnitude of the applied force but are known to include transient pore generation, cytoplasmic extrusions, altered metabolic output, reduced proliferation and even cell death (150, 151). In addition, this phenomenon may in fact be reinforced by the presence of high concentrations of microcarriers, which are likely to damage cells as a result of bead-to-bead collisions and impacting with the impeller or vessel wall (152). Importantly, when considering the expansion of stem cells, shear stresses have also been demonstrated to initiate lineage-specific differentiation in a number of specific cases, including the endothelial and osteogenic differentiation of BM-MSCs (153, 154). This type of behaviour is particularly pertinent given the apparent therapeutic potential of undifferentiated MSCs as a result of their distinct secretory profile, which would almost certainly be lost if differentiation were to occur. Intriguingly, it appears that bubbles produced during mixing and as a result of culture gassing using a sparger, may also cause significant damage to cultured cells when utilising conventional bioreactor systems (155). This impact is thought to primarily occur as a result of the so-called 'air-liquid interfacial effect', which refers to the massively destructive forces generated when a bubble ruptures at the surface of the culture medium. In many cases the impact of this phenomenon is thought to depend almost exclusively upon bubble size, with the presence of sub-2mm diameter bubbles leading to increased cell loss due to their decreased rate of climb through the liquid and likelihood of interacting with and carrying more cells to the surface (156). Additionally, smaller bubbles have a tendency to be retained at the air-liquid interface in the form of foam, which can trap cells within a nutrient-deprived environment (156). This is not to say that mechanical forces cannot have a beneficial impact on stem cell survival when applied in a highly controlled manner however. Luo *et al* (2011) demonstrated that laminar shear stresses of fifteen dyne/cm<sup>2</sup> could suppress apoptosis in MSCs as a direct consequence of increased Bcl-2 expression, a potent anti-apoptotic gene (157). It should be noted that this effect coincided with cell cycle arrest and cells entering a quiescent-like state, limiting its immediate applicability but not undermining its overall relevance (157).

In order to address the concerns discussed above regarding microcarrier usage and shear-induced cell damage, a number of low-force or microcarrier-free bioreactor alternatives have been developed. The rotating wall vessel bioreactor for instance, consists of a rotating cylinder of liquid in which cells or particles are constantly falling, causing them to remain suspended without the need for violent or turbulent mixing (158). In fact, the forces generated on microcarrier beads under these conditions can be as low as 1.8 to 3.2 dyne/cm<sup>2</sup>, well below the values referenced earlier in this section, that were seen to cause cell cycle arrest in BM-MSCs (159). Unfortunately, the mixing method employed in these types of vessels typically leads to cell aggregation or inhibition of growth as a direct result of the gravity-annulling environment produced within the reactor (158). Hollow fibre bioreactors also offer an interesting alternative to stirred tank or wave systems, negating the need for microcarriers due to the large surface area-to-volume ratio inherent to the design. These vessels are made up of a large tube containing a huge quantity of parallel capillaries arranged as a bundle. Cells can occupy either the extra-capillary or intra-capillary space depending upon the specific requirements of the cells, with no need for subculture or bulk-feeding due to the perfusion of medium through the fibres. Regrettably, issues with culture monitoring and scale-up seriously limit the use of this type of technology in a commercial setting (160). Additionally, due to difficulties regarding cell release following expansion, hollow fibre bioreactors are likely most useful in producing stem cell-derived products, such as conditioned media or exosomes, rather than bulk cell generation.

## 1.4 Stem cell culture medium

### 1.4.1 The importance of culture medium

Culture medium represents one of the single most important and most variable components of any mammalian cell culture process. The primary responsibility of this solution is to provide cells with the nutrients they require in order to survive and proliferate *in vitro*. The fundamental components of any functional mammalian cell culture medium include a metabolic substrate; typically glucose, alongside various essential amino acids, vitamins, minerals and lipids, all helping to drive processes such as cellular respiration, protein production, cellular repair and ensure proper enzyme functionality (161). In the case of adherent cell populations, such as MSCs, medium also often contains various extracellular matrix (ECM) proteins, which act to

facilitate cell-substrate interactions. The inclusion of soluble matrix proteins can be substituted with the use of pre-coated surfaces if a more defined substrate composition or pattern of deposition are required, such as when spatially organising differentiation for the purposes of artificial tissue generation. Such surfaces can also be reused following harvest, making them a cost-effective alternative to soluble protein inclusion, despite increased preparation times prior to their initial use. While not directly relevant to most stem cell-based processes; within the biologics industry, medium may also be supplemented with additional non-essential amino acids for the purposes of accommodating the increased demands of antibody production. A strategy similar to this could potentially be adopted if stem cell bi-products, such as exosomes, became the primary target of future manufacturing efforts. Finally, it is important to note that cell culture medium often also contains various ancillary supplements, such as pH indicators (e.g. phenol red) and mechano-protectants (e.g. Pluronic ® F-68) (162).

In the following sections, we will examine the primary components of mammalian cell culture medium in greater detail, with particular emphasis being paid to supplement origin, safety and consistency.

#### 1.4.2 Foetal bovine serum

Mammalian cell culture medium is typically made up of three distinct elements; basal medium, which contains glucose alongside an array of different amino acids, minerals and vitamins, a primary growth supplement in the form of serum or an equivalent alternative, and finally any additional supplements absent from the other two components. Foetal bovine serum (FBS) represents the single most commonly utilised primary growth supplement for mammalian cell cultures and, as its name suggests, is derived from the processed and sterilised blood of foetal calves. The resultant solution contains a myriad of different amino acids, vitamins, minerals, cytokines, growth hormones and metabolic bi-products, which can adequately support the survival and proliferation of adult-derived stem cells in long-term culture (163). Alongside promoting cell growth, FBS also serves to facilitate cell-surface interactions by supplying a number of different ECM proteins, as well as acting as a potent mechano-protectant in dynamic culture environments (164). It is likely for these reasons that the United States Food and Drug Administration reported that over 80% of the MSC-based investigational new products in 2014 utilised FBS during their manufacture (165).

Despite the extensive benefits of utilising FBS and its prevalence throughout the industry, a number of important factors impact upon its continued use within both the academic and commercial sectors, particularly when considering the manufacture of cell therapies for use in human patients. Firstly, the xenogeneic origin of the material must be considered, which brings with it the risk of both pathogen transfer and unwanted immunogenic reactions in human cell recipients. Whilst it is true that the use of FBS could result in products being contaminated with bacteria, fungi, mycoplasma or virus particles, the combined use of sub-micron filtration and radiation treatment is typically adequate to alleviate these concerns (166). Of greater importance, is the possibility of endotoxin or prion protein content, which can be addressed through heat-inactivation but only at the detriment of overall serum potency (166).

When compared to the aforementioned contamination concerns, the immunogenic impact of FBS is a far more difficult problem to tackle. In fact, a number of ATMP-based clinical trials have reported some level of serum-elicited immune response in their associated human subjects. For example, Horwitz *et al* (2002) described antibody production against FBS components in one of six patients treated with BM-MSCs, with similar responses having also been seen in individuals treated with non-stem cell based cellular therapeutics (167, 168). Intriguingly, groups such as Cho *et al* (2009) have demonstrated that AD-MSCs retain their immunomodulatory functions following culture in FBS, with no apparent immune responses being reported following transfer to murine models (169). It has been suggested that FBS may be inherently less immunogenic to mice, limiting the applicability of these findings to human recipients, however to date this hypothesis remains unconfirmed (170).

Given the biological source of FBS, serum variability is also an important concern. Despite having been utilised for over half a century, FBS remains very poorly characterised, with some reports suggesting that it may contain as many as 1800 different proteins and 4000 distinct metabolites (171). This compositional inconsistency has been seen to impact cell growth and differentiation by a number of different research groups, though only limited investigations have examined the extent with which these differences can affect adult-derived stem cell populations (172). One study, using adult retinal pigment epithelial cells, discovered that differences in cell growth between FBS batches correlated to variability in Insulin-like growth factor binding protein-4 (IBGFBP-4) and insulin-like growth factor-2 (IGF-2) concentrations within the supplement (173). In addition, batches of FBS most readily capable of supporting cell proliferation were seen to contain fibroblast FGF-2 and TGF- $\beta$ 1, which were absent from the low-growth samples and act as potent mitogens during mammalian cell culture (173). While

pooling of different serum batches during manufacture does go some way to alleviating this problem, factors such as cattle health, feed composition and sub-species related differences are unlikely to be accommodated for via this method due to current farming practices.

Alongside the issues detailed above, the recent surge in interest for stem cell-based therapeutics has led to an increased demand for FBS, which the current market may not be able to adequately respond to. Serum manufacture is heavily dependent upon the state of the beef and dairy industries due to its status as a bi-product and as such does not operate independently based upon demand alone. In addition, the countries responsible for supplying the majority of the world's FBS; namely New Zealand, Australia, Brazil and South Africa are distant from those that utilise it (the UK, Europe and the US), making interruption of supply a more likely occurrence (171). Poor regulation within the serum industry has also led to cases of quality tampering and batch doping, such as with GE Healthcare in 2011 (171). When combined with the inherent variability of the product, the use of FBS for the production of human therapeutics seems thwart with problems. In fact, the regulatory requirements in regard to ATMP quality and consistency, along with difficulties concerning process scale-up and supply, make it increasingly difficult to justify the use of FBS when developing a new therapeutic. Finally, it is important to note that the use of FBS also raises a number of ethical concerns, primarily in regard to animal welfare and farming standards. Currently, calf foetuses are thought to suffocate as a result of their mother's slaughter prior to serum extraction, however some individuals have suggested that due to their immature state, these animals are likely to survive much longer than originally suspected, indicating that conventional FBS production methods may require thorough reform should the industry continue to be supported.

#### 1.4.3 Non-defined alternatives to foetal bovine serum

In order to address the xenogeneic nature of FBS, which can potentially lead to cross-species disease transmission or immune activation, a number of human-derived alternatives have been proposed. The most apparent substitute for FBS is the use of human serum (HS), which is typically produced via a process of chemically-induced clot formation followed by filtration (174). It is theorised that HS should be able to better support the growth of human-derived stem cells as a result of species compatibility and that the use of AB-serum, which lacks both A and B-type blood antigens, should minimise any associated immunoreactivity concerns (175). When utilising human AB-serum for the expansion of human MSCs, Marques dos Santos *et al*

(2017) reported maintained surface marker expression, immunomodulatory phenotype and karyotypic stability when compared to culture in FBS supplemented medium (174). In addition to its use as a nutrient source during growth, HS has also been shown to support cell survival during chilled transport, a role typically reserved for FBS. Mizuno *et al* (2017) demonstrated that synovial MSCs held at 4 °C and 13 °C in HS for up to 48 hours retained both their tri-lineage differentiation potential and surface marker expression, alongside their proliferative capacity once re-seeded into conditions suitable for expansion (176).

Alongside the use of human serum itself, many groups have examined the potential of a number of HS-derived products, produced via more extensive processing of the material prior to use. Human platelet lysate (hPL) for example, is manufactured through repeated freeze-thaw cycling of whole serum, resulting in the disruption of the platelet plasma membrane and subsequent release of a wide range of different cytokines and growth factors into the product (177). This platelet lysate step has been shown to lead to significant increases in FGF-2, TGF- $\beta$ 1, IGF-1 and platelet-derived growth factor-AB (PDGF-AB) content in hPL when compared to FBS, all of which are known to readily support mammalian cell growth *in vitro* (178). This may explain the improved MSC proliferation reported by groups such as Matthyssen *et al* (2017) when using hPL (179). As with whole serum, surface marker expression and tri-lineage potential were retained following culture in PL (179). Furthermore, the use of lysate was not seen to bring about the senescence-like effects observed by some groups when utilising FBS, enhancing expression of various cyclin proteins and decreasing p21 and p27 cell cycle inhibitor activity in AD-MSCs following long term expansion (180, 181).

As with animal-derived products, the use of supplements derived from human tissues brings with it serious risks of disease transmission, made even more concerning due to donor/patient species compatibility. Interestingly, the cyclic freeze-thaw step used to produce PL from whole serum samples may in fact act to eliminate many possible bacterial and fungal pathogens, improving product safety. Furthermore, the extensive pre-screening assays already associated with blood and serum donation, the chief sources of lysate, offer a robust layer of protection from a variety of pathogens, including hepatitis and HIV. Despite this promise however, it should be noted that the use of plasma lysate is not without issue. For instance, Oikonomopoulos *et al* (2015) reported that culture in hPL inhibited the immunosuppressive effects of both bone marrow and adipose-derived hMSCs (180). This phenomenon was seen to persist even when cells were pre-primed with Interferon gamma (IFN- $\gamma$ ), a pro-inflammatory

cytokine known to augment the immunomodulatory impact of MSCs when grown using FBS (182).

In addition to platelet lysate, several other HS-derived supplements have also been proposed for use with adult stem cell populations, including platelet rich plasma (PRP) and platelet rich fibrin (PRF). PRP is produced through the biochemical activation of clot formation without platelet lysis and results in supplements containing growth factor and cytokine levels equivalent to those seen during natural wound healing processes (183). PRF on the other hand, is manufactured in a similar manner to PRP but the natural clotting mechanism is utilised to invoke cytokine secretion which is then followed by controlled clot compression in order to facilitate growth factor release (183). Due to the use of endogenous biochemical agents in PRP production and the need to ensure their removal from the resultant material, PRF is seen by many as more suitable for use in ATMP manufacture. Importantly, PRF has been seen to adequately support the expansion and possible osteogenic differentiation of dental pulp-derived MSCs *in vitro* (183). One factor to consider however, is that PRF has demonstrated the ability to successfully prime MSCs for chondrogenic differentiation in a dose dependant manner, making its use in the production of undifferentiated cells potentially problematic, particularly if likely to be exposed to additional chondrogenic stimuli (184).

Unfortunately, the use of HS, PL, PRP and PRF do not address the consistency issues associated with FBS, due to their similar biological nature. In fact, due to the relatively small scale at which these human-based supplements are produced, manufacturing processes vary significantly between groups, potentially leading to inconsistencies in product quality and suitability. Additionally, supply is also a concern, with limited availability resulting from the therapeutic need for blood donations and while it is true that recent research has shown that PL derived from out-of-date blood samples is equally capable of supporting cell growth, supply shortages remain an ever-present threat (185). Finally, it is important to note that plant-derived alternatives have also been explored for use in stem cell expansion, with Lee *et al* (186) demonstrating that vegetable soy peptides are capable of supporting the growth of both AD-MSCs and UCB-MSCs in serum-free conditions. As with serum-based supplements before them however, the lack of characterisation of such materials makes them potentially unsuitable for therapeutic manufacturing processes, despite being readily available and pathogen free.

#### 1.4.4 Chemically defined serum-free medium

As stated in the previous sections, inconsistency in raw material composition represents one of the single most important concerns regarding the use of biologically-sourced media supplements, whether they be of animal, human or even botanical origin. Whilst it is true that so called Quality by Design (QbD) strategies incorporating Process Analytical Technologies (PAT) can be utilised to help accommodate this inherent variability, the development of chemically defined media offers manufacturers a method of essentially eliminating this problem in its entirety. As its name suggests, chemically-defined medium is typically formulated from a basal mixture of selected amino acids, vitamins, minerals and metabolic substrates supplemented with a variety of different cytokines and growth factors. Importantly, these bioactive molecules are produced through biopharmaceutical processes, rather than being extracted from animal sources due to the unwanted variability and potentially dangerous immunogenicity issues that can occur as a result.

In the decades since the initial isolation of MSCs, a number of compatible chemically defined media formulations have become commercially available, including Mesencult-XF (Stemcell Technologies) and Mosaic hMSC Serum Free Medium (Becton Dickinson), both of which have been shown to readily support the isolation of primary cells alongside their expansion (187, 188). Unfortunately, despite the efficacy of these products, they remain prohibitively expensive when compared to the use of serum or serum-derived supplements. Furthermore, the combination of supply monopoly due to their proprietary nature and the strict regulatory guidelines relating to changes in ongoing production processes, could potentially lead to high price variability and market exploitation if left unchecked. In fact, whilst the secrecy surrounding the compositions of these media is entirely justified, it does raise concerns regarding their use in research, where uncovering causal relationships relies upon a thorough understanding of all the associated factors.

In response to these issues, a limited number of research groups have developed chemically defined media formulations for use with MSCs, many choosing to utilise pre-existing media compositions originally developed for use with other types of stem cells in a quest to speed up this process. To this end, Rajala *et al* (2010), successfully expanded AD-MSCs in a modified version of a readily available ESC medium, reporting significantly higher rates of proliferation when compared to growth in allogeneic human serum (189). Similarly, *Mimura et al* (2010) reported the use of an adapted form of hESF9 ESC medium in the expansion of an immortalised

human MSC line. Troublingly, the cells grown in defined conditions displayed a substantially different surface marker profile than cells cultured in conventional serum-supplemented medium, with increased pluripotency-related marker expression (190). This type of observation exemplifies one of the most important criticisms of this kind of approach to medium development, namely that a lack of formulation specificity can potentially lead to altered cell behaviour or unwanted lineage transition following even short times in culture. In addition, the inclusion of unnecessary components within the medium carried over from its initial inception will likely lead to increased production costs, unless lengthy and convoluted re-optimisation processes are carried out in order to identify and eliminate these factors.

In light of this, the development of entirely novel media formulations, tailored exclusively for the expansion of MSCs may represent a more promising strategy when moving forward. Unfortunately, the results of such activities to date have remained highly variable and typically lacking when compared to the use of serum. Liu *et al* (2006) for instance, reported the successful growth of umbilical cord-derived MSCs in defined conditions, with maintained tri-lineage differentiation potential and marker expression but saw only one-fiftieth of the fold-expansion demonstrated for similar cells in FBS supplemented medium over nine to ten total subcultures (191). More recently, Wu *et al* (2016) described the culture of UC-MSCs in a novel chemically-defined medium capable of preserving their unique immunomodulatory properties (192). Again however, the associated cell growth was seen to be noticeably poorer than in comparable serum supplemented cultures (192). Even one of the most encouraging investigations in recent years, described by Jung *et al* (2010) is not without its problems. In this study, the researchers developed a novel defined medium formulation capable of facilitating the rapid *in vitro* expansion of MSCs, maintaining their multipotency and even enabling isolation in serum-free conditions (193). Despite these promising results however, it is important to note that this research was conducted exclusively through the use of commercially-sourced cells derived from healthy donors, seriously limiting the applicability of these findings when considering autologous MSC-based therapies. Furthermore, the highly complex nature of the resulting formulation may eliminate any potential cost benefits arising from the use of non-commercial medium.

As with conventional serum-supplemented culture medium, chemically defined medium has also been utilised as a foundation from which to differentiate stem cell populations towards selected lineages for the purposes of tissue replacement. Of particular interest, is the process of chondrogenesis, which has been shown to benefit from induction under serum-free conditions

as a result of the extracellular matrix damage associated with exposure to blood-derived products (194, 195). Finally, it is important to note that the activity of cryopreservation, which has typically relied upon the use of serum, has also been successfully demonstrated under chemically defined conditions. Lopez *et al* (2016), described the cryopreservation of adipose-derived MSCs in a solution comprised of a combination of antioxidants, synthetic polymers and permeating protective agents, with cells retaining their multipotency and karyotypic stability following revival (196).

## 1.5 Methods of media development and supplement screening

As we have seen in the previous sections, the use of chemically-defined xeno-free medium for the expansion, differentiation and cryopreservation of cells is paramount to ensuring the safety, efficacy and cost-effectiveness of advanced MSC-based therapeutics. To date however, the research associated with medium development within this field has seen only limited success, with the most promising formulations having been applied solely to the culture of model cell lines derived from healthy donors, whilst also remaining prohibitively expensive due to their relative complexity. One factor which typically remains undiscussed in regard to this topic, is the choice of screening strategy utilised within the associated studies. In the following sections, we will briefly review the types of statistical approaches that can be utilised when screening supplements for use in culture medium and highlight the respective benefits and shortcomings of each.

### 1.5.1 One-factor-at-a-time screening methods

As their name suggests, one-factor-at-a-time (OFAT) strategies involve examining experimental factors in isolation in a sequential manner and represent the most basic approach that can be applied to supplement screening activities. Whilst their relative simplicity has resulted in countless research groups employing this type of method in the past, the popularity of the OFAT approach has dropped significantly in recent years. The primary reason for this is that OFAT strategies fail to examine interactions between factors and as a result cannot identify potentially significant synergistic relationships amongst screened components (197). In addition, the process of assessing a large number of factors in this way can be both highly time-consuming and, as a direct consequence, extremely expensive.

### 1.5.2 Design of experiments and multifactorial approaches

In response to the issues described above concerning sequential supplement screening, many groups are now utilising Design of Experiments (DoE) or multifactorial statistical approaches during medium development. For instance, so called full factorial experimental designs involve looking at every possible combination of a set of factors and assessing not only their individual contributions to a given outcome but also any combined effects (198). Unfortunately, whilst this specific approach can provide researchers with an incredibly detailed understanding of a given process, the financial and time-related investments involved can be significant. Adding a single additional concentration value (level) and supplement type to a simple two-level two-factor design for example, increases the number of experimental combinations from four to twenty-seven, requiring a massive increase in reagent costs and set-up time for only a small change in strategy. In order to circumvent these concerns, streamlined experimental designs can be employed, such as a Plackett-Burman approach.

Developed by statisticians Robin L. Plackett and J.P. Burman in 1946, the appropriately named Plackett-Burman design, reduces the number of experimental runs or combinations to the absolute minimum required in order to accurately assess the impact of any main effects on an outcome of interest (199). This is achieved by implementing a complex aliasing system that confounds main effects with any associated higher order interactions, resulting in a condensed design (199). As can be expected of such an approach however, higher order interaction effects cannot be resolved, limiting the use of Plackett-Burman designs to settings in which the contribution of such effects is likely negligible. One possible alternative to this type of approach is the application of a fractional-factorial design, which function in a very similar manner but due to their flexibility can be tailored to resolve higher order interactions depending upon the scope of the activities in question. In fact, such designs are most applicable when dealing with relationships for which there is already a level of understanding, making it less likely that researchers will overlook any potential factor interactions and fail to design the associated investigation accordingly. Furthermore, it is important to note that following the use of a fractional factorial, researchers may wish to consider utilising a responsive surface methodology, such as a central composite design (CCD), to more accurately pin-point the optimal factor values required in order to achieve the desired cellular response (200).

### 1.5.3 Computational systems and random global searching

In addition to sequential and multifactorial statistical approaches to component screening, the use of significantly more complex computational methods is also now being explored. One such strategy, is the application of genetic algorithms to medium development. As their name suggests, these models were initially developed as a means of solving optimisation-related problems using concepts borrowed from evolutionary biology (201). Unfortunately, despite promising results in related fields, very few papers have explored the use of these types of systems in the development of chemically-defined culture medium for use with mammalian stem cells (202, 203). This gap is likely a result of the very high skill threshold required in order to produce and properly utilise such models. Whilst it is possible that the multidisciplinary nature of regenerative medicine may in time facilitate the adoption of these techniques, at the present time they remain far too esoteric to see widespread use.

### 1.6 Project overview and aims

The change to chemically defined serum-free culture medium must be explored as early as possible within the typical ATMP developmental process. Despite the substantial advantages associated with this shift, commercially available formulations remain prohibitively expensive, whilst academic research has focused on the use of model cell populations, generating results that may not be applicable to primary autologous MSCs due to their widely varied *in vitro* culture potential (204, 205). Furthermore, many of these media have been built from existing non-MSC formulations or have included a wide range of expensive supplements, limiting both their specificity and cost-effectiveness. Here we developed a new minimal chemically-defined serum-free medium for use in the expansion of primary MSCs, after first demonstrating the impact of serum variability on cell growth and gene expression. In order to develop this medium, a two-step system was utilised. In the first step, a series of fractional factorial screening experiments were performed in order to rapidly assess the ability of various supplements to support MSC metabolism in serum-deprived conditions. In the second step, a full factorial formulation evaluation was performed as a means of understanding the relative contributions of each of the previously selected supplements. Additionally, a set of readily available extracellular matrix proteins were assessed for their ability to support MSC surface

adhesion in serum-free conditions, for use as part of a single complete chemically-defined culture process.

Aims:

1. Evaluate the comparability of primary BM-MSCs isolated from osteoarthritic patients and a model immortalised MSC cell line.
2. Assess the impact of raw material variability on MSC proliferation and gene expression in regard to both foetal bovine and human serum.
3. Begin development of a characterised cytokine-supplemented serum-free medium for use in the expansion of primary MSCs using a Design of Experiments-based methodology.
4. Compare and contrast the characteristics of cells grown in serum-free medium with those cultured in conventional serum-supplemented conditions.
5. Screen a series of extracellular matrix proteins for use in conjunction with the previously described serum-free medium, as a means of better facilitating cell/surface interactions.

## 2 Chapter 2: Materials and methods

### 2.1 Cell culture

#### 2.1.1 Tissue collection and informed consent

All of the human tissue samples processed during the course of this project were handled in accordance with the relevant rules and regulations as laid out in the UK Human Tissue Act 2004, the UK Human Tissue (Quality and Safety for Human Application) Regulations 2007 and the European Directives on Tissues and Cells (2004/23/EC, 2006/17/EC, 2006/86/EC). All related project activities were assessed and approved by the National Research Ethics Committee prior to commencement of the project (IRAS project ID: 166522). Informed consent was gathered for each of the specimens used and collection was carried out in accordance to Newcastle University ethical and technical regulations. Samples were anonymised in such a way as to ensure that those working directly with the material could not identify the individual from whom the tissue was taken, whilst still retaining a high level of obfuscated traceability. It should be noted that due to the limited availability of donor samples, no specific exclusion criteria were applied during the course of this investigation.

#### 2.1.2 Cell culture standards

In order to help reduce the risks of bacterial and fungal contamination, both cell isolation and cell expansion were performed within a sterile class II biological safety cabinet. In addition, all materials and equipment, together with the safety cabinets themselves, were sterilised using a 70% v/v ethanol solution. Cell culture media together with all other non-sterile liquid reagents were filtered through 0.22  $\mu\text{m}$  syringe filters prior to use and all waste liquids, plastic disposables and cells were treated with Virkon (SP Services) before disposal. A suitably high standard of aseptic laboratory technique was maintained throughout the cell culture process, with cultures being routinely checked using an inverted phase contrast microscope. Liquid culture medium and wash buffers were stored at 4 °C and replaced every four weeks in order to minimise the impacts of nutrient degradation and contamination on cell quality. Finally, as a means of protecting cells from the potentially negative effects of cold-induced and pH-induced stress, culture flasks were only removed from the incubators when absolutely necessary and all liquid reagents warmed to 37 °C in a water bath prior to use.

### 2.1.3 Primary cell isolation

Human BM-MSCs were isolated based on a modified version of the method first described by Pittenger *et al* (1999) and then later used by groups such as Mareschi *et al* (2012) (210, 211). MSCs were separated out based upon a combination of density-based centrifugation and their plastic adherent nature, with figure 2.1 providing an overview of the isolation process.

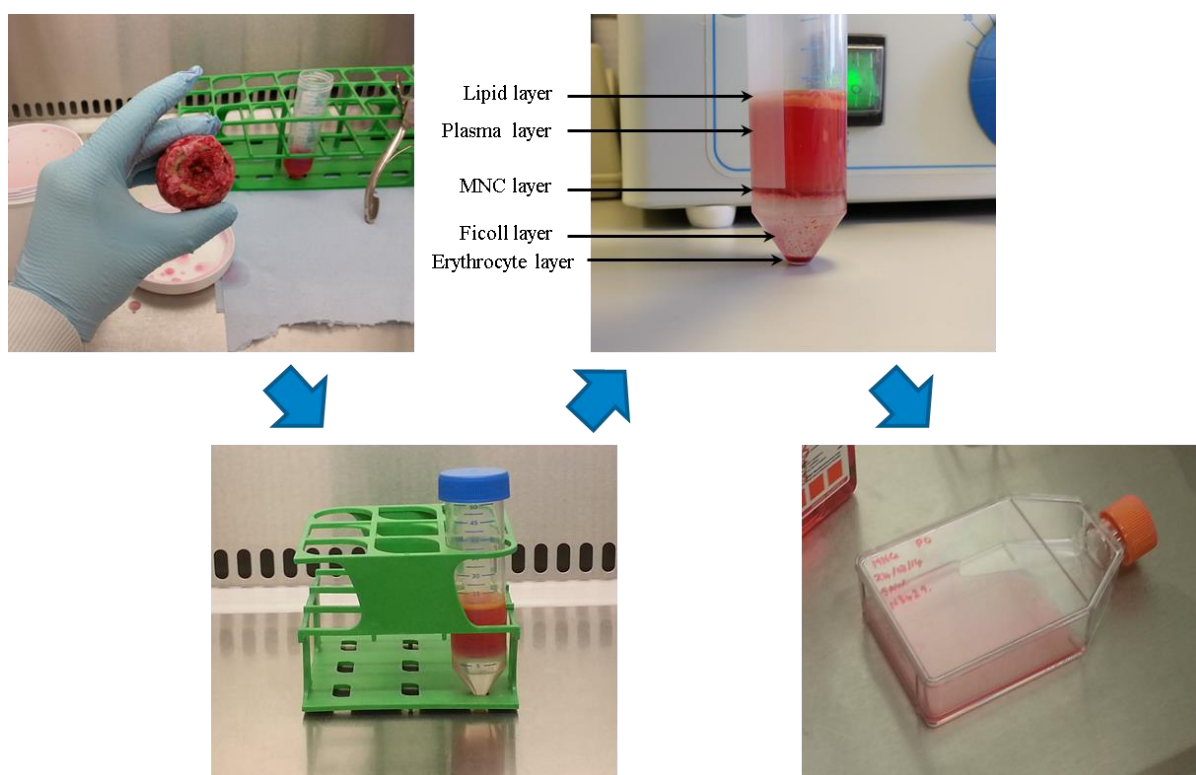


**Figure 2.1 The hBM-MSC isolation process**

The process begins with trabecular bone removal and washing (a), followed by suspension on top of Ficoll-Paque centrifugation solution (b). After centrifugation a clear pattern of banding can be seen, with the MNC band residing between the plasma and ficoll layers (c). The MNC layer is then removed, washed in a dedicated buffer, resuspended in cell culture medium and seeded in a T-75 culture flask.

To begin with, trabecular bone was removed from the neck of the femur and the inside of the femoral head, washed in 10 mL of unsupplemented MSC culture medium (as per table 2.1 without the inclusion of FGF-2) and filtered in order to help remove any contaminating bone fragments or connective tissue from the resultant cell solution. The filtered bone wash was then suspended upon 10 mL of Ficoll-Paque Premium 1.073 (GE Healthcare Life Sciences)

centrifugation solution and centrifuged for 40 mins at 800 x g. Following centrifugation, the MNC layer was removed and resuspended in a solution of 5 mM ethylenediaminetetraacetic acid (EDTA, Sigma) and 0.2% w/v bovine serum albumin (BSA, Sigma); henceforth referred to as MSC wash buffer, before again being centrifuged at 800 x g at room temperature for 10 minutes. Finally, the resultant supernatant was aspirated away, the cell pellet resuspended in unsupplemented MSC culture medium and the cell solution seeded into a plastic T-75 tissue culture flask (see 2.1.4). The flask was then placed into an incubator at 37 °C and 5% CO<sub>2</sub> for two days. Following this two day period, the culture medium within the flask was aspirated away, the flask surface washed twice with sterile Dulbecco's phosphate buffered saline (DPBS, Sigma) and the unsupplemented culture medium replaced.

It is important to note that due to the propensity for hBM-MSCs to form tightly grouped colonies immediately following isolation, a single 'lift and re-seed' step was commonly included within the initial culture period in order to help redistribute the cells and prevent non-specific differentiation. This process was performed in much the same manner as the passage procedure detailed below in section 2.1.4, with the exception that the cells were re-seeded into a single flask following trypsinization rather than being spread across multiple flasks. Additionally, the culture medium applied to the cells following this 'lift and re-seed' process was supplemented with FGF-2,(Peprotech) as per table 2.1.

#### 2.1.4 Primary cell expansion

hBM-MSCs were cultured across a range of different sizes of Corning® vent capped tissue culture-treated flasks (Sigma) as appropriate, most commonly including the 75 cm<sup>2</sup> (T-75) variant whenever possible. Cells were expanded in normoxic conditions at 37 °C and 5% CO<sub>2</sub>, using the standard MSC culture medium detailed below in table 2.1. The culture medium within each of the flasks was replaced every 2 to 3 days in order to ensure maximum nutrient availability.

Components	Quantity/Concentration	Supplier
DMEM (low glucose/1x10 <sup>4</sup> mg/mL)	Dependant on volume	Sigma
Heat-treated batch-tested FBS	10% v/v	Life Technologies
GlutaMax (200mM)	1% v/v	Life Technologies
Penicillin-Streptomycin (10,000 U/mL)	1% v/v	Life Technologies
Fibroblast Growth Factor-2 (FGF-2)	8 ng/mL	Peprtech

**Table 2.1 Standard MSC culture medium composition**

It should be noted that the FBS used to produce this medium, which was utilised in all subsequent experimental activities, was designated 'FBS 1' during the FBS variability assessment detailed in Chapter 4.

Upon reaching between 70% and 80% confluence, the cell monolayers were subjected to substrate dissociation and re-seeding; henceforth referred to as cell passage or subculture. It should be noted that when exceeding 85% confluence MSCs have been observed to undergo osteogenic priming, taking on a distinctly altered morphological appearance. As a direct result of this phenomenon, all cell cultures were regularly checked through visual assessment as a means of ensuring that the aforementioned 80% confluence threshold was not exceeded. This was performed using a 0.5 g/L trypsin and 0.2 g/L EDTA solution (Sigma), which acts to disrupt integrin-mediated cell-substrate associations. Initially, the culture medium was aspirated away from the flasks and the cells washed with sterile DPBS. Next, trypsin/EDTA solution was applied to the flasks at a volume of 0.5 mL per 25 cm<sup>2</sup> of total culture area. The cells were then incubated for 3 to 4 minutes, cell detachment verified using an inverted light microscope and the trypsin/EDTA solution neutralised using an excess volume of standard MSC culture medium. The resultant cell solution was then centrifuged at 1200 rpm for 5 minutes before being resuspended in 30 mL of culture medium and split across three new T-75 tissue culture-treated flasks

#### 2.1.5 Primary cell cryopreservation and recovery

In order to ensure the long term preservation of isolated hBM-MSCs, a cryoprotectant solution made up of heat-treated FBS and 10% v/v dimethyl sulfoxide (DMSO, Sigma); henceforth referred to as freezing medium, was applied to cells immediately prior to cryopreservation.

To begin the process, cells were first passaged and then resuspended within chilled freezing medium at a density of  $1 \times 10^6$  cells per mL, before being decanted into 1.2 mL Corning® cryogenic vials (Sigma). The vials were then cooled overnight at a controlled rate of approximately 1 °C/minute using an isopropyl alcohol-filled Mr. Frosty™ freezing container (ThermoFisher Scientific) stored at -80 °C. Following this time, the vials were transferred to liquid nitrogen for long-term storage and their details logged in an associated paper-based cataloguing system.

Since DMSO has been shown to have significant cytotoxic effects, cell recovery was performed as rapidly as possible. The contents of the previously frozen vials were allowed to partially thaw whilst stored on ice, before being resuspended in 9 mL of standard MSC culture medium. The resultant cell suspensions were then centrifuged at 1200 rpm for 5 mins, the cell pellets resuspended in 10 mL of standard MSC culture medium and finally seeded into a single T-75 tissue culture flask. The flasks were then incubated in standard culture conditions for 2 days, before the resulting cell monolayers were washed twice with sterile DPBS and the culture medium replaced.

#### 2.1.6 Cell line donation and culture

Telomerase (hTERT) immortalised human MSCs, henceforth referred to as Y201s, were kindly donated by Dr Paul Genever of the University of York Department Of Biology. These cells, which have been shown to have consistent morphological and phenotypic characteristics even after extended periods of expansion, were utilised in the current investigation as a representative and readily available benchmark with which to compare the responses of primary patient-derived MSCs.

The expansion, passage, cryopreservation and thawing practices associated with the Y201 cells were the same as those described for the primary hBM-MSCs in sections 2.1.4 and 2.1.5, with one noteworthy exception. Due to their rapid rate of growth, the culture medium used to expand the Y201 cell line was not supplemented with FGF-2 but was otherwise identical to the formulation given in table 2.1.

## 2.2 Quantification of cell number and metabolic activity

### 2.2.1 Haemocytometer-based cell counting

Manual cell enumeration was performed using a standard Neubauer haemocytometer, with two identical 20  $\mu\text{L}$  counting chambers. Cells were counted whilst in suspension immediately following removal from their substrate via the use of trypsin (see 2.1.4), either as part of the regular passaging process or as part of a cell seeding exercise. The haemocytometer's two counting surfaces were divided into 16 large squares, each of which was further subdivided into 16 smaller squares. Cell number was first determined by counting the amount of cells present within each of the 4 large corner squares of a single chamber and dividing that number by the number of squares counted. This average 'per large square' value was then divided by 2 and multiplied by  $1 \times 10^4$  in order to calculate the total number of cells per millilitre of solution. The requirement to divide the average number of cells per large square by 2 and then multiply by  $1 \times 10^4$  was derived directly from the dimensions of the larger haemocytometer squares themselves, which hold a total volume of  $2 \times 10^{-4}$  mL ( $0.1 \text{ cm} \times 0.1 \text{ cm} \times 0.02 \text{ cm}$ ). This entire counting process was then repeated for the second chamber and an average of the two 'per millilitre' values used as the final estimate.

In addition to simply counting cells, this haemocytometer-based process was also used to quickly assess the viability of cells when necessary. In order to do this, samples of the cell suspension were mixed 1:1 with a 0.25% v/v solution of trypan blue (Sigma) in DPBS before being loaded into the chambers. Cells seen to be stained blue were considered dead or irreparably damaged and hence discounted from the enumeration process.

### 2.2.2 MTT assay

In section 5.3.1, the metabolic activity of hBM-MSCs seeded into 24-well plates at a density of  $2.5 \times 10^3$  cells per  $\text{cm}^2$  was determined using an MTT assay. In order to perform the assay, thiazolyl blue tetrazolium bromide powder (MTT, Sigma) was added to standard culture medium at a concentration of 0.5 mg/mL and the mixture sterile filtered using a  $0.22 \mu\text{m}$  filter attached to an appropriately sized syringe. The sterile MTT solution was then applied directly to the cell monolayers at a volume of 500  $\mu\text{L}$  per well. The plates were then incubated at  $37 \text{ }^\circ\text{C}$  in 5%  $\text{CO}_2$  for 2 hours, before the MTT solution was removed and the cells washed twice in

DPBS. Undiluted DMSO was then applied to the cells in order to lyse them, releasing any formazan present within the cytoplasm. The plates were then returned to the incubator for 20 minutes in order to ensure complete cell lysis and homogeneous dispersal of the formazan throughout the resultant solution. 200  $\mu$ L samples of the DMSO solubilised formazan were then transferred to a transparent 96-well plate and the absorbance of the samples measured at 570 nm using a Sunrise™ 96-well plate reader (Tecan). It should be noted that the absorbance values resulting from these analyses were normalised to DMSO-background controls prior to evaluation. Additionally, it should also be remarked that during each of the described incubation periods, the MTT and solubilised formazan solutions were shielded from unnecessary exposure to light due to their high level of sensitivity.

### 2.2.3 PrestoBlue assay

In sections 4.3.1 and 5.3.3, the metabolic activity of hBM-MSCs and Y201s seeded into 24-well plates at a density of  $2.5 \times 10^3$  cells per  $\text{cm}^2$  was determined using a PrestoBlue® assay. The assay was performed by first mixing the pre-made PrestoBlue® solution (Sigma) 1:10 with standard MSC culture medium as per the manufactures instructions. The cell monolayers were then washed using DPBS and the reagent mixture applied at a volume of 300  $\mu$ L per well. The well plates were then wrapped in tin foil as a means of protecting the light sensitive PrestoBlue® reagent from unnecessary exposure and incubated for 2 hours at 37 °C and 5% CO<sub>2</sub>. Following incubation, 200  $\mu$ L samples of the PrestoBlue® mixture were taken from each of the wells and transferred to a transparent 96-well plate for assessment. This was done using an LS 50 B luminescence spectrometer (Perkin Elmer) with excitation and emission wavelengths of 560 nm and 590 nm respectively.

### 2.2.4 PicoGreen assay

A Quant-iT™ PicoGreen® dsDNA assay (ThermoFisher Scientific) was used in order to quantify cell number following PrestoBlue® metabolic assessment in sections 4.3.1 and 5.3.3. In addition, the assay was also used independently in section 7.3.4 as a means of cell enumeration. Initially, cells seeded into 24-well plates at a density of  $2.5 \times 10^3$  cells per  $\text{cm}^2$  were lysed using a standard freeze-thaw methodology. In brief, the cell monolayers were

washed twice with DPBS and 300  $\mu$ L of DNase-free water (Sigma) added to each of them. The plates were then stored at  $-80^{\circ}\text{C}$  for a minimum of 1 hour in order to fully freeze the liquid in each of the wells. Next the cells were rapidly thawed in an incubator at  $37^{\circ}\text{C}$ ; completing a single freeze/thaw cycle. Finally, the plates were subjected to two more freeze/thaw cycles in order to ensure complete cell lysis within each of the wells.

During the final sample thaw, the PicoGreen® reagent and associated buffers were prepared according to the manufacturer's instructions. To begin with, an appropriate amount of TE buffer was prepared by diluting the x20 concentrated buffer mixture provided in the assay kit 1:20 in sterile DPBS. This buffer was then used to dilute the PicoGreen® reagent 1:200 to create a working solution of the dye. Both the TE buffer and PicoGreen® mixture were kept on ice until needed, with the PicoGreen® mixture being shielded from any unnecessary exposure to light given its high level of sensitivity. Immediately following lysis, 100  $\mu$ L samples of the cell lysate were transferred into white opaque-walled 96-well plates, after which 100  $\mu$ L of the diluted PicoGreen® mixture was also added. The plates were then allowed to sit on ice for 5 minutes, before being read using a FLUOstar OPTIMA fluorescent spectrometer (BMG LABTECH) at excitation and emission wavelengths of 480 nm and 520 nm respectively.

It should be noted that standard curves were produced for both the primary hBM-MSCs and the Y201 cell line, using cells seeded at known concentrations of  $1.25 \times 10^3$ ,  $2.5 \times 10^3$ ,  $5 \times 10^3$ ,  $1 \times 10^4$ ,  $2 \times 10^4$  and  $4 \times 10^4$ . In all cases appropriate control conditions were included within each of the plates as a means of measuring background fluorescence levels. Instrument gain was manually set using the most densely seeded samples taken from the standard curve plates and kept constant throughout the course of the investigation.

### 2.2.5 Alkaline phosphatase activity assay

Alkaline phosphatase (ALP) activity was determined using a p-nitrophenyl phosphate (pNPP) liquid substrate system (Sigma). Cells seeded into 24-well plates at a density of  $2.5 \times 10^3$  cells per  $\text{cm}^2$  were washed in DPBS and fixed using a pre-warmed 4% w/v paraformaldehyde (PFA, Sigma) solution in DPBS for 20 minutes at room temperature. The PFA solution was then removed, the samples washed again using DPBS and incubated for a further 10 minutes in 0.1 M TRIS (Sigma) buffered DPBS. Following this 10 minute period, the samples were again washed in DPBS and 250  $\mu$ L of undiluted pNPP added to each well. The plates were wrapped

in tin foil to protect the light sensitive pNPP reagent from unwanted exposure and incubated at 37 °C for 15 minutes. 200 µL samples were then taken from each of the wells and transferred into an appropriate number of transparent 96-well plates, which were measured for absorbance at 405nm using a Sunrise™ 96-well plate reader. All sample plates were run alongside appropriate background absorbance controls and normalised to cell number, which was determined using the PicoGreen® assay described in section 2.2.3.

## 2.3 Directed tri-lineage differentiation

### 2.3.1 Osteogenic differentiation

The osteogenic differentiation process began by seeding either hBM-MSCs or Y201s at a density of  $4 \times 10^4$  cells per well across an appropriate number of tissue culture-treated 24-well plates, using the supplemented osteogenic differentiation medium described below in table 2.2. It should be noted that the cells were allowed to reach over 90% confluence on their previous substrate prior to seeding, as a means of priming them for osteogenic differentiation. Following this initial seeding process, the cells continued to be cultured for a further 14 days at 37 °C and 5% CO<sub>2</sub>. Their medium was replaced every 3 days with fresh osteogenic differentiation medium, based upon a formulation by Wang *et al* (2016), and the cells regularly observed for any apparent morphological changes (212).

Components	Quantity/Concentration	Supplier
DMEM (low glucose)	Dependant on volume	Sigma
Foetal bovine serum	10% v/v	Life Technologies
GlutaMax (200mM)	1% v/v	Life Technologies
Penicillin-Streptomycin (10,000 U/mL)	1% v/v	Life Technologies
Dexamethasone	100 nM	Sigma
B-Glycerophosphate disodium salt hydrate	10 mM	Sigma
L-Ascorbic acid	50 µg/mL	Sigma

**Table 2.2 Osteogenic medium composition**

### 2.3.2 Chondrogenic differentiation

Chondrogenic differentiation was performed using a combination of pellet-cultured cells and a supplemented medium formulation based on the composition described by Meretoja *et al* (2012) (213). To begin with, either hBM-MSCs or Y201s were pelleted across an appropriate number of V-bottomed 96-well plates (Sigma) at a density of  $2 \times 10^5$  cells per well. The cells were both seeded and then subsequently cultured using the chondrogenic differentiation medium detailed in table 2.3. The culture process proceeded for 14 days at 37 °C and 5% CO<sub>2</sub>, with medium changes being conducted every 3 days.

Components	Quantity/Concentration	Supplier
DMEM (high glucose/ $4.5 \times 10^4$ mg/mL)	Dependant on volume	Sigma
GlutaMax (200mM)	1% v/v	Life Technologies
Penicillin-Streptomycin (10,000 U/mL)	1% v/v	Life Technologies
Dexamethasone	100 nM	Sigma
L-Ascorbic acid	50 µg/mL	Sigma
Proline	40 µg/mL	Sigma
Transforming growth factor beta-3	10 ng/mL	Peprotech
Insulin Transferrin Selenium (ITS)	1% v/v	Sigma

**Table 2.3 Chondrogenic medium formulation**

### 2.3.3 Adipogenic differentiation

The adipogenic differentiation process followed a similar methodology to that of the osteogenic differentiation procedure described above in section 2.3.1. Cells were seeded into tissue culture-treated 24-well plates at a density of  $4 \times 10^4$  cells per well. The cells were then cultured for 14 days at 37 °C and 5% CO<sub>2</sub> using the adipogenic differentiation medium detailed in table 2.4, which is based upon the formulation first published by Neubauer *et al* (2004) (214). Medium changes were performed every 3 days, alongside regular cell morphology checks.

Components	Quantity/Concentration	Supplier
DMEM (low glucose)	Dependant on volume	Sigma
Foetal bovine serum	10% v/v	Life Technologies
GlutaMax (200mM)	1% v/v	Life Technologies
Penicillin-Streptomycin (10,000 U/mL)	1% v/v	Life Technologies
Dexamethasone	1 $\mu$ M	Sigma
Insulin	10 $\mu$ g/mL	Sigma
Indomethacin	60 $\mu$ M	Sigma
3-isobutyl-1-methylxanthine (IBMX)	50 $\mu$ g/mL	Sigma

**Table 2.4 Adipogenic medium composition**

## 2.4 Flow cytometry

### 2.4.1 Cell staining and cytometric analysis

Flow cytometry was utilised in sections 3.3.3, 3.3.4, 4.3.4 and 6.3.4 in order to characterise the surface marker profiles of the cells described there. To begin the staining and flow cytometry procedure, cells were manually counted (see 2.2.1) immediately following trypsinization (see 2.1.4), with  $3 \times 10^4$  cells being added to each of an appropriate number of Corning® Falcon® Round-bottom polystyrene tubes (Sigma). The cells were then washed in 1 mL of FACS buffer, made up of a sterile filtered solution of 1 mM EDTA and 10% v/v FBS in DPBS. It should be noted that following centrifugation, the liquid supernatant in the tubes was quickly tipped off rather than being aspirated away, due to the round-bottomed nature of the tubes offering no protection to any resultant cell pellet.

Next, the cells were resuspended in 50  $\mu$ L of FACS buffer and the required amounts of both the isotype or test antibodies added to each of the appropriate tubes, in accordance with the details given below in tables 2.5 and 2.6. The tubes were then wrapped in tin foil due to the light sensitivity of the fluorescent molecules and stored at 4 °C for 15 minutes. Following refrigeration, the cells were washed in 200  $\mu$ L of FACS buffer, resuspended in 400  $\mu$ L of FACS buffer, wrapped in tin foil and stored in the fridge until required. Immediately before the tubes were taken to the flow cytometer, 50  $\mu$ L of a 10  $\mu$ g/mL 4',6-Diamidino-2-phenylindole dihydrochloride (DAPI, Sigma) solution was added to each of them. A FACSCanto II (BD

Biosciences) flow cytometer was used to analyse all of the samples, with the associated excitation wavelengths and emission filter values for each of the fluorochromes being given in table 2.7.

<b>Fluorochrome-Antibody name</b>	<b>Volume</b>	<b>Supplier</b>
PE-migG1	1 $\mu$ L	BD Biosciences
APC-migG1	16 $\mu$ L	BD Biosciences
FITC-migG1	4 $\mu$ L	BD Biosciences
FITC-migG2b	2 $\mu$ L	BD Biosciences
PerCP Cy5.5-migG1	8 $\mu$ L	BD Biosciences
APC-H7-migG2a	1 $\mu$ L	BD Biosciences

**Table 2.5 Isotype control antibody list**

<b>Fluorochrome-Antibody name</b>	<b>Volume</b>	<b>Supplier</b>
PE-CD73	4 $\mu$ L	BD Biosciences
APC-CD105	2 $\mu$ L	BD Biosciences
FITC-CD14	4 $\mu$ L	BD Biosciences
FITC-CD19	4 $\mu$ L	BD Biosciences
FITC-CD34	4 $\mu$ L	BD Biosciences
FITC-CD45	4 $\mu$ L	BD Biosciences
PerCP Cy5.5-CD90	2 $\mu$ L	BD Biosciences
APC-H7-HLA-DR	4 $\mu$ L	BD Biosciences

**Table 2.6 Test condition antibody list**

Fluorochrome name	Excitation wavelength	Emission filter values
PE	488 nm	585/42 nm
APC	635 nm	660/20 nm
FITC	488 nm	530/30 nm
PerCP Cy5.5	488 nm	670/LP nm
APC-H7	635 nm	780/60 nm
DAPI	405 nm	450/50 nm

**Table 2.7 Fluorochrome excitation and emission filter wavelength values**

Emission band pass (BP) filter wavelengths are displayed alongside their respective tolerance limits. The filter associated with PerCP Cy5.5 is labelled as long pass (LP) and permits all wavelengths above the listed value.

Alongside the test and isotype runs, which were produced for each individual experimental condition, a single set of compensation controls was also created. These control tubes were produced in the same manner as the test and isotype runs, with two primary exceptions. Firstly, cells were not employed in these runs, with positive and negative compensation beads (BD Sciences) being used in their place at a volume of one drop each per tube in accordance with the manufacturer's instructions. Secondly, the beads were individually stained for each of the markers, as opposed to being simultaneously stained, as were the test and isotype samples. Table 2.8 below provides details of the staining procedure used for the single-stained compensation controls.

Fluorochrome-Antibody name	Volume	Supplier
Unstained cells	N/A	N/A
PE-CD73	4 $\mu$ L	BD Biosciences
APC-CD105	4 $\mu$ L	BD Biosciences
FITC-CD45	4 $\mu$ L	BD Biosciences
PerCP Cy5.5-CD90	4 $\mu$ L	BD Biosciences
APC-H7-HLA-DR	4 $\mu$ L	BD Biosciences

**Table 2.8 Compensation control and voltage calibration antibody list**

Lastly, it is important to note that in order to initially calibrate the flow cytometer amplification voltages, a set of single stained primary hBM-MSCs and single stained Y201s were utilised. Again this process followed the same protocol as for the isotype and test conditions but with the cells again being stained with a single antibody per tube, as described in table 2.8. Unlike the isotype and compensation controls, the single stained voltage calibration runs were performed only once over the entire course of the investigation due to the relative stability of the flow cytometer's settings. All data analysis was performed using the Flowing Software® flow cytometry data analysis software.

#### 2.4.2 Assessing the impact of FGF-2 supplementation on surface marker expression

In section 3.3.4 as part of the cell characterisation process, the impact of FGF-2 supplementation on the surface marker profile of hBM-MSCs was assessed using flow cytometry. Upon reaching 80% confluence following isolation (see 2.1.3), passage 0 cells were trypsinized and manually counted according to the instructions given in sections 2.1.4 and 2.2.1 respectively. As per section 2.4.1, samples of these cell populations were taken and their surface marker profiles assessed using flow cytometry. The remaining cells were re-seeded across two new T-75 flasks, one of which contained standard MSC culture medium complete with 8 ng/mL of FGF-2 (see table 2.1), whilst the other contained this same medium without the supplementary cytokine. The cells were then cultured for 6 days, with a single medium change being performed half way through this process. Following the 6 day period, the cells in both the FGF-2 supplemented and unsupplemented conditions were again trypsinized and manually counted, before being assessed using flow cytometry. The remaining FGF-2 supplemented cells were then re-seeded across two new T-75 flasks, one of which continued to be treated with the supplemented medium, while the other contained unsupplemented medium only. These cells were then cultured for a further 6 days in the same manner as the previous culture step, before being trypsinized, manually counted and assessed using flow cytometry one final time. An overview of the culture process is given below in figure 2.2.

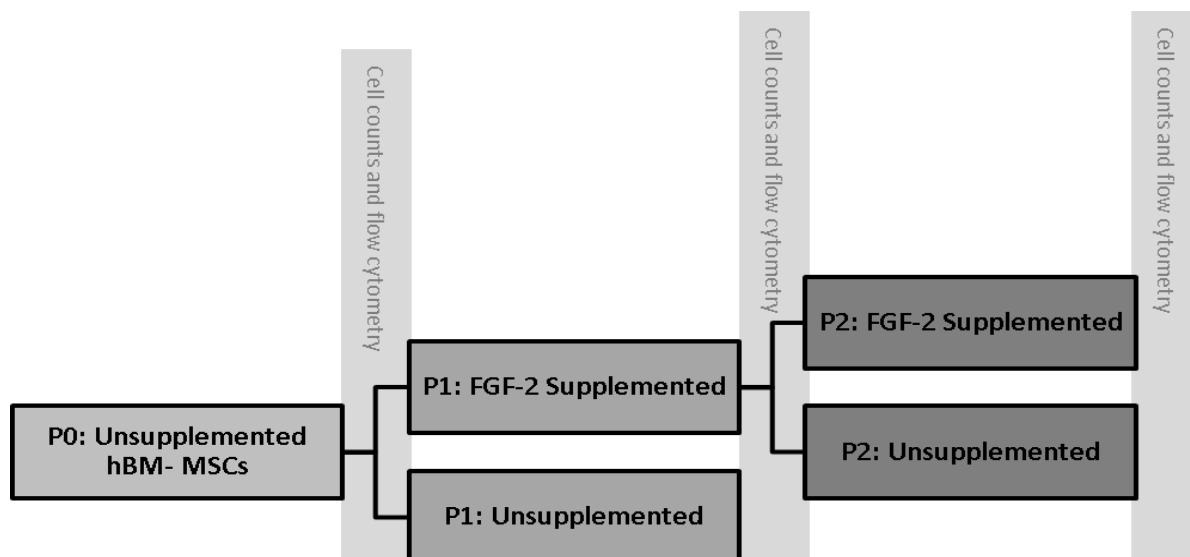


**Figure 2.2 Culture process used in assessing the impact of FGF-2 supplementation on surface marker profile**

Upon either reaching 80% confluence or following 6 days in culture, samples from each of the cell populations were manually counted and assessed using flow cytometry. Unsupplemented P1 cells were not re-seeded following sample collection due to the poor growth seen in these populations.

### 2.4.3 Identifying endothelial marker expression

In section 6.3.4, hBM-MSCs and Y201s were assessed in regard to their expression of the endothelial surface marker CD31 in addition to the markers given in table 2.6. With the exception of the use of 4  $\mu$ L of FITC-conjugated CD31 (BD Biosciences) in each of the test conditions, the assay was performed precisely as described in section 2.4.1.

## 2.5 Cell staining procedures

### 2.5.1 Cytoskeletal staining

In sections 4.3.2 and 7.3.4 hBM-MSCs and Y201s were subject to cytoskeletal staining using a combination of Fluorescein Isothiocyanate-labelled Phalloidin (Sigma) and DAPI. To begin with, cells seeded into 24-well plates at a density of  $5 \times 10^3$  cells per  $\text{cm}^2$  were fixed using a 4% PFA solution in DPBS for 20 minutes at room temperature. Prior to staining, the fixed cell

monolayers were washed twice with a 0.1% v/v solution of tween-20 (Sigma) in DPBS. Next, a 0.1% v/v solution of Fluorescein Isothiocyanate-labelled Phalloidin in DPBS was applied to the cells at a volume of 250  $\mu$ L per well, the plates covered in tin foil and the samples left to sit at room temperature for 1 hour. Following this time, the cells were washed twice, again using the 0.1 % v/v solution of tween-20 in DPBS. Next, 250  $\mu$ L of a 1  $\mu$ g/mL solution of DAPI in DPBS was applied to each of the wells, the plates covered in tin foil and the samples left to sit at room temperature for 15 minutes. The cells were then washed twice using a 0.1% v/v solution of tween-20 in DPBS and covered in 1 mL of DPBS for storage. Finally, the cells were imaged using a Nikon TiE fluorescence wide-field inverted microscope. Images were taken from ten randomly selected points across the surface of each well and analysed using the procedure described in section 2.5.6.

### 2.5.2 Acetylated low density lipoprotein uptake assay

Cells grown in tissue culture-treated 24-well plates were incubated with 10  $\mu$ g/mL of DiI-complexed acetylated low density lipoprotein (DiI-acLDL, ThermoFisher Scientific) in standard culture medium (see 2.1.4) for 4 hours at 37 °C and 5% CO<sub>2</sub>. The plates were wrapped in tin foil during incubation due to the sensitivity of the fluorescent compound. Following incubation, the medium was removed from each of the wells, the cells washed twice with DPBS and fixed using a 4% v/v PFA solution for 20 minutes at room temperature. As with the staining process, the plates were again wrapped in tin foil during fixation. Finally, 1 mL of DPBS was added to each of the wells and the cells imaged using a Nikon TiE fluorescence wide-field inverted microscope.

### 2.5.3 Staining for osteogenic differentiation

Cells undergoing osteogenic differentiation as a result of the methodology detailed in section 2.3.1 were identified using Alizarin Red-S histological staining. The plated cells and associated controls were fixed using a 4% PFA solution for 20 minutes at room temperature following the described 14 day culture period. A working solution of the stain was prepared by dissolving 2 g of Alizarin Red-S (Sigma) into 100 mL of dH<sub>2</sub>O, before adjusting the pH to between 4.1 and 4.3 using hydrochloric acid (HCL). To begin the staining process, the cell monolayers were

washed twice using DPBS and 250  $\mu$ L of the 2% v/v Alizarin Red-S solution added to each of the wells. It should be noted that this solution was filtered through a 0.22  $\mu$ m polyethersulphone (PES) syringe filter (Sigma) prior to use. The plates were then wrapped in tin foil and incubated at room temperature for 10 minutes. Following incubation, the excess stain was removed from the wells, the cell monolayers washed thoroughly using dH<sub>2</sub>O and then each of them covered in 0.5 mL of DPBS. The cells were imaged using a Nikon TiE fluorescence wide-field inverted microscope in phase-contrast mode.

#### 2.5.4 Staining for chondrogenic differentiation

In order to identify cells undergoing chondrogenesis as a result of the differentiation procedure described in section 2.3.2, histological staining of pellet sections was performed using Toluidine Blue. The cell pellets were fixed overnight in a 10% formalin solution (Sigma), after being carefully washed using DPBS. The formalin solution was then removed from the plates and the pellets again washed in DPBS. Next, the pellets were incubated up through a series of graduated ethanol solutions, namely 25%, 50% and finally 75% v/v in dH<sub>2</sub>O. Each of the pellets was then removed from its well, wrapped in lint-free tissue paper, dipped in a 70% v/v ethanol solution, loaded into an appropriately labelled tissue cassette and stored in 70% v/v ethanol. The prepared cell pellets were then embedded in paraffin, sectioned at a thickness of 4  $\mu$ m and attached to pre-charged VFM twinfrost microscope slides (CellPath). It should be noted that the aforementioned embedding and sectioning processes were undertaken by the staff at the Newcastle University Biobank service.

Toluidine Blue staining was performed by first deparaffinising the pellet sections in a 100% v/v xylene solution for 4 minutes, followed by rehydration through a series of graded ethanol solutions for 2 minutes each. These solutions ranged from 100% v/v down to 50% v/v in increments of 10% and included a final dH<sub>2</sub>O hydration step. Next the sections were immersed in a 0.1% w/v solution of Toluidine Blue in dH<sub>2</sub>O for 10 minutes. The sections were then washed thoroughly using dH<sub>2</sub>O and quickly dehydrated by being dipped 10 times each in a 95% v/v and then a 100% v/v ethanol solution. Finally, the sections were immersed briefly in a 100% v/v xylene solution in order to complete the dehydration process and a coverslip mounted to each of them using Fluoroshield™ mounting medium (Sigma). The cells were imaged using a Nikon TiE fluorescence wide-field inverted microscope in phase-contrast mode.

### 2.5.5 Staining for adipogenic differentiation

Oil Red-O histological staining was used to identify adipogenesis in cells differentiated according to the methodology described in section 2.3.3. Immediately following the 14 day differentiation process, the plated cells and associated controls were fixed using a 4% PFA solution for 20 minutes at room temperature. A working Oil Red-O solution was prepared by mixing 30 mL of Oil Red-O (Sigma) with 20 mL of dH<sub>2</sub>O. The solution was then allowed to sit for 10 minutes at room temperature before being filtered. The previously fixed cells were washed twice using dH<sub>2</sub>O and incubated for 5 minutes in a 60% v/v isopropanol (Sigma) solution. The isopropanol was then aspirated away, 250 µL of the working Oil Red-O solution added to each of the wells and the plates left at room temperature for 10 minutes. Next, the excess Oil Red-O stain was removed and the cells again washed using 60% isopropanol. Finally, the cells were rinsed thoroughly in distilled water, before 0.5 mL of DPBS was added to each of the wells and the cells imaged using a Nikon TiE fluorescence wide field inverted microscope in phase-contrast mode.

### 2.5.6 Automated image analysis

Images produced according to the methodology detailed in section 2.5.1 were analysed using the built-in functions of the Nikon NIS Elements AR software. The DAPI-stained nuclei in each image were counted using bright-spot detection, whilst a combination of threshold and local-contrast pre-processing were used to accurately determine the FITC-stained area present within each image. A measure of the FITC-stained area per cell was then calculated by dividing the FITC-stained area for a given image by the associated number of nuclei.

## 2.6 RNA extraction and gene expression analysis

### 2.6.1 RNA extraction

Cell lysis and subsequent ribonucleic acid (RNA) extraction were performed using QIAshredder homogenizer columns (Qiagen) and RNeasy® Minikits (Qiagen) respectively. Due the inherent compatibility of the homogenizer and extraction columns, both processes

were performed together in accordance with their shared manufacturer's instructions. In order to begin the process, an appropriate amount of the supplied Buffer RLT lysis solution and Buffer RPE solution were prepared through the addition of 10  $\mu\text{L}/\text{mL}$  of  $\beta$ -mercaptoethanol ( $\beta$ -ME) and 4 volumes of ethanol respectively. The cells were then trypsinized (see 2.1.4) and manually counted (see 2.2.1). Approximately  $1.5 \times 10^5$  to  $2 \times 10^5$  cells were used per sample whenever possible, while for smaller or less proliferative samples, the entire cell population was used whenever necessary. After being harvested, the cells were then lysed through the addition of 350  $\mu\text{L}$  of the previously prepared Buffer RLT solution, which was then gently mixed in order to help disrupt the cells, before being transferred to a QIAshredder column and centrifuged for 2 minutes at full speed in a micro-centrifuge.

Immediately following lysis, 350  $\mu\text{L}$  of a 70% v/v ethanol solution was added to each of the lysate samples, the samples were then mixed well via pipetting and transferred in their entirety to a set of RNeasy® spin columns, each located within their own individual 2 mL collection tube. The columns were then centrifuged at 10000 x g for 15 seconds and the flow-through discarded. Next, the columns were subjected to a series of three individual wash steps, the first two of which again required centrifugation at 10000 x g for a further 15 seconds following the addition of 700  $\mu\text{L}$  of the supplied Buffer RW1 solution and 500  $\mu\text{L}$  of the previously prepared Buffer RPE solution respectively. The third wash step again saw 500  $\mu\text{L}$  of the Buffer RPE solution being added to each of the columns, before the samples were centrifuged for 2 minutes at 10000 x g. Flow-through was discarded after each of the previously detailed wash steps.

Next the columns were transferred to a new set of 2 mL collection tubes and centrifuged at full speed for 1 minute in order to dry the column membranes. Finally, the columns were transferred once more, this time to a set of 1.5 mL collection tubes and any associated RNA eluted. This was done by adding 30  $\mu\text{L}$  of the supplied RNase-free water directly to the column membranes, before centrifuging them for 1 minute at 10000 x g. The column itself was then discarded and the quality of the resultant RNA-rich water solution evaluated using the methodology described below in section 2.6.2.

## 2.6.2 RNA quality assessment

The RNA solutions produced using the extraction procedure described in section 2.6.1 were evaluated using a NanoDrop 1000 spectrophotometer (Thermo Scientific). In order to perform

the analysis, a 20  $\mu\text{L}$  sample of RNA solution was loaded onto the NanoDrop after the machine had first been 'blanked' using a 20  $\mu\text{L}$  sample of RNase-free water (Sigma). The equipment was wiped clean with lint-free tissue paper and again 'blanked' to RNase-free water between each sample. In the event that a given sample contained too high a concentration of RNA for use in genetic characterisation, the solution would be diluted as required with RNase-free water and assessed again. Following evaluation, the RNA samples were stored in appropriately labelled 0.5 mL tubes at  $-80\text{ }^{\circ}\text{C}$  until required.

### 2.6.3 NanoString nCounter gene expression analysis

All of the NanoString nCounter<sup>®</sup> data presented in sections 4.3.5 and 6.3.5 of this thesis was collected by Dr Kile Green of the Newcastle University Institute of Cellular Medicine, using nCounter<sup>®</sup> Stem Cell Gene Expression Codesets (NanoString Technologies). The full gene list for these stem cell expression panels can be found in Appendix A.

The process of running an nCounter<sup>®</sup> panel can be split into three distinct phases; namely hybridization, purification/immobilisation and counting. The RNA samples used in this process were extracted via the methodology described in section 2.6.1, quality assessed using the technique detailed in section 2.6.2 and diluted to a concentration of 30 ng/mL prior to use. Both the hybridisation and purification/immobilisation steps were performed using an nCounter<sup>®</sup> Prep Station (NanoString Technologies) automated liquid handling unit, over the course of a 2.5 hour period. During hybridization, capture and reporter probes were added to 5  $\mu\text{L}$  volumes of each of the associated RNA samples and allowed to hybridize. Next, during the purification/immobilisation step, the excess probes were removed and the probe-transcript complexes aligned and immobilised in the supplied nCounter<sup>®</sup> cartridge. Finally, the cartridge was transferred to an nCounter<sup>®</sup> Digital Analyser unit (NanoString Technologies) for counting, where the barcoded molecules were imaged and raw expression data collected. The results of the nCounter<sup>®</sup> assay were then exported as a series of comma separated values (.CSV) files for subsequent analysis and evaluation.

## 2.7 Identifying and characterising cellular protein secretions

### 2.7.1 Cell culture medium sample collection

All of the collected medium samples were taken from cultures grown in T-75 flasks in accordance with the methodology described in section 2.1.4. Each of the 10 mL samples was collected in a 15 mL Corning® Falcon® centrifuge tube (Sigma) and centrifuged at 800 x g for 5 minutes, in order to remove any remaining cellular debris. Following centrifugation, the samples were each transferred to a new 15 mL centrifuge tube and stored at -80°C. Corning® Falcon® polypropylene tubes were specifically selected for sample collection due to their material composition, which resists protein adsorption helping to ensure that any proteins present within the samples remained in solution.

Medium samples were collected from 7 different experimental conditions, the specifics of which are given below in table 2.9. Upon sample collection the cells in each condition were trypsinized (See 2.1.4) and counted using a haemocytometer (see 2.2.1) for use in data normalisation. It is important to note that the cells used in the ‘normal’ hBM-MSK condition at Passage 0 were re-seeded across three new flasks after being counted, for use in the Passage 1 stage of the ‘Normal’, ‘S-F’ and ‘TNF’ conditions. The Passage 1 and 2 ‘Normal’ condition cells were similarly used to form the basis of the Passage 2 and 3 ‘Normal’, ‘S-F’ and ‘TNF’ conditions respectively. With the obvious exception of the ‘Serum-Free’ (S-F) samples, a single batch of FBS was used to prepare all of the culture medium collected throughout this process, as a means of eliminating the potential impact of batch-to-batch variability on cell behaviour or subsequent assay performance. The Tumour Necrosis Factor- $\alpha$  (TNF- $\alpha$ ) and Lipopolysaccharide (LPS) used in the ‘TNF’ and ‘LPS’ medium preparations were purchased from Peptotech and Sigma respectively. It should be noted that these conditions were included within the study purely as a means of ensuring that the cells under investigation were capable of reactive protein secretion and to identify the profile of factors produced by these cells when exposed to an inflammatory (non-optimal) environment.

Condition Name	Time in Culture	Medium Formulation and Supplements
MSC P0	5 Days	Standard Culture Medium
MSC P1/P2/P3 Normal	5 Days	Standard Culture Medium
MSC P1/P2/P3 S-F	5 Days	See Section 2.10.2 (Table 2.13)
MSC P1/P2/P3 TNF	2 Days	Standard Medium + 50 ng/mL TNF- $\alpha$
MSC LPS Control	2 Days	Standard Medium + 200 ng/mL LPS
Y201 Normal	5 Days	Standard Culture Medium
Y201 S-F	5 Days	See Section 2.10.2 (Table 2.13)
FBS Control	N/A	N/A (FBS only)

**Table 2.9 Protein secretion culture details**

With the exception of the S-F and FBS Control conditions, the standard culture medium described in section 2.1.3 was used as a basis for all of the culture processes described here. The FBS control condition samples were comprised of undiluted volumes of foetal bovine serum, which had not come into contact with cells of any kind.

## 2.7.2 Meso Scale Discovery immunoassay

The medium samples collected according to the process described above in section 2.7.1 were characterised using a V-PLEX Human Biomarker 40-Plex immunoassay (Meso Scale Discovery). This assay was performed in accordance with the manufacturer's instructions and with the assistance of Mr John Butler. A full list of the 40 biomarkers assessed using this assay can be found in Appendix B. It should be noted, that due to the inclusion of FGF-2 in all of the medium formulations used during the course of this investigation, FGF-2 itself was excluded from the analysis process. Similarly, TNF- $\alpha$  concentrations were not assessed for the TNF- $\alpha$  treated cell populations given the relatively high concentrations used.

In brief, the V-PLEX immunoassay was performed as follows. Initially, the plates were blocked using the supplied blocking reagent, sealed and incubated for 1 hour at room temperature on a shaking platform set at 800 rpm. Next, the plates were washed three times with the supplied buffer solution and 50  $\mu$ L volumes of the diluted calibrator, control and sample solutions added to each of the appropriate wells. The plates were then sealed and incubated at room temperature for 2 hours on a shaking platform set at 800 rpm. Following this, the plates were again washed three times and 25  $\mu$ L volumes of the appropriate detection antibodies added to each of the wells. As with the previous step, the plates were then sealed and incubated at room temperature for 2 hours on a shaking platform. Finally, the plates were again washed three times, before

150  $\mu$ L of the supplied read-buffer was added to each well and the plates analysed using a Meso Scale Discover Sector Imager 6000.

## 2.8 Preparing aminosilane functionalised glass surfaces

### 2.8.1 Pre-preparation of glass surfaces

Standard sized VFM twinfrost glass microscope slides (CellPath) were initially pre-cleaned using one of two different methods; the first consisted of emersion in a 1:1 solution of methanol (Sigma) and concentrated hydrochloric acid (Sigma) for 30 minutes prior to rinsing in de-ionised water ( $\text{dH}_2\text{O}$ ) and drying under a steady stream of nitrogen gas. The second method utilised the exact same acid-solvent immersion protocol as the first but was immediately followed by a 3 minute exposure to air plasma within a PDC-32G plasma cleaner (Harrick Plasma). The treated slides were then stored in sealed containers under an inert atmosphere of nitrogen gas prior to use.

### 2.8.2 Silanization of glass surfaces

Glass slides pre-cleaned according to the procedure described in section 2.8.1 were aminosilane functionalized using either (3-aminopropyl)triethoxysilane (APTES, Sigma) or 3-aminopropyl(diethoxy)methylsilane (APDEMS, Sigma) split across one of three different solution-based methods. Aqueous-APTES treated slides were functionalised as per the protocol proposed by Yadav *et al* (2014) (215). A stock solution of 50% v/v methanol (Sigma), 47.5% v/v APTES and 2.5% v/v ultrapure water was prepared and allowed to age at 4 °C overnight. Before use, the stock solution was further diluted 1:500 in methanol, in order to produce a working solution with an APTES concentration of 0.095% v/v. Pre-cleaned glass slides were then immersed in the aqueous APTES solution for 40 minutes at room temperature. Anhydrous-APTES and anhydrous-APDEMS treated slides were submerged in either a 0.1% v/v solution of APTES in anhydrous toluene or a 0.1% v/v solution of APDEMS in anhydrous toluene for 40 minutes. All of the aminosilane treated slides were then rinsed with anhydrous toluene and dried under a steady stream of nitrogen gas, before being heated to 110°C for 30 minutes in a MINO 30 SS Laboratory Oven (Genlab). As with the cleaned glass slides before

them, the treated slides were stored in sealed containers under an inert atmosphere of nitrogen gas.

### 2.8.3 Measuring water contact angle

Static water contact angle measurements were taken at five different points across each of the prepared glass surfaces using a Cam 101 Tensiometer (KSV Instruments) and represented the average of the measured left and right angles for each of the assessed points. It should be noted that the droplets of liquid used to assess the water contact angles were allowed to sit for 40 seconds prior to any measurements being taken, as a means of ensuring that they had settled into position and were hence representative of a truly static contact angle.

### 2.8.4 Measuring surface amine content

Acid orange-7 (AO-7) is an organic dye which binds to protonated amine groups and can be used to identify their presence and relative abundance on the surface of a given material. The AO-7 assay was performed by first exposing treated glass surfaces to a 500 $\mu$ M solution of orange-II sodium salt (AO-7, Sigma) in dH<sub>2</sub>O at pH 3 for approximately 24 hours at room temperature, after which the slides were rinsed three times in dH<sub>2</sub>O at pH 3 in order to remove any non-adsorbed dye. Following washing, the surfaces were immersed in dH<sub>2</sub>O at pH13 for 15 minutes at room temperature as a means of releasing any bound dye, the level of which was quantified using a spectrophotometer reading absorbance at 482 nm with a 600 nm reference wavelength. 50 mL skirted Corning® Falcon® tubes (Sigma) were used to hold each of the individual glass slides during incubation with both the AO-7 solution and the alkaline dH<sub>2</sub>O solution, with 10 mL of each liquid being sufficient to cover an area of 7.65 cm<sup>2</sup> at the bottom of each slide. The relative pH levels of the distilled water and AO-7 solutions were regulated using either a dilute hydrochloric acid solution or a dilute sodium hydroxide solution depending upon the required pH values. In addition to the samples themselves, a series of control solutions of known AO-7 concentrations were also tested as a means of developing a standard curve for the assay (Figure 2.3). This curve was then used to convert the experimental data values into ‘amine groups per area squared’ measurements for the purposes of interpretation.



**Figure 2.3 An AO-7 standard curve plated into 96-well plate format**

The plate contains samples of the AO-7 reagent at concentrations ranging from 100nM up to 500µM. Increases in the intensity of the yellow/orange colouration of the samples can be seen to correlate with the increase in reagent concentration.

#### 2.8.5 Surfaces characterisation via x-ray photoelectron spectroscopy

X-ray photoelectron spectroscopic analysis of the aminosilane treated surfaces described in section 7.3.2 was carried out by the Nexus National EPSRC XPS Users' Facility (Newcastle University) using a Thermo Scientific Theta Probe Angle-Resolved X-ray Photoelectron Spectrometer (ARXPS) System. The elemental composition of the slides was assessed at two different points across each of the surfaces, with analysis of the resultant spectra being carried out using the CasaXPS software package.

#### 2.8.6 Assessing aminosilane layer stability in aqueous conditions

With the intention of assessing the aqueous stability of the aminosilane layers formed as a result of using the three different silanization methodologies described in section 2.8.2, slides coated using each of these methods were incubated for either 0, 15, 30 and 60 minutes in dH<sub>2</sub>O at 37°C. The aminosilane treated slides were each fully immersed in dH<sub>2</sub>O within individually allocated 50mL Corning® Falcon® centrifuge tubes and were dried under a stream of nitrogen gas immediately after removal from aqueous conditions. The slides were then stored in sealed containers under an inert atmosphere of nitrogen gas prior to assessment, which was performed using static water contact angle measurements. It should be noted that these measurements

were taken exactly as described in section 2.8.3 with the exception that only three points were measured per slide, due to the increased number of slides associated with this investigation.

As a means of helping validate any potential links between diminished water contact angle and decreased aminosilane layer integrity, an AO-7 assay (see 2.8.4) was performed using only the methodology that appeared to produce the most stable layers as indicated by the associated water contact angle data.

## 2.9 Screening selected extracellular matrix proteins in regard to cell adhesion and morphology

### 2.9.1 Surface preparation

The following procedure was used in order to prepare aminosilane coated surfaces for use in screening a selected set of extracellular matrix proteins. To begin with, a series of 13 mm diameter borosilicate glass coverslips (Scientific Laboratory Supplies) were APDEMS treated as per the process described in section 2.8.2. The coverslips were then transferred into an appropriate number of Corning® non-treated 24-well plates (Sigma), at one coverslip per well. Next, the plates were UV treated for 30 minutes using a bench-top sterilization unit. 250 µL volumes of a 25% v/v glutaraldehyde solution in dH<sub>2</sub>O were then added to each of the wells and the plates incubated for 30 minutes at room temperature. Following incubation, the wells and coverslips were washed three times each using DPBS and stored at 4 °C until required.

### 2.9.2 Experimental set-up and cell seeding

Plates produced according to the methodology described above in section 2.9.1 were used as a basis from which to screen an array of different combinations of ECM proteins in regard to their impact on both hBM-MSK and Y201 adhesion and morphology. Initially, the plates were removed from storage and washed twice with DPBS. Next, the various combinations of the different proteins were added across the plates at volumes of 500 µL per well and the plates incubated for 2 hours at 37 °C. A two-level three-factor (2<sup>3</sup>) full factorial design was used to construct the experiment, an overview of which is given in table 2.10. It is important to note that the total amount of protein in each of the experimental conditions was kept constant, with

only the specific composition changing between runs. A single positive control condition of 10% v/v FBS in Hank's Buffered Saline Solution (Sigma, HBSS) and a single negative control condition of 0.5% w/v BSA in HBSS were also included.

Run designation	Fibronectin	Vitronectin	Fibrinogen	Total Protein
1	0 µg	0 µg	0 µg	0 µg
2	10 µg	0 µg	0 µg	10 µg
3	0 µg	10 µg	0 µg	10 µg
4	0 µg	0 µg	10 µg	10 µg
5	5 µg	5 µg	0 µg	10 µg
6	5 µg	0 µg	5 µg	10 µg
7	0 µg	5 µg	5 µg	10 µg
8	3.3 µg	3.3 µg	3.3 µg	10 µg
0 (Centre)	1.6 µg	1.6 µg	1.6 µg	5 µg

**Table 2.10 Overview of the 2<sup>3</sup> factorial design used for ECM protein screening**

The total protein content of each corner point was kept constant throughout the detailed design due to the substantial impact that protein concentration is known to have on cell-substrate interactions. A single literal centre point was included as a means of assessing curvature within the design, a clear indicator that the concentrations being employed are far higher than those actually required in order to illicit the observed effects.

Following incubation, the protein solutions were aspirated from the wells and the wells washed twice with DPBS. Next, cells were trypsinized, manually counted and seeded across the plates at  $1 \times 10^4$  cells per well, using standard MSC culture medium without the inclusion of FBS. The plates were then incubated for 4 hours at 37 °C and 5% CO<sub>2</sub>. After this period, the wells were washed with DPBS in order to remove any unattached cells and the cells fixed using a 4% w/v solution of PFA in DPBS for 20 minutes at room temperature. 500 µL volumes of DPBS were then added to each well and the plates stored at 4 °C until required for analysis. The cells were assessed using a combination of the PicoGreen® assay described in section 2.2.4 and the cytoskeletal staining procedure described in section 2.5.1. Due to the destructive nature of the PicoGreen® assay, separate plates were prepared for this purpose in which the cells were not fixed immediately following the screening process.

## 2.10 Design of experiments and statistical analyses

### 2.10.1 Fractional factorial supplement screening

Twelve different cytokines and commonly used culture supplements were screened across three individual sets of  $2^{4-1}$  fractional factorial experiments, with four factors being investigated per design (see table 2.11). The supplements were assessed on their ability to support the metabolic functions of hBM-MSCs in serum-deprived conditions. Cells were seeded at a density of  $2.5 \times 10^3$  cells per  $\text{cm}^2$  in 24-well plates using standard MSC culture medium and incubated overnight at  $37^\circ\text{C}$  and 5%  $\text{CO}_2$ . Following incubation, the cells were washed three times using DPBS and cytokine-supplemented serum-free medium solutions added to each of the appropriate wells in accordance with the design given in table 2.12. The basal medium used to produce the serum-free solutions was a commercially available 1:1 combination of DMEM and Ham's F-12 Nutrient Mixture (DMEM/F-12, Sigma), supplemented with 1% v/v GlutaMax (200 mM) and 1% v/v Penicillin-Streptomycin (10,000 U/mL). The cells were then cultured for 5 days at  $37^\circ\text{C}$  and 5%  $\text{CO}_2$ , without media changes. Following this 5 day culture period, the metabolic activity of the cells was assessed using an MTT assay as described in section 2.2.2. It should be noted that an FBS control condition, in which the cells were cultured for the 5 day period in standard MSC culture medium, was also included in each of the experiments.

	<b>Designation</b>	<b>Component 1</b>	<b>Component 2</b>	<b>Component 3</b>	<b>Component 4</b>
<b>Name</b>	Screening	FGF-2	SITE	PDGF-BB	TGF- $\beta$ 1
<b>Concentration</b>	Experiment 1	25 ng/mL	1.75% v/v	5 ng/mL	2.5 ng/mL
<b>Supplier</b>		Peprotech	Sigma	Peprotech	Peprotech
<b>Name</b>		Screening	Ascorbic Acid	SDF-1 $\alpha$	IL-6
<b>Concentration</b>	Experiment 2	80 $\mu\text{g/mL}$	50 ng/mL	10 ng/mL	100 ng/mL
<b>Supplier</b>		Sigma	Peprotech	Peprotech	Peprotech
<b>Name</b>		Screening	BMP-3	VEGF	ROCK
<b>Concentration</b>	Experiment 3	100 ng/mL	20 ng/mL	4 $\mu\text{g/mL}$	100 ng/mL
<b>Supplier</b>		Peprotech	Peprotech	Sigma	Peprotech

**Table 2.11 Overview of the cytokines and culture supplements assessed over the course of three separate screening experiments**

The listed components are as follows: Fibroblast Growth Factor-2 (FGF-2), Selenium Insulin Transferrin Ethanolamine (SITE), Platelet Derived Growth Factor-BB (PDGF-BB), Transforming Growth Factor- $\beta$ 1 (TGF-

$\beta$ 1), Ascorbic Acid (AA), Stromal Cell Derived Factor-1 $\alpha$  (SDF-1 $\alpha$ ), Interleukin-6 (IL-6), Heparin Binding EGF-like Growth Factor (HB-EGF), Bone Morphogenetic Protein-3 (BMP-3), Vascular Endothelial Growth Factor (VEGF), Rho-associated protein Kinase-inhibitor Y-27632 (ROCK) and Thymosin- $\beta$ 4 (Thy- $\beta$ 4).

Run designation	Component 1	Component 2	Component 3	Component 4
1	-	-	-	-
2	+	-	-	+
3	-	+	-	+
4	+	+	-	-
5	-	-	+	+
6	+	-	+	-
7	-	+	+	-
8	+	+	+	+
0 (Centre)	0	0	0	0

**Table 2.12 Overview of the 2<sup>4-1</sup> fractional factorial experimental design used in supplement screening**

The experimental design detailed here was used across all three of the individual component lists given in table 2.11. A '+' symbol indicates the inclusion of a given component at the listed concentration, whilst a '-' symbol indicates that the corresponding component was not included in a particular run.

### 2.10.2 Full factorial formulation assessment

Following the fractional factorial experiments described above in section 2.10.1, a set of full factorial designs were utilised in order to assess the suitability of a serum-free medium formulation derived from the most promising of the screened cytokines and growth supplements (see table 2.13). hBM-MSCs and Y201s were seeded at a density of 2.5x10<sup>3</sup> cells per cm<sup>2</sup> in 24-well plates using standard MSC culture medium and incubated overnight at 37 °C and 5% CO<sub>2</sub>. Following incubation, the cells were washed three times using DPBS and cytokine-supplemented serum-free medium solutions added to each of the appropriate wells in accordance with the design given in table 2.14. The basal medium used to produce these solutions was the same as the one used in the fractional factorial screening experiments (see 2.10.1). The cells were then cultured for 5 days at 37 °C and 5% CO<sub>2</sub>, without media changes. Following culture, metabolic activity levels and total cell numbers were determined for each of the plates using PrestoBlue® and PicoGreen® assays respectively (see 2.2.3 and 2.2.4). It

should be noted that, as with the fractional screening experiments before them, an FBS control condition was also included in each of the full factorial designs.

	<b>Component 1</b>	<b>Component 2</b>	<b>Component 3</b>	<b>Component 4</b>
<b>Name</b>	FGF-2	SITE	PDGF-BB	TGF- $\beta$ 1
<b>Concentration</b>	25 ng/mL	1.75% v/v	5 ng/mL	2.5 ng/mL
<b>Supplier</b>	Peprtech	Sigma	Peprtech	Peprtech

**Table 2.13 Overview of the cytokines and culture supplements used in the assessed serum-free medium formulation**

The listed components are as follows: Fibroblast Growth Factor-2 (FGF-2), Selenium Insulin Transferrin Ethanolamine (SITE), Platelet Derived Growth Factor-BB (PDGF-BB) and Transforming Growth Factor- $\beta$ 1 (TGF- $\beta$ 1).

Run designation	Component 1	Component 2	Component 3	Component 4
1	-	-	-	-
2	+	-	-	-
3	-	+	-	-
4	-	-	+	-
5	-	-	-	+
6	+	+	-	-
7	+	-	+	-
8	+	-	-	+
9	-	+	+	-
10	-	+	-	+
11	-	-	+	+
12	+	+	+	-
13	-	+	+	+
14	+	+	-	+
15	+	-	+	+
16	+	+	+	+
0 (Centre)	0	0	0	0

**Table 2.14 Overview of the 2<sup>4</sup> full factorial experimental design used in formulation assessment**

The experimental design detailed here was used in conjunction with the component list given in table 2.13. A '+' symbol indicates the inclusion of a given component at the listed concentration, whilst a '-' symbol indicates that the corresponding component was not included in a particular run.

### 2.10.3 Data handling and statistical analyses

All of the experiments described in this investigation were independently repeated a minimum of three times, with at least three technical replicates being included for each individual condition. Biological replicates were conducted using either hBM-MSC populations isolated from distinct donors or individually thawed Y201 samples with different passage numbers. Parametric analyses were used whenever possible, with the associated non-parametric alternatives being applied only when data transformation was seen to be ineffective. All raw data was assessed in regard to the normality of the associated residuals and homoscedasticity, as appropriate. Literal centre points were included in all fractional and full factorial designs as

a means of assessing curvature within the resultant data set, a clear indicator of diminishing returns within the context of the associated design space. In addition, where appropriate experimental data sets were split into blocks based on primary cell donor or cell line passage number, in order to assess the impact of these factors on the cells responses to cytokine supplementation. Microsoft® Excel 2016 was used for data storage, graphical representation of data and descriptive analysis, whilst Minitab 16 was used in all instances of inferential analysis and factorial design. A critical value ( $\alpha$ ) of 0.05 was used throughout the entire course of this project.

## 3 Chapter 3: Primary mesenchymal stromal cell and cell line characterisation

### 3.1 Introduction

Different types of mammalian cells have been shown on numerous occasions to possess distinct metabolic, nutritional and micro-environmental requirements in order to ensure their continued growth and phenotypic stability *in vitro*. For instance, Kato & Gospodarowicz (1984) demonstrated that low density cultures of rabbit-derived chondrocytes require a complex combination of high-density lipoprotein, transferrin, FGF-2, hydrocortisone and epidermal growth factor in order to actively proliferate in serum-free conditions (216). Conversely, whilst insulin was shown to have no beneficial effects on cell growth in the aforementioned study, this same supplement was demonstrated to significantly improve the proliferation of human umbilical vein endothelial cells (HUVECs) during prolonged *in vitro* expansion (217).

In light of these substantial differences, it is apparent that any study utilising primary cells should include relevant characterisation activities, especially given the large amounts of variability inherent to both the proliferative and metabolic features of such cells. Here, we utilised The International Society for Cellular Therapy's (ISCT) criteria for the identification of MSCs as the primary means by which to characterise the donor-derived cells used as part of this investigation. It was also important that cells belonging to the immortalised Y201 line were similarly assessed, as a means of evaluating their suitability for use as a consistent control group during subsequent activities. It should be noted that any significant deviations from the criteria laid out by the ISCT triggered further investigation, the results of which can be found within the confines of this chapter.

### 3.2 Aims

1. To assess the morphological, differentiation and surface marker properties of both the primary and immortalised cells used during the course of this investigation with respect to those typical for hBM-MSCs.
2. To evaluate the potential impact of FGF-2 supplementation on surface marker expression in primary hBM-MSCs.

### 3.3 Results

#### 3.3.1 Morphological characterisation

Human bone marrow-derived MSCs were commonly seen to adopt a classical spindle-like morphology following isolation, as shown below in figure 3.1. A range of additional morphological conformations were also observed during culture, with a general shift towards a more flattened and rounded shape becoming apparent over extended periods of expansion. Similarly, Y201 cells were also seen to adopt a spindle-like morphology but displayed little to no variability in regard to their shape despite prolonged time in culture. It should be noted however, that if allowed to reach confluence levels of over 90%, these cells began to display an almost cuboidal appearance, which persisted over subsequent sub-cultures.

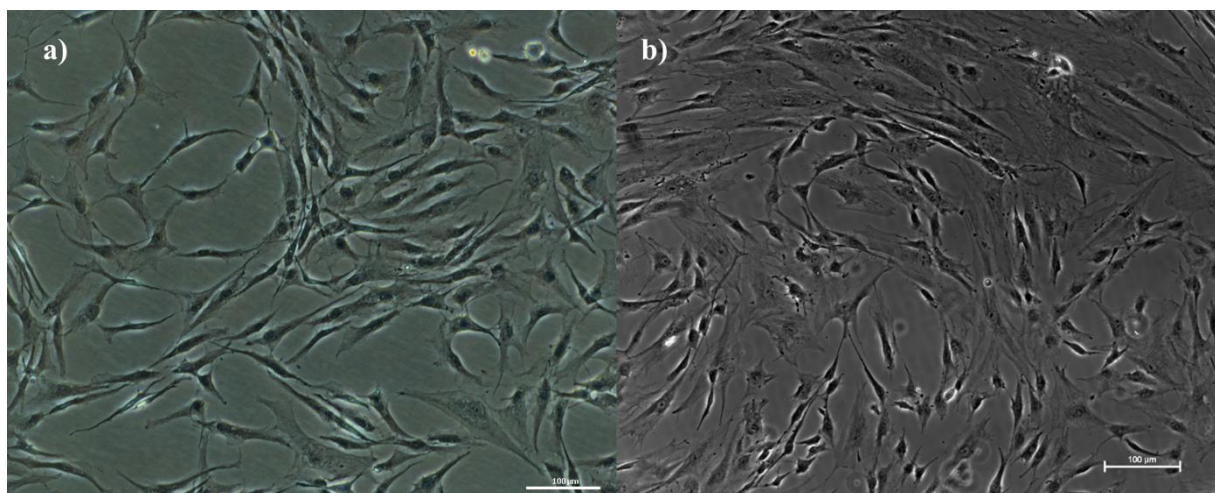


**Figure 3.1 Representative phase contrast micrographs of cell belonging to the Y201 line together with primary hBM-MSCs**

All included scale bars are indicative of a 100 µm length. a) Y201s. b) hBM-MSC

#### 3.3.2 Tri-lineage differentiation potential

Following 14 days of culture in adipogenic conditions, primary hBM-MSCs were seen to produce fat droplets, readily stained by Oil Red-O and considered indicative of directed adipogenic differentiation. Similarly, these same cells were seen to produce small Alizarin Red-S stainable mineral deposits typical of osteogenic differentiation following exposure to appropriate culture conditions. Despite the diffuse blue colouration seen across the embedded

sections following pellet culture and subsequent staining, no clear indications of directed chondrogenic differentiation were observed in regard to the hBM-MSCs utilised during the course of this investigation.

As with the primary cells before them, cells belonging to the Y201 cell line were readily seen to generate fat droplets and mineralised deposits characteristic of adipogenic differentiation and osteogenic differentiation respectively. It should be noted that the osteogenic features displayed by these cells were substantially more pronounced than those seen in the primary hBM-MSCs. In addition, the adipogenic features of these cells were seen to be less distinct on visual evaluation than those of the patient-derived cells. Given the formative nature of this aspect of the investigation however, no further analysis was deemed necessary when going forward. Similar to the primary hBM-MSCs mentioned above, the toluidine blue stained Y201 sections displayed only a subtle change in colouration following the chondrogenic differentiation process, suggesting a lack of phenotypic shift. Control groups grown in the absence of differentiation-induction media were included in both the hBM-MSC and Y201 osteogenic, adipogenic and chondrogenic staining processes. No apparent morphological or phenotypic changes consistent with tri-lineage differentiation were observed within any of these control groups. Representative images of the cells discussed here, alongside all associated controls, can be found below in figures 3.2 and 3.3.

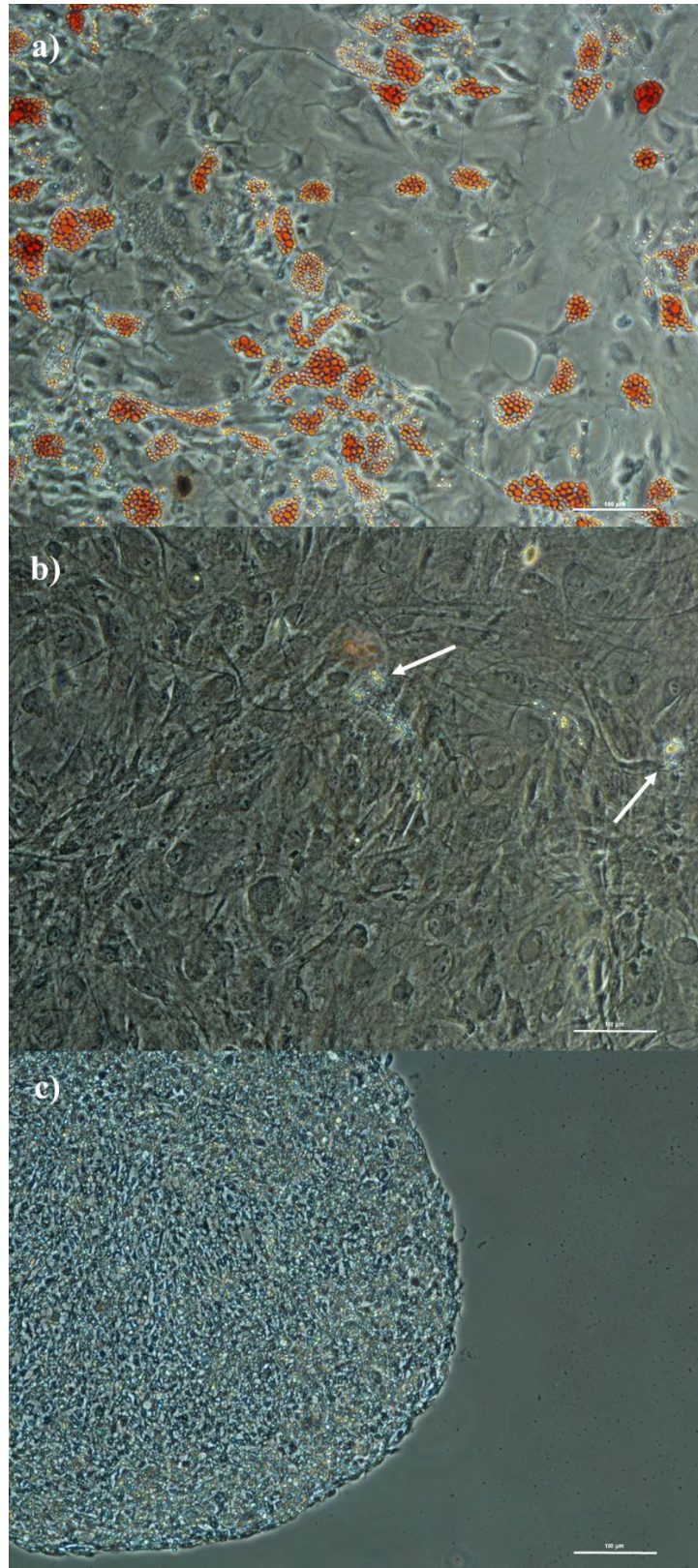


**Figure 3.2 Phase contrast images of tri-lineage differentiated BM-MSCs**

All included scale bars are indicative of a 100  $\mu\text{m}$  length. a) Oil Red-O stained fat droplets following adipogenic differentiation. b) Alizarin Red-S stained mineral deposits in osteogenically differentiated cells (as indicated by the associated arrows). c) A Toluidine Blue stained section of pellet cultured cells exposed to chondrogenic medium, with no clear indications of differentiation.

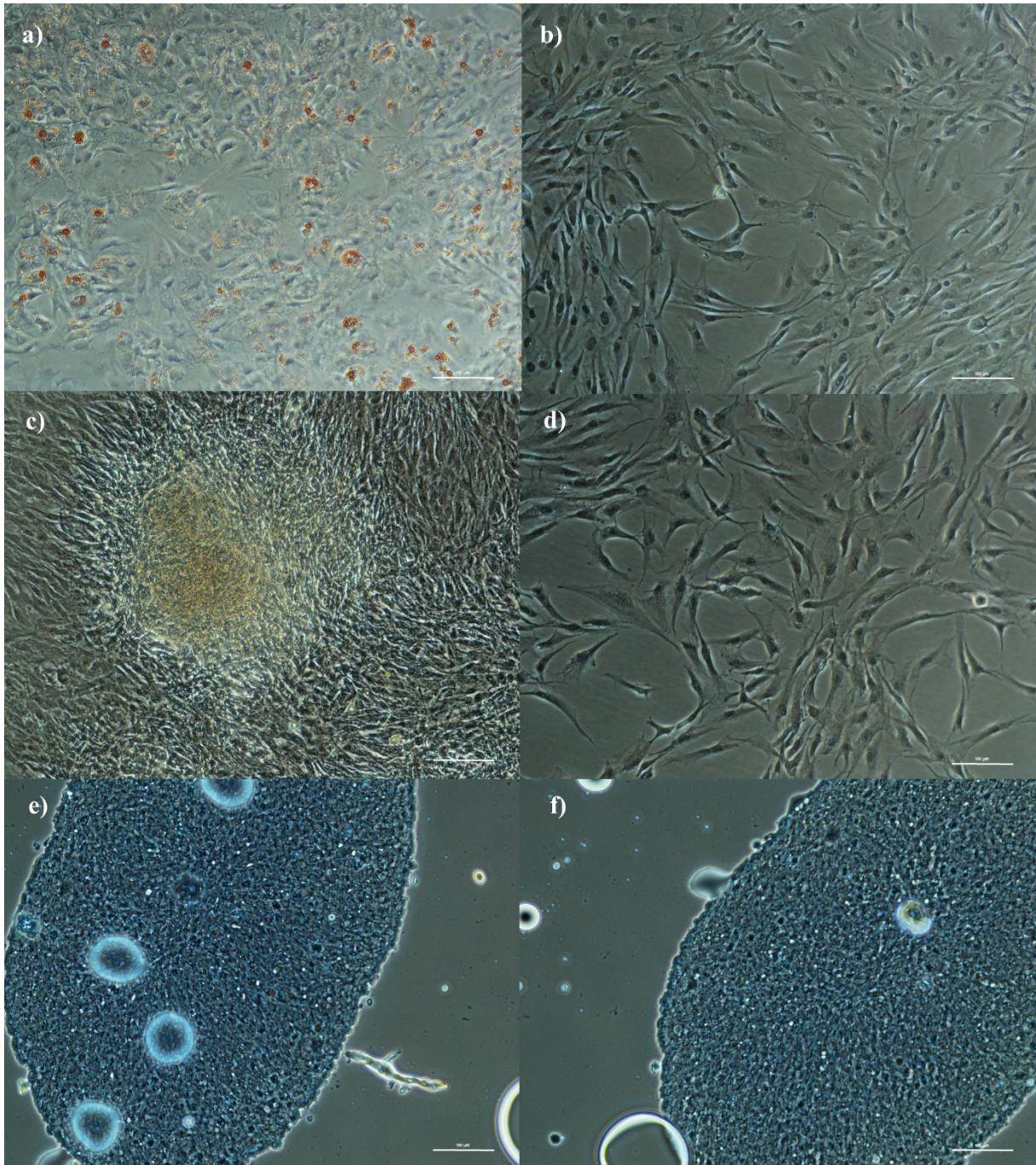


**Figure 3.3 Phase contrast images of tri-lineage differentiated Y201s**

All included scale bars are indicative of a 100  $\mu\text{m}$  length. a) Oil Red-O stained fat droplets following adipogenic differentiation. b) Cells grown in standard culture conditions stained with Oil Red-O. c) Alizarin Red-S stained mineral deposits in osteogenically differentiated cells. d) Cells grown in standard culture conditions and stained with Alizarin Red-S. e) A Toluidine Blue stained section of pellet cultured cells exposed to chondrogenic medium, with no clear indications of differentiation. f) Cells grown in pellet culture without chondrogenic induction medium and stained with Toluidine Blue.

### 3.3.3 Surface marker expression

Three different populations of cells isolated from human donor femoral heads were characterised using flow cytometry against the International Society for Cellular Therapy's (ISCT) criteria for identifying MSCs. The gating strategy utilised during this process is detailed below in figure 3.4. Cells showed an average viability of 96.8% based on their DAPI staining profile, with 39.2% of this sub-population of living cells matching the MSC characterisation criteria on average. Investigation of the gating process revealed that a substantial proportion of viable cells were not identified as MSC-like on the basis of their positive expression of HLA-DR. Exclusion of this marker was seen to boost the average number of MSC-like cells to 97.4%, revealing a significant shift over the previous value ( $t(2)=4.55$ ,  $P=0.045$ ).

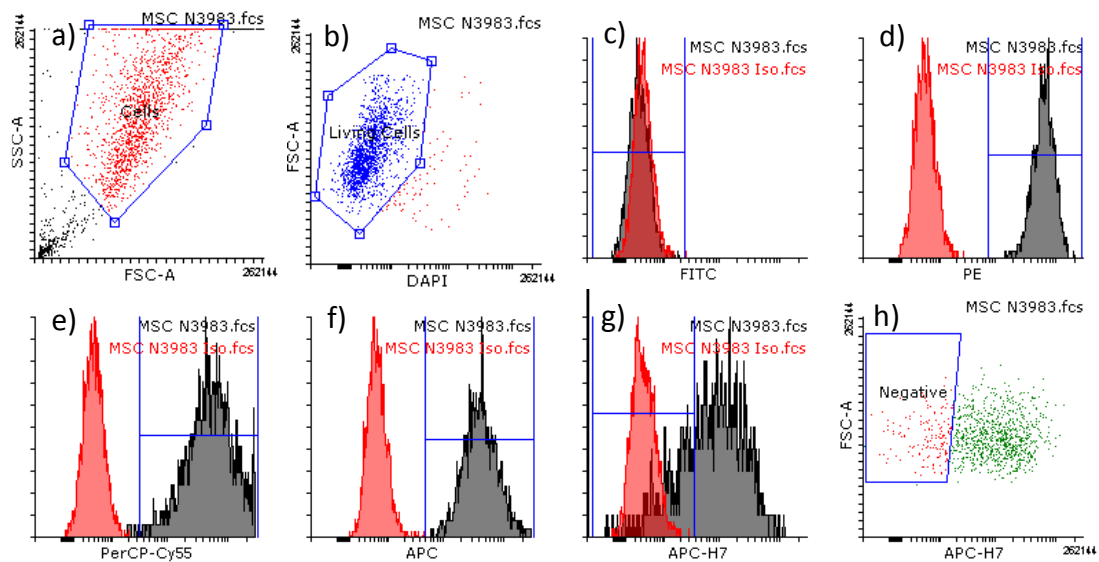


**Figure 3.4 Example dot plots and histograms representative of the typical gating strategy used to characterise BM-MSCs**

a) Cells were initially distinguished from cellular-debris on the basis of their SSC-A to FSC-A ratio. b) Living cells were then identified due to their lack of staining with DAPI. c-g) BM-MSCs were characterised based on the International Society for Cellular Therapy's (ISCT) criteria for the identification of MSCs. Namely, the combination of their lack of expression of CD14, CD19, CD34 and CD45 (FITC), positive expression of CD73 (PE), CD90 (PerCP-Cy55) and CD105 (APC), and finally the absence of HLA-DR (ACP-H7) expression. The black curves on each of the displayed histograms represent the plotted sample data, whilst the associated red curves correspond to the matching isotype controls. Blue gates signify the BM-MSCs acceptance criteria using for characterisation based on the positioning of isotype control data. h) A dot plot of APC-H7 staining against FSC-A is included due to the unusual pattern of HLA-DR expression seen in all of the cell populations assessed.

Alongside the donor-derived cells, three different cultures belonging to the Y201 cell line were also evaluated, revealing an average viability of 95.7%. An example of the gating process

utilised during this activity is given below in figure 3.5. Unlike the primary cells before them, no significant shift in the proportion of living Y201s identified with or without the inclusion of the HLA-DR marker was seen ( $t(2)=0.08$ ,  $P=0.943$ ). It is thought that the overall reduction in the number of MSC-like cells identified in the Y201 cultures (89.6% pre HLA-DR and 89.6% post HLA-DR) when compared to the pre HLA-DR primary populations was brought about by the existence of a small sub-group of CD73 negative cells, which can clearly be seen in image d) of figure 3.5.

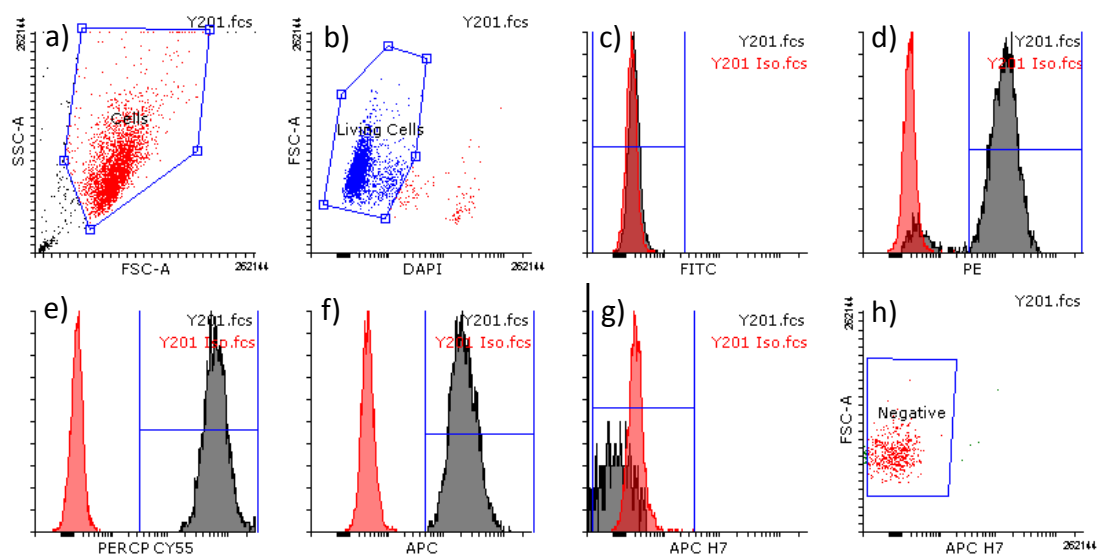


**Figure 3.5 Example dot plots and histograms representative of the typical gating strategy used to characterise cells belonging to the Y201 cell line**

a) Cells were initially distinguished from cellular-debris on the basis of their SSC-A to FSC-A ratio. b) Living cells were then identified due to their lack of staining with DAPI. c-g) As with the primary BM-MSCs, Y201s were characterised based on the International Society for Cellular Therapy's (ISCT) criteria for the identification of MSCs. Namely, the combination of their lack of expression of CD14, CD19, CD34 and CD45 (FITC), positive expression of CD73 (PE), CD90 (PerCP-Cy55) and CD105 (APC), and finally the absence of HLA-DR (ACP-H7) expression. The black curves on each of the displayed histograms represent the plotted sample data, whilst the associated red curves correspond to the matching isotype controls. Blue gates signify the BM-MSC acceptance criteria using for characterisation based on the positioning of isotype control data. h) A dot plot of APC-H7 staining vs FSC-A is included for comparison to primary cells.

### 3.3.4 Assessing the impact of fibroblast growth factor-2 supplementation on surface marker expression

As a result of the high HLA-DR expression levels identified during primary MSC characterisation, an investigation was performed in order to assess the potential impact of FGF-

2 supplementation on the expression of this marker over two successive subcultures following initial isolation. Flow cytometry data showed a significant reduction in the average percentage of MSC-like cells identified post HLA-DR when cultures were supplemented with bFGF at both passage 1 ( $t(3)=3.52$ ,  $P=0.039$ ) and passage 2 ( $t(3)=11.36$ ,  $P=0.001$ ), as seen below in figures 3.6 and 3.7. In addition, there was no significant reduction in the average percentage of MSC-like cells pre and post HLA-DR when bFGF was removed from previously supplemented cells, suggesting that any associated effect may potentially be reversible ( $t(3)=2.18$ ,  $P=0.117$ ).

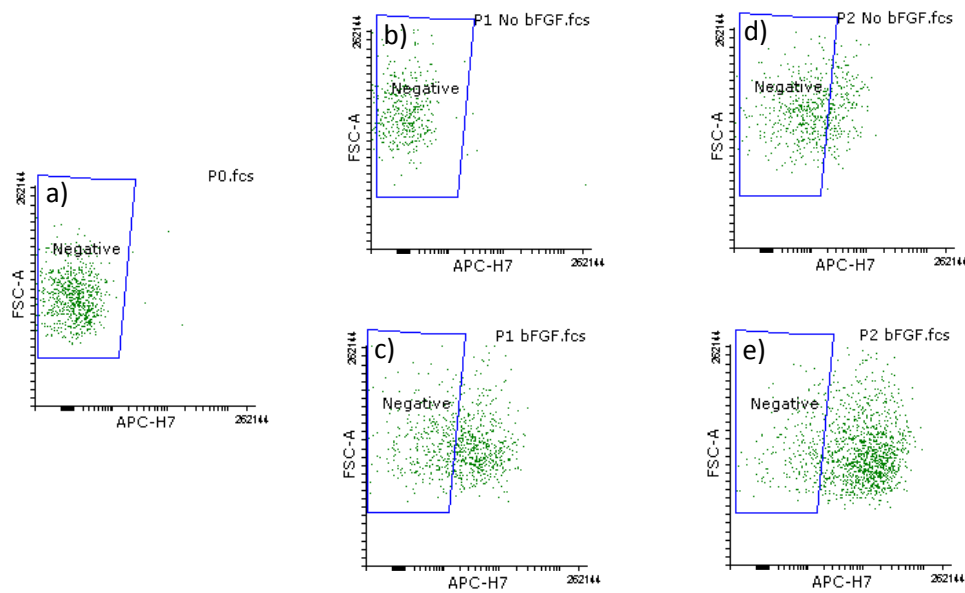


**Figure 3.6 Representative dot plots showing the expression of HLA-DR in BM-MSCs following expansion in bFGF supplemented and un-supplemented media across three subsequent subcultures**

a) Cells cultured without supplementary bFGF showing negligible expression of HLA-DR at P0 b) Cells at P1 continuing to display negligible levels of HLA-DR following expansion in un-supplemented media. c) Cells at P1 cultured with supplementary bFGF expressing increased levels of surface-bound HLA-DR. d) Cells showing a decrease in HLA-DR expression at P2 following expansion in un-supplemented media. e) Cells at P2 cultured with supplementary bFGF again showing increased HLA-DR expression.

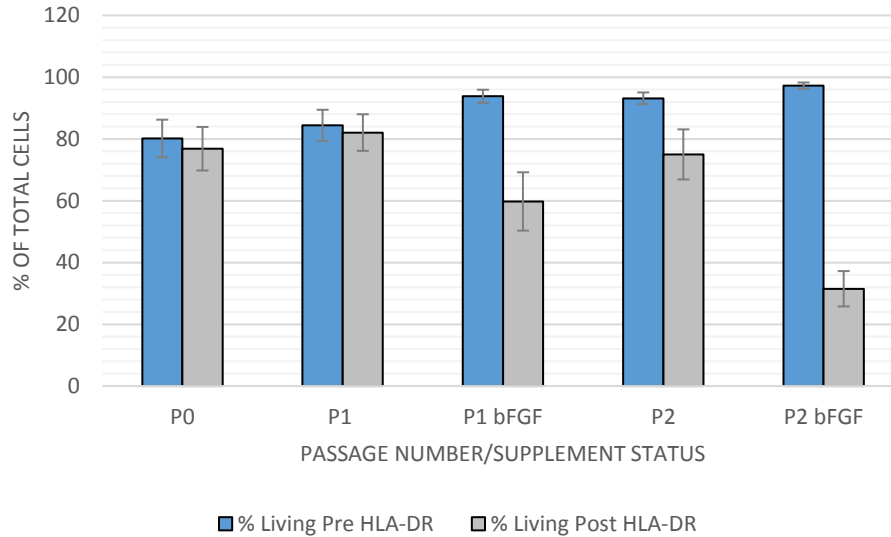


**Figure 3.7 Mean percentages of living BM-MSCs remaining prior to and following selection based on lack of expression of HLA-DR**

Error bars indicate the standard error of the mean for n=4. Cells were cultured over a number of successive subcultures with or without bFGF supplementation as indicated.

### 3.4 Discussion

Over the course of this chapter, the two principle cell populations utilised during this investigation were characterised in regard to their morphology, tri-lineage differentiation potential and surface marker profiles. Upon visual examination, both primary BM-MSCs and Y201s were seen to display morphological characteristics typical of MSCs, possessing an elongated spindle-like morphology. Immortalised cells were seen to appear smaller in size than primary patient-derived cells and to display a substantially more consistent morphology between cultured populations. In regard to their tri-lineage differentiation, both cell types were capable of osteogenic and adipogenic differentiation, identified by the production of mineralized nodules and lipid droplets respectively. Conversely, neither Y201s nor primary cells were able to undergo chondrogenic differentiation following culture in appropriate conditions. Whilst it has been demonstrated that MSCs derived from aged osteoarthritic donors undergoing joint replacement surgery have significantly reduced chondrogenic potential, this should not be the case for cells belonging to the Y201 cell line (221). These results may suggest that rather than lacking in tri-lineage potential, the method of inducing chondrogenic differentiation utilised here was not compatible with these cells. It should be noted that, based upon visual assessment alone, primary cells appeared to show increased fat droplet formation when compared to Y201s, whilst Y201s had larger mineralised deposits on average than

patient-derived cells. It could be that this observation suggests some level of lineage bias between the two groups but this cannot be confirmed without the use of gene expression analysis or a similarly quantitative assessment.

The results of the surface marker analysis for both cell types were consistent with the ISCT criteria for MSC identification, with the exception of HLA-DR, which was seen to be positively expressed in the primary cell populations. It should be noted that some groups have demonstrated increased HLA-DR expression in cells derived from diseased patients and that the pro-inflammatory conditions present within osteoarthritic synovial joints can also lead to aberrant expression of HLA class-II molecules (222). Despite this, no HLA-DR expression was seen in very early stage cultures, suggesting that some element of the expansion process itself was likely impacting upon the surface marker profile of these cells. FGF-2 was identified as a possible culprit, given its apparent ability to cause immunogenic activation of MSCs, in spite of its continued use throughout the industry as a mitogenic supplement (223, 224). The results of the associated investigation, revealed that expansion with FGF-2 did indeed lead to significant increases in HLA-DR expression over successive subcultures. Unfortunately, the primary cell populations utilised here were incapable of growing for more than a single passage without FGF-2 supplementation, necessitating its continued inclusion within the medium. Incidentally however, it was observed that the aforementioned increases in HLA-DR expression resulting from FGF-2 use were at least partially reversible and that removal of the cytokine from the medium would result in reduced expression. As a direct result, where appropriate cells were cultured without FGF-2 for a single passage immediately prior to experimental use, in order to help reduce the impact of this phenomenon on any subsequent investigations.

## 4 Chapter 4: Assessing the variability of foetal bovine serum as a cell culture supplement

### 4.1 Introduction

Foetal bovine serum represents one of the most commonly applied media supplements used within modern mammalian cell culture processes, particularly with regard to small scale research-related activities. This complex mixture of ions, amino acids, vitamins and proteins not only provides cells with the nutrients required for effective *in vitro* growth but also supplies additional buffering capacity and protection from shear forces. Despite these benefits however, the xenogeneic nature of FBS raises many questions regarding its safety and the reliability of supply, with its variable composition acting a main point of contention during process development and scale-up activities. Interestingly, whilst an overwhelming amount of anecdotal evidence exists regarding the potential impact of serum variability on cell proliferation and survival, very little experimental data can be found to support such claims.

As a direct result of this gap in current knowledge, we chose to assess the impact of both batch to batch variability and variability between different serum types on the key phenotypic, metabolic and genetic characteristics of primary hBM-MSCs and Y201s. It is important to note that Y201s were included in this study chiefly as a means of helping to distinguish any apparent batch-related effects from those arising as an artefact of the donor variability inherent to primary cells. Similarly, a second type of serum was included within the investigation; namely human serum, in order to act as a reference point from which to assess the relative variability between different FBS batches. Finally, it should also be noted that the batch of FBS designated here as 'FBS 1' was utilised in all activities requiring the inclusion of serum described outside of this chapter, including the isolation, expansion and cryopreservation of primary cell populations detailed in section 2.1.

### 4.2 Aims

1. To evaluate the impact of foetal bovine serum batch variability on hBM-MSC growth, metabolic activity and surface marker characteristics.

2. To assess whether the apparent effects of foetal bovine serum variability on cell proliferation and metabolic activity can be linked to altered gene expression in hBM-MSCs and Y201s.

## 4.3 Results

### 4.3.1 Cell growth and metabolic activity

Following five days of culture, both primary hBM-MSCs and Y201s were seen to display variable peak cell densities depending upon the batch and type of serum to which they were exposed, as seen below in figures 4.1 and 4.2. The results of a one-way ANOVA on the primary cell data revealed significant differences between the total cell counts recorded for day five ( $F(23)=6.00$ ,  $P=0.001$ ), with FBS 1 showing significantly reduced growth when compared to each of the three tested human serum (HS) batches. Analysis of the Y201 data at day five uncovered a similarly significant result ( $F(23)=231.44$ ,  $P=0.000$ ), with growth using FBS batches 2 and 3 resulting in a significant reduction in peak cell density when contrasted against the other six serum batches. Additionally, FBS 1; the use of which resulted in the highest recorded average day five Y201 cell count, gave rise to values that were statistically distinct from those of FBS 4, HS 1 and HS 2.

Figures 4.3 and 4.4 show the normalised metabolic activity for each of the different serum groups displayed by primary hBM-MSCs and Y201s respectively. Despite a general trend towards reduced metabolic activity in cells exposed to serum with poor growth profiles, no statistically significant effects were identified.

Utilising the growth curves seen in figures 4.1 and 4.2, a set of average doubling times were calculated for the two different cell types when cultured in each of the tested serum batches, using the equation  $\text{Doubling Time (hrs)} = (24 * \text{LOG}(2)) / (\text{LOG}(\text{Cell Count on Day 3}) - \text{LOG}(\text{Cell Count on Day 2}))$ . Analysis of these results, which are given in figures 4.5 and 4.6, revealed significant differences within both the MSC ( $F(23)=3.82$ ,  $P=0.013$ ) and Y201 ( $F(23)=26.77$ ,  $P=0.000$ ) data sets. For primary cells, growth in FBS 3 was seen to significantly increase doubling times when compared to all three of the human serum types used, whilst for the Y201s, FBS 2 and 3 were seen to promote increased doubling times when contrasted against all of the other tested batches of serum.

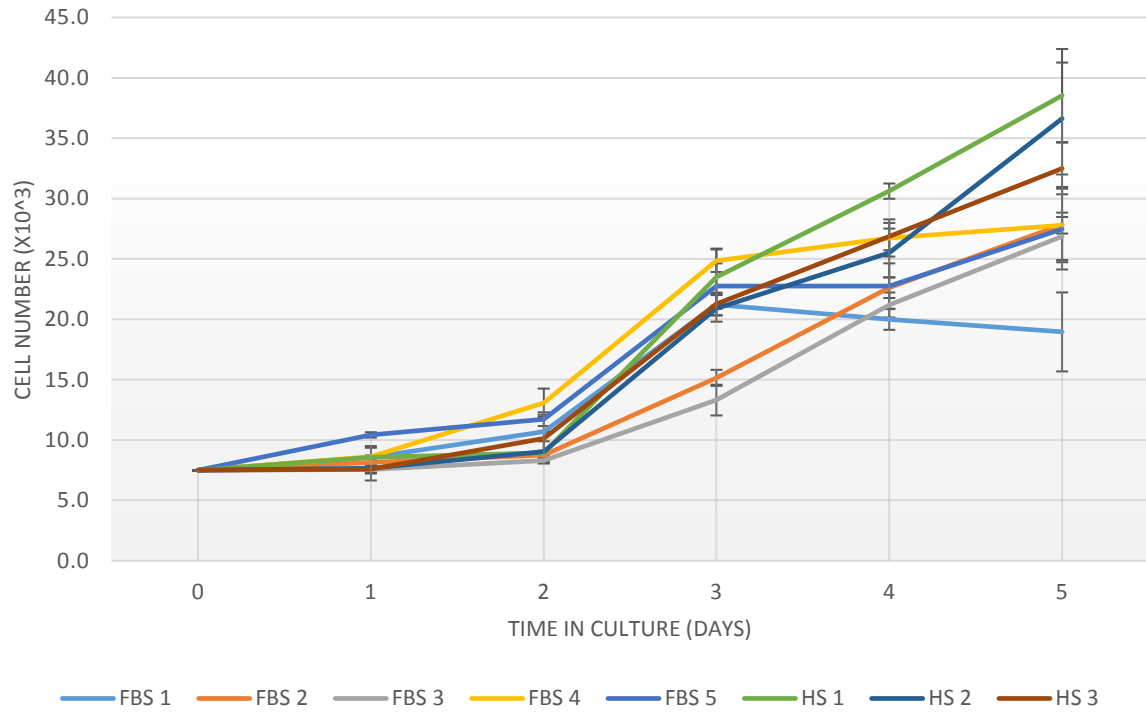


**Figure 4.1 Mean hBM-MSc numbers across a 5 day culture period for each of the tested FBS and human serum types**

Error bars indicate the standard error of the mean for n=3. Day 0 cell numbers represent the seeding density ( $7.5 \times 10^3$  cells per well) used at the outset of this experiment.

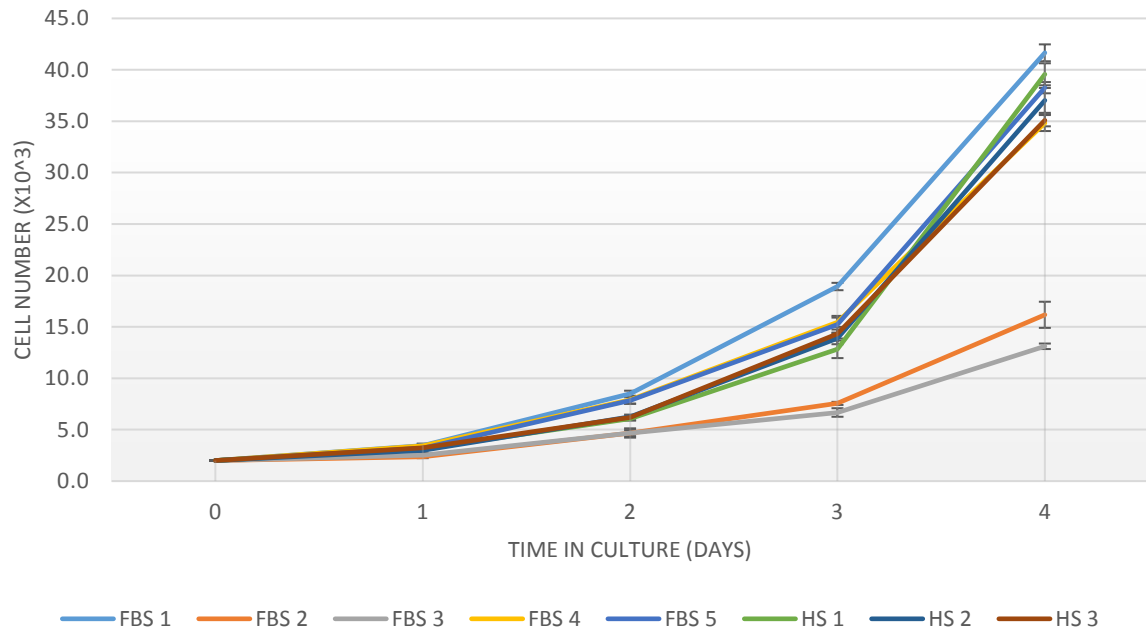


**Figure 4.2 Mean Y201 cell numbers across a 5 day culture period for each of the tested FBS and human serum types**

Error bars indicate the standard error of the mean for n=3. Day 0 cell numbers represent the seeding density ( $2 \times 10^3$  cells per well) used at the outset of this experiment.

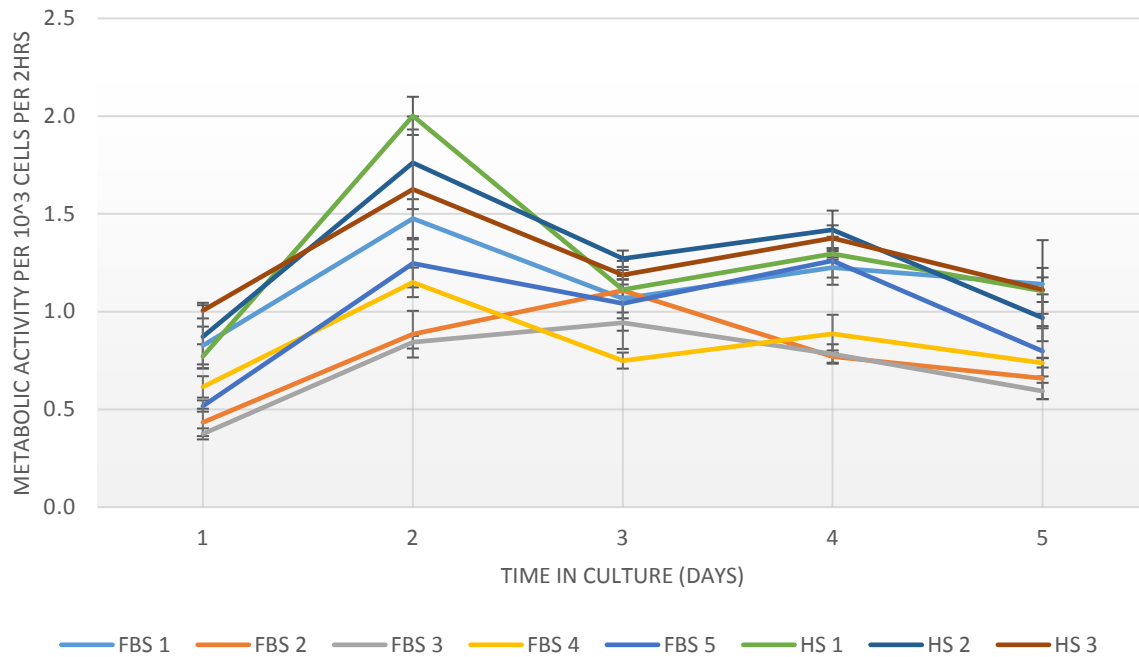


**Figure 4.3 Mean BM-MSC metabolic activity normalised to cell number across a 5 day culture period for each of the tested FBS and human serum types**

Error bars indicate the standard error of the mean for n=3. Metabolic activity rates could not be derived at the time of seeding (Day 0) due to the low numbers of cells present together with the relative sensitivity of the Alamar blue assay used.

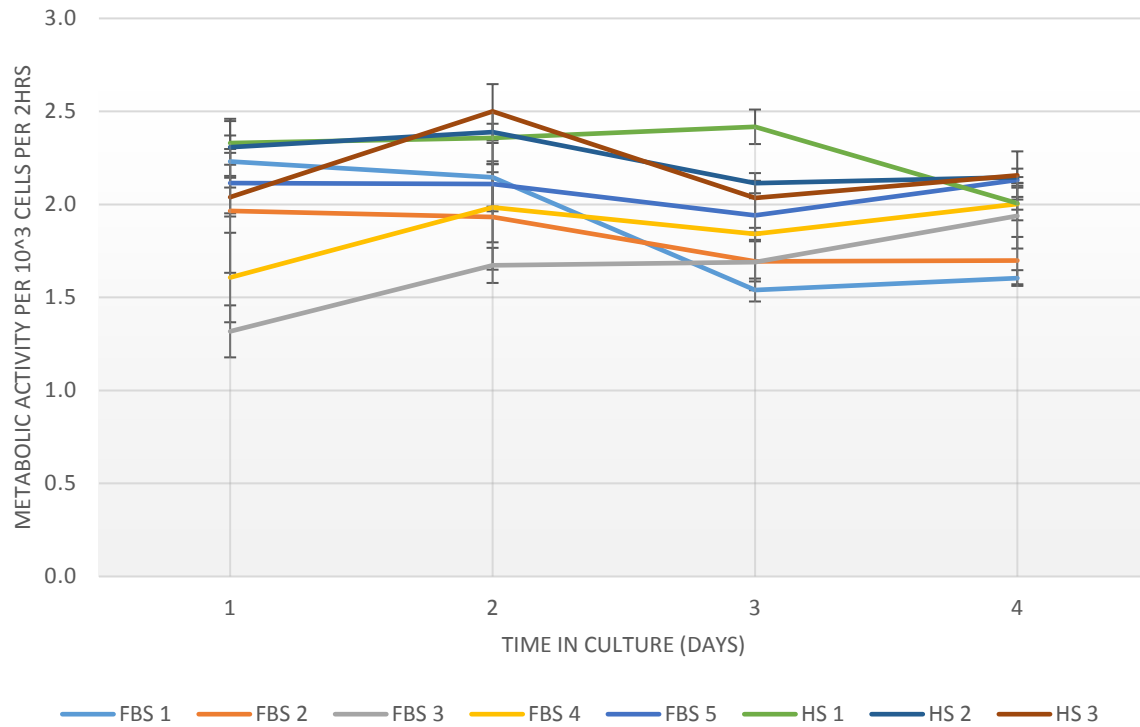


**Figure 4.4 Mean Y201 cell metabolic activity normalised to cell number across a 5 day culture period for each of the tested FBS and human serum types**

Error bars indicate the standard error of the mean for n=3. Metabolic activity rates could not be derived at the time of seeding (Day 0) due to the low numbers of cells present together with the relative sensitivity of the Alamar blue assay used.

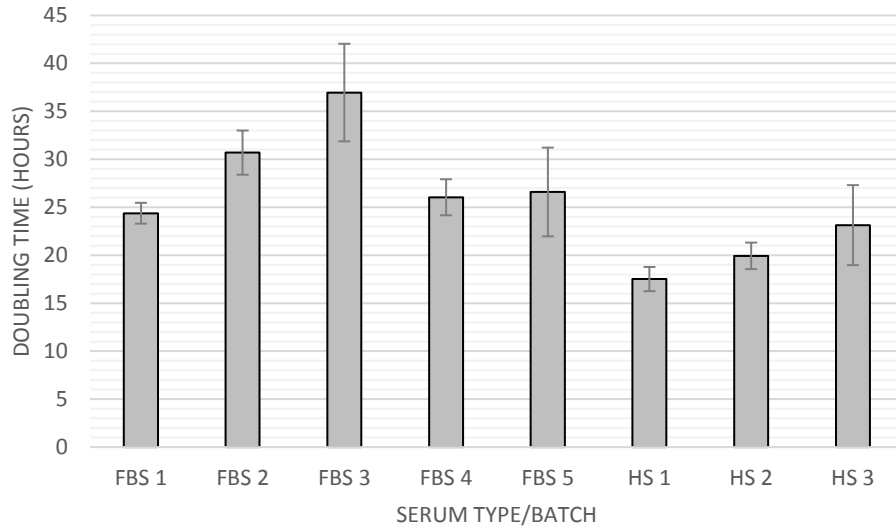


**Figure 4.5 Mean hBM-MSC doubling times during the exponential growth phase of a 5 day culture period for each of the tested FBS and human serum types**

Error bars indicate the standard error of the mean for n=3. The exponential growth phase of the cells was thought to reside between days 2 and 3 of the culture and was determined through visual examination of the cell numbers shown in figure 4.1 following log conversion (figure not included).

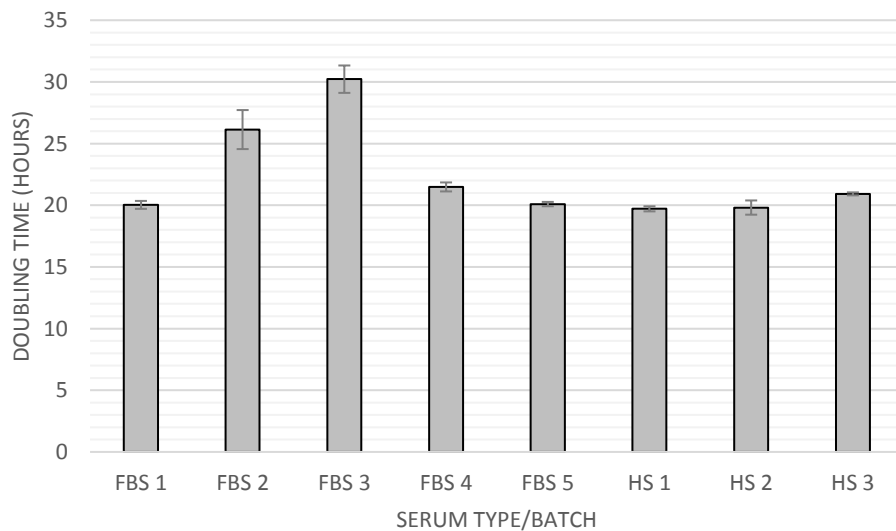


**Figure 4.6 Mean Y201 cell doubling times during the exponential growth phase of a 5 day culture period for each of the tested FBS and human serum types**

Error bars indicate the standard error of the mean for n=3. The exponential growth phase of the cells was thought to reside between days 1 and 4 of the culture and was determined through visual examination of the cell numbers shown in figure 4.1 following log conversion (figure not included).

#### 4.3.2 Cell morphology

Both MSCs and Y201s were seen to display growth-associated morphological features following five days of culture in a range of different types and batches of serum. Individual primary hBM-MSCs showed either pronounced elongation or an expanded circular shape when exposed to FBS seen to have negative effects on cell growth. Conversely, cells expanded in human or foetal serum seen to support cell growth displayed typical stromal cell morphology, similar to that documented in section 3.3.1. As with the primary cells before them, Y201s displayed a more flattened morphology when cultured in low-proliferation serum, whilst these same cells showed a standard spindle-like morphology when expanded in high-proliferation FBS. Unlike the donor-derived cells however, Y201s exposed to human serum took on a highly consistent flattened and circular morphology.

Image analysis for primary hBM-MSCs revealed that expansion in HS 1 promoted the highest level of overall growth ( $F(23)=9.85$ ,  $P=0.000$ ), with an associated average cell number significantly distinct from that of any of the bovine-derived serum batches used. In contrast to the results given above in section 4.2.1, the use of FBS 1 did not result in a rapid decline in cell density following 2 days of culture. As with cell number, a significant effect was also identified in regard to cell area ( $F(23)=20.22$ ,  $P=0.000$ ). hBM-MSCs grown in any of the three human-derived serum batches used, showed a significant decrease in area when compared to those cultured in serum of bovine origin.

For cells belonging to the Y201 lineage, serum batch and type were again seen to have a significant effect on cell growth ( $F(23)=17.36$ ,  $P=0.000$ ). HS 1 was observed to promote the highest average overall growth, being significantly greater than that seen for FBS 1, 2, 3 and 4. Conversely, the use of FBS 3 resulted in the lowest average cell count, being defined as statistically distinct from each of the other recorded values with the exception of FBS 2, which was similarly poor. A significant effect was also identified in regard to Y201 area ( $F(23)=2.50$ ,  $P=0.026$ ), with the per cell area of HS 1 cultured cells being shown to be significantly different from that of cells grown in FBS 3, which was associated with one of the lowest recorded average cell densities.

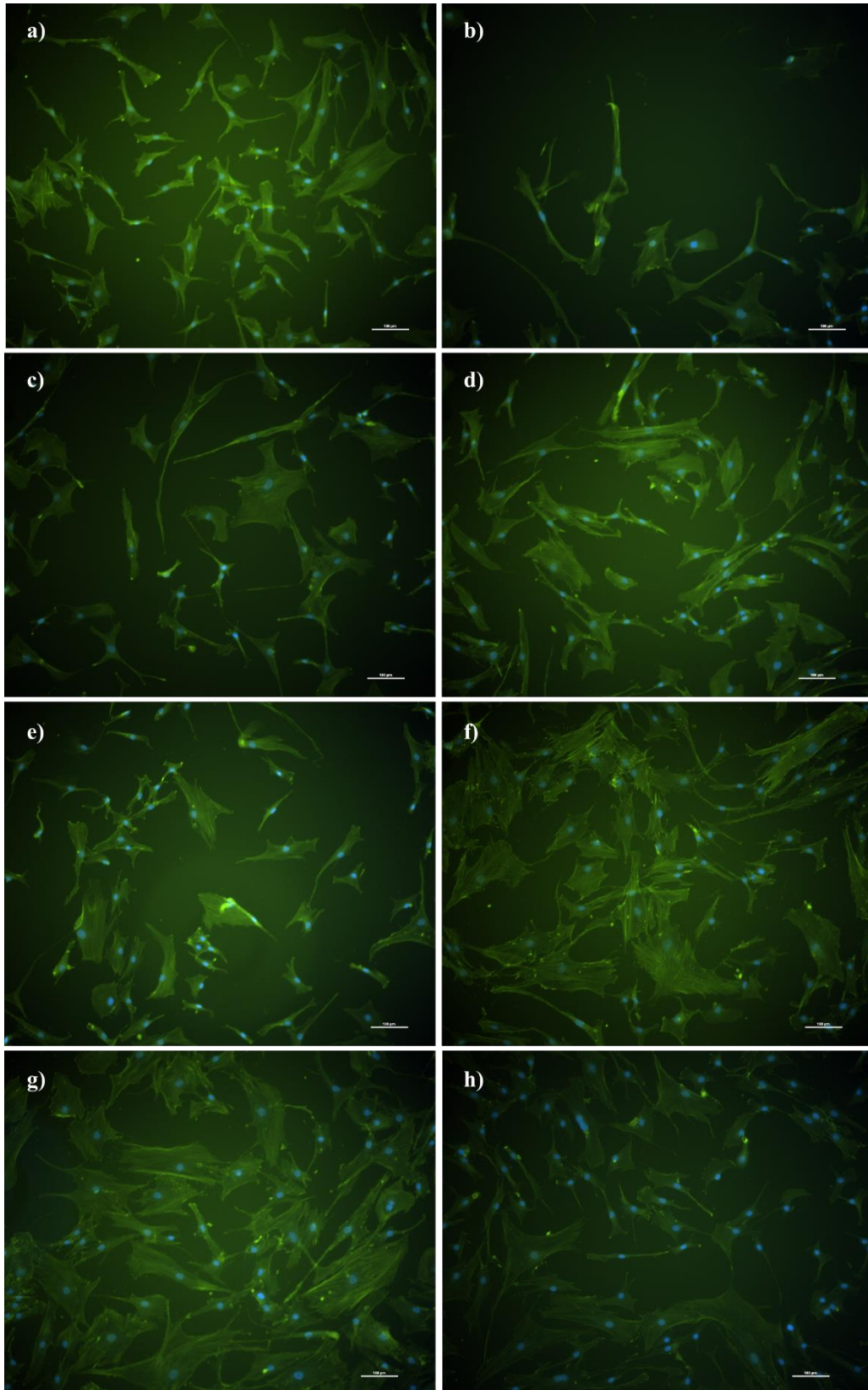


**Figure 4.7** Fluorescent microscopy images of Phalloidin and DAPI stained hBM-MSCs following culture in a series of different FBS and human serum batches

All included scale bars are indicative of a 100  $\mu\text{m}$  length. a) FBS Batch 1. b) FBS Batch 2. c) FBS Batch 3. d) FBS Batch 4. e) FBS Batch 5. f) Human Serum Batch 1. g) Human Serum Batch 2. h) Human Serum Batch 3.

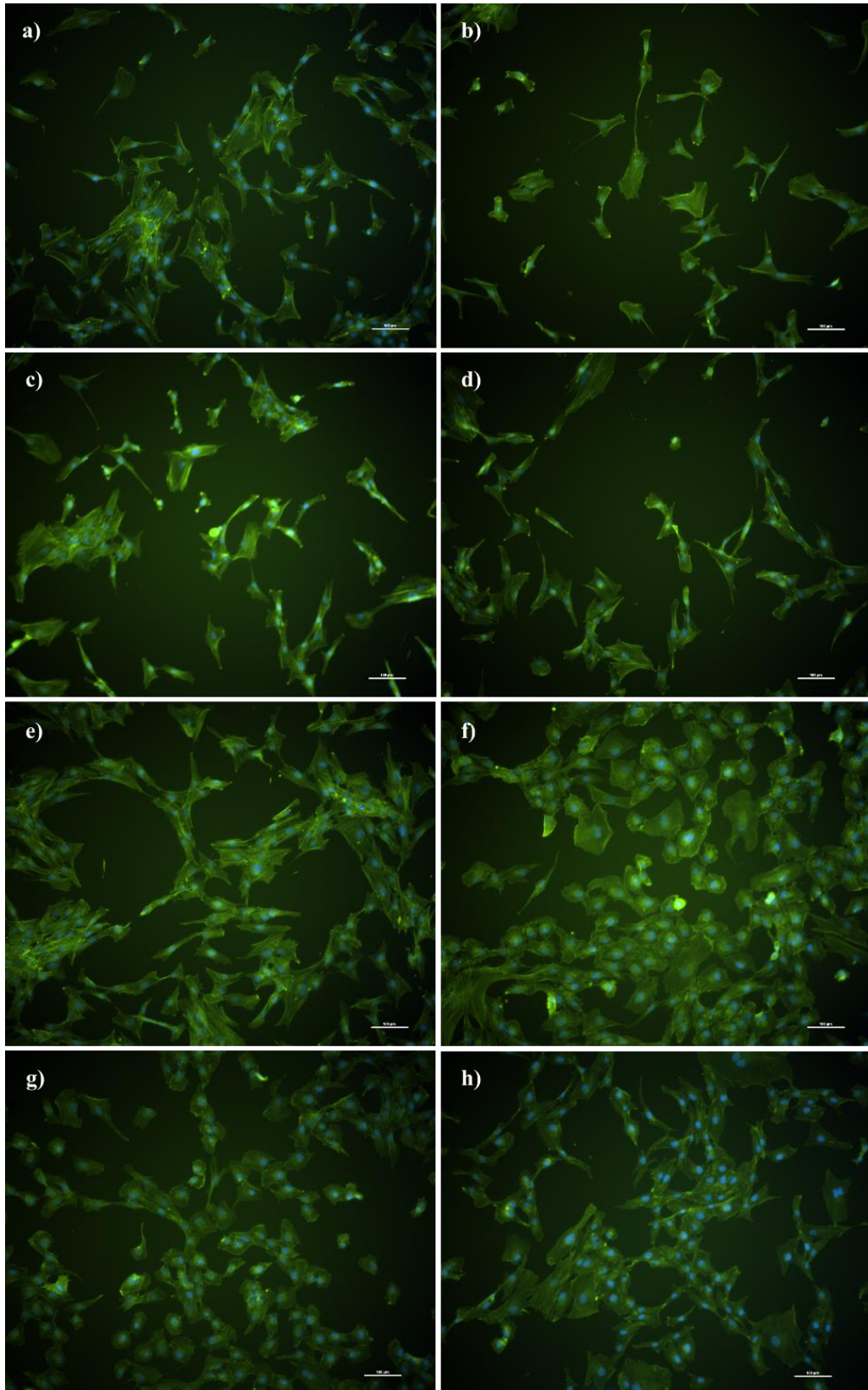


**Figure 4.8** Fluorescent microscopy images of Phalloidin and DAPI stained Y201s following culture in a series of different FBS and human serum batches

All included scale bars are indicative of a 100  $\mu\text{m}$  length. a) FBS Batch 1. b) FBS Batch 2. c) FBS Batch 3. d) FBS Batch 4. e) FBS Batch 5. f) Human Serum Batch 1. g) Human Serum Batch 2. h) Human Serum Batch 3.

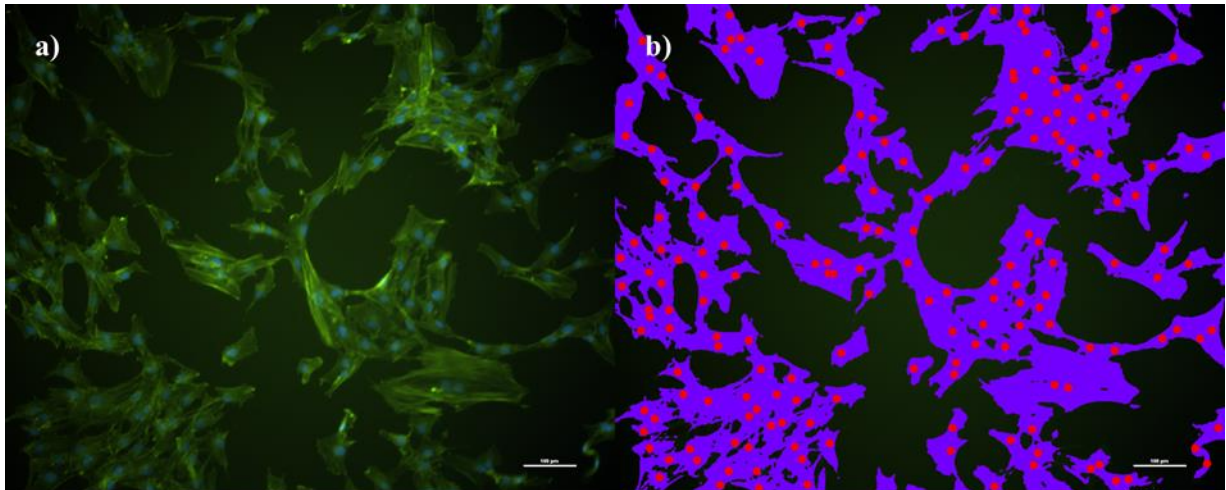


**Figure 4.9** Fluorescent microscopy image of Phalloidin and DAPI stained Y201s alongside the same image overlaid with an analysis mask used to quantify cell number and area

All included scale bars are indicative of a 100 µm length. a) Phalloidin and DAPI stained cells. b) Analysis mask with red coloured nuclei and purple coloured bodies.

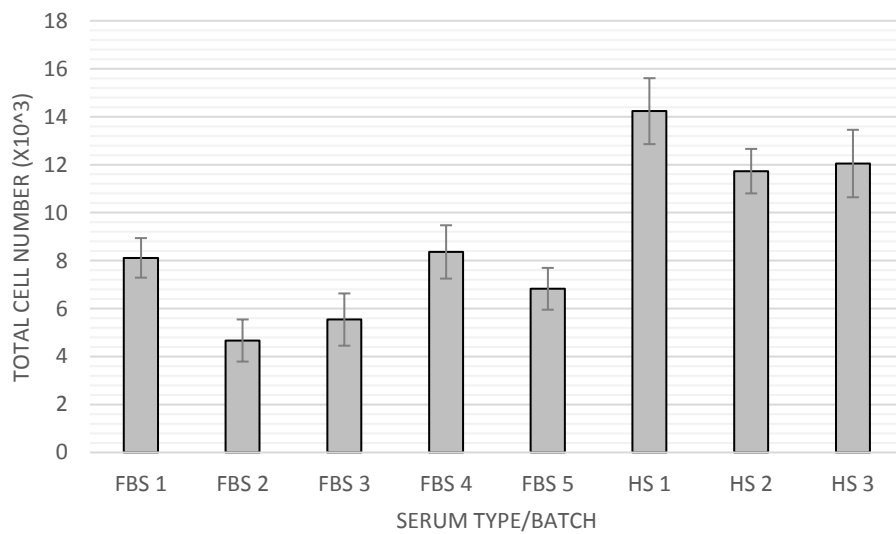


**Figure 4.10** Mean total hBM-MSC numbers on the final day of culture (day 5) for each of the tested FBS and human serum batches

Error bars indicate the standard error of the mean for n=3. Cell numbers were calculated from counts of the DAPI stained nuclei taken using dedicated image analysis software.

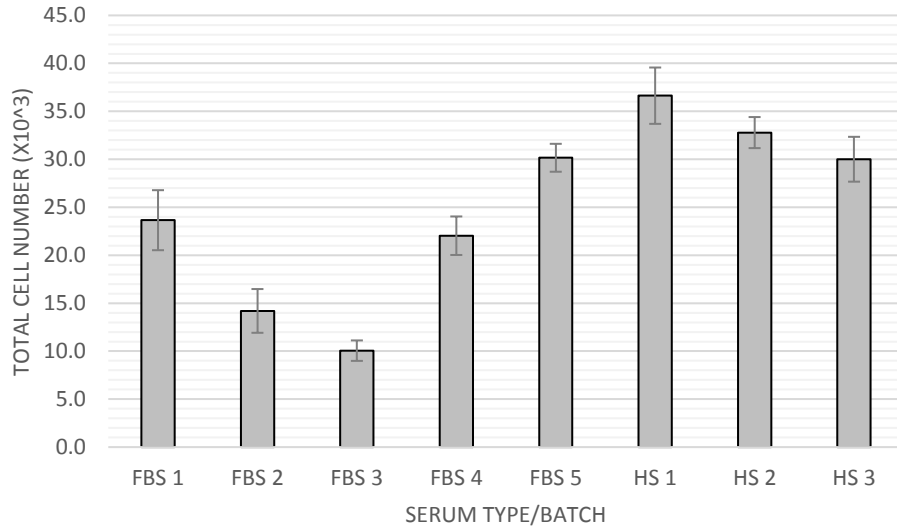


**Figure 4.11 Mean total Y201 cell numbers on the final day of culture (day 4) for each of the tested FBS and human serum batches**

Error bars indicate the standard error of the mean for n=3. Cell numbers were calculated from counts of the DAPI stained nuclei taken using dedicated image analysis software.

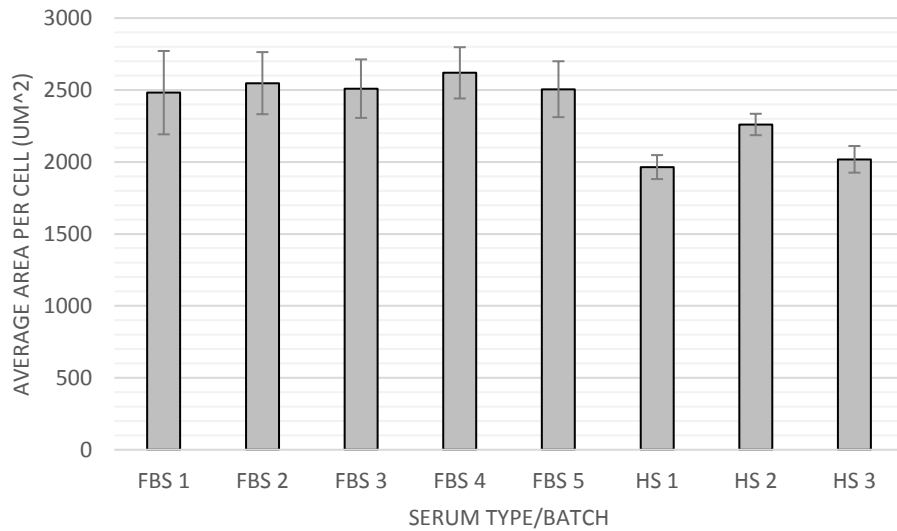


**Figure 4.12 Mean hBM-MSC area per cell on the final day of culture (day 5) for each of the tested FBS and human serum batches**

Error bars indicate the standard error of the mean for n=3. Per cell areas were calculated by measuring the total phalloidin stained area for a given image and then dividing this value by the total number of DAPI stained nuclei present.

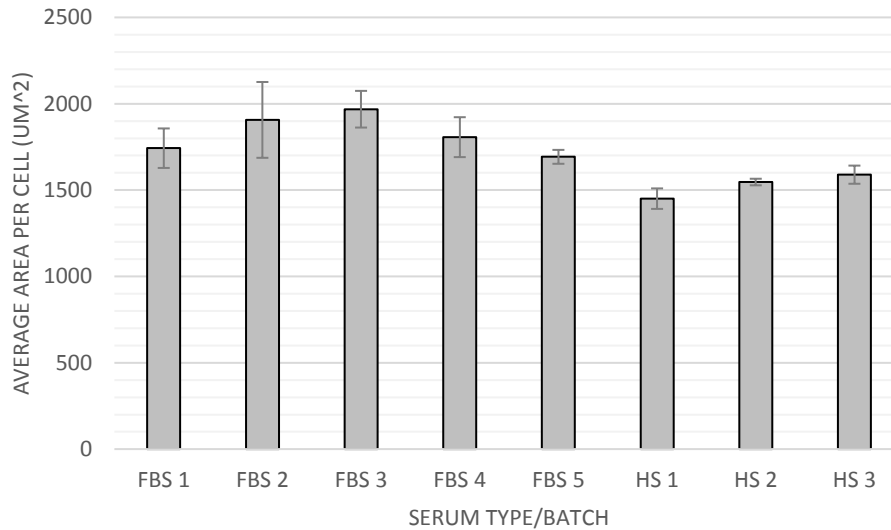


**Figure 4.13 Mean Y201 area per cell on the final day of culture (day 4) for each of the tested FBS and human serum batches**

Error bars indicate the standard error of the mean for  $n=3$ . Per cell areas were calculated by measuring the total phalloidin stained area for a given image and then dividing this value by the total number of DAPI stained nuclei present.

#### 4.3.3 Alkaline phosphatase activity

Statistically significant differences in primary hBM-MSC alkaline phosphatase (ALP) activity were identified at all of the tested timepoints; namely day three ( $F(23)=37.85$ ,  $P=0.000$ ), day four ( $F(23)=8.52$ ,  $P=0.000$ ) and day five ( $F(23)=11.91$ ,  $P=0.000$ ). On each of these days, expansion in FBS batches 2 and 3 was seen to result in significantly reduced ALP activity, specifically when compared to all other serum batches on day three, batches FBS 5, HS 1, HS 2 and HS 3 on day four and batches FBS 1, FBS 4, HS 1, HS 2 and HS 3 on day five.

Data associated with Y201 cell growth showed no similar trend, despite the identification of significant differences on both day three ( $F(23)=28.61$ ,  $P=0.000$ ) and day four ( $F(23)=24.74$ ,  $P=0.000$ ). On day three, growth in FBS 1, 4 and 5 was shown to result in significantly reduced ALP activity when compared to all other batches, whilst expansion in HS 1 led to a significant increase in ALP activity when contrasted against all other batches with the exception of FBS 2 and 3. On day four, HS 1 was again seen to result in the highest level of ALP activity when

compared to all other conditions except HS 3, whilst FBS 1 and 4 were seen to significantly reduce ALP activity when contrasted against all of the other groups.

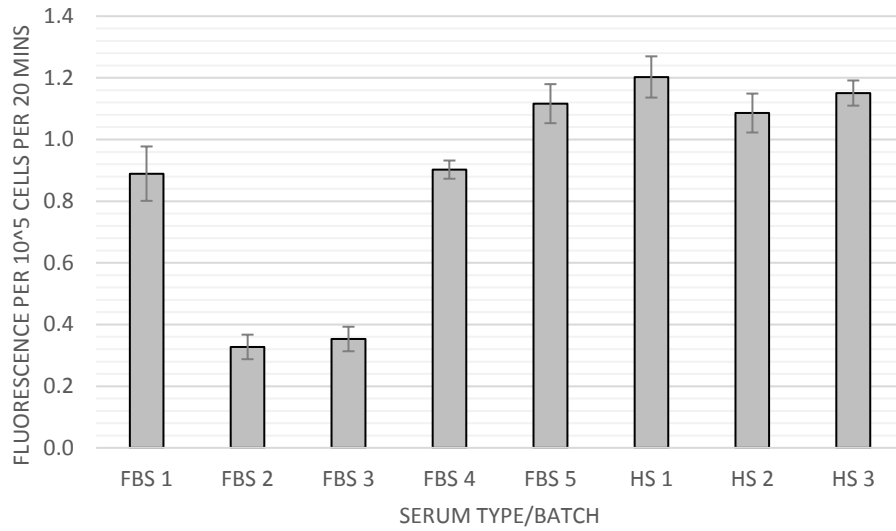


**Figure 4.14 Mean alkaline phosphatase activity as indicated by fluorescence per  $10^5$  hBM-MSCs on day 3 of culture for each of the tested FBS and human serum batches**

Error bars indicate the standard error of the mean for  $n=3$ . The fluorescence values indicated here were calculated for a 20 minute assay incubation time.

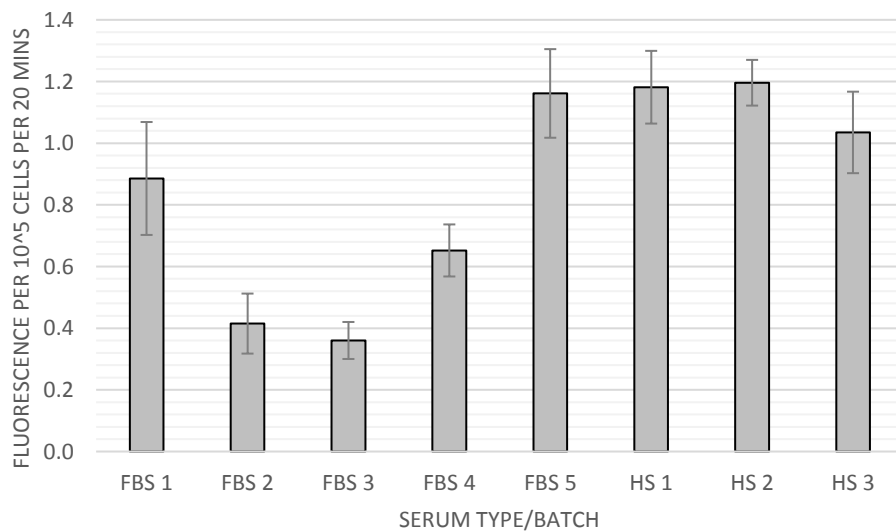


**Figure 4.15 Mean alkaline phosphatase activity as indicated by fluorescence per  $10^5$  hBM-MSCs on day 4 of culture for each of the tested FBS and human serum batches**

Error bars indicate the standard error of the mean for n=3. The fluorescence values indicated here were calculated for a 20 minute assay incubation time.

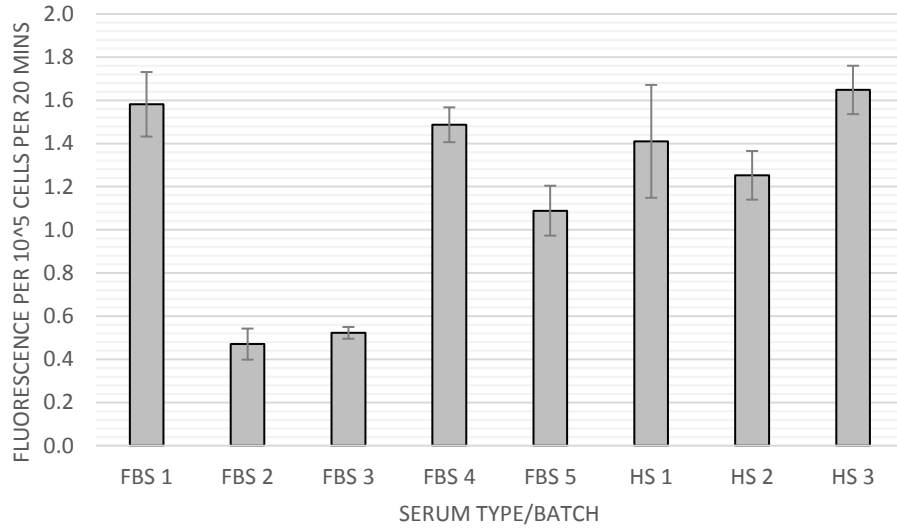


**Figure 4.16 Mean alkaline phosphatase activity as indicated by fluorescence per 10<sup>5</sup> hBM-MSCs on the final day of culture (day 5) for each of the tested FBS and human serum batches**

Error bars indicate the standard error of the mean for n=3. The fluorescence values indicated here were calculated for a 20 minute assay incubation time.

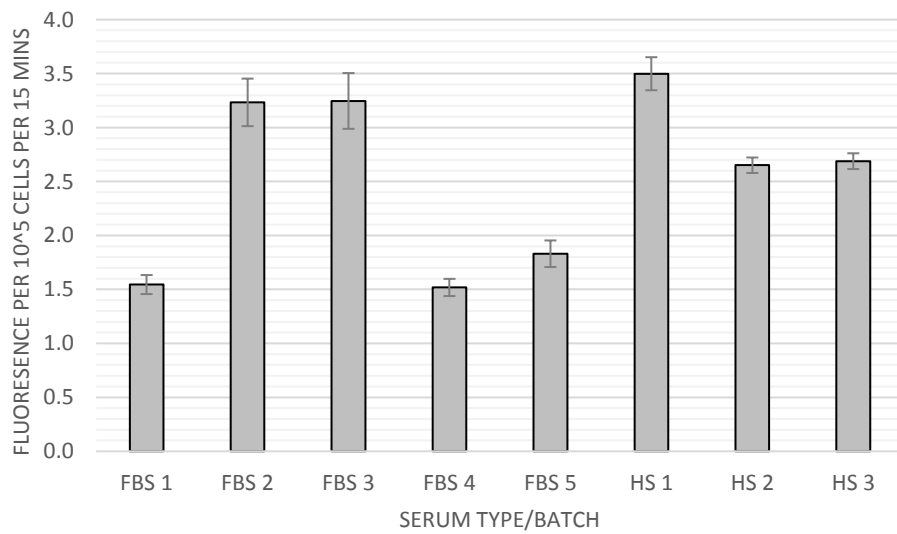


**Figure 4.17 Mean alkaline phosphatase activity as indicated by fluorescence per 10<sup>5</sup> Y201s on day 3 of culture for each of the tested FBS and human serum batches**

Error bars indicate the standard error of the mean for n=3. The fluorescence values indicated here were calculated for a 15 minute assay incubation time.

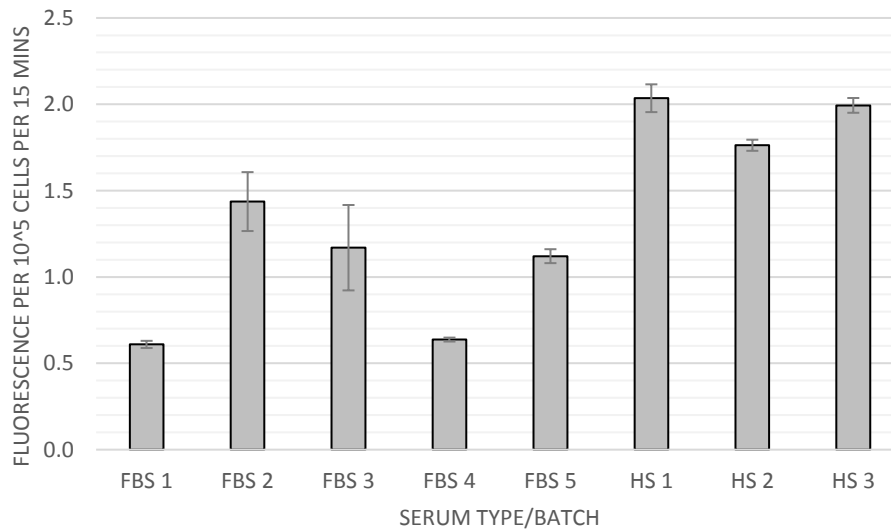


**Figure 4.18 Mean alkaline phosphatase activity as indicated by fluorescence per 10<sup>5</sup> Y201s on the final of culture (day 4) for each of the tested FBS and human serum batches**

Error bars indicate the standard error of the mean for n=3. The fluorescence values indicated here were calculated for a 15 minute assay incubation time.

#### 4.3.4 Surface marker expression

Following on from the results given in section 4.3.3, the surface marker profiles of hBM-MSCs and Y201s expanded in both low-growth and high-growth inducing FBS were evaluated. For primary hBM-MSCs, FBS 4 was identified as inducing the highest level of growth amongst the tested batches of foetal serum, whilst FBS 3 was considered to induce the lowest. Despite the apparent negative impact of FBS 1 on the growth of primary cells, the rapid decline in cell number observed when utilising this serum appeared suspicious, leading the use of FBS 3 as a suitable alternative. For Y201s, expansion in FBS 1 was seen to produce the highest peak cell densities, whilst the use of FBS 3 was seen to result in the lowest.

Analysis of the resultant data revealed no significant differences in marker expression between cells grown in high-growth versus low-growth foetal bovine serum for either of the two tested cell types when utilising the standard ISCT stromal cell panel described in section 2.4.1.

#### 4.3.5 Gene expression analysis

hBM-MSCs cultured in high and low-growth batches of serum were shown to display 2-fold or greater differences in the expression of twenty-six individual stem cell-associated genes, with the relative log<sub>2</sub> expression values and directionality of each, displayed below in figure 4.19. Of this number, twenty-one were found to be statistically significant, including a variety of key lineage specific genes such as PPARG, COL1A1 and IGF1, as shown in table 4.1. Serum batch variability was also seen to impact upon Y201 gene expression (see Figure 4.20), with a total of seven different genes displaying a 2-fold or greater shift; of which five; namely NOTCH3, RAB23, PPARG, LDLR and FZD8, were shown to be statistically significant during subsequent analysis (table 4.2).

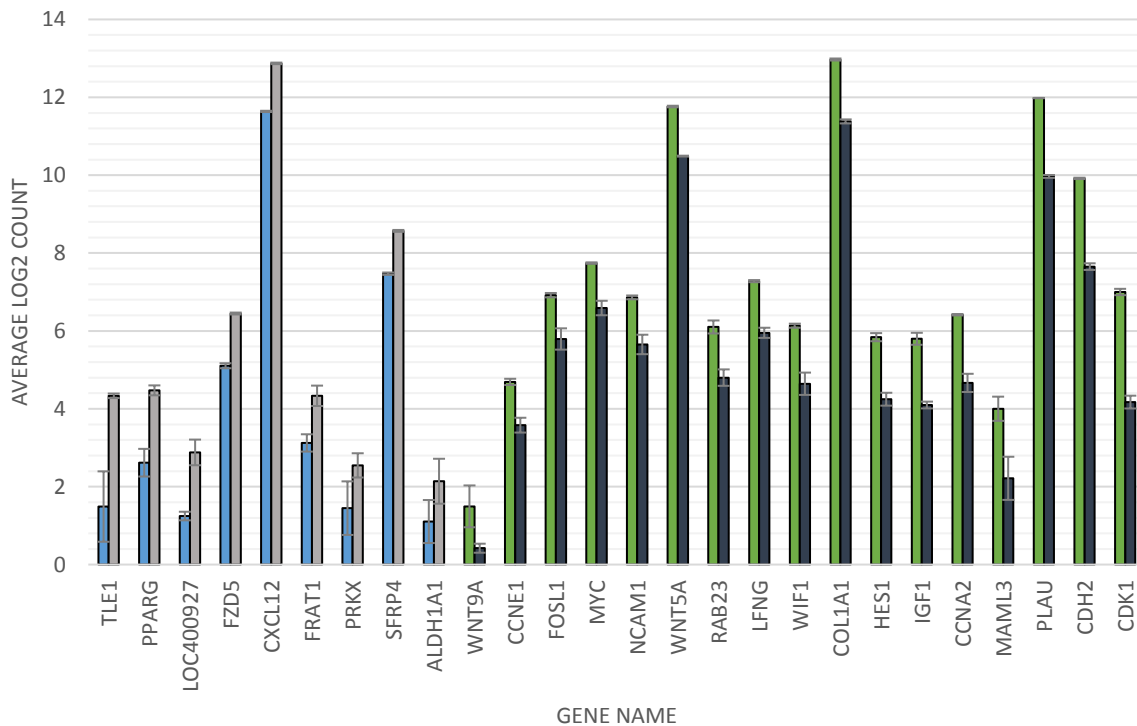


**Figure 4.19 Mean expression levels for BM-MSC-derived gene transcripts showing a minimum of 2-fold change following culture in high-growth rate FBS (FBS 4) when compared to low-growth rate FBS (FBS 3) presented in the form of log<sub>2</sub> transformed count data**

Error bars indicate the standard error of the mean for n=3. Pairs of bars coloured light blue and grey represent those genes for which expression was seen to increase following culture in a high-growth rate batch of FBS, whilst the opposite is true for those shown in green and dark blue. Bars on the left of each pair (light blue/green) are indicative of values associated with culture in a batch of FBS resulting in lower levels of cell proliferation, whereas those on the right (grey/dark blue) are linked to a batch of FBS seen to improve cell growth rates.

Gene Name	P-value	t-statistic
PPARG	0.02	4.93
LOC400927	0.03	4.70
FZD5	0.00	19.49
CXCL12	0.00	48.25
FRAT1	0.03	3.53
SFRP4	0.00	28.46
CCNE1	0.02	-5.37
FOSL1	0.05	-4.03
MYC	0.02	-6.18
NCAM1	0.04	-4.74
WNT5A	0.00	-55.5
RAB23	0.01	-4.84
LFNG	0.01	-10.00
WIF1	0.03	-5.12
COL1A1	0.00	-27.49
HES1	0.00	-8.15
IGF1	0.00	-9.63
CCNA2	0.02	-7.47
PLAU	0.00	-54.49
CDH2	0.00	-25.92
CDK1	0.00	-15.40

**Table 4.1 P-values and t-statistics associated with all genes seen to display a minimum of 2-fold change in expression at statistically significant levels in BM-MSCs following culture in high-growth rate FBS (FBS 4) when compared to low-growth rate FBS (FBS 3)**

The twenty-one genes listed here were seen to display significant differences in expression when cells were grown in high-growth rate FBS when compared to low-growth rate serum.

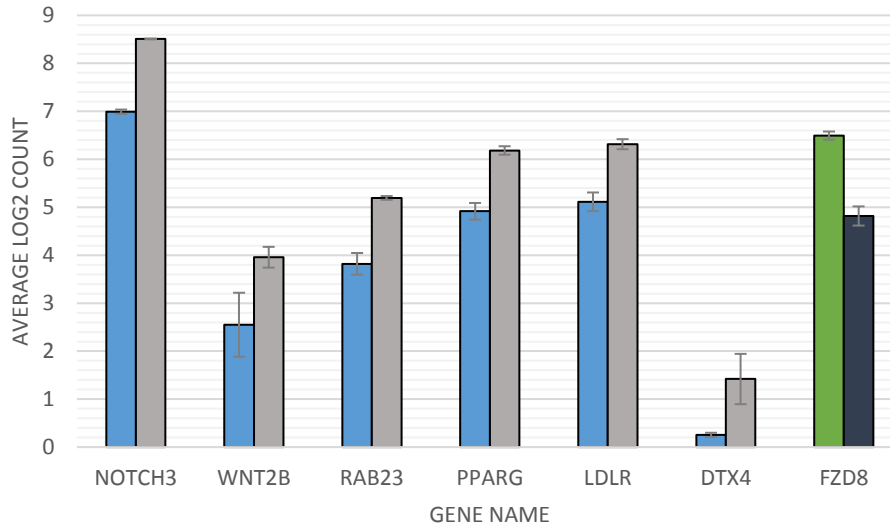


**Figure 4.20 Mean expression levels for Y201-derived gene transcripts showing a minimum of 2-fold change following culture in high-growth rate FBS (FBS 1) when compared to low-growth rate FBS (FBS 3) presented in the form of log<sub>2</sub> transformed count data**

Error bars indicate the standard error of the mean for n=3. Pairs of bars coloured light blue and grey represent those genes for which expression was seen to increase following culture in a high-growth rate batch of FBS, whilst the opposite is true for those shown in green and dark blue. Bars on the left of each pair (light blue/green) are indicative of values associated with culture in a batch of FBS resulting in lower levels of cell proliferation, whereas those on the right (grey/dark blue) are linked to a batch of FBS seen to improve cell growth rates.

Gene Name	P-value	t-statistic
NOTCH3	0.00	32.90
RAB23	0.02	5.99
PPARG	0.01	6.51
LDLR	0.01	5.43
FZD8	0.01	-7.70

**Table 4.2 P-values and t-statistics associated with all genes seen to display a minimum of 2-fold change in expression at statistically significant levels in Y201s following culture in high-growth rate FBS (FBS 1) when compared to low-growth rate FBS (FBS 3)**

The five genes listed here were seen to display significant differences in expression when cells were grown in high-growth rate FBS when compared to low-growth rate serum.

#### 4.4 Discussion

FBS variability constitutes one of the single most compelling reasons for utilising serum-free medium during mammalian cell culture processes. Despite this however, the extent to which the variability effects cell behaviour has not been extensively researched. To this end, we

assessed the extent to which both batch variability and supplier variability impacted upon MSC and Y201 proliferation, metabolism, morphology, surface marker profile and gene expression. In addition, a series of different batches of human serum were also included within the study, as a means of comparing the efficacy of the two supplements in light of the growing popularity of human-derived alternatives to FBS.

If we begin by examining cell growth and metabolic activity data, the results of the investigation clearly demonstrate that FBS variability can seriously impact upon cell growth, with the use of batches 2 and 3 resulting in significantly reduced cell densities at each stage during the culture process. These two batches were derived from a different supplier than the remaining three, suggesting that supplier variability may impact on serum performance more than lot-to-lot variation. This would make sense given that companies typically source FBS from different countries, which utilise distinct sub-species of cattle and have unique regional feed compositions. Intriguingly, no significant batch variability was seen within either of the two suppliers, both for human and foetal serum. It is likely that modernised production processes together with pooling of batches have reduced the impact of lot-to-lot variability on cell growth. It is possible that the cells experience and respond only to broad differences in serum composition due to the very high concentrations of many of the key nutrients within the supplement, which are likely far in excess of the levels required by the cells. One interesting distinction between the two cell types, is their response to the use of human serum. Whilst the primary cells appear to grow best in HS; with the efficacy of FBS appearing to decline at around day 3 of culture in most cases, Y201 expansion was equivalent in both supplements. It is important to note that the improved proliferation seen in the primary cell populations may represent a transient artefact of the change to human serum that will not persist through long-term culture. In regard to the metabolic activity data associated with these cultures, no consistent impact of serum type, batch or supplier could be identified.

The above-mentioned results were corroborated by those of the morphology assessment and related image analysis activities. Both primary MSCs and Y201s were seen to display significantly poorer growth in FBS batches 2 and 3, with the cells grown using these supplements displaying morphological features representative of increased cellular stress. Intriguingly, Y201s cultured in human serum demonstrated a shift in morphology, distinct from that seen when using any of the included batches of FBS. One possible suggestion, is that the cells could be responding to differences in extracellular matrix composition within the two

types of serum, which has been suggested as an explanation of similar morphological changes in MSC populations when cultured in HS (225).

In regard to alkaline phosphatase, primary cells showed increased levels of expression when cultured in serum more capable of supporting growth, an observation consistent with the use of high density culture as an osteogenic priming method for these cells. It is likely that increased levels of cells confluence in these cultures led to increased inter-cell interaction and some level of osteogenic priming. Interestingly, the inverse relationship was displayed by the Y201s and whilst the mechanisms underpinning this remain a mystery, it does suggest that these cells are not entirely representative of the populations from which they were derived.

The impact of FBS batch variation on gene expression revealed a number of intriguing results, again suggesting that a certain level of distinction exists between the two cell types utilised here. Beginning with the primary cells, a total of twenty-one genes showed statistically significant 2-fold or greater differences in expression when cells were cultured in low-growth versus high-growth serum. These genes; given below in table 4.3, can be seen to fall into a number of broad categories based on the direction of the observed change in expression. For instance, those genes which underwent increased expression in high-growth FBS were most commonly linked to general cell signalling processes, together with adipogenic differentiation. Interestingly, CDH2; which here showed a reduction in activity, is known to be linked to MSC adipogenesis when displaying diminished expression, corresponding to the above observation (226). Conversely, RAB23, IGF1, COL1A1 and CDH2 which have all been linked to chondrogenic differentiation in MSCs, were seen here to decrease in expression following cell culture in high-growth serum compared to low (227, 228, 226). Additionally, reductions in WNT5A and CDH2 activity are known to correspond to decreased osteogenic activity, potentially suggesting that growth in high-proliferation serum may result in decreased osteochondral potential in primary cells (229, 226).

Gene Name	Directionality	Function
PPARG	Increased	Fatty acid storage and adipogenesis
LOC400927	Increased	Cell signalling
FZD5	Increased	Receptor for the Wnt5A ligand
CXCL12	Increased	Angiogenesis, stem cell recruitment and migration
FRAT1	Increased	Wnt/ $\beta$ -catenin signalling, tumorigenesis
SFRP4	Increased	Insulin secretion, apoptosis, cell signalling
CCNE1	Reduced	Cell cycle regulation
FOSL1	Reduced	Regulation of proliferation and differentiation
MYC	Reduced	Cell cycle regulation, proliferation, apoptosis, stem cell renewal
NCAM1	Reduced	Differentiation, cell adhesion
WNT5A	Reduced	Proliferation, differentiation, inflammatory disease
RAB23	Reduced	Differentiation, chondrogenesis
LFNG	Reduced	Development, cell fate
WIF1	Reduced	Inhibits Wnt/ $\beta$ -catenin signalling
COL1A1	Reduced	Type-1 collagen formation, chondrogenesis
HES1	Reduced	Differentiation
IGF1	Reduced	Proliferation, chondrogenesis
CCNA2	Reduced	Cell cycle regulation
PLAU	Reduced	Migration, extracellular matrix degradation
CDH2	Reduced	Cell-cell interactions/adhesion
CDK1	Reduced	Cell cycle regulation

**Table 4.3 The directionality of change and general functions of genes showing a statistically significant 2-fold or greater change in expression following BM-MSC culture in high-growth rate FBS (FBS 4) when compared to low-growth rate FBS (FBS 3).**

Unlike primary MSCs before them, Y201s showed changes in expression for only a limited number of genes when cultured in high-growth serum, as seen below in table 4.4. Intriguingly, increases in both osteo-chondral and adipogenic genes were observed when utilising these cells (227, 230). It is unlikely that changes in the activity of a single gene per lineage would significantly impact upon cell phenotype or differentiation potential, however the stark contrast in response between the immortalised and primary cells does suggest that serum variability can impact even related cell types in very different ways.

Gene Name	Directionality	Function
NOTCH3	Increased	Osteogenesis
RAB23	Increased	Differentiation, chondrogenesis
PPARG	Increased	Fatty acid storage and adipogenesis
LDLR	Increased	Endocytosis
FZD8	Reduced	Receptor for the Wnt ligands

**Table 4.4** The directionality of change and general functions of genes showing a statistically significant 2-fold or greater change in expression following Y201 culture in high-growth rate FBS (FBS 1) when compared to low-growth rate FBS (FBS 3).

## 5 Chapter 5: Supplementing medium for improved cell growth and survivability in nutrient-deprived conditions

### 5.1 Introduction

In light of the findings presented in the previous chapter, the continued use of FBS as a primary media supplement in mammalian cell culture appears potentially ill-advised. Of particular concern is the apparent impact of batch to batch variability on cell proliferation and gene expression.

In order to help eliminate the need for serum, work began on the development of a novel serum-free medium for use in the expansion of hBM-MSCs and MSC-derived cell lines. A two-tiered design of experiments approach was utilised in order to screen components for the liquid portion of the media. In the first round of the investigation, a set of 12 different commonly used cytokines, growth factors and supplements were screened in sets of four for their ability to maintain cell growth in serum-deprived conditions. In the second round of testing, the most promising candidates from the initial screening were assessed in combination, using both total cell number and normalised metabolic activity, as a means of identifying the most effective formulation for use in serum-free culture.

### 5.2 Aims

1. To utilise a Design of Experiments methodology to evaluate the potential of twelve different cytokines, growth factors and commonly used medium supplements to assist in hBM-MSCs and Y201 survival in serum-deprived conditions.
2. To identify the most effective formulation of the previously screened components for use in forming the basis of a novel serum-free medium.

## 5.3 Results

### 5.3.1 Supplement screening

Twelve different cytokines and commonly used growth supplements were screened over the course of three separate fractional factorial investigations, having been separated into the three distinct groups detailed below in table 5.1. This table also includes the primary references associated with each of the molecules' initial choice and final concentrations. It should be noted that the concentrations utilised here were in many instances higher than those listed in the associated literature as a means of helping to ensure that any related effects would be detected by the employed experimental designs, despite increasing the likelihood of significant curvature effects also being included. Analysis of the data generated for group 1 revealed main effects for bFGF ( $F(26)=20.09$ ,  $P=0.000$ ), SITE ( $F(26)=32.71$ ,  $P=0.000$ ), PDGF-BB ( $F(26)=7.84$ ,  $P=0.013$ ) and TGF- $\beta$ 1 ( $F(26)=17.36$ ,  $P=0.001$ ), with each of these supplements being shown to significantly increase primary MSC metabolic activity in serum-deprived conditions. In addition, three individual two-way interaction effects were also identified, namely between bFGF and SITE ( $F(26)=8.76$ ,  $P=0.009$ ), bFGF and PDGF-BB ( $F(26)=8.43$ ,  $P=0.010$ ) and lastly bFGF and TGF- $\beta$ 1 ( $F(26)=6.14$ ,  $P=0.025$ ). Each of the associated supplements was seen to have a positive synergistic effect on cell metabolic activity when used as part of its identified pair. It should be noted that due to the confounding strategy applied here, no additional two-way or three-way interactions were examined as part of the implemented design. Finally, a significant curvature effect ( $F(26)=19.70$ ,  $P=0.000$ ) was also revealed, suggesting that the supplement concentrations used here were in excess of the minimal values required to impact upon MSC behaviour.

Across supplement groups 2 and 3, three significant main effects were identified, the first for IL-6 ( $F(26)=7.42$ ,  $P=0.013$ ), the second for HB-EGF ( $F(26)=10.61$ ,  $P=0.004$ ) and the third for ROCK ( $F(26)=5.98$ ,  $P=0.025$ ). The inclusion of either IL-6 or ROCK at the tested concentrations was shown to significantly reduce MSC metabolic activity in serum-deprived conditions. Despite the apparent positive impact of HB-EGF supplementation, a combination of the small associated effect size (see figure 5.1 below) and lack of reproducibility during subsequent testing (data not included) resulted in its exclusion from all later investigations.

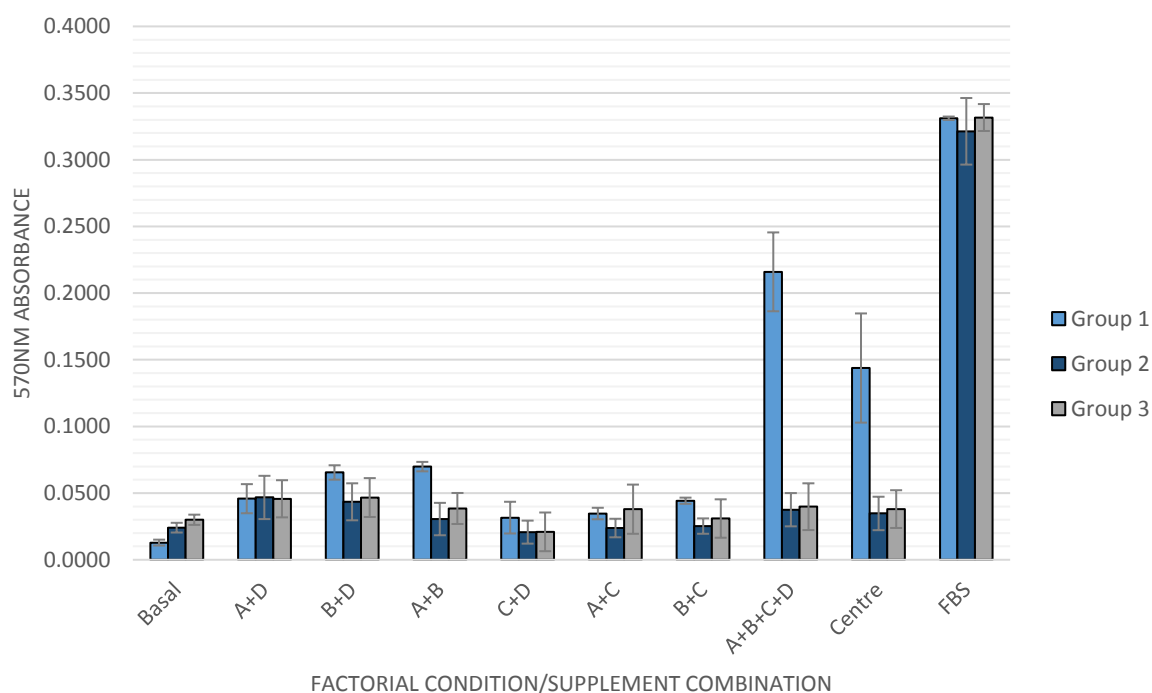


**Figure 5.1 Mean 570nm absorbance values for each of the three fractional factorial investigations used to screen potential serum-free medium supplements**

Error bars indicate the standard error of the mean for n=3. The coded designations of the supplements used in each of the three experimental rounds are described below in table 5.1. Centre point conditions represent the use of a combination of all the associated supplements at half the concentrations seen in the other factorial groupings and act as a means of assessing curvature within the design, a clear indicator that the concentrations being employed are far higher than those actually required in order to illicit the observed effects.

	<b>Component A</b>	<b>Component B</b>	<b>Component C</b>	<b>Component D</b>
<b>Group 1</b>	FGF-2 <sup>(231)</sup>	SITE <sup>(231)</sup>	PDGF-BB <sup>(193)</sup>	TGF- $\beta$ 1 <sup>(232)</sup>
<b>Group 2</b>	Ascorbic Acid <sup>(233)</sup>	SDF-1 $\alpha$ <sup>(234)</sup>	IL-6 <sup>(235)</sup>	HB-EGF <sup>(236)</sup>
<b>Group 3</b>	BMP-3 <sup>(237)</sup>	VEGF <sup>(238)</sup>	ROCK <sup>(239)</sup>	Thy- $\beta$ 4 <sup>(240)</sup>

**Table 5.1 Coded designations used for the supplements investigated in each of the three rounds of fractional factorial screening experiments, alongside the key references used to determine supplement inclusion and concentration.**

### 5.3.2 Full factorial formulation assessment

Following on from the results of the screening process described above in section 5.3.1, a 2-level full factorial formulation investigation was undertaken using the factors associated with screening group 1, as shown in figure 5.1. The highest level of cell growth in serum-deprived conditions was associated with the use of all four factors in combination at their maximum respective concentration values ( $22.2 \times 10^3$  cells). Analysis of the total cell number data for hBM-MSCs revealed four significant main effects, five significant two-way interactions and two significant three-way interactions, each of which are described in table 5.2. As with the analysis of the screening data for group 1, a significant curvature effect was also revealed, again suggesting that the supplement concentrations utilised were well above the minimal values required to impact cell behaviour in the manner described. In addition, a substantial block-based effect was also identified with regard to this data set, highlighting the existence of significant between-donor hBM-MSC variability.

Analysis of the Y201 cell number data for this same group of factors, revealed a similar set of four significant main effects alongside a pair of significant two-way interactions and a single four-way interaction, all of which are described below in table 5.3. Again, significant curvature and block effects were identified during the analysis, with the highest average cell number being associated with the use of factors A, B and D in combination ( $35.3 \times 10^3$  cells). It is important to note, that the total cell number value associated with this grouping is almost identical to that seen when using all four of the tested factors in combination ( $35.1 \times 10^3$  cells), as seen in figure 5.3.

As with the cell number data before it, examination of the normalised-metabolic activity data revealed an array of significant main effects and interaction effects for the hBM-MSC investigation. These results followed the same trend as seen for the total cell number values from the same data set, with four significant main effects, five significant two-way interactions and two significant three-way interactions alongside significant curvature and block-related effects, as shown in table 5.4. Interestingly, the Y201 data was not seen to follow a similar trend to the associated cell number data, with only a single main effect and block-related effect being identified, as displayed below in table 5.5.

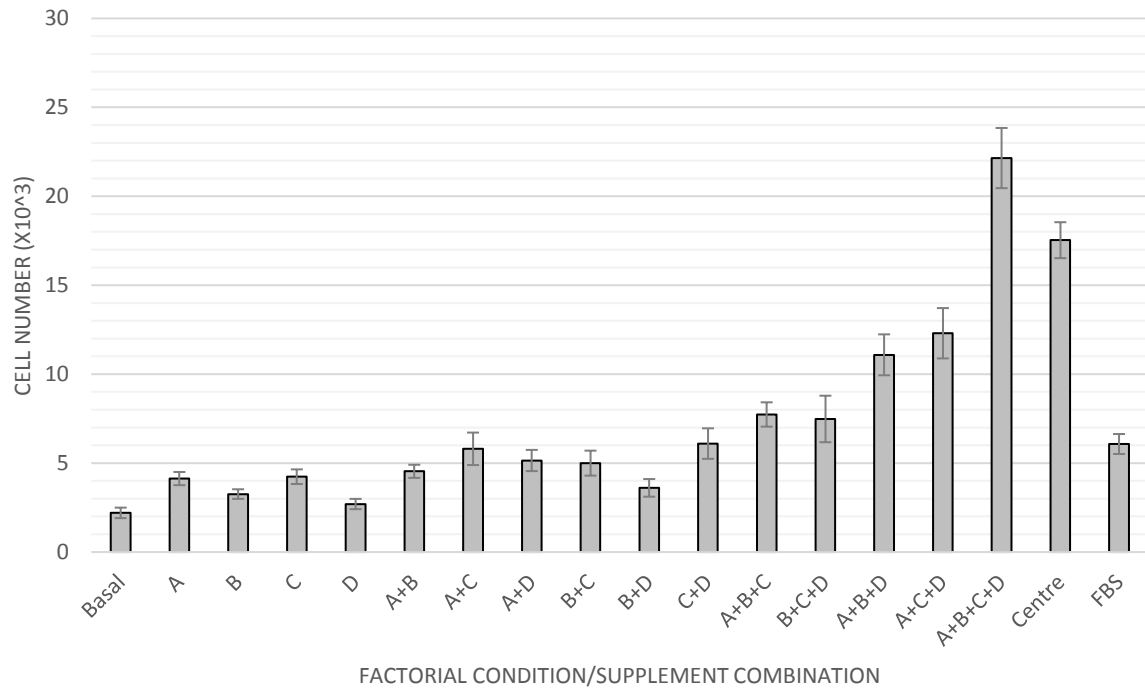


**Figure 5.2 Mean BM-MSc numbers for each of the supplement combinations included within the full-factorial formulation assessment**

Error bars indicate the standard error of the mean for n=3. The coded designations of the supplements used in each of the three experimental rounds are as described in the Group 1 row of table 5.1. Centre point conditions represent the use of a combination of all the associated supplements at half the concentrations seen in the other factorial groupings and act as a means of assessing curvature within the design, a clear indicator that the concentrations being employed are far higher than those actually required in order to illicit the observed effects.

Factor/Source	F-statistic	P-value
<b>Main Effects</b>		
bFGF	78.21	0.000
SITE	26.36	0.000
PDGF-BB	62.10	0.000
TGF- $\beta$ 1	60.43	0.000
<b>Two-way Interactions</b>		
bFGF*SITE	10.47	0.003
bFGF*PDGF-BB	7.72	0.009
bFGF*TGF- $\beta$ 1	28.90	0.000
SITE*TGF- $\beta$ 1	10.33	0.003
PDGF-BB*TGF- $\beta$ 1	15.12	0.000
<b>Three-way Interactions</b>		
bFGF*SITE*TGF- $\beta$ 1	8.98	0.005
bFGF*PDGF-BB*TGF- $\beta$ 1	5.17	0.029
<b>Additional Effects</b>		
Blocks	12.76	0.000
Curvature	93.90	0.000

**Table 5.2 Main effects and interactions table for hBM-MSc total cell number data**

The displayed values represent all of statistically significant main effects and interaction effects identified during analysis of the total cell number data associated with primary MSC factorial formulation experiment described in section 2.2.2. The total degrees of freedom for this analysis was 50.

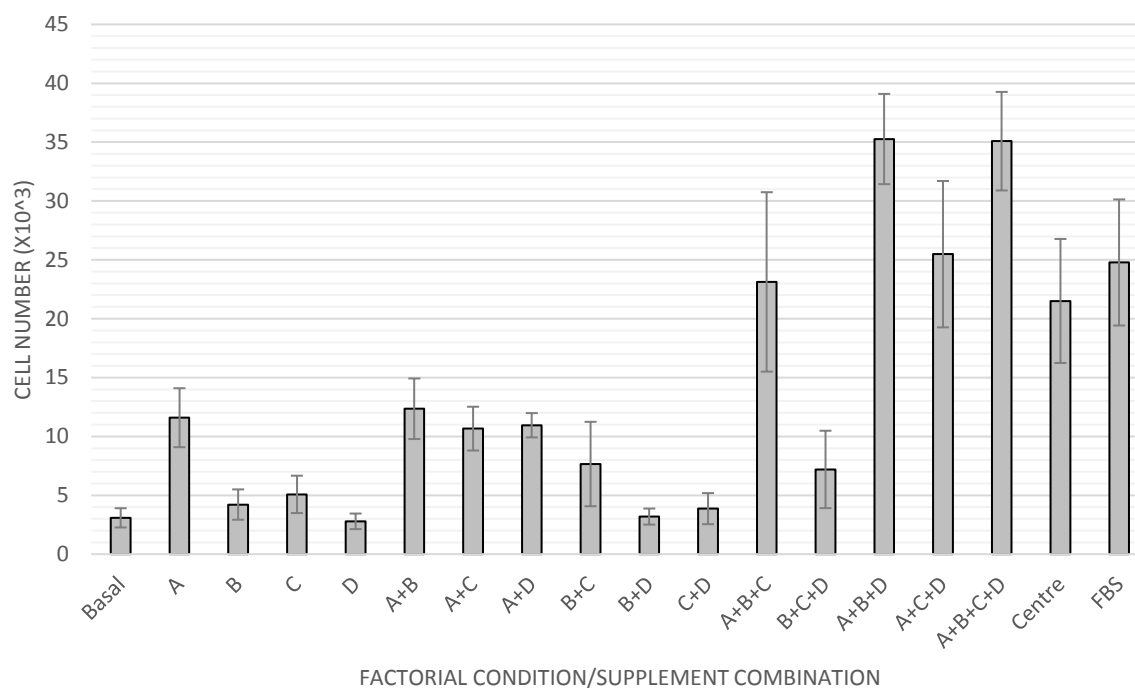


**Figure 5.3 Mean Y201 cell number for each of the supplement combinations included within the full-factorial formulation assessment**

Error bars indicate the standard error of the mean for n=3. The coded designations of the supplements used in each of the three experimental rounds are as described in the Group 1 row of table 5.1. Centre point conditions represent the use of a combination of all the associated supplements at half the concentrations seen in the other factorial groupings and act as a means of assessing curvature within the design, a clear indicator that the concentrations being employed are far higher than those actually required in order to illicit the observed effects.

Factor/Source	F-statistic	P-value
<b>Main Effects</b>		
bFGF	94.48	0.000
SITE	17.33	0.000
PDGF-BB	7.01	0.012
TGF-β1	12.34	0.001
<b>Two-way Interactions</b>		
bFGF*SITE	9.17	0.005
bFGF*TGF-β1	15.75	0.000
<b>Four-way Interactions</b>		
bFGF*SITE*PDGF-BB*TGF-β1	4.53	0.041
<b>Additional Effects</b>		
Blocks	4.04	0.027
Curvature	6.95	0.013

**Table 5.3 Main effects and interactions table for Y201 total cell number data**

The displayed values represent all of statistically significant main effects and interaction effects identified during analysis of the total cell number data associated with the Y201 factorial formulation experiment described in section 2.2.2. The total degrees of freedom for this analysis was 50.

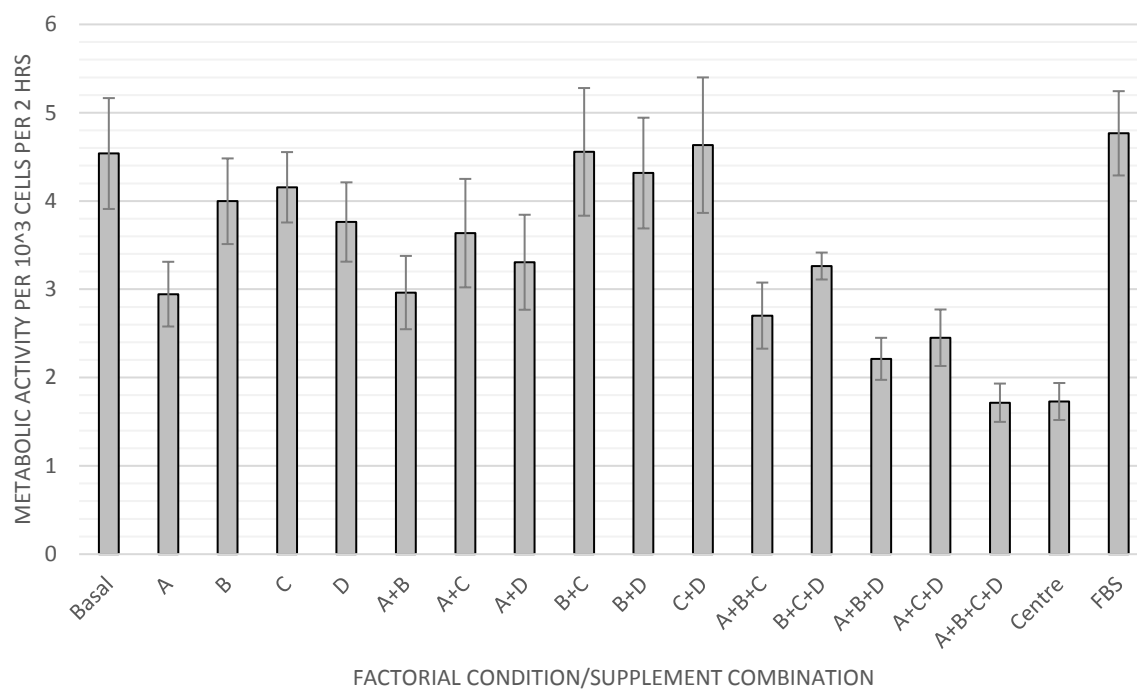


**Figure 5.4 Mean BM-MSC metabolic activity normalised to total cell number for each of the supplement combinations included within the full-factorial formulation assessment**

Error bars indicate the standard error of the mean for n=3. The coded designations of the supplements used in each of the three experimental rounds are as described in the Group 1 row of table 5.1.

Factor/Source	F-statistic	P-value
<b>Main Effects</b>		
bFGF	76.16	0.000
SITE	26.98	0.000
PDGF-BB	60.33	0.000
TGF- $\beta$ 1	58.69	0.000
<b>Two-way Interactions</b>		
bFGF*SITE	9.87	0.003
bFGF*PDGF-BB	8.11	0.007
bFGF*TGF- $\beta$ 1	29.54	0.000
SITE*TGF- $\beta$ 1	9.74	0.004
PDGF-BB*TGF- $\beta$ 1	15.63	0.000
<b>Three-way Interactions</b>		
bFGF*SITE*TGF- $\beta$ 1	9.40	0.004
bFGF*PDGF-BB*TGF- $\beta$ 1	4.77	0.036
<b>Additional Effects</b>		
Blocks	12.69	0.000
Curvature	92.76	0.000

**Table 5.4 Main effects and interactions table for hBM-MSC normalised-metabolic activity data**

The displayed values represent all of statistically significant main effects and interaction effects identified during analysis of the cell number-normalised metabolic activity data associated with the primary MSC factorial formulation experiment. The total degrees of freedom for this analysis was 50.

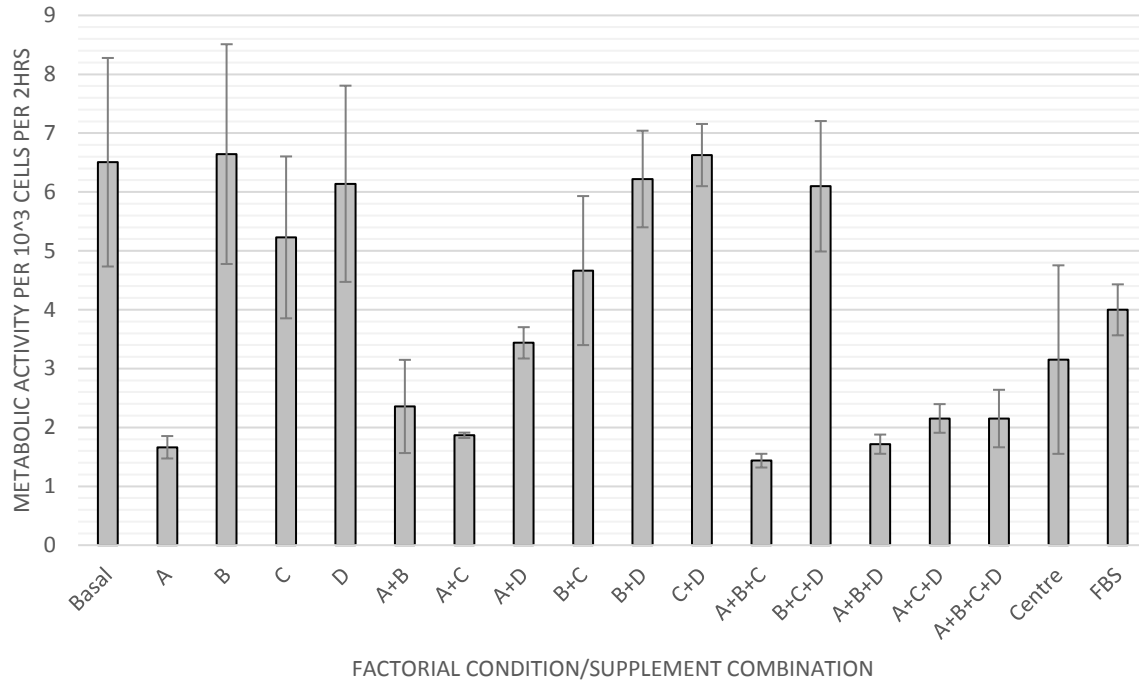


**Figure 5.5 Mean Y201 metabolic activity normalised to total cell number for each of the supplement combinations included within the full-factorial formulation assessment**

Error bars indicate the standard error of the mean for n=3. The coded designations of the supplements used in each of the three experimental rounds are as described in the Group 1 row of table 5.1. Centre point conditions represent the use of a combination of all the associated supplements at half the concentrations seen in the other factorial groupings and act as a means of assessing curvature within the design, a clear indicator that the concentrations being employed are far higher than those actually required in order to illicit the observed effects.

Factor/Source	F-statistic	P-value
<b>Main Effects</b>		
bFGF	77.28	0.000
<b>Additional Effects</b>		
Blocks	4.27	0.020

**Table 5.5 Main effects and interactions table for Y201 normalised-metabolic activity data**

The displayed values represent all of statistically significant main effects and interaction effects identified during analysis of the cell number-normalised metabolic activity data associated with the Y201 factorial formulation experiment. It should be noted that no significant interaction effects were revealed during this analysis, for which the total degrees of freedom was 50.

## 5.4 Discussion

Here we examined the impact of twelve different cytokines and growth supplements on the metabolic activity of primary human-derived MSCs in serum deprived conditions, using a series of three fractional factorial investigations. It is important to note that whilst increased metabolic activity does not necessarily correlate directly to increased proliferation, this method of assessing supplement efficacy represented the most cost-effective and efficient technique available. The results of this investigation revealed seven supplements to possess statistically significant main effects. Of these six, the impact of HB-EGF was found to be unconfirmable in subsequent follow-up experiments, whilst the use of IL-6 and ROCK had significant detrimental effects on cell metabolism. The remaining four, namely FGF-2, SITE, PDGF-BB and TGF- $\beta$ 1, were observed to support continued cellular activity in the absence of serum both individually and in any one of the three possible two-way combinations. Importantly, overall metabolic activity levels were seen to remain lower than those of cells grown in FBS-supplemented medium, suggesting but not necessarily indicating, reduced proliferation in cytokine-supplemented serum-deprived conditions.

Following on from the results of the fractional screening experiments, a full factorial formulation assessment of a medium made up of the group 1 supplements was performed. The results of this experiment confirmed those of the earlier screening activities, with each of the four factors having a statistically significant effect on cell proliferation in nutrient-deprived conditions. Again, all associated two-way interactions were shown to be positively synergistic, alongside two of the possible three-way interactions. These results correspond to the findings of groups such as Ng *et al* (2008), who demonstrated that interruption in any one of the FGF-2, PDGF-BB and TGF- $\beta$ 1 associated signalling pathways was sufficient to inhibit MSC growth, while the combination of these three molecules was capable of supporting continued cell survival in the absence of serum when utilising a commercially available serum-free basal medium (231). These findings are then further reinforced by the apparent interaction between FGF-2 and insulin-related signalling, with insulin-like growth factors having been seen to enhance the mitogenic impact of FGF-2 in umbilical cord-derived MSCs (241).

Alongside the primary cell work detailed above, a full factorial assessment was also performed using cells belonging to the immortalised Y201 cell line. The results of this experiment were similar to those observed for the primary MSCs, with all four of the group 1 supplements significantly improving cell proliferation in serum-deprived conditions. Interestingly, the

impact of PDGF-BB on cell growth appeared reduced when compared to primary cells. This effect may explain the lack any three-way interaction effects in the Y201 data group, with the two-way interactions mimicking the three-way interactions of the MSC-related results without PDGF-BB involvement.

Finally, if we examine the normalised metabolic activity data for both cell groups, we can see that per cell metabolic activity decreases in serum-free conditions as proliferation increases. The normalised metabolic activity of cells cultured in a combination of all four of the assessed supplements can be seen to be lower than that of any other experimental group for the primary cells, whilst it remains one of the lowest for the Y201s. These observations are particularly interesting when comparing the earlier screening study and the full factorial investigation. It was unknown following the fractional factorial study, whether FBS was outcompeting the most effective combination of serum-free supplements in regard to metabolic activity alone or cell number. It appears now, that the high normalised metabolic activity of primary cells grown in the presence of FBS resulted in the aforementioned disparity, and that the serum-free medium described here is capable of generating higher cell densities than growth in comparable serum-supplemented conditions.

## 6 Chapter 6: Investigating the characteristics of cells following expansion in supplemented serum-free medium

### 6.1 Introduction

Following on from the findings of the previous chapter in which an effective serum-free medium formulation was identified, it became necessary to determine whether cells grown in this medium would retain their distinctive and highly desirable MSC-related characteristics over time. Two key features of the cells were of primary concern, namely their ability to undergo tri-lineage differentiation and their unique secretory profiles, both of which have been directly linked to the therapeutic potential of MSCs.

Many research groups have sought to utilise the differentiation potential of MSCs to help replace damaged or degrading tissues via integration with native material. For example, Chen *et al* (2006) were able to differentiate cells from the same canine donor population into both osteoblasts and chondrocytes through the use of a synthetic biphasic biomaterial scaffold in an attempt to treat osteochondral defects (218). In regard to their distinctive secretory behaviours, it has been suggested that MSCs can be successfully utilised for purposes such as assisting in the re-establishment of cardiac function following myocardial infarction and aiding in the regeneration of transected rodent spinal cords, solely as a result of this phenomenon alone without the need for local engraftment (219, 220).

It should be noted that whilst the majority of the assays used in this section directly reflect those initially utilised to characterise the cells in chapter 3, additional attention was paid to both the genetic and secretory profiles of the cells in order to help properly ascertain the medium's potential impact on the two key therapeutic features mentioned above.

### 6.2 Aims

1. To determine the extent to which hBM-MSCs and Y201s grown in serum-free medium retain the characteristic morphological, differentiation and surface marker properties of their cell type.
2. To assess whether the documented morphological changes occurring as a result of serum-free culture are indicative of endothelial differentiation.

3. To identify and characterise any differences in hBM-MSC and Y201 gene expression or secretory profile between cells grown in serum-free versus serum-supplemented conditions.

## 6.3 Results

### 6.3.1 Morphological characterisation

Following culture in serum-free conditions both hBM-MSCs and Y201s displayed a morphology distinct from that of comparable cells grown in serum-supplemented medium. Numerous clumped cell masses became apparent within the cultures after as little as 3 days, whilst individual cells were seen to take on elongated shapes with lengthy processes joining together the aforementioned aggregates. Figures 6.1 and 6.2 display representative images of the cells described here.

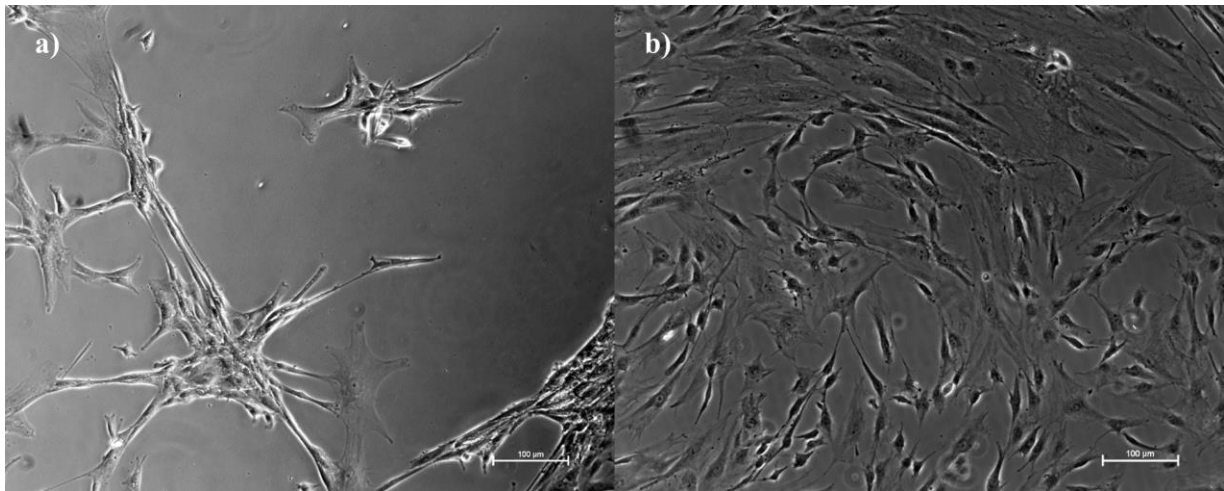


**Figure 6.1 Phase contrast images of hBM-MSCs grown in serum-free conditions alongside those grown in standard serum-supplemented medium**

All included scale bars are indicative of a 100 µm length. a) Cells grown in serum-free conditions displaying altered morphological traits. b) Cells grown in serum-supplemented medium (included for reference).

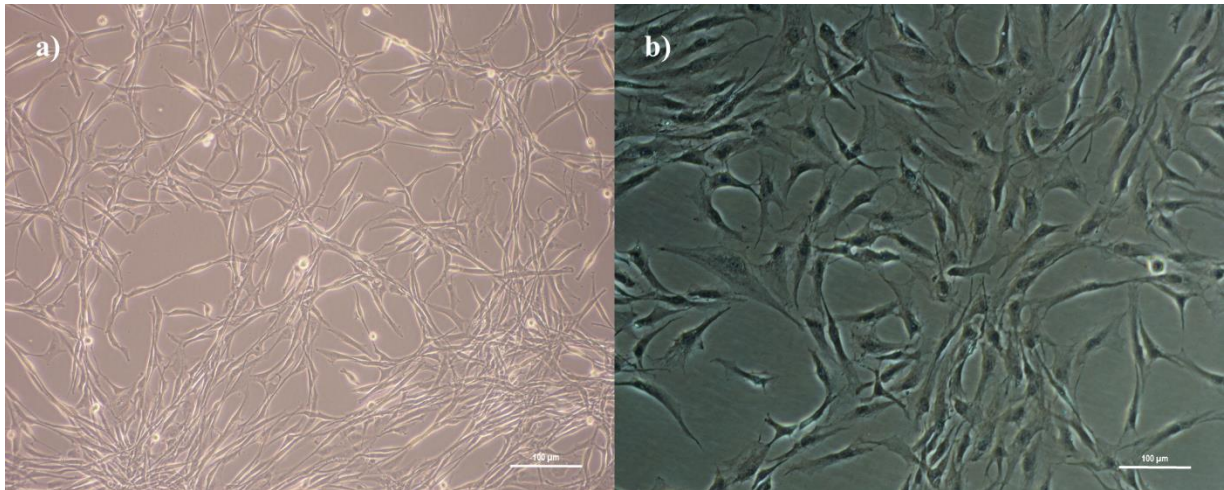


**Figure 6.2 Phase contrast images of Y201s grown in serum-free conditions alongside those grown in standard serum-supplemented medium**

All included scale bars are indicative of a 100 µm length. a) Cells grown in serum-free conditions displaying altered morphological traits. b) Cells grown in serum-supplemented medium (included for reference).

### 6.3.2 Tri-lineage differentiation potential

hBM-MSCs grown in serum-free conditions were seen to display fat droplet and mineral deposition following culture in adipogenic and osteogenic medium respectively. As with the serum supplemented cells discussed in section 3.3.2, no clear signs of chondrogenic differentiation were seen following pellet culture in appropriate medium and subsequent staining with Toluidine Blue.

Y201 cells cultured in serum-free medium displayed similar levels of adipogenic and osteogenic differentiation as their serum-supplemented counterparts, discussed in section 3.3.2. Again, cells undergoing adipogenic differentiation were seen to produce fat droplets consistent with such behaviour, whilst those undergoing the osteogenic differentiation process formed deposits of mineralised material. In keeping with the results described in chapter 3, no apparent signs of chondrogenic differentiation were seen when utilising Y201s grown in the absence of serum. Control groups, cultured in standard FBS supplemented conditions following initial growth in serum-free medium were included for reference. No observable indications of differentiation were seen in any of these control conditions after appropriate histological staining. Representative images of the cells described here can be found below in figures 6.3 and 6.4.

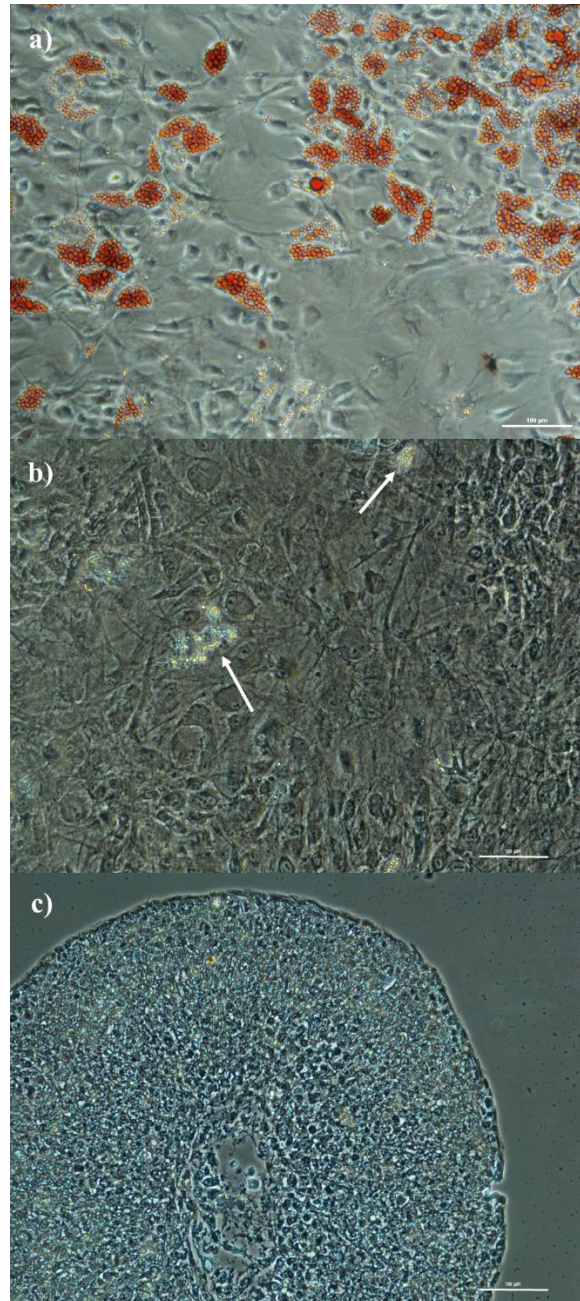


**Figure 6.3 Phase contrast images of tri-lineage differentiated hBM-MSCs following culture in serum-free conditions**

All included scale bars are indicative of a 100  $\mu\text{m}$  length. a) Oil Red-O stained fat droplets following adipogenic differentiation of cells grown in serum-free medium. b) Alizarin Red-S stained mineral deposits in osteogenically differentiated cells (as indicated by the associated arrows) following serum-free culture. c) A Toluidine Blue stained section of pellet cultured serum-free conditioned cells exposed to chondrogenic medium, with no clear indications of differentiation.

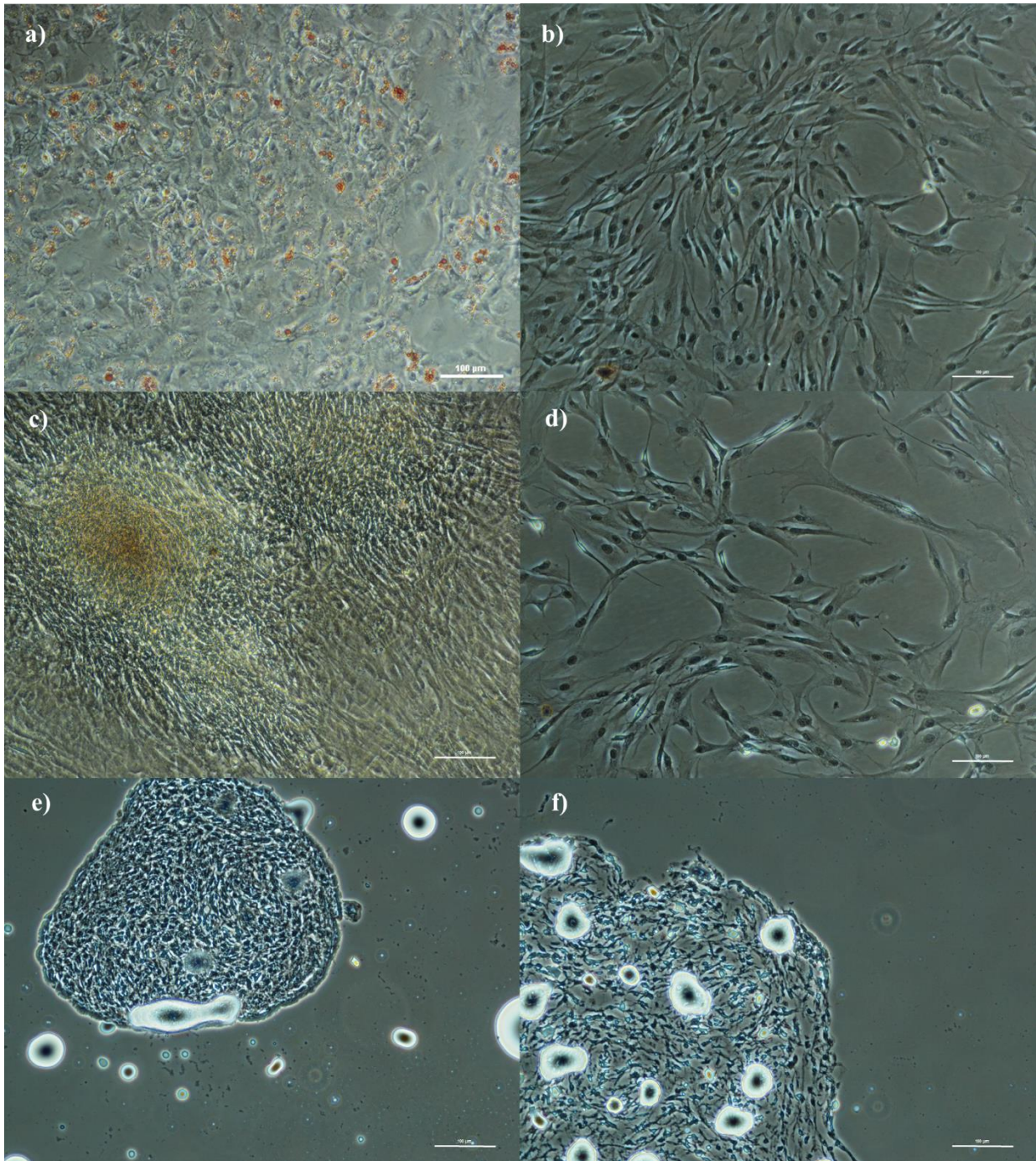


**Figure 6.4 Phase contrast images of tri-lineage differentiated Y201s following culture in serum-free conditions**

All included scale bars are indicative of a 100  $\mu\text{m}$  length. a) Oil Red-O stained fat droplets following adipogenic differentiation. b) Cells grown in standard conditions following serum-free culture and stained with Oil Red-O. c) Alizarin Red-S stained mineral deposits in osteogenically differentiated cells. d) Cells grown in standard conditions following serum-free culture and stained with Alizarin Red-S. e) A Toluidine Blue stained section of pellet cultured cells exposed to chondrogenic medium, with no clear indications of differentiation. f) Cells grown in pellet culture without chondrogenic induction medium and stained with Toluidine Blue. The artefacts present within this image represent pockets of trapped air which do not impact upon the value of the micrograph.

### 6.3.3 Cellular ac-LDL uptake

No fluorescent signal was detected in any of the ac-LDL treated cell cultures following growth in serum-free conditions. Similarly, no staining was observed in any of the associated control samples, cultured in standard serum-supplemented medium.

### 6.3.4 Surface marker expression

Analysis of the surface marker profiles of both primary hBM-MSCs ( $t(2)=14.14$ ,  $P=0.005$ ) and Y201s ( $t(2)=11.38$ ,  $P=0.008$ ) revealed significant decreases in CD105 expression for cells grown in serum-free medium when compared to standard FBS-supplemented conditions. Despite appearances, no significant differences were seen with regard to any of the other tested markers; including HLA-DR, which appeared to display subtly reduced expression in serum-free conditions as shown below in figures 6.5 and 6.6.

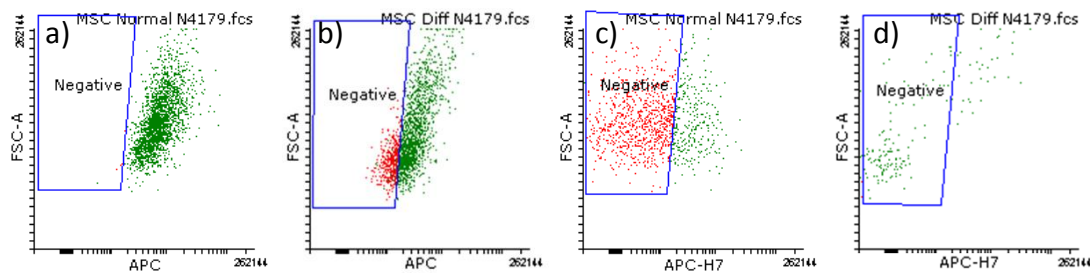


**Figure 6.5 Representative dot plots indicative of BM-MSC CD105 and HLA-DR expression following expansion in serum-supplemented and serum-free conditions**

Gate positioning for negative populations was determined using associated isotype control data. a) CD105 expression as determined by APC staining in BM-MSCs expanded in standard serum-supplemented conditions. b) CD105 expression in BM-MSCs cultured using serum-free medium. c) HLA-DR expression as determined by APC-H7 staining in BM-MSCs expanded in standard serum-supplemented conditions. d) HLA-DR expression in BM-MSCs cultured using serum-free medium.

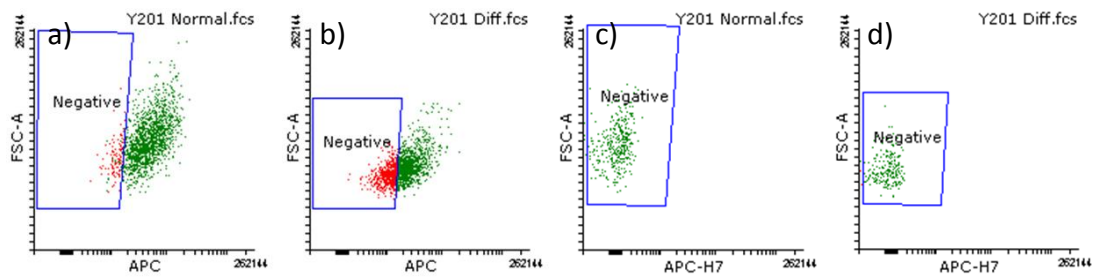


**Figure 6.6 Representative dot plots indicative of Y201 CD105 and HLA-DR expression following expansion in serum-supplemented and serum-free conditions**

Gate positioning for negative populations was determined using associated isotype control data. a) CD105 expression as determined by APC staining in Y201s expanded in standard serum-supplemented conditions. b) CD105 expression in Y201s cultured using serum-free medium. c) HLA-DR expression as determined by APC-H7 staining in Y201s expanded in standard serum-supplemented conditions. d) HLA-DR expression in Y201s cultured using serum-free medium.

### 6.3.5 Gene expression analysis

hBM-MSCs cultured using the serum-free medium formulation identified above in chapter 5 were seen to display 2-fold or greater changes in the expression of twenty-four different stem cell-associated genes, of which only a single sequence was shown to display a statistically significant shift. Y201s grown in these same conditions displayed 2-fold or greater changes in the expression of twenty individual genes, with fourteen showing a statistically significant difference when compared to culture using standard serum-supplemented medium. The log<sub>2</sub> expression values and relative directionality of each of the associated changes for the two datasets can be found below in figures 6.7 and 6.8, whilst the respective P-values and t-statistics are located in tables 6.1 and 6.2.

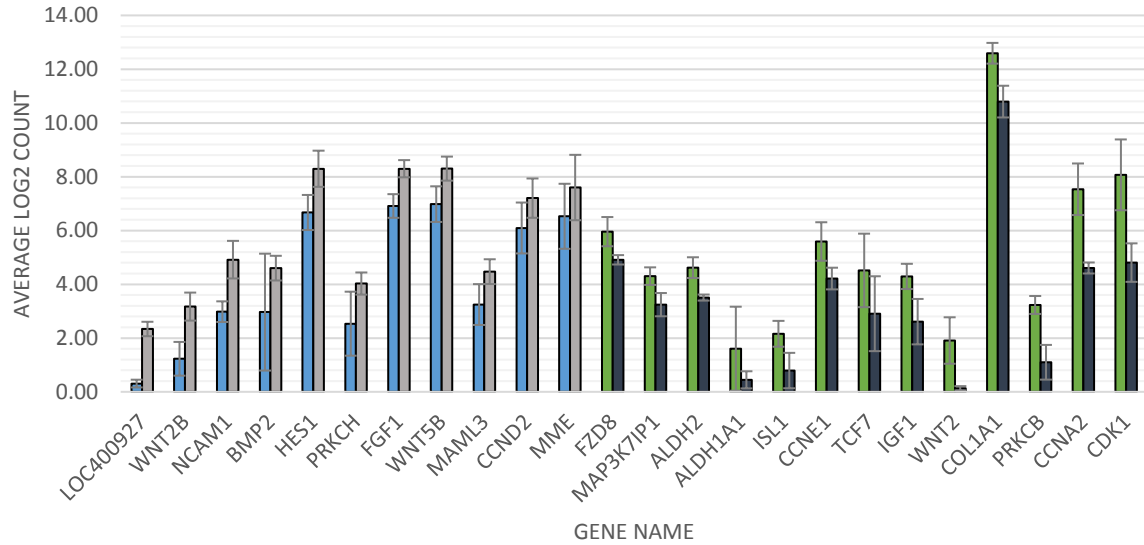


**Figure 6.7 Mean expression levels for all hBM-MSC-derived gene transcripts showing a minimum of 2-fold change following expansion in serum-free media when compared to standard serum-supplemented conditions presented in the form of log<sub>2</sub> transformed count data**

Error bars indicate the standard error of the mean for n=3. Pairs of bars coloured light blue and grey represent those genes for which expression was seen to increase following growth in the serum-free conditions, whilst the opposite is true for those shown in green and dark blue. Bars on the left of each pair (light blue/green) are indicative of values associated with growth in standard serum-supplemented media, whereas those on the right (grey/dark blue) are linked to serum-free culture.

Gene Name	P-value	t-statistic
LOC400927	0.01	6.67
<b>WNT2B</b>	<b>0.08</b>	<b>2.38</b>
<b>NCAM1</b>	<b>0.09</b>	<b>2.42</b>
<b>BMP2</b>	<b>0.53</b>	<b>0.74</b>
<b>HES1</b>	<b>0.16</b>	<b>1.73</b>
<b>PRKCH</b>	<b>0.34</b>	<b>1.19</b>
<b>FGF1</b>	<b>0.07</b>	<b>2.55</b>
<b>WNT5B</b>	<b>0.18</b>	<b>1.65</b>
<b>MAML3</b>	<b>0.25</b>	<b>1.38</b>
<b>CCND2</b>	<b>0.41</b>	<b>0.93</b>
<b>MME</b>	<b>0.57</b>	<b>0.62</b>
<b>FZD8</b>	<b>0.19</b>	<b>-1.84</b>
<b>MAP3K7IP1</b>	<b>0.13</b>	<b>-1.96</b>
<b>ALDH2</b>	<b>0.09</b>	<b>-2.77</b>
<b>ALDH1A1</b>	<b>0.54</b>	<b>-0.73</b>
<b>ISL1</b>	<b>0.17</b>	<b>-1.68</b>
<b>CCNE1</b>	<b>0.19</b>	<b>-1.67</b>
<b>TCF7</b>	<b>0.46</b>	<b>-0.82</b>
<b>IGF1</b>	<b>0.18</b>	<b>-1.74</b>
<b>WNT2</b>	<b>0.18</b>	<b>-2.04</b>
<b>COL1A1</b>	<b>0.07</b>	<b>-2.55</b>
<b>PRKCB</b>	<b>0.06</b>	<b>-2.93</b>
<b>CCNA2</b>	<b>0.09</b>	<b>-2.99</b>
<b>CDK1</b>	<b>0.12</b>	<b>-2.18</b>

**Table 6.1 P-values and t-statistics associated with all genes seen to display a minimum of 2-fold change in expression in hBM-MSCs following culture in serum-free medium when compared to a standard serum-supplemented formulation**

The twenty-three genes highlighted in bold were associated with P-values above the 0.05 threshold, suggesting a lack of statistical significance with regard to the changes in expression seen. The single remaining gene showed significant differences in expression when cells were expanded using serum-free medium rather than in serum-supplemented conditions

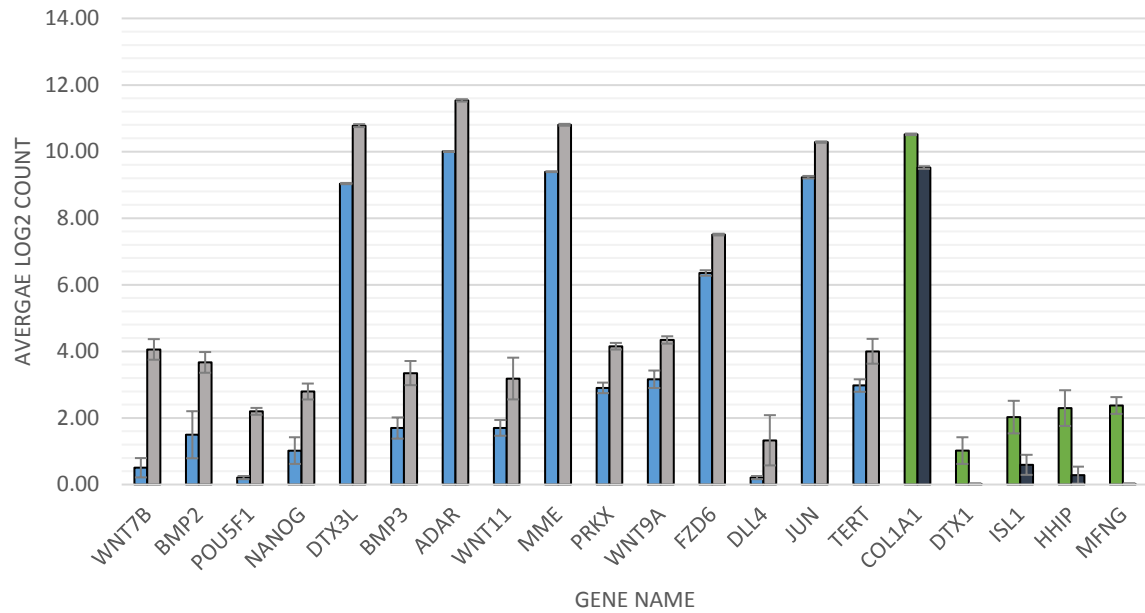


**Figure 6.8 Mean expression levels for all Y201-derived gene transcripts showing a minimum of 2-fold change following expansion in serum-free media when compared to standard serum-supplemented conditions presented in the form of log<sub>2</sub> transformed count data**

Error bars indicate the standard error of the mean for n=3. Pairs of bars coloured light blue and grey represent those genes for which expression was seen to increase following growth in the serum-free conditions, whilst the opposite is true for those shown in green and dark blue. Bars on the left of each pair (light blue/green) are indicative of values associated with growth in standard serum-supplemented media, whereas those on the right (grey/dark blue) are linked to serum-free culture.

Gene Name	P-value	t-statistic
WNT7B	0.00	8.38
<b>BMP2</b>	<b>0.07</b>	<b>2.81</b>
POU5F1	0.00	17.67
NANOG	0.03	3.79
DTX3L	0.00	36.28
BMP3	0.03	3.42
ADAR	0.00	42.78
<b>WNT11</b>	<b>0.13</b>	<b>2.21</b>
MME	0.00	46.06
PRKX	0.00	6.69
WNT9A	0.03	4.15
FZD6	0.00	13.38
<b>DLL4</b>	<b>0.28</b>	<b>1.48</b>
JUN	0.00	25.01
<b>TERT</b>	<b>0.09</b>	<b>2.46</b>
COL1A1	0.00	-21.53
<b>DTX1</b>	<b>0.13</b>	<b>-2.49</b>
<b>ISL1</b>	<b>0.08</b>	<b>-2.50</b>
HHIP	0.05	-3.39
MFNG	0.01	-9.33

**Table 6.2 P-values and t-statistics associated with all genes seen to display a minimum of 2-fold change in expression in Y201s following culture in serum-free medium when compared to a standard serum-supplemented formulation**

The six genes highlighted in bold were associated with P-values above the 0.05 threshold, suggesting a lack of statistical significance with regard to the changes in expression seen. The remaining fourteen genes showed significant differences in expression when cells were expanded using serum-free medium rather than in serum-supplemented conditions

### 6.3.6 Identifying and characterising cell protein secretions

Of the forty factors included within the panel, a total of twenty-five were seen to be expressed at measurable levels within the primary hBM-MSC associated media samples (see figure 6.9). Activity from the remaining fifteen stayed below the threshold of measurement for the MSD assay, resulting in their exclusion from all subsequent analyses. Similarly, cells belonging to the Y201 lineage were seen to exhibit poor expression across all forty of the investigated factors and as such were also excluded from all later analyses. Due the multi-dimensional nature of the data set, Principle Component Analysis (PCA) was performed on the relative expression values for each of the experimental groupings, following normalisation to total cell number. PCA condenses complex data sets into a limited number of overarching variables, known as principle components, defined by their ability to adequately convey the maximum amount of variability within the source data, whilst allowing reconstruction of the original values if

necessary. In essence, these principle components accurately summarise the original data set in the most concise way possible. In this particular instance, a total of ten principle components (PCs) were extracted from the data, an overview of which can be seen across table 6.3 and figure 6.10. Importantly, over 70% of the observed variability associated with the data set was seen to be explained utilising the first 2 principle components alone, the respective elements of which are summarised in tables 6.4 and 6.5. When plotted as a score plot, as seen in figure 6.11, the experimental groups displayed a distinct pattern of clustering, with the first PC separating the TNF- $\alpha$  treated cells from the untreated cells, whilst the serum-free and serum-supplemented groups were distinguished based upon their interaction with PC2. Finally it is important to note that, whilst no passage-related effects were identified, analysis of the LPS control data did show that both IL-8 and sVCAM-1 secretion increased considerably when compared to all of the other measurable factors with the exception of IP-10, MCP-1 and VEGF (F(23)=3.79, P=0.000), each of which showed relatively high levels of expression following exposure of cells to LPS (see figure 6.12).

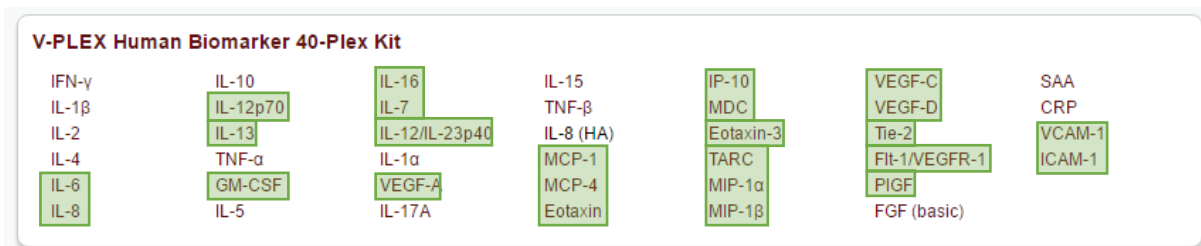


**Figure 6.9 Overview of the V-PLEX Human biomarker panel**

All entries highlighted in green were seen to display a measurable level of expression in some or all of the experimental groups and as a direct result, were included in all subsequent analyses.

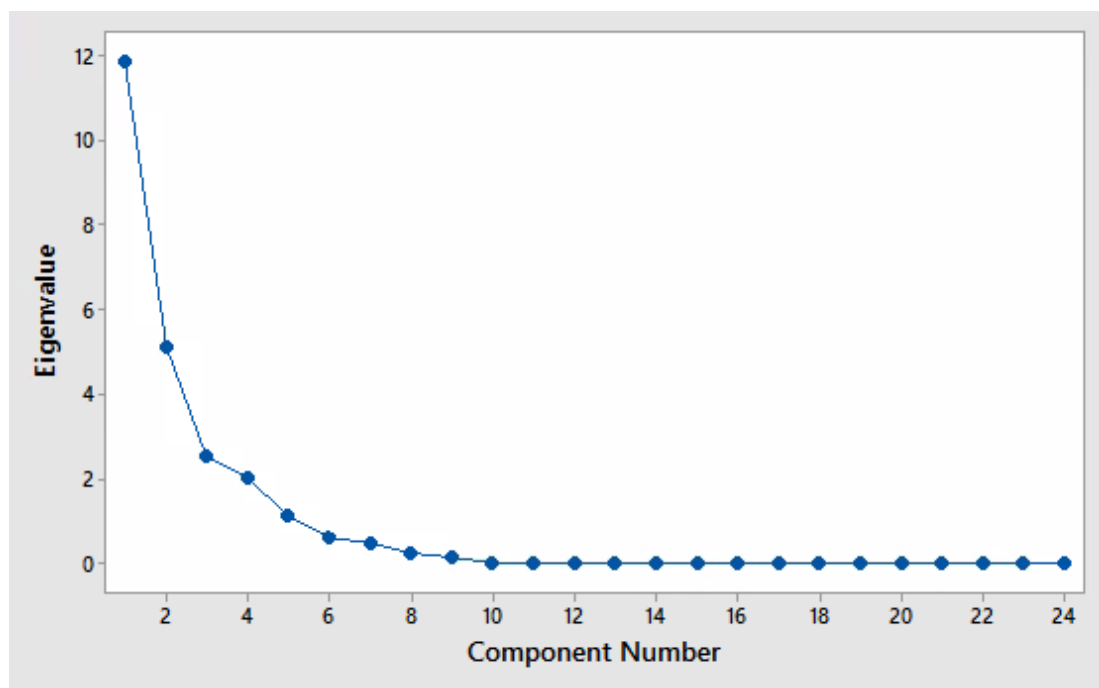


**Figure 6.10** Scree plot corresponding to the analysis of the combined serum-free, serum-supplemented and TNF-treated data sets

The plot shows a rapid early descent followed by a gradual slope downwards, indicating that the first two principle components likely correspond to the vast majority of the variability present within the data, as would be expected when utilising PCA on an appropriately structured data set.

	PC1	PC2	PC3	PC4	PC5	PC6	PC7	PC8	PC9	PC10
Eigenvalue	11.839	5.113	2.540	1.985	1.097	0.591	0.467	0.236	0.133	0.000
Proportion	0.493	0.213	0.106	0.083	0.046	0.025	0.019	0.100	0.006	0.000
Cumulative	0.439	0.706	0.812	0.895	0.941	0.965	0.985	0.994	1.000	1.000

**Table 6.3** Overview of the first 10 principle components identified for the combined serum-free, serum-supplemented and TNF-treated data sets.

Eigenvalues, proportion of explained variability and cumulative proportion of variability are each included within their respective rows.

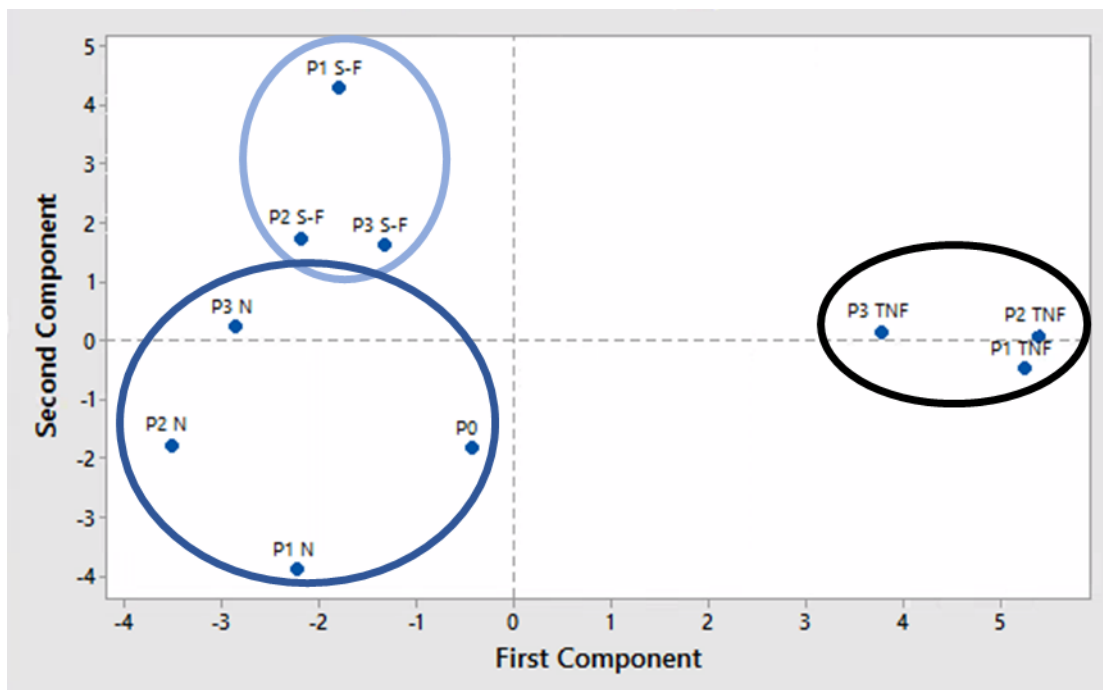


**Figure 6.11** Score plot for the first two identified principle components

Circled collections of data points indicate the impact of PC1 and PC2 on the various experimental groupings. PC1 can be seen to help distinguish between TNF-treated and untreated cells, whilst the serum-free and serum-supplemented conditions can be separated based upon their interaction with PC2.

Principle Component 1	
Positive	Negative
Eotaxin-3	MCP-4
IL-8	PIGF
IP-10	Tie-2
MIP-1 $\alpha$	VEGF
MIP-1 $\beta$	VEGF-C
TARC	VEGF-D
GM-CSF	IL-16
sICAM-1	IL-7
IL-12 P70	sVCAM-1
IL-13	
IL-6	

**Table 6.4** Experimental factors seen to contribute to Principle Component 1

Factors were distinguished as positive or negative depending upon whether they were seen to increase or decrease in-line with the stated principle component.

Principle Component 2	
Positive	Negative
Eotaxin	PIGF
Eotaxin-3	IL-7
MCP-1	
MIP-1 $\beta$	
TARC	
sFlt-1	
Tie-2	
VEGF	
VEGF-C	
VEGF-D	
IL-16	

**Table 6.5 Experimental factors seen to contribute to Principle Component 2**

Factors were distinguished as positive or negative depending upon whether they were seen to increase or decrease in-line with the stated principle component.

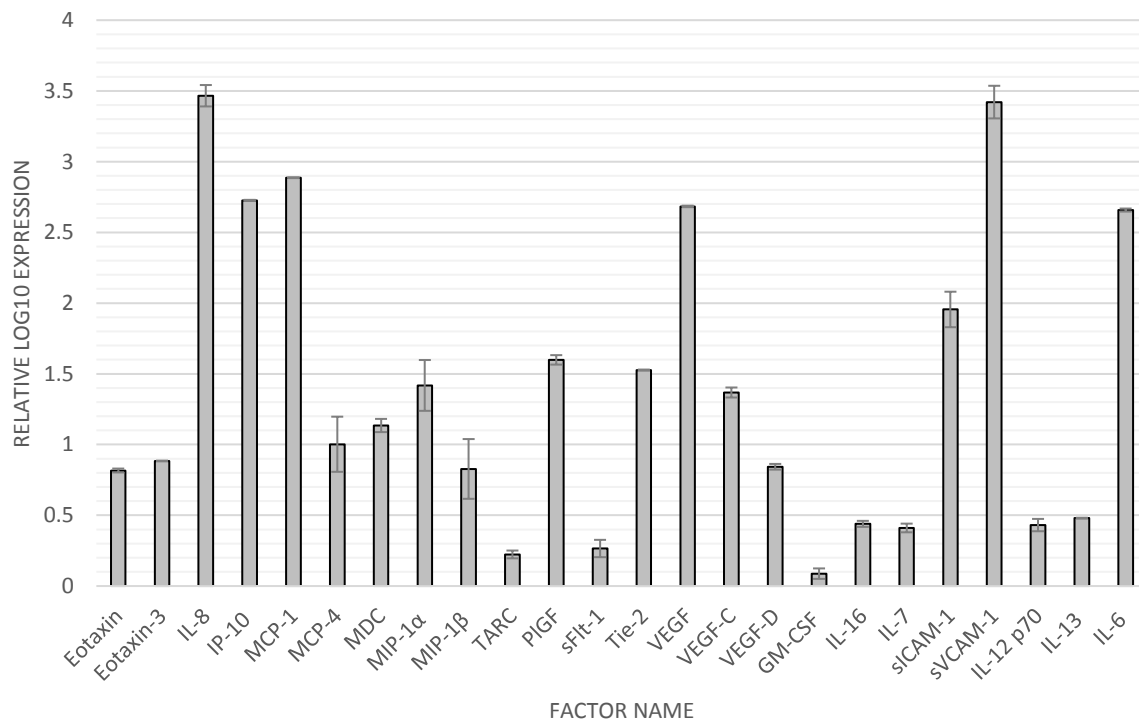


**Figure 6.12 Log<sub>10</sub> transformed normalised expression data for LPS treated hBM-MSCs**

Error bars indicate the standard error for n=3. hBM-MSCs can be seen to readily secrete a wide range of different factors in response to LPS exposure.

## 6.4 Discussion

Following on from the findings of the previous chapter, in which it was shown that primary and immortalised MSCs could be successfully expanded in a serum-free medium supplemented with FGF-2, SITE, PDGF-BB and TGF- $\beta$ 1, the characteristics of these cells were assessed. Both MSCs and Y201s were seen to undergo a significantly shift in morphology following five days in serum-free culture. The specifics of this change appeared endothelial in nature, due to the elongated tube-like protrusions seen between larger cell aggregates. As a direct result, CD31 was included within the subsequent surface marker analysis, whilst an ac-LDL uptake assay was also performed. Interestingly, no fluorescence was detected following treatment of the cells with fluorophore-conjugated ac-LDL, nor was any expression of CD31. In fact, the only surface marker-related distinction between the serum-free and serum-supplemented cell groups, came in the form of significantly reduced CD105 expression, which was observed across both of the tested cell types. This decrease, is consistent with the findings of Lee *et al* (2017) and Brohlin *et al* (2017), and is thought to have a detrimental effect on the therapeutic potential of these cells in the treatment of myocardial infarction (242, 243, 244). It is important to note however, that CD105 negative murine MSCs have been shown to better regulate immune system activation as a result of increased IL-6 secretion, potentially suggesting altered, rather than diminished, clinical relevance following serum-free expansion (245). Intriguingly, the HLA-DR expression profiles of Y201s grown in serum-free medium containing high concentrations of FGF-2 remained negative for HLA-DR expression, implying that some element of cell origin is likely involved in the interaction explored earlier in section 3.3.4.

Despite differences in cell morphology and marker expression, no readily apparent changes in the differentiation potential of the cells grown in serum-free medium were detected. Again, no chondrogenic differentiation was observed in either of the tested cell groups, reaffirming the hypothesis that either a protocol or cell-related issue was to blame. In regard to gene expression, whilst only a single cell-signalling related gene saw significant changes in expression for the primary MSCs (table 6.6), a total of fourteen genes displayed significant 2-fold or greater change for the Y201 cell group. As can be seen below in table 6.7, increases in expression occurred for a range of genes linked to cell self-renewal, stemness, proliferation and DNA repair. These findings support those of Lotz *et al* (2013), who reported that supplementation with FGF-2 helped to maintain the iPSC undifferentiated phenotype in prolonged culture through interactions with stemness-related genes such as nanog (246). It is important to note

that only a very limited number of genes showing 2-fold or greater change irrespective of significance were consistent between the two cell groups, again indicating a distinct lack of similarity between the primary and immortalised cells.

Gene Name	Directionality	Function
LOC400927	Increased	Cell signalling

**Table 6.6** The directionality of change and general functions of genes showing a statistically significant 2-fold or greater change in expression following BM-MSC culture in serum-free medium when compared to serum-supplemented conditions.

Gene Name	Directionality	Function
WNT7B	Increased	Proliferation, differentiation
POU5F1	Increased	Self-renewal, osteogenesis
NANOG	Increased	Self-renewal, stemness
DTX3L	Increased	DNA repair
BMP3	Increased	Proliferation, inhibition of osteogenesis
ADAR	Increased	Purine metabolism
MME	Increased	Peptide cleavage
PRKX	Increased	Differentiation
WNT9A	Increased	Proliferation, differentiation
FZD6	Increased	Receptor for the WNT4 ligand
JUN	Increased	Cell cycle regulation, anti-apoptotic
COL1A1	Reduced	Type-1 collagen formation, chondrogenesis
HHIP	Reduced	Developmental processes
MFNG	Reduced	Developmental processes

**Table 6.7** The directionality of change and general functions of genes showing a statistically significant 2-fold or greater change in expression following Y201 culture in serum-free medium when compared to serum-supplemented conditions.

Finally, as can be seen from the protein analysis data displayed in section 6.3.6, the secretory profile of primary cells cultured in serum-free medium is quite distinct from that of cells expanded in FBS-supplemented conditions. Of primary importance is the apparent reduction in angiogenic potential displayed by cells grown in serum-free medium, which appeared to express reduced PIGF and increased sFlt-1 activity, which are known to promote and inhibit vascularisation respectively. These findings support earlier indications of reduced therapeutic potential in ischemia-related conditions, in which the activation of neo-vascularisation is known to play an important role. Intriguingly, in contrast to related reports regarding CD105-reduced cells, primary MSCs displayed increased expression of molecules responsible for the recruitment of immune cells such as Eotaxin, Eotaxin-3, IL-16, TARC and MCP-1, the vast

majority of which are linked to eosinophil and monocyte enlistment. Taken together, these results suggest that cells cultured in the medium described here could be of use in the treatment of conditions linked to infection with multicellular parasites.

## 7 Chapter 7: Screening extracellular matrix proteins for enhanced cellular adhesion and viability

### 7.1 Introduction

In chapter 5, a medium formulation was identified that effectively supported the proliferation of MSCs in serum-deprived conditions. However, due to the multifaceted nature of foetal bovine serum, which provides both nutritional support and the proteins required for cell-substrate adhesion, it became necessary to screen extracellular matrix proteins for inclusion within the formulation as a means of completely eliminating the need for serum.

As with the liquid components before them, a design of experiments approach was utilised in order to screen selected ECM proteins in regard to their ability to support cell adhesion in the absence of serum. Unlike the previous system however, a single set of factorial experiments was performed due to the limited number of proteins being investigated, with these specific molecules having been selected based on a combination of availability, cost and literature investigation (247, 248, 249). Prior to beginning the screening process a series of aminosilane functionalised glass surfaces were produced and characterised, in order to provide a suitable substrate on which to assess protein efficacy in a consistent and controlled manner.

### 7.2 Aims

1. To produce and characterise aminosilane functionalised glass surfaces for use in protein screening.
2. To screen a selected set of different extracellular matrix proteins in regard to their effects upon cell adhesion and viability, utilising a factorial design of experiments methodology.

## 7.3 Results

### 7.3.1 Surface cleaning and pre-functionalisation

Contact angle measurements of glass slides cleaned using the two different methods described above in section 2.8.1 were seen to be significantly reduced when compared to those of comparable untreated surfaces ( $F(8)=117.07$ ,  $P=0.000$ ). Subsequent pairwise analyses showed that slides treated with the combined acid/solvent and plasma cleaning regimes had significantly lower static contact angles than those subjected to the acid/solvent mixture alone ( $P<0.05$ ). Images of the water contact angles displayed by each of the tested surfaces are provided below in figure 7.1. Figure 7.2 contains a graphical representation of the mean contact angles and associated standard error values for each of the methods used.

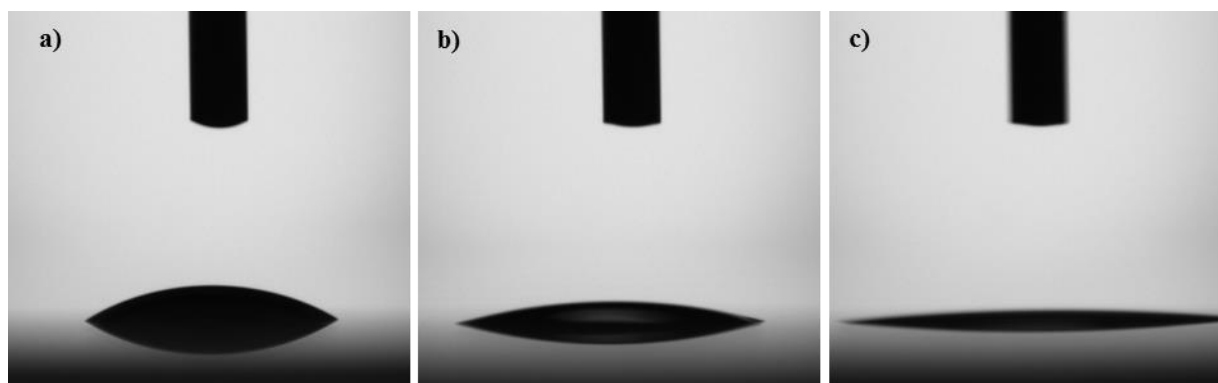


**Figure 7.1 Representative images of static water contact angles taken on each of the cleaned surfaces along with uncleaned controls**

a) Uncleaned glass. b) Acid/solvent cleaned glass. c) Acid/solvent and plasma cleaned glass.

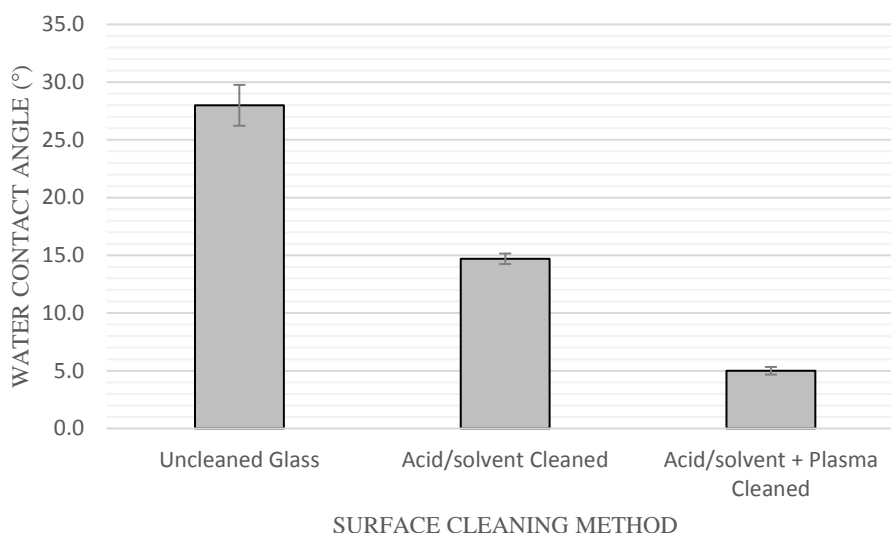


**Figure 7.2 Mean contact angle values for each of the cleaning methods used and associated controls**

Error bars indicate the standard error of the mean for n=3.

### 7.3.2 Characterisation of aminosilane functionalised surfaces

Evaluation of the average contact angles of glass slides following one of three different aminosilane functionalisation techniques revealed a statistically significant effect ( $F(11)=1655.59$ ,  $P=0.000$ ), with all three methods resulting in substantially increased angles when compared to toluene-treated controls. In addition, the average contact angles for each of the three treatment processes were significantly different from each other; as shown in figures 7.3 and 7.4, suggesting possible changes in surface quality depending upon the method used.

In accordance to the contact angle data, the results of a subsequent AO-7 assay confirmed the presence of significant differences between the amine-group content of aminosilane treated slides and associated controls ( $F(11)=29.60$ ,  $p 0.000$ ). The highest recorded amine-group content was attributed to anhydrous APTES coated surfaces, coinciding with the high average contact angle value associated with these slides (figure 7.5).

Alongside contact angle and amino-group content assessment, the elemental composition of the treated surfaces was also evaluated, the results of which are summarised across figures 7.6, 7.7, 7.8 7.9 and 7.10. Significant differences in nitrogen ( $F(7)=46.24$ ,  $P=0.001$ ), carbon ( $F(7)=104.87$ ,  $P=0.000$ ), oxygen ( $F(7)=128.53$ ,  $P=0.000$ ) and silicon ( $F(7)=43.49$ ,  $P=0.002$ ) content were identified between the coated slides and any associated toluene-treated controls. Significant increases in nitrogen and carbon content consistent with aminosilane

functionalisation were seen across all of the treated groups when contrasted against untreated controls. Conversely, significant reductions in oxygen and silicon content were revealed, likely due to masking of the underlying glass surfaces by layers of aminosilane. A number of differences between the various treatment types were also identified, with aqueous APTES treated substrates displaying significantly increased nitrogen, oxygen and silicon at the same time as significantly lower carbon content than surfaces coated using either of the other two tested treatment methods. No significant differences were seen between either of the two anhydrous treatment methods for any of the assessed elements.

Finally, the stability of the aminosilane coatings produced using the three different treatment processes were assessed in heated aqueous conditions via both contact angle and AO-7 measurements. The results of this evaluation can be seen below in figures 7.11 and 7.12, with all of the treated surfaces showing a decline in average contact angle and amine-group content over time. Anhydrous APDEMS treated surfaces were revealed to retain the highest average contact angle and amine-group content following prolonged exposure to an aqueous environment.

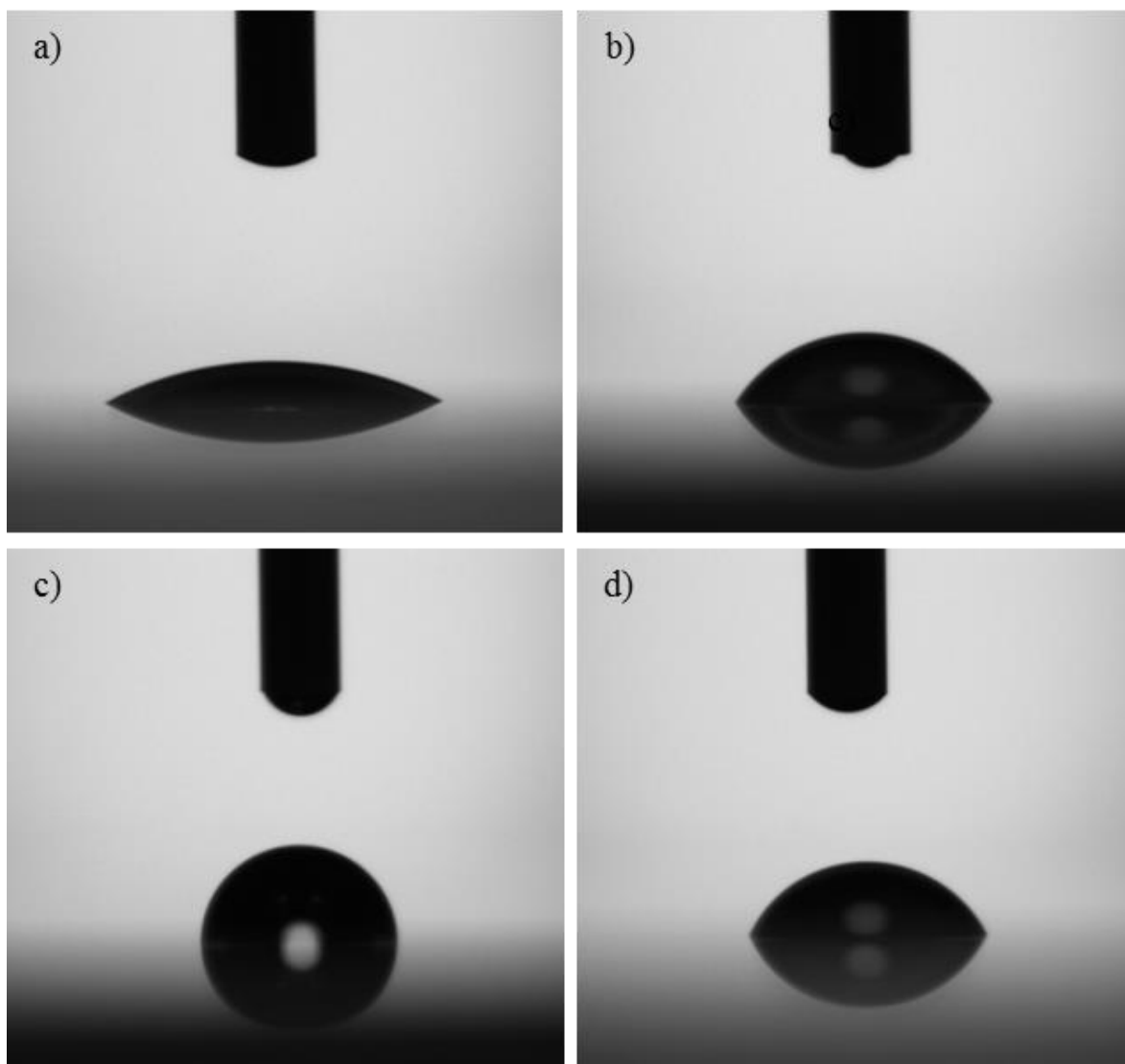


**Figure 7.3 Representative images of static water contact angles taken on each of the aminosilane functionalised surfaces alongside appropriate controls**

a) Toluene control. b) Aqueous APTES. c) Anhydrous APTES. d) Anhydrous APDEMS.

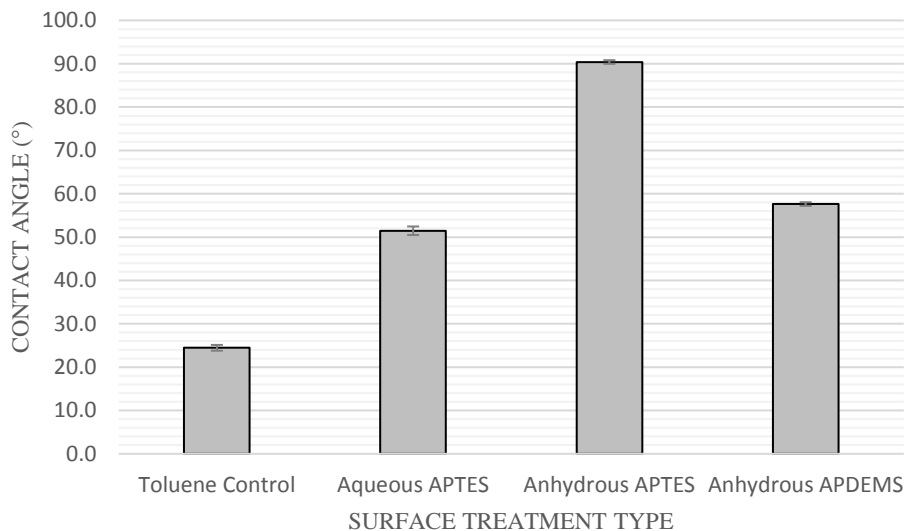


**Figure 7.4 Mean contact angle values for each of the aminosilane functionalisation methods used and associated controls**

Error bars indicate the standard error of the mean for n=3.

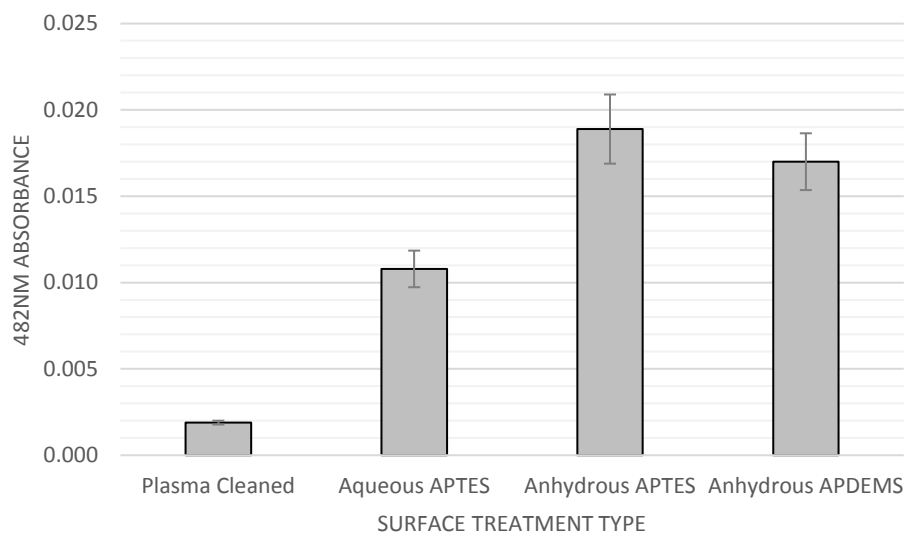


**Figure 7.5 Mean 482nm absorbance values for alkaline washes taken for each of the assessed aminosilane functionalisation methods and associated controls following treatment with Acid Orange-7**

Error bars indicate the standard error of the mean for n=3.

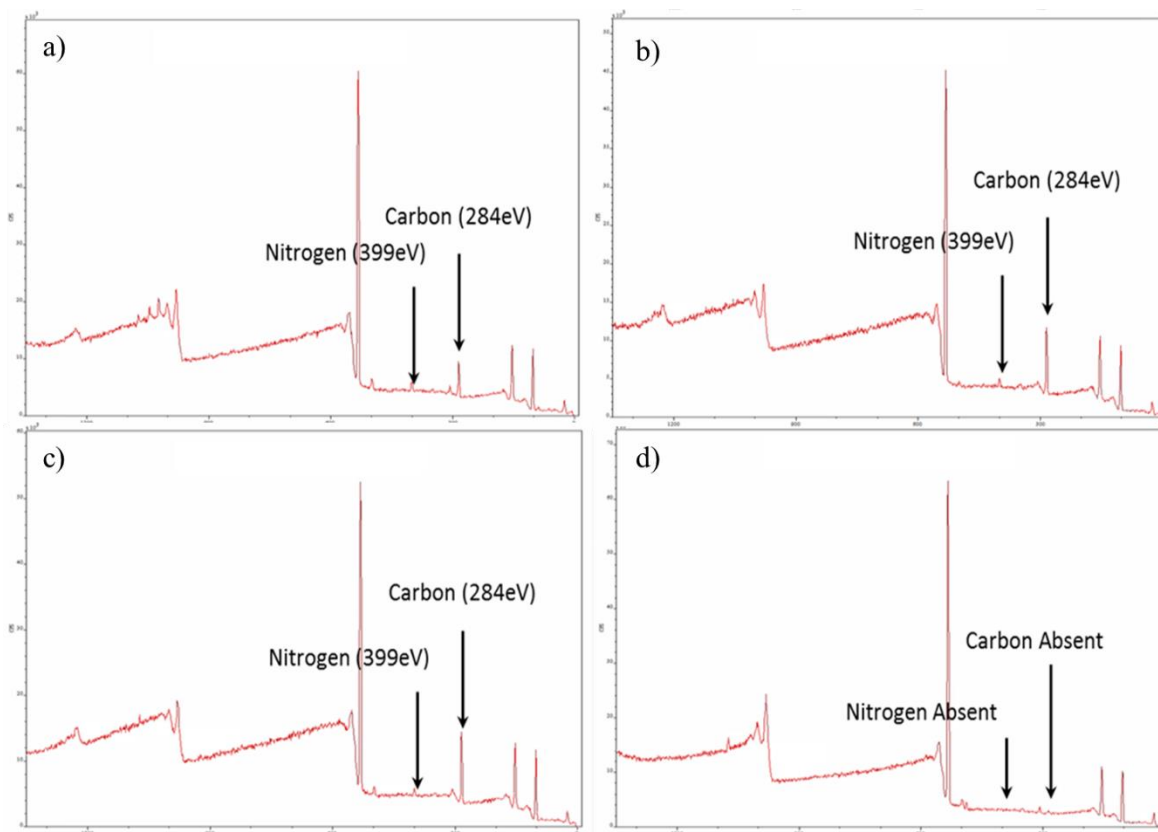


**Figure 7.6 Representative XPS survey spectra showing increased carbon and nitrogen presence on aminosilane functionalised glass surfaces versus controls**

a) Aqueous APTES. B) Anhydrous APTES. C) Anhydrous APDEMS d) Untreated Control.

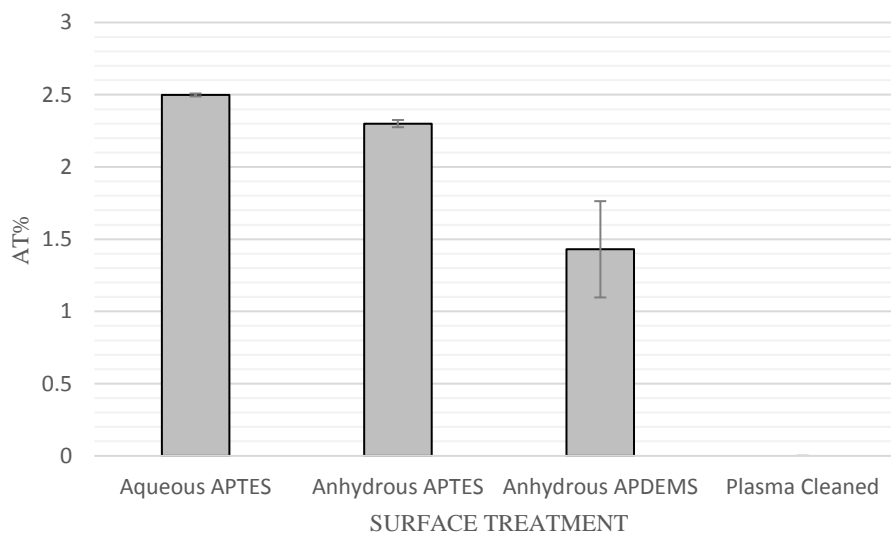


**Figure 7.7 Mean percentage surface nitrogen (N1s) content for each of the aminosilane functionalisation methods used and associated controls**

Error bars indicate the standard error of the mean for n=3.

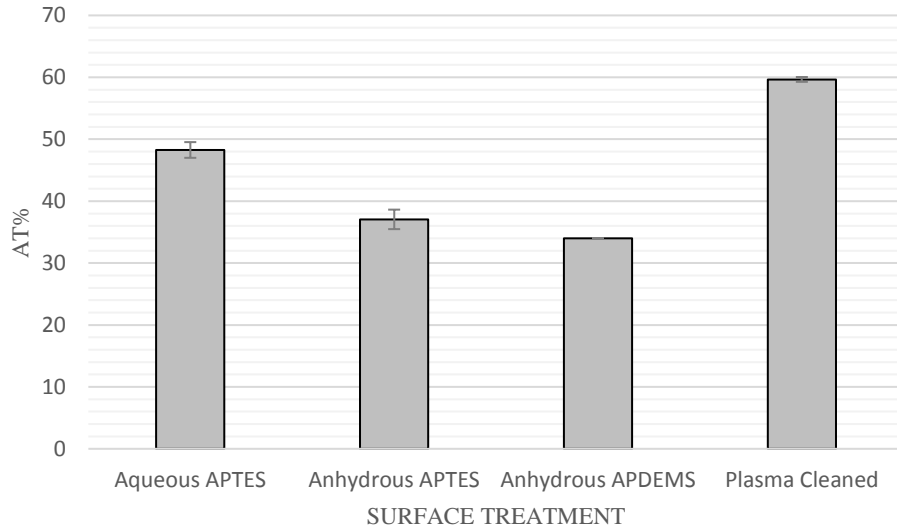


**Figure 7.8 Mean percentage surface oxygen (O1s) content for each of the aminosilane functionalisation methods used and associated controls**

Error bars indicate the standard error of the mean for n=3.

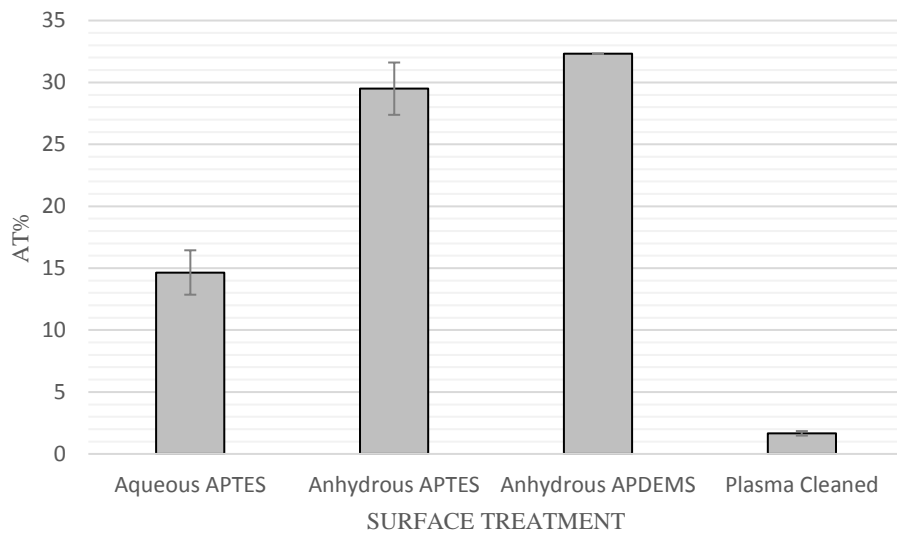


**Figure 7.9 Mean percentage surface carbon (C1s) content for each of the aminosilane functionalisation methods used and associated controls**

Error bars indicate the standard error of the mean for n=3.

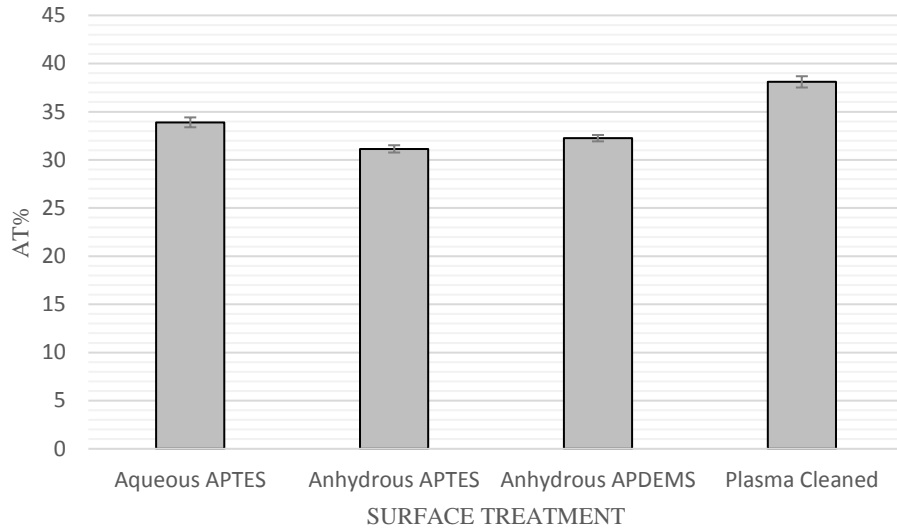


**Figure 7.10 Mean percentage surface silicon (Si 2p) content for each of the aminosilane functionalisation methods used and associated controls**

Error bars indicate the standard error of the mean for n=3.

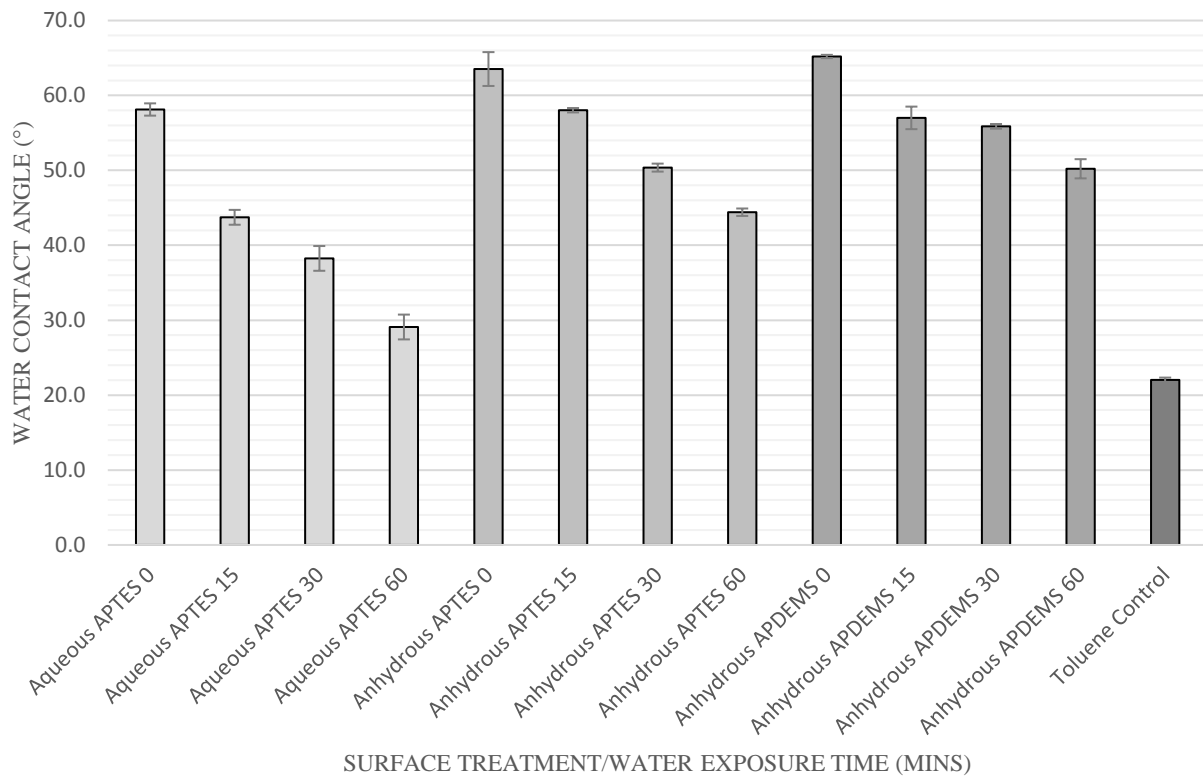


**Figure 7.11 Mean contact angles of aminosilane functionalised surfaces following water-mediated degradation for 0, 15, 30 and 60 minutes**

Error bars indicate the standard error of the mean for n=3. A toluene treated control is included for reference.

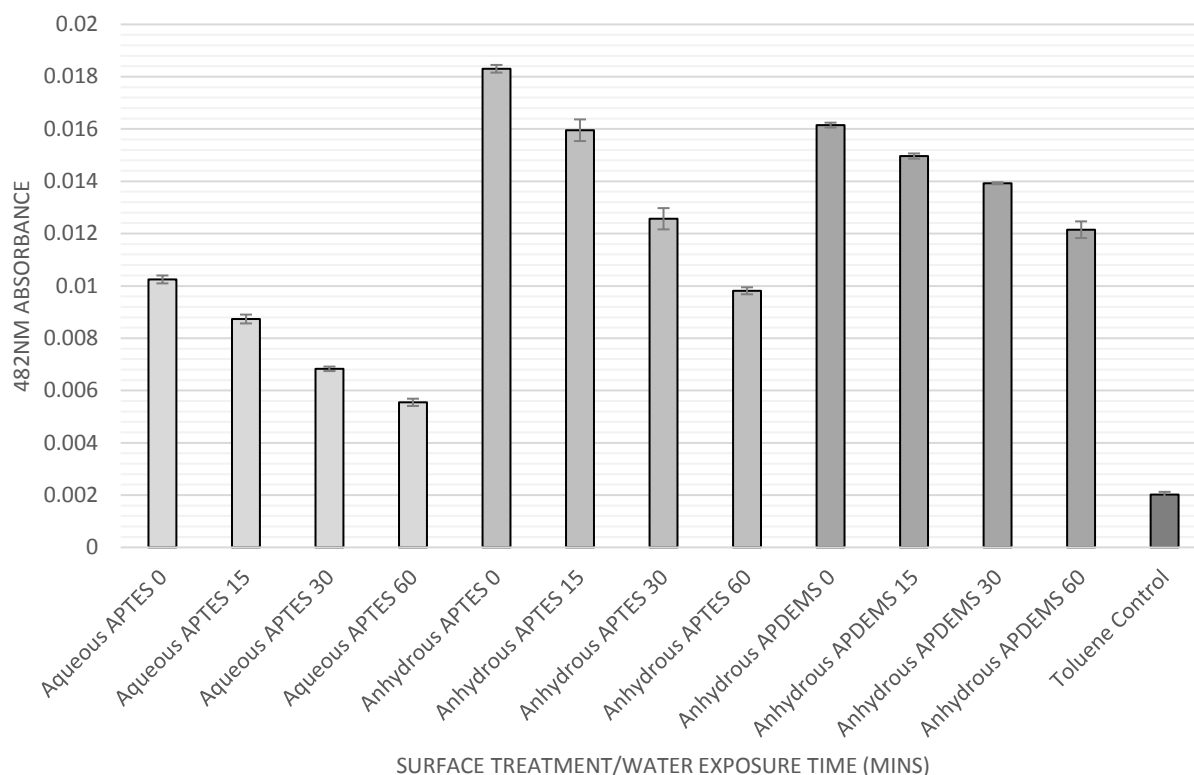


**Figure 7.12 Mean 482nm absorbance values for each of the tested aminosilane functionalisation methods following water-mediated degradation for 0, 15, 30 and 60 minutes**

Error bars indicate the standard error of the mean for n=3. A toluene treated control is included for reference.

### 7.3.3 Screening of extracellular matrix proteins

The morphological characteristic of primary hBM-MSCs exposed to fibronectin, vitronectin and fibrinogen individually and in combination were/ consistent with both the characterisation images displayed in section 3.3.1 and the FBS controls detailed here (figures 7.13 and 7.14). Cells exposed to untreated and bovine serum albumin-coated controls appeared smaller and less spread-out than those grown on protein-treated surfaces. Y201s showed a similar shift in morphology under these same conditions, with cells grown on ECM protein-coated substrates continuing to display classic MSC-like morphology irrespective of the specific protein or proteins to which they were exposed (figures 7.15 and 7.16).

Analysis of the primary cell retention data for each of the protein combinations utilised here revealed a single significant main effect and a single significant 2-way interaction. The use of fibrinogen was shown to significantly reduce the ability of these cells to adhere to glass surfaces when compared to all other conditions ( $F(26)=12.94$ ,  $P=0.002$ ), whilst the combination of fibronectin and vitronectin was seen to result in a significant increase in the total number of

cells retained ( $F(26)=25.98$ ,  $P=0.000$ ) giving rise to values equivalent to those recorded for the associated FBS-controls.

Unlike with the donor-derived cells before them, no significant main effects or interactions were identified with regard to the Y201 cells groups, with all experimental conditions and associated centre points displaying similar levels of cell retention.

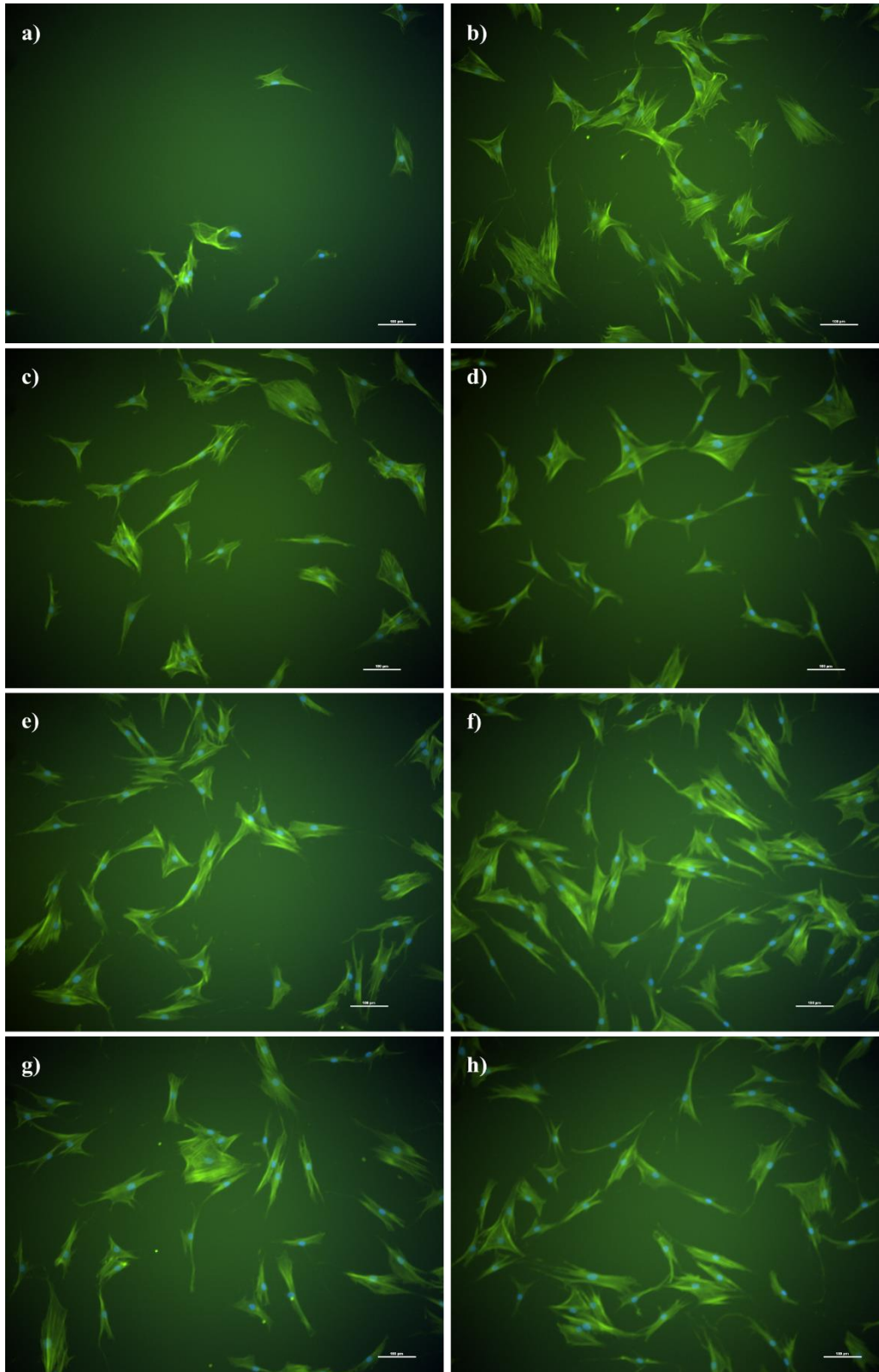


**Figure 7.13** Fluorescent microscopy images of Phalloidin and DAPI stained hBM-MSCs following 8 hours of culture on aminosilane coated glass functionalised with different combinations of extracellular matrix proteins

All included scale bars are indicative of a 100  $\mu\text{m}$  length. a) No supplementary proteins. b) 10  $\mu\text{g}/\text{mL}$  fibronectin. c) 10  $\mu\text{g}/\text{mL}$  vitronectin. d) 10  $\mu\text{g}/\text{mL}$  fibrinogen. e) 5  $\mu\text{g}/\text{mL}$  fibronectin and 5  $\mu\text{g}/\text{mL}$  vitronectin. f) 5  $\mu\text{g}/\text{mL}$  fibronectin and 5  $\mu\text{g}/\text{mL}$  fibrinogen. g) 5  $\mu\text{g}/\text{mL}$  vitronectin and 5  $\mu\text{g}/\text{mL}$  fibrinogen. h) 3.3  $\mu\text{g}/\text{mL}$  each of fibronectin, vitronectin and fibrinogen.

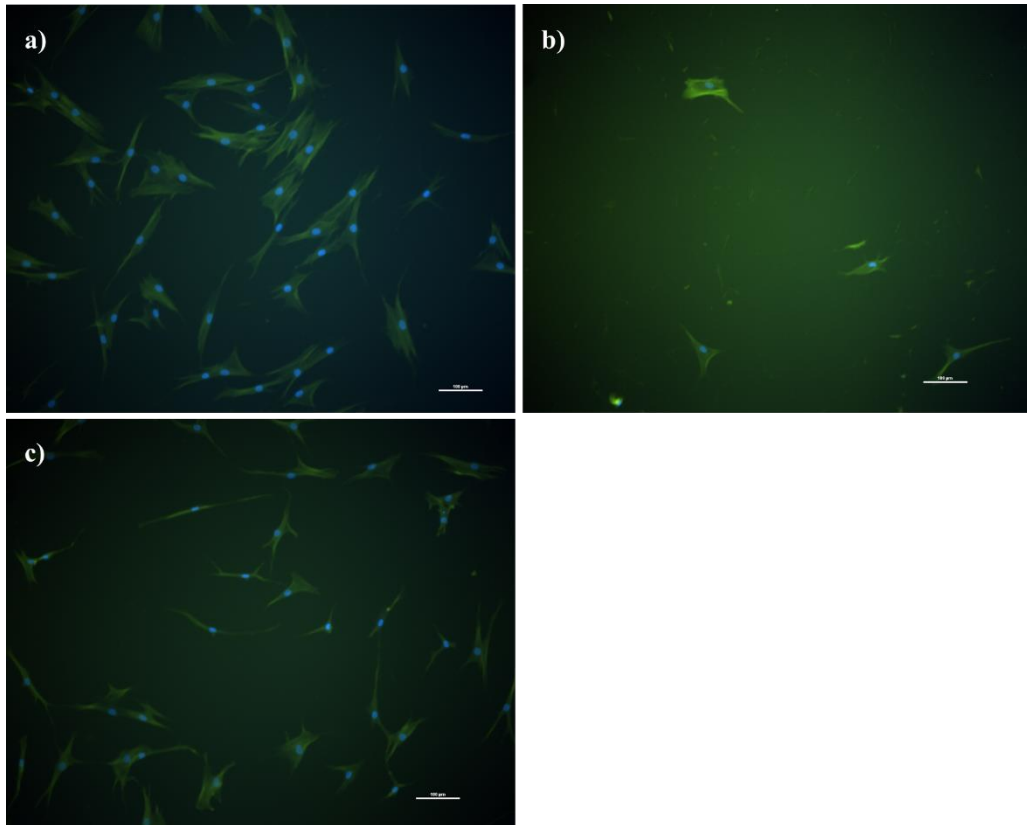


**Figure 7.14** Fluorescent microscopy images of Phalloidin and DAPI stained hBM-MSCs following 8 hours of culture on aminosilane coated glass functionalised with different combinations of extracellular matrix proteins

All included scale bars are indicative of a 100  $\mu\text{m}$  length. a) DoE centre point treated with 1.6  $\mu\text{g}/\text{mL}$  each of fibronectin, vitronectin and fibrinogen. b) 0.5% w/v BSA-treated negative control. c) FBS-treated positive control.

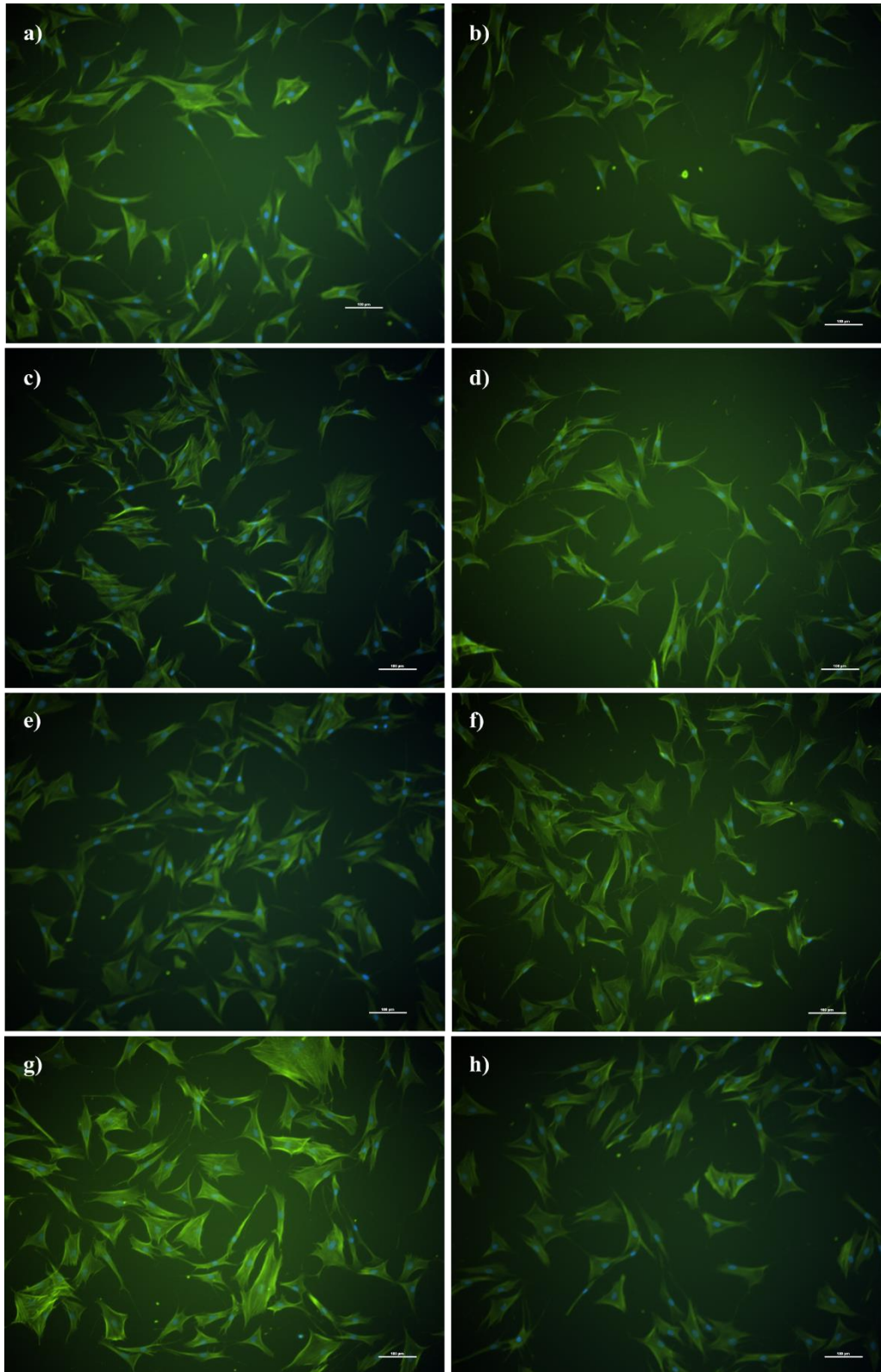


**Figure 7.15** Fluorescent microscopy images of Phalloidin and DAPI stained Y201s following 8 hours of culture on aminosilane coated glass functionalised with different combinations of extracellular matrix proteins

All included scale bars are indicative of a 100  $\mu\text{m}$  length. a) No supplementary proteins. b) 10  $\mu\text{g}/\text{mL}$  fibronectin. c) 10  $\mu\text{g}/\text{mL}$  vitronectin. d) 10  $\mu\text{g}/\text{mL}$  fibrinogen. e) 5  $\mu\text{g}/\text{mL}$  fibronectin and 5  $\mu\text{g}/\text{mL}$  vitronectin. f) 5  $\mu\text{g}/\text{mL}$  fibronectin and 5  $\mu\text{g}/\text{mL}$  fibrinogen. g) 5  $\mu\text{g}/\text{mL}$  vitronectin and 5  $\mu\text{g}/\text{mL}$  fibrinogen. h) 3.3  $\mu\text{g}/\text{mL}$  each of fibronectin, vitronectin and fibrinogen.

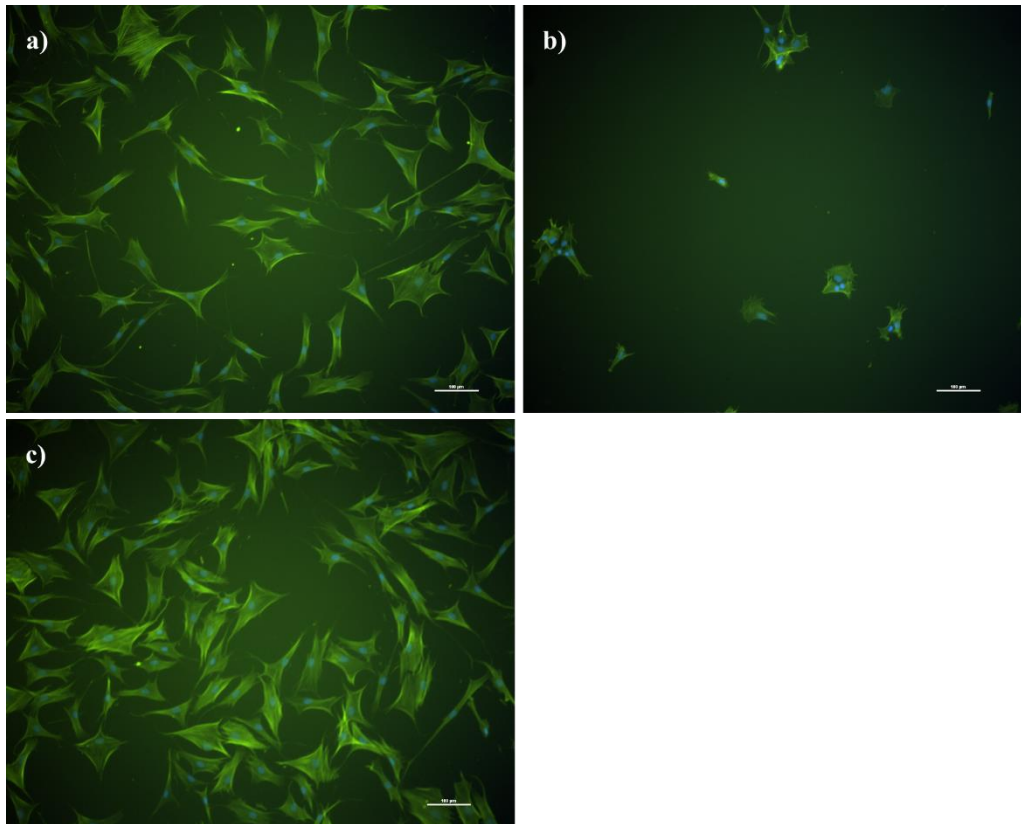


**Figure 7.16** Fluorescent microscopy images of Phalloidin and DAPI stained Y201s following 8 hours of culture on aminosilane coated glass functionalised with different combinations of extracellular matrix proteins

All included scale bars are indicative of a 100 µm length. a) DoE centre point treated with 1.6 µg/mL each of fibronectin, vitronectin and fibrinogen. b) 0.5% w/v BSA-treated negative control. c) FBS-treated positive control.

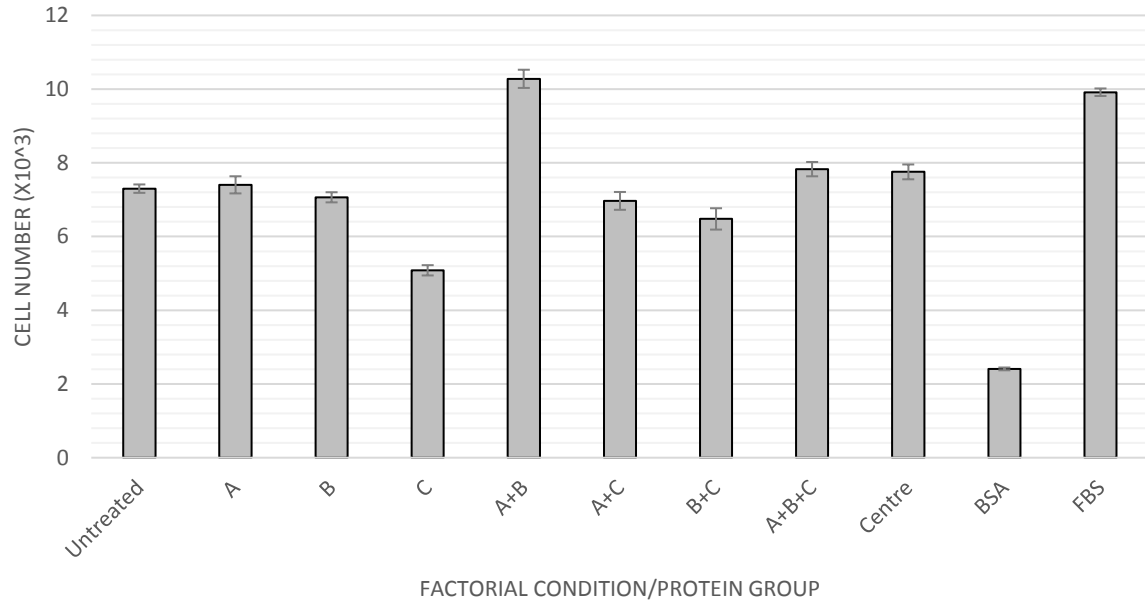


**Figure 7.17 Mean BM-MSc numbers retained on surfaces coated with each of the extracellular matrix protein combinations included within the full-factorial functionalisation assessment**

Error bars indicate the standard error of the mean for n=3. The coded designations of the proteins used in this investigation were as follows: A) Fibronectin, B) Vitronectin, C) Fibrinogen. Included centre point conditions represents the use of a combination of all the associated supplements at half the concentrations seen in the other factorial groupings. BSA and FBS conditions were included as negative and positive controls respectively.

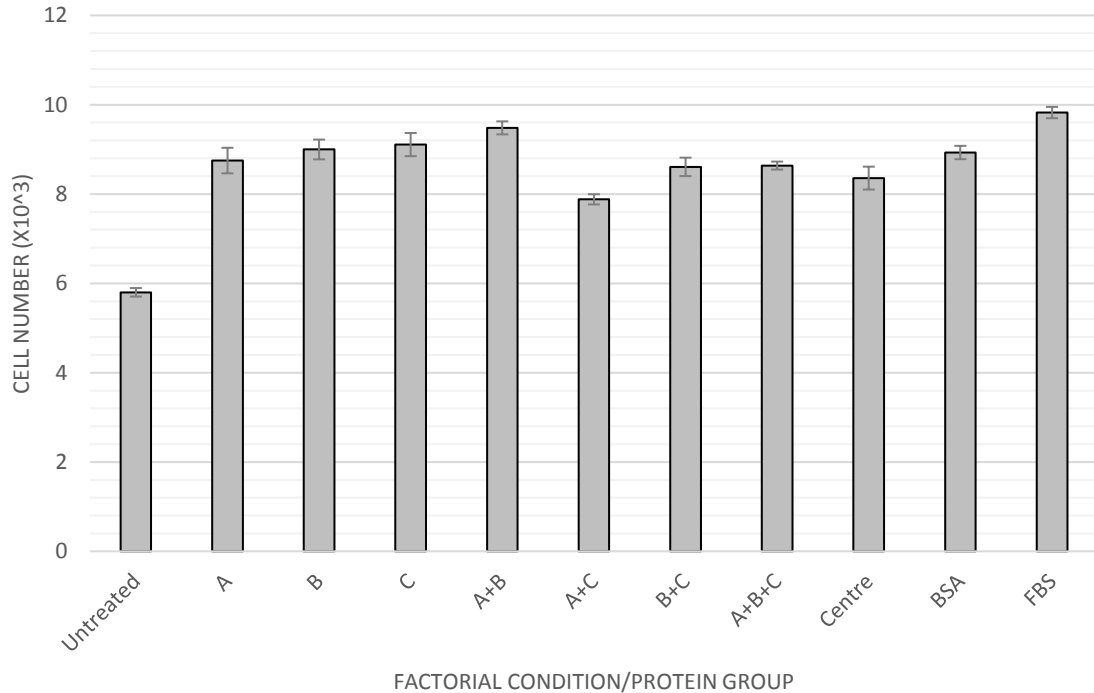


**Figure 7.18 Mean Y201 cell numbers retained on surfaces coated with each of the extracellular matrix protein combinations included within the full-factorial functionalisation assessment**

Error bars indicate the standard error of the mean for n=3. The coded designations of the proteins used in this investigation were as follows: A) Fibronectin, B) Vitronectin, C) Fibrinogen. Included centre point conditions represent the use of a combination of all the associated supplements at half the concentrations seen in the other factorial groupings. BSA and FBS conditions were included as negative and positive controls respectively.

## 7.4 Discussion

In this chapter, we successfully produced aminosilane coated glass surfaces capable of tolerating extended exposure to aqueous conditions for the purposes of ECM protein screening. It was determined that of the three methods used, anhydrous treatment with APDEMS was the most stable, coinciding with the findings of Yadav *et al* (2014) (250). This enhanced stability ensured coating retention following aldehyde functionalisation and subsequent protein binding.

Results from the primary MSC extracellular matrix protein screening revealed that the use of a combination of fibronectin and vitronectin was most effective at assisting cell adhesion in the absence of serum. This finding is supported by high levels of  $\beta 1$ ,  $\alpha 4$ ,  $\alpha 5$ ,  $\alpha 8$ ,  $\alpha 9$  and  $\alpha V$  expression seen in MSCs, which are known to directly mediate binding to fibronectin and vitronectin RGD sequence motifs (247). Intriguingly, an apparent reduction in cell attachment was observed when utilising fibrinogen, even in combination with the other two proteins. It is likely that this is the direct result of limited  $\beta 2$  and  $\beta 3$  expression by these cells, with groups

such as Majumdar *et al* (2000) reporting only 2.4%  $\beta$ 2 expression in passage-zero adipose-derived MSCs when compared to 87.5%  $\beta$ 1 activity (251). It is important to note that no apparent differences in cell morphology were observed between any of the tested protein combinations (excluding the untreated surfaces and negative controls), all of which appeared consistent with those of the FBS-control.

With regard to the Y201 data set, no significant effects were seen in relation to cell retention or morphology across any of the tested protein groups. It is thought that the rapid generation of ECM proteins by these cells is likely to have rendered them refractory to the different surface treatments under examination; including the untreated and BSA-control conditions, and that a shortened incubation period would be required in order to properly highlight any potential interactions.

## 8 Chapter 8: Discussion and conclusions

### 8.1 Summary of Results

At the outset of this thesis, variability in the composition of foetal bovine serum was shown to significantly impact the proliferation of both primary and immortalised MSCs. Additionally, gene expression was also seen to be affected, whilst common quality-attributes such as morphology and surface marker profile remained unchanged. As a result of this, a novel defined serum-free medium formulation was developed, based on an initial screening of twelve different cytokines, growth factors and commonly used culture supplements. This medium, which was formulated from a combination of DMEM and Ham's F12 nutrient mix supplemented with FGF-2, SITE, PDGF-BB and TGF- $\beta$ 1, was shown to support cell growth in the absence of serum, leading to the generation of cell numbers in excess of those observed for comparable FBS-supplemented cultures. Cells retained their inherent differentiation potential and expressed an MSC-like surface marker profile, with the exception of reduced CD105 expression. Despite this, both primary and immortalised cells underwent significant morphological changes following growth in serum-free conditions, with the secretory profile of primary MSCs showing a marked increase in immune-cell recruitment proteins together with a decrease in angiogenic potential. Cells belonging to the immortalised Y201 line on the other hand, were seen to undergo increased expression of self-renewal and stemness-related genes when cultured in the serum-free medium formulation described here. This disparity may highlight a distinct difference in the responses of model healthy cell populations and patient-derived cell populations, with donor variability significantly impacting upon the efficacy of novel serum-free medium formulations and the characteristics of cells expanded using them. Finally, screening of extracellular matrix proteins revealed that a combination of fibronectin and vitronectin was sufficient to promote primary cell adhesion in serum-free conditions, producing a straight-forward surface treatment for use in combination with the medium formulation described here.

## 8.2 Discussion

### 8.2.1 Cell Characterisation

The primary MSCs isolated and described in this work appeared to display many of the identifying characteristics of model mesenchymal stromal cells, with the exception of their lack of chondrogenic differentiation and increased HLA-DR expression. The first of these deviations is likely due to either a lack of compatibility between the cells and the chondrogenic differentiation method used or the osteoarthritic nature of the donor material itself. It has been demonstrated that MSCs derived from the bone marrow of patients with advanced osteoarthritis have substantially reduced chondrogenic potential (221). Intriguingly, this phenomenon was coupled with a decline in adipogenic potential, an effect which was not documented here due to a lack of comparable healthy donor cells from which to develop a baseline. In fact, the stark lack of chondrogenic differentiation in both the primary and immortalised cells, which have previously been shown to be capable of producing cartilage, suggests that the induction method used here was likely insufficient to initiate change and may have led to this lack observable chondrogenesis. Ideally, it would be of interest to trial a number of alternative methods using these cells, as well as testing the efficacy of the original method using a model cell population isolated from a healthy donor as a means of pin pointing the root cause of this issue.

The second deviation relating to the characterisation of the primary cells utilised here was associated with their abnormal expression of HLA-DR. It was initially assumed that, as with the lack of chondrogenic differentiation, this phenomenon was a direct result of the osteoarthritic nature of the patients from which the cells were isolated, with a number of groups having observed increased HLA-DR expression in individuals suffering from lymphoproliferative, connective or inflammatory disorders (222, 252). Upon further investigation however it was shown that the increased HLA-DR expression described here was likely due to the use of supplementary FGF-2 during in vitro expansion of the donor cell populations. These findings make this one of only a handful of studies to have demonstrated this possible link and the only one to have done so in primary bone marrow-derived MSCs. It is important to note however, that the functionality of this surface marker has not been investigated and that its increased expression cannot be assumed to have altered the immunogenic properties of the cells in this particular instance. Further study in the form of T-

helper cell activation assays would be required in order to draw any firm conclusions regarding the functionality of this marker.

### 8.2.2 Foetal bovine serum batch variability

Despite the discrepancies discussed above, the use of the primary cells characterised here was continued throughout the remainder of this work due to the limited supply of suitable cell populations available alongside their cost-effective nature and reliability of supply. Following directly on from this, these cells were utilised to demonstrate for the first time, the impact of FBS batch variability on MSC proliferation and gene expression. It is important to note that at this time the specific effects of the variable genes highlighted here are unknown with regards to MSC therapeutic efficacy but it is likely that at least some of them are linked to the changes in proliferation that were documented alongside them. Intriguingly, the morphology and surface marker profiles of these cells showed little variation when exposed to high versus low proliferation serum. Not only do these findings suggest that FBS is not a suitable supplement for the production of MSCs in a consistent and reproducible manner, it also suggests that two of the key quality parameters used to determine cell suitability prior to academic or clinical use, namely morphology and surface marker profile, are unlikely to highlight important shifts in cell behaviour as a result of seemingly subtle changes in raw material source.

### 8.2.3 Supplement screening for serum-free medium development

Following the conclusion of the supplement screening investigations detailed in chapter 5 it was revealed that contrary to the findings of previous studies (see table 5.1) none of the group two or group three molecules were seen to significantly improve MSC growth in serum-deprived conditions. Not only did many of these supplements have little to no effect on cell survival, but IL-6 and ROCK were seen to significantly inhibit proliferation in the tested conditions. It is possible that the combinations of supplements utilised here had a negative impact upon the group two and group three molecules but re-testing each of these factors in combination with each other, together with the group one supplements would be in direct opposition to the time-saving reasoning behind utilising a grouped fractional factorial design. More importantly, this departure from the expected may suggest that a literature review was not the most appropriate method of selecting molecules for inclusion within the study and that

an alternative process should have been undertaken. One possible approach would be the use of a dedicated-depletion study, in which the components of fresh human serum are compared to those of culture-conditioned human serum as a means of identifying what factors are being utilised by the cells and hence what they require in order to proliferate *in vitro*. This particular type of method does require access to an array of analytical techniques capable of accurately characterising the composition of the liquid medium, such as mass spectrometry, which is typically considered both an expensive and technically demanding method to use, and remained outside the scope of the present investigation.

In contrast to the results referenced above, FGF-2, ITSX, PDGF-BB and TGF- $\beta$ 1 were seen to synergistically improve MSC proliferation in serum-deprived conditions in-line with the findings of previous groups. Additionally, the curvature effect seen in the associated design suggests that the lower concentrations used in the literature may in fact be sufficient to elicit the desired response. Unfortunately, these cells displayed significant changes in morphology, CD105 expression, gene expression and cytokine secretion in response to expansion within the described medium. Whilst it appeared at first glance that the cells could have been differentiating towards an unknown endothelial lineage based on their morphological shift, the lack of ac-LDL staining and CD-34 expression together with a decrease in overall vascularisation-related cytokine secretion suggested that this was likely not the case. It is interesting to note that the differences in gene expression and secretory profile observed following serum-free culture did not overlap with those seen when cells were cultured in a low-growth batch of FBS or when undergoing an immune response (as when treated with TNF). It is possible that these differences were the result of the cells entering some sort of stressed state as a direct result of the removal of serum however the author hypothesises that the changes in morphology and gene expression described here are linked to detachment from the surfaces onto which the cells were initially seeded. This phenomenon may have occurred as a result of the limited nature of the initial surface coating (treatment with FBS), which may have been sufficient for immediate attachment but limited following extensive cell proliferation. It would be interesting to see whether the use of the surfaces identified in chapter 7 of this investigation would alleviate the documented effects or whether the inclusion of further supplements to the mixture could act to bring these cells back in-line with their serum-cultured counterparts.

Alternatively, it should be noted that MSCs as we know them are an artefact of their original isolation and culture methods, with our current criteria for identification being based upon these factors. It may be that the cells described here simply represent a distinct sub-type of MSC

arising from this method of culture with unique therapeutic properties. As documented earlier, the re-vascularisation potential of these cells is likely to be reduced when compared to those of serum-cultured populations due to their reduced PlGF and increased sFlt-1 production, however their adipogenic, osteogenic and immunomodulatory properties are likely intact. Interestingly this decreased angiogenic potential is also coupled with increased VEGF-C and VEGF-D production. Whilst these factors do have some limited angiogenic properties, they are primarily associated with lymphangiogenesis, particularly when in the presence of inhibitors such as sFlt-1, which would significantly reduce the impact of the VEGF-A also being produced by these cells (253). When taken in combination with the recruitment of monocytes as a consequence of secreted IL-16 and MCP-1, which themselves play an important role in lymphangiogenesis, it appears likely that these cells could potentially be utilised in the treatment of conditions characterised by impaired lymphatic vessel formation and oedema (253).

Alongside the aforementioned changes in secretory profile, a significant reduction in CD105 expression was also observed in cells grown using the current serum-free medium formulation. These findings coincide with those of Anderson *et al* (2013) who identified a subpopulation of CD105 negative cells showing increased osteogenic and adipogenic differentiation potential following growth in serum-free conditions (245). Similarly Brohlin *et al* (2017) observed reduced expression of CD105 in MSC populations cultured in defined serum-free conditions and whilst this change also coincided with an alteration in cell morphology, this was not consistent with the changes documented here (243). It is important to mention that differentiation was not quantified during the course of the current investigation, making it impossible to accurately gauge whether the cells were capable of increased osteogenic and adipogenic differentiation following serum-free culture.

One issue that must be highlighted here is the relative cost of the serum-free medium formulation described in this study, which was calculated at £57.46 per 500 mL at the time of writing. When compared to standard FBS-containing medium at £155.25, HS-containing medium at £882.25 and finally commercially available serum-free medium at £182.90, it is clear that the current approach has the potential to be the one of the most cost effective means of culturing MSCs *in vitro*. It is of course important to note that this estimate does not take into account the costs of the ECM proteins required in order to facilitate serum-free cell attachment, as it is difficult to accurately estimate the functional surface area associated with a fixed volume of liquid media given the vast array of different culture systems available. It is likely that a

proportion of this expensive will be offset by the refinement of the medium however, as it appears from the significant curvature effect seen within the experimental design that the concentrations of each of the included components are capable of being reduced without impacting the efficacy of the formulation. Of course, it is also likely that additional factors will need to be included within the medium in order to bring the characteristics of the cultured cells back in line with those of FBS-supplemented populations, assuming that the inclusion of the ECM-treated surfaces described in chapter 8 does not alleviate these concerns.

#### 8.2.4 Screening of ECM Proteins for enhanced cell adhesion in serum free conditions

The final component of this study which must be discussed is the aforementioned ECM screening investigation, from which we can see that for primary MSCs a combination of vitronectin and fibronectin resulted in the best overall cell attachment. It is likely that this effect occurred as a direct consequence of the types of integrins possessed by these cells and their respective binding properties when associated with the three investigated ECM proteins. MSCs have been shown to widely express a variety of integrin subunits with affinity for fibrinogen and vitronectin, such as  $\beta 1\alpha 3$ ,  $\beta 1\alpha 5$  and  $\beta 1\alpha V$  but little to no expression of fibrinogen-specific subunits such as  $\beta 2\alpha X$  or  $\beta 2\alpha M$  (247). It may be that the inclusion of fibrinogen reduces the overall amount of protein accessible for integrin binding due to a lack of fibrinogen-specific subunits and significant overlap in binding with both fibronectin and vitronectin. The subunits displayed by the cells however, have greater or lesser affinity to fibronectin and vitronectin respectively, limiting the amount of overlap and providing a surface with more available attachment points per unit weight of total protein when this combination is used. It should be noted that the associated Y201 screening experiment likely failed to reveal any significant effects due to the length of time the cells were allowed to attach to the surfaces for before assessment. Ideally this experiment should be repeated with a shortened initial binding time.

It is at this point that it is necessary to comment on the suitability of the Y201 cell line as a model for primary cells during media development. As has clearly been demonstrated over the course of this investigation, the responses of these cells to both cytokine supplementation and culture in serum-free conditions differ substantially from those of isolated primary MSCs. In fact, in many cases the highly proliferative nature of the Y201s confers them a level of resilience to supplementation with potentially inhibitory factors, whilst masking the impact of anything but the most pronounced positive effects. Overall, whilst the use of immortalised cell lines in media screening can represent a highly cost effective approach, the lack of similarity

between Y201s and primary bone marrow-derived MSCs severely limits their usefulness in this particular case.

### 8.3 Conclusions

1. Variability inherent to the composition of foetal bovine serum is capable of impacting the proliferation and gene expression of both primary and immortalised MSCs.
2. Basal medium supplemented with FGF-2, SITE, PDGF-BB and TGF- $\beta$ 1 is able to support the proliferation of primary and immortalised MSCs in the absence of serum, generating total cell numbers in excess of those recorded using FBS-treated cultures.
3. Expansion in the serum-free medium described here, resulted in altered cell morphology, CD105 expression and secreted protein production in primary human MSCs, potentially altering their therapeutic potential.
4. Immortalised MSCs were seen to undergo similar changes in morphology and surface marker profile to primary cell populations when cultured in serum-free medium but with increased expression of self-renewal and stemness related genes.
5. A combination of fibronectin and vitronectin was capable of supporting primary and immortalised cell adhesion in serum-free conditions, with morphology comparable to that of serum-supplemented cells.

### 8.4 Future Directions

1. Optimise the formulation of the serum-free medium by reducing the concentration of each of the included supplements, eliminating curvature within the associated experimental design and producing a more cost effective solution.
2. Combine the fibronectin and vitronectin functionalised surfaces with the serum-free medium formulation over multiple successive passages, assessing cell proliferation, metabolic activity, tri-lineage differentiation potential and surface marker profile.
3. Attempt to isolate primary cells into the combined serum-free system, with the potential of screening an array of additional supplements in order to help better support this activity.
4. Incorporate primary cells isolated from healthy donors into the existing investigation as an additional control element.

## References

1. Kirsner RS, Marston WA, Snyder RJ, Lee TD, Cargill DI & Slade HB. Spray-applied cell therapy with human allogeneic fibroblasts and keratinocytes for the treatment of chronic venous leg ulcers: a phase 2, multicentre, double-blind, randomised, placebo-controlled trial. *The Lancet*. 2012; 380(9846): 977-985.
2. Han EQ, Li XL, Wang CR, Li TF & Han SY. Chimeric antigen receptor-engineered T cells for cancer immunotherapy: progress and challenges. *Journal of Haematology & Oncology*. 2013; 6(47).
3. Nerem RM. Regenerative medicine: the emergence of an industry. *The Journal of the Royal Society: Interface*. 2010; 7(Suppl 6): 771-775.
4. Lysaght MJ, Jaklenec A & Deweerd E. Great Expectations: Private Sector Activity in Tissue Engineering, Regenerative Medicine and Stem Cell Therapeutics. *Tissue Engineering: Part A*. 2008; 14(2): 305-315.
5. Werner M, Ruffin M & West E. *Regenerative Medicines: a paradigm shift in healthcare*. 2011. Retrieved 2017 from [www.ddw-online.com](http://www.ddw-online.com).
6. Sumant, O. Regenerative Medicines Market by technology (Cell Therapy, Gene Therapy, Tissue Engineering, Small Molecules & Biologics), Material (Biodegradable Synthetic Polymers, Scaffold, Hydrogel & Collagen, Transgenic, Fibroblasts, Small Molecules and Biologics) - Global Opportunity Analysis and Industry Forecast, 2015 – 2022. *Pharmaceuticals*. 2016.
7. The Department of Business, Innovation and Skills. *Taking Stock of Regenerative Medicine in the United Kingdom*. 2011.
8. Fee R. *The Cost of Clinical Trials*. 2007. Retrieved 2013 from [www.dddmag.com](http://www.dddmag.com). Accessed 28/08/2017.
9. Ambrose WM, Schein O & Elisseeff J. A Tale of Two Tissues: Stem Cells in Cartilage and Corneal Tissue Engineering. *Current Stem Cell Research & Therapy*, 2010, 5: 37-48.

10. Bajada S, Mazakova I, Richardson JB et al. Updates on stem cells and their applications in regenerative medicine. *Journal of Tissue Engineering and Regenerative Medicine*, 2008; 2: 169-183.
11. Barberi T, Willis LM, Socci ND, et al. Derivation of multipotent mesenchymal precursors from human embryonic stem cells. *PLoS Medicine*, 2005; 2(6): e161.
12. Zeng X. Human Embryonic Stem Cells: Mechanisms to Escape Replicative Senescence? *Stem Cell Reviews*, 2007; 3(4): 270-279.
13. Goldring CE, Duffy PA, Benvenisty N, et al. Assessing the safety of stem cell therapeutics. *Cell Stem Cell* 2011; 8: 618–628.
14. ViaCyte, ViaCyte, Inc. Announces FDA Acceptance of IND to Commence Clinical Trial of VC-01™ Candidate Cell Replacement Therapy for Type 1 Diabetes. Available at <http://viacyte.com/press-releases/viacyte-inc-announces-fda-acceptance-of-ind-to-commence-clinical-trial-of-vc-01-candidate-cell-replacement-therapy-for-type-1-diabetes/>, 2014. Accessed 28/08/2017.
15. Schwartz SD, Regillo CD, Lam BL et al. Human embryonic stem cell-derived retinal pigment epithelium in patients with age-related macular degeneration and Stargardt's macular dystrophy: Follow-up of two open-label phase 1/2 studies. *The Lancet*, 2015; 385(9967): 509–516.
16. Sharon N, Mor I, Golan-lev T, et al. Molecular and functional characterizations of gastrula organizer cells derived from human embryonic stem cells. *Stem Cells*, 2011; 29: 600-608.
17. Spence JR, Mayhew CN, Rankin SA, et al. Directed differentiation of human pluripotent stem cells into intestinal tissue in vitro. *Nature*, 2011; 470: 105-109.
18. Jukes JM, Both SK, Leusink A, et al. Endochondral bone tissue engineering using embryonic stem cells. *Proceedings of the National Academy of Sciences of the United States of America*, 2008a; 105: 6840–6845.
19. Jukes JM, van Blitterswijk CA & de Boer J. Skeletal tissue engineering using embryonic stem cells. *Journal of Tissue Engineering and Regenerative Medicine*, 2010; 4: 165-180.

20. Kahan B, Magliocca J, Merriam F, et al. Elimination of tumorigenic stem cells from differentiated progeny and selection of definitive endoderm reveals a Pdx1<sup>+</sup> foregut endoderm stem cell lineage. *Stem Cell Research*, 2011; 6(2): 143-157.
21. Ben-David U, Gan QF, Golan-Lev T, et al. Selective Elimination of Human Pluripotent Stem Cells by an Oleate Synthesis Inhibitor Discovered in a High-Throughput Screen. *Cell Stem Cell*, 2013; 12(2): 167-179.
22. Li L, Baroja ML, Majumdar A, et al. Human embryonic stem cells possess immune-privileged properties. *Stem Cells*, 2004; 22(4): 448-456.
23. Drukker M, Katz G, Urbach A, et al. Characterization of the expression of MHC proteins in human embryonic stem cells. *Proceedings of the National Academy of Sciences of the United States of America*, 2002; 99(15): 9864-9869.
24. Swijnenburg RJ, Schrepfer S, Cao F, et al. In vivo imaging of embryonic stem cells reveals patterns of survival and immune rejection following transplantation. *Stem Cells Dev.*, 2008; 17(6): 1023-1029.
25. Hanahan D & Weinberg RA. Hallmarks of cancer: The next generation. *Cell*, 2011; 144(5): 646–674.
26. Pearl JI, Kean LS, Davis MM, et al. Pluripotent Stem Cells: Immune to the immune system? *Science Translational Medicine*, 2012; 4(164): 164ps25.
27. Avior Y, Lezmi E, Yanuka D, et al. Modeling Developmental Tumorigenic Aspects of Trilateral Retinoblastoma via Human Embryonic Stem Cells. *Stem Cell Reports*, 2017; 8: 1354-1365.
28. Mayshar Y, Yanuka O, & Benvenisty N. Teratogen screening using transcriptome profiling of differentiating human embryonic stem cells. *Journal of Cellular and Molecular Medicine*, 2011; 15(6): 1393-1401.
29. Towns CR & Jones DG. Stem cells, embryos, and the environment: a context for both science and ethics. *Journal of Medical Ethics*, 2003; 30(4): 410-413.
30. Mali P & Cheng L. Concise Review: Human Cell Engineering: Cellular Reprogramming and Genome Editing. *Stem Cells*, 2012; 30(1): 75-81.

31. Yamanaka S. Induced Pluripotent Stem Cells: Past, Present, and Future. *Cell Stem Cell*, 2012; 10(6): 678-684.
32. Takahashi K & Yamanaka S. Induction of Pluripotent Stem Cells from Mouse Embryonic and Adult Fibroblast Cultures by Defined Factors. *Cell*, 2006; 126: 663-676.
33. Pan C, Lu B, Chen H, et al. Reprogramming Human Fibroblasts using HIV-1 TAT recombinant proteins OCT4, SOX2, KLF4 and c-MYC. *Molecular Biology Reports*, 2010; 37(4): 2117-2124.
34. Cai S, Hou J, Fujino M, et al. iPSC-Derived Regulatory Dendritic Cells Inhibit Allograft Rejection by Generating Alloantigen-Specific Regulatory T Cells. *Stem Cell Reports*, 2017, 8: 1174-1189.
35. Espejel S, Roll GR, McLaughlin KJ, et al. Induced pluripotent stem cell-derived hepatocytes have the functional and proliferative capabilities needed for liver regeneration in mice. *The Journal of Clinical Investigation*, 2010; 120(9): 3120–3126.
36. Rami F, Beni SN, Kahnamooi MM, et al. Recent advances in Therapeutic Application of Induced Pluripotent Stem Cells. *Cellular Reprogramming*. 2017; 19(2): 65-74.
37. Bedel A, Beliveau F, Lamrissi-Garcia I, et al. Preventing Pluripotent Cell Teratoma in Regenerative Medicine Applied to Hematology Disorder. *Stem Cells Translational Medicine*, 2017; 6: 382-393.
38. Chen H, Li Y, Lin X, et al. Functional disruption of human leukocyte antigen II in human embryonic stem cell. *Biological Research*, 2015; 48: 59.
39. Kim K, Doi Am Wen B, et al. Epigenetic memory in induced pluripotent stem cells. *Nature*, 2010; 467: 285-290.
40. Boulting GL, Kiskinis E, Croft GF, et al. A functionally characterized test set of human induced pluripotent stem cells. *Nature Biotechnology*, 2011; 29(3): 279–286.
41. Kramer AS, Harvey AR, Plant GW, et al. Systematic Review of Induced Pluripotent Stem Cell Technology as a Potential Clinical Therapy for Spinal Cord Injury. *Cell Transplantation*, 2013; 22: 571-617.

42. Inak G, Lorenz C, Lisowski P, et al. Concise Review: Induced Pluripotent Stem Cell-Based Drug Discovery for Mitochondrial Disease. *Stem Cells*, 2017; 35: 1655-1662.
43. Ko HC & Gelb BD. Concise Review: Drug Discovery in the Age of the Induced Pluripotent Stem Cell. *Stem Cells Translational Medicine*, 2014; 3: 500-509.
44. Lesage S & Brice A. Parkinson's disease: from monogenic forms to genetic susceptibility factors. *Human Molecular Genetics*, 2009; 18(R1): R48-59.
45. Obeso JA, Rodriguez-Oroz MC, Goetz CG, et al. Missing pieces in the Parkinson's disease puzzle. *Nature Medicine*, 2010; 16: 653–661.
46. Su YC & Qi X. Inhibition of excessive mitochondrial fission reduced aberrant autophagy and neuronal damage caused by LRRK2 G2019S mutation. *Human Molecular Genetics*, 2013; 22(22): 4545–4561.
47. Ananiev G, Williams EC, Li H, et al. Isogenic pairs of wild type and mutant induced pluripotent stem cell (iPSC) lines from Rett syndrome patients as in vitro disease model. *PLoS ONE*, 2011; 6(9): e25255.
48. Cheung AYL, Horvath LM, Grafodatskaya D, et al. Isolation of MECP2-null Rett Syndrome patient hiPS cells and isogenic controls through X-chromosome inactivation. *Human Molecular Genetics*, 2011; 20: 2103–2115.
49. Hass R, Kasper C, Böhm S, et al. Different populations and sources of human mesenchymal stem cells (MSC): A comparison of adult and neonatal tissue-derived MSC. *Cell Communication & Signaling*, 2011; 9: 12.
50. Chao YH, Wu HP, Chan CK, et al. Umbilical Cord-Derived Mesenchymal Stem Cells for Hematopoietic Stem Cell Transplantation. *Journal of Biomedicine and Biotechnology*, 2012; 2012: 759503.
51. Anker PS, Scherjon SA, der Kaur CK, et al. Isolation of Mesenchymal Stem Cells of Fetal or Maternal Origin from Human Placenta. *Stem Cells*, 2004; 22(7): 1338-1345.
52. Yadav PS, Singh RK & Singh B. Fetal Stem Cells in Farm Animals: Applications in Health and Production. *Agricultural Research*, 2012; 1(1): 67-77.

53. Malgieri A, Kantzari E, Patrizi MP, et al. Bone marrow and umbilical cord blood human mesenchymal stem cells: state of the art. *International Journal of Clinical and Experimental Medicine*, 2010; 3(4): 248-269.
54. Davies JE, Walker JT & Keating A. Concise Review: Wharton's Jelly: The Rich, but Enigmatic, Source of Mesenchymal Stromal Cells. *Stem Cells Translational Medicine*, 2017; 6: 1620-1630.
55. Lu L., Shen RN & Broxmeyer, HE. Stem cells from bone marrow, umbilical cord blood and peripheral blood for clinical application: Current status and future application. *Critical Reviews in Oncology/Hematology*, 1996; 22(2): 61-78.
56. Zhu Y, Yang Y, Zhang Y, et al. Placental mesenchymal stem cells of fetal and maternal origins demonstrate different therapeutic potentials. *Stem Cell Research & Therapy*, 2014; 5: 48.
57. Loukogeorgakis SP & Coppi PD. Concise Review: Amniotic Fluid Stem Cells: The Known, the Unknown, and Potential Regenerative Medicine Applications. *Stem Cells*, 2017; 35: 1663-1673.
58. Jaing TH. Umbilical Cord Blood: A Trustworthy Source of Multipotent Stem Cells for Regenerative Medicine. *Cell Transplantation*, 2014; 23: 493-496.
59. Jin HJ, Bae YK, Kim M, et al, Comparative Analysis of Human Mesenchymal Stem Cells from Bone Marrow, Adipose Tissue, and Umbilical Cord Blood as Sources of Cell Therapy. *International Journal of Molecular Sciences*, 2013; 14(9): 17989-8001.
60. Mareschi K, Biasin E, Piacibello W, et al. Isolation of human mesenchymal stem cells: bone marrow versus umbilical cord blood. *Haematologica*, 2001; 86(10): 1099–1110.
61. Wexler SA, Donaldson C, Denning-Kendall P, et al. Adult bone marrow is a rich source of human mesenchymal “stem” cells but umbilical cord and mobilized adult blood are not. *British Journal of Haematology*, 2003; 121(2): 368–374.
62. Miller FD & Kaplan DR. Mobilizing Endogenous Stem Cells for Repair and Regeneration: Are We There Yet? *Cell Stem Cell*, 2012; 10(6): 650-652.

63. Holyoake TL, Nicolini FE & Eaves CJ. Functional differences between transplantable human hematopoietic stem cells from fetal liver, cord blood, and adult marrow. *Experimental Hematology*, 1999; 27(9): 1418–1427.
64. Rebel VI, Miller CL, Thornbury GR, et al. A comparison of long-term repopulating hematopoietic stem cells in fetal liver and adult bone marrow from the mouse. *Experimental Hematology*, 1996; 24(5): 638–648.
65. O'Donoghue K & Fisk NM. Fetal stem cells. *Best Practice & Research Clinical Obstetrics and Gynaecology*, 2004; 18(6): 853-875.
66. Malik N. Allogeneic Versus Autologous Stem-Cell Therapy. *BioPharm International*, 2012; 25(7).
67. Bakhtiari P & Djalilian A. Update on Limbal Stem Cell Transplantation. *Middle East African Journal of Ophthalmology*, 2010; 17(1): 9-14.
68. Van Buskirk EM. The Anatomy of the Limbus. *Eye*, 1989; 3: 101-108.
69. Dua HS & Azuara-Blanco A. Autologous limbal transplantation in patients with unilateral corneal stem cell deficiency. *The British Journal of Ophthalmology*, 2000; 84(3): 273-278.
70. Pellegrini G, Traverso CE, Franzi AT, et al. Long-term restoration of damaged corneal surfaces with autologous cultivated corneal epithelium. *The Lancet*, 1997; 349(9057): 990-993.
71. Dumont NA, Wang YX, von Maltzahn J, et al. Dystrophin expression in muscle stem cells regulated their polarity and asymmetric division. *Nature Medicine*, 2015; 21(12): 1455-63.
72. Alvarez-Buylla A & Lim DA. For the Long Run: Maintaining Germinal Niches in the Adult Brain. *Neuron*, 2004; 41: 683-686.
73. Taupin P. Adult neurogenesis in the mammalian central nervous system: functionality and potential clinical interest. *Medical Science Monitor: International Medical Journal of Experimental and Clinical Research*, 2005; 11(7): RA247-252.

74. Lévesque MF, Neuman T & Rezak M. Therapeutic Microinjection of Autologous Adult Human Neural Stem Cells and Differentiated Neurons for Parkinson's Disease: Five-Year Post-Operative Outcome. *The Open Stem Cell Journal*, 2009; 1: 20-29.
75. Karaoz E, Demircan PC, Saglam O, et al. Human dental pulp stem cells demonstrate better neural and epithelial stem cell properties than bone marrow-derived mesenchymal stem cells. *Histochemistry and Cell Biology*, 2011; 136(4): 455-473.
76. Yasui T, Mabuchi Y, Morikawa S, et al. Isolation of dental pulp stem cells with high osteogenic potential. *Inflammation and Regeneration*, 2017; 37: 8.
77. Kawai G, Ohno T, Kawaguchi T, et al. Human Dental Pulp Facilitates Bone Regeneration in a Rat Bone Defect Model. *Bone and Tissue Regeneration Insights*, 2013; 4: 1-10.
78. Wang F, Jia Y, Liu J, et al. Dental pulp stem cells promote regeneration of damaged neuron cells on the cellular model of Alzheimer's disease. *Cell Biology International*, 2017; 41: 639-650.
79. Kuwabara T & Asashima M. Regenerative medicine using adult neural stem cells: the potential for diabetes therapy and other pharmaceutical applications. *Journal of Molecular Cell Biology*, 2012; 4: 133-139.
80. Kuwabara T, Kagalwala MN, Onuma Y, et al. Insulin biosynthesis in neuronal progenitors derived from adult hippocampus and the olfactory bulb. *EMBO Molecular Medicine*, 2011; 3: 742-754.
81. Park B, Yoo KH & Kim C. Hematopoietic stem cell expansion and generation: the ways to make a breakthrough. *Blood Research*, 2015; 50(4): 194-203.
82. Bryder D, Rossi DJ & Weissman IL. Hematopoietic Stem Cells: The Paradigmatic Tissue-Specific Stem Cell. *The American Journal of Pathology*, 2006; 169(2): 338-46.
83. Weissman IL. Translating Stem and Progenitor Cell Biology to the Clinic: Barriers and Opportunities. *Science*, 2000; 287(5457): 1442-1446.
84. Gschweng E, Oliveira SD & Kohn DB. Hematopoietic Stem Cells for Cancer Immunotherapy. *Immunological Reviews*, 2014; 257(1): 237-249.

85. Smith DJ, Liu S, Ji S, et al. Genetic engineering of hematopoietic stem cells to generate invariant natural killer T cell. *PNAS*, 2015; 112(5): 1523-1528.
86. Zomorodian E & Eslaminejad MB. Mesenchymal Stem Cells as a Potent Cell Source for Bone Regeneration. *Stem Cells International*, 2011; 2012(2012), Article ID 980353.
87. Friedenstein AJ, Chailakhjan RK & Lalykina KS. The development of fibroblast colonies in monolayer cultures of guinea-pig bone marrow and spleen cells. *Cell and Tissue Kinetics*, 1970; 3(4): 393–403.
88. Lindner U, Kramer J, Rohwedel J, et al. Mesenchymal Stem or Stromal Cells: Toward a Better Understanding of Their Biology? *Transfusion Medicine and Hemotherapy*, 2010; 37: 75-83.
89. Bonab MM, Alimoghaddam K, Talebian F, et al. Aging of mesenchymal stem cell in vitro. *BMC Cell Biology*, 2006; 7: 14.
90. Wu X, Wang W, Meng C, et al. Regulation of differentiation in trabecular bone-derived mesenchymal stem cells by T cell activation and inflammation. *Oncology Reports*, 2013; 30: 2211-2219.
91. de Sousa EB, Casado PL, Neto VM, et al. Synovial fluid and synovial membrane mesenchymal stem cells: latest discoveries and therapeutic perspectives. *Stem Cell Research & Therapy*, 2014; 5: 112.
92. Fat tissue: an underappreciated source of stem cells for biotechnology. *Trends in Biotechnology*, 2006; 24: 150-154.
93. Bosch P, Musgrave DS, Lee JY, et al. Osteoprogenitor cells within skeletal muscle. *Journal of Orthopaedic Research*, 2000; 18(6): 933-944.
94. Griffiths MJ, Bonnet D, Janes SM. Stem cells of the alveolar epithelium. *The Lancet*, 2005; 366: 249-260.
95. Beltrami AP, Barlucchi L, Torella D, et al. Adult cardiac stem cells are multipotent and support myocardial regeneration. *Cell*, 2003; 114: 763-776.

96. Cao C, Dong Y & Dong Y. Study on culture and in vitro osteogenesis of blood-derived human mesenchymal stem cells. *Zhongguo Xiu Fu Chong Jian Wai Ke Za Zhi*, 2005; 19: 642-647.
97. Dominici M, le Blanc K, Mueller I, et al. Minimal criteria for defining multipotent mesenchymal stromal cells. The International Society for Cellular Therapy position statement. *Cytotherapy*, 2006; 8(4): 315-317.
98. Deskins DL, Bastakoty D, Sarawati S, et al. Human Mesenchymal Stromal Cells: Identifying Assays to Predict Potency for Therapeutic Selection. *Stem Cells Translation Medicine*, 2013; 2: 151-158.
99. Fox AJS, Bedi A & Rodeo SA. The Basic Science of Articular Cartilage: Structure, Composition, and Function. *Sports Health*, 2009; 1(6): 461-468.
100. Huey DJ, Hu JC & Athanasiou KA. Unlike Bone, Cartilage Regeneration Remains Elusive. *Science*, 2012; 16: 917-921.
101. Ghezzi CE, Marelli B, Donelli I, et al. Multilayered dense collagen-silk fibroin hybrid: a platform for mesenchymal stem cell differentiation towards chondrogenic and osteogenic lineages. *Journal of Tissue Engineering and Regenerative Medicine*, 2017; 11: 2046-2059.
102. Hofmann S, Knecht S, Langer R, et al. Cartilage-like Tissue Engineering Using Silk Scaffolds and Mesenchymal Stem Cells. *Tissue Engineering*, 2006; 12(10): 2729-2738.
103. Huang CY, Reuben PM, D'Ippolito G, et al. Chondrogenesis of human bone marrow-derived mesenchymal stem cells in agarose culture. *Anat Rec A Discov Mol Cell Evol Biol*. 2004;278(1): 428-436.
104. Quarto R, Mastrogiacomo M, Cancedda R, et al. Repair of large bone defects with the use of autologous bone marrow stromal cells. *The New England Journal of Medicine*, 2001; 344(5): 385-386.
105. Maiti SK, Ninu AR, Sangeetha P, et al. Mesenchymal stem cells-seeded bio-ceramic construct for bone regeneration in large critical-size bone defect in rabbit. *Journal of Stem Cells & Regenerative Medicine*, 2016; 12(2): 87-99.

106. Tondreau T, Dejeneffe M, Meuleman N, et al. Gene expression pattern of functional neuronal cells derived from human bone marrow mesenchymal stromal cells. *BMC Genetics*, 2008; 9: 166.
107. Zeng R, Wang LW, Hu ZB, et al, Differentiation of human bone marrow mesenchymal stem cells into neuron-like cells in vitro. *Spine*, 2011; 36(13): 997–1005.
108. Ma N, Gai H, Mei J, et al. Bone marrow mesenchymal stem cells can differentiate into type II alveolar epithelial cells in vitro. *Cell Biology International*, 2011; 35(12): 1261–1266.
109. Ullah I, Subbarao RB & Rho GJ. Human mesenchymal stem cells – current trends and future prospective. *Bioscience Reports*, 2015; 35: e00191.
110. Gneccchi M, Danieli P, Malpass G, et al. Paracrine mechanisms of mesenchymal stem cells in tissue repair. *Methods in Molecular Biology*, 2016; 1416: 123-146.
111. Kusuma GD, Carthew J, Lim R, et al. Effect of the Microenvironment on Mesenchymal Stem Cell Paracrine Signaling: Opportunities to Engineer the Therapeutic Effect. *Stem Cells and Development*, 2017; 26(9): 617-631.
112. Kuraitis D, Giordano C, Ruel M, et al. Exploiting extracellular matrix-stem cell interactions: a review of natural materials for therapeutic muscle regeneration. *Biomaterials*, 2012; 33(2): 428–443.
113. Khubutiya MS, Vagabov AV, Temnov AA, et al. Paracrine mechanisms of proliferative, anti-apoptotic and anti-inflammatory effects of mesenchymal stromal cells in models of acute organ injury. *Cytotherapy* 16(5): 579–585.
114. Karantalis V & Hare JM. Use of Mesenchymal Stem Cells for Therapy of Cardiac Disease. *Circulation Research*, 2015; 116(8): 1413-1430.
115. Mirotsoy M, Zhang Z, Deb A, et al. Secreted frizzled related protein 2 (Sfrp2) is the key Akt-mesenchymal stem cell-released paracrine factor mediating myocardial survival and repair. *Proceedings of the National Academy of Sciences of the United States of America*, 2007; 104(5): 1643-1648.

116. Block GJ, Ohkouchi S, Fung F, et al. Multipotent stromal cells are activated to reduce apoptosis in part by upregulation and secretion of stanniocalcin-1. *Stem Cells*, 2009; 27(3): 670-681.
117. Young NS, Calado RT & Scheinberg P. Current concepts in the pathophysiology and treatment of aplastic anemia. *Blood*, 2006; 108(8): 2509-2519.
118. Pang Y, Xiao HW, Zhang H, et al. Allogenic Bone Marrow-Derived Mesenchymal Stromal Cells Expanded In Vitro for Treatment of Aplastic Anemia: A Multicenter Phase II Trial. *Stem cells Translational Medicine*, 2017; 6: 1569-1575.
119. Usha L, Rao G, II KC, et al. Mesenchymal Stem Cells Develop Tumor Tropism but Do Not Accelerate Breast Cancer Tumorigenesis in a Somatic Mouse Breast Cancer Model. *PLOS ONE*, 2013; 8(9): e67895.
120. Ohta Y, Hamaguchi A, Ootaki M, et al. Intravenous infusion of adipose-derived stem/stromal cells improves functional recovery of rats with spinal cord injury. *Cytotherapy*, 2017; 19: 839-848.
121. Harman RM, Yang S, He MK, et al. Antimicrobial peptides secreted by equine mesenchymal stromal cells inhibit the growth of bacteria commonly found in skin wounds. *Stem Cell Research & Therapy*, 2017; 8: 157.
122. Amable PR, Teixeira MVT, Carias RBV, et al. Protein synthesis and secretion in human mesenchymal cells derived from bone marrow, adipose tissue and Wharton's jelly. *Stem Cell Research & Therapy*, 2014; 5: 53.
123. Siegel G, Kluba T, Hermanutz-Klein U, et al. Phenotype, donor age and gender affect function of human bone marrow-derived mesenchymal stromal cells. *BMC Medicine*, 2013; 11: 146
124. Ryan JM, Barry FP, Murphy JM, et al. Mesenchymal stem cells avoid allogeneic rejection. *Journal of Inflammation*, 2005; 2: 8.
125. Schwartz RE, Reyes M, Koodie L, et al. Multipotent adult progenitor cells from bone marrow differentiate into functional hepatocyte-like cells. *The Journal of Clinical Investigation*, 2002; 109(10): 1291-1302.

126. Trounson A & McDonald C. Stem Cell Therapies in Clinical Trials: Progress and Challenges. *Cell Stem Cell*, 2015, 17: 11-22.
127. Elseberg C, Leber J, Weidner T, et al. The Challenge of Human Mesenchymal Stromal Cell Expansion: Current and Prospective Answers. New Insights into Cell Culture Technology, Dr. Sivakumar Joghi Thatha Gowder (Ed.), *InTech*, 2017; DOI: 10.5772/66901. Available from: <https://www.intechopen.com/books/new-insights-into-cell-culture-technology/the-challenge-of-human-mesenchymal-stromal-cell-expansion-current-and-prospective-answers>
128. Pittenger MF, Le Blanc K, Phinney DG, et al. MSCs: Scientific Support for Multiple Therapies. *Stem Cells International*, 2015; 2015, Article ID 280572.
129. Chabannon C, Caunday-Rigot O, Faucher C, et al. Accreditation and regulations in cell therapy. *ISBT Science Series*, 2016; 11(Suppl. 1): 271-276.
130. Haagdoorens M, Van Acker SI, Van Gerwen V, et al. Limbal Stem Cell Deficiency: Current Treatment Options and Emerging Therapies. *Stem Cells International*, 2016; 2016: Article ID 9798374.
131. Ratcliffe E, Glen KE, Naing MW, et al. Current status and perspectives on stem cell-based therapies undergoing clinical trials for regenerative medicine: case studies. *British Medical Bulletin*, 2013; 108: 73-94.
132. Schrepfer S, Deuse T, Reichenspurner H, et al. Stem Cell Transplantation: The Lung Barrier. *Transplantation Proceedings*, 2007; 39: 573-576.
133. Ryan JA. Evolution of Cell Culture Surfaces. *Biofiles*, 2008; 3.8: 21. URL: <http://www.sigmaaldrich.com/technical-documents/articles/biofiles/evolution-of-cell.html#ref>
134. Amstein CF & Hartman PA. Adaptation of Plastic Surfaces for Tissue Culture by Glow Discharge. *Journal of Clinical Microbiology*, 1975; 2(1): 46-54.
135. Ramsey WS, Hertl W, Nowlan ED, et al. Surface treatments and cell attachment. *In Vitro*, 1984; 20(10): 802-808.

136. Godara P, McFarland CD & Nordon RE. Design of bioreactors for mesenchymal stem cell tissue engineering. *Journal of Chemical Technology and Biotechnology*, 2008; 83: 408-420.
137. Titus K, Klimovich V, Rothenberg M, et al. Closed System Cell Culture Protocol Using HYPERStack Vessels with Gas Permeable Material Technology. *Journal of Visualized Experiments*, 2010; 45: e2499.
138. Rowley J, Abraham E, Campbell A, et al. Meeting Lot-Size Challenges of Manufacturing Adherent Cells for Therapy. *BioPress International*, 2012; 10(3): 16-22.
139. Thomas RJ, Chandra A, Liu Y, et al. Manufacture of a human mesenchymal stem cell population using an automated cell culture platform. *Cytotechnology*, 2007; 55(1): 31-39.
140. Eibes G, dos Santos F, Andrade PZ, et al. Maximizing the *ex vivo* expansion of human mesenchymal stem cells using a microcarrier-based stirred culture system. *Journal of Biotechnology*, 2010; 146: 194-197.
141. Hewitt CJ, Lee K, Nienow AW, et al. Expansion of human mesenchymal stem cells on microcarriers. *Biotechnology Letters*, 2011; 33(11): 2325-2335.
142. Santos FD, Andrade PZ, Abecasis MM, et al. Toward a Clinical-Grade Expansion of Mesenchymal Stem Cells from Human Sources: A Microcarrier-Based Culture System Under Xeno-Free Conditions. *Tissue Engineering. Part C, Methods*, 2011; 17(12): 1201-1210.
143. Stupack DG. Integrins as a distinct subtype of dependence receptors. *Cell Death and Differentiation*, 2005; 12: 1021-1030.
144. Kato D, Takeuchi M, Sakurai T, et al. The design of polymer microcarrier surfaces for enhances cell growth. *Biomaterials*, 2003; 24: 4253-4264.
145. van der Velden-de Groot CAM. Microcarrier technology, present status and perspective. *Cytotechnology*, 1995; 18(1-2): 51-56.
146. Qui QQ, Ducheyne P & Ayyaswamy PS. Fabrication, Characterization and Evaluation of Bioceramic Hollow Microspheres Used as Microcarriers for 3-D Bone Tissue Formation in Rotating Bioreactors. *Biomaterials*, 1999; 20(11): 989-1001.

147. Schirmaier C, Jossen V, Kaiser SC, et al. Scale-up of adipose tissue-derived mesenchymal stem cell production in stirred single-use bioreactors under low-serum conditions. *Engineering in Life Sciences*, 2014; 14: 292-303.
148. Timmins NE, Kiel M, Günther M, et al. Closed System Isolation and Scalable Expansion of Human Placental Mesenchymal Stem Cells. *Biotechnology and Bioengineering*, 2012; 109(7): 1817-1826.
149. Nienow AW, Rafiq QA, Coopman K, et al. A potentially scalable method for the harvesting of hMSCs from microcarriers. *Biochemical Engineering Journal*, 2014; 85: 79-88.
150. Mardikar SH & Niranjana K. Observations on the Shear damage to Different Animal Cells in a Concentric Cylinder Viscometer. *Biotechnology and Bioengineering*, 2000; 68(6): 697-704.
151. Augenstein DC, Sinskey AJ & Wang DIC. Effect of Shear on the Death of Two Strains of Mammalian Tissue Cells. *Biotechnology and Bioengineering*, 1971; XIII: 409-418.
152. Merten OW. Advance in cell culture: anchorage dependence. *Philosophical transactions of the Royal Society of London. Service B, Biological Sciences*, 2015; 370(1661): 20140040.
153. Dong JD, Gu YQ, Li CM, et al. Response of mesenchymal stem cells to shear stress in tissue engineered vascular grafts. *Acta Pharmacologica Sinica*, 2009; 30(5): 530-536.
154. Yourek G, McCormick SM, Mao JJ, et al. Shear stress induces osteogenic differentiation of human mesenchymal stem cells. *Regenerative Medicine*, 2010; 5(5): 713-724.
155. Wu J. Mechanisms of animal cell damage associated with gas bubbles and cell protection by medium additives. *Journal of Biotechnology*, 1995; 43: 81-94.
156. Chisti Y. Animal-cell damage in sparged bioreactors. *Trends in Biotechnology*, 2000; 18(10): 420-432.
157. Luo W, Xiong W, Zhou J, et al. Laminar shear stress delivers cell cycle arrests and anti-apoptosis to mesenchymal stem cells. *Acta Biochimica et Biophysica Sinica*, 2011; 43(3): 210-216.

158. Ulbrich C, Wehland M, Pietsch J, et al. The Impact of Simulated and Real Microgravity on Bone Cells and Mesenchymal Stem Cells. *BioMed Research International*, 2014; 2014: Article ID 928507.
159. Liu T, Li X, Sun X, et al. Analysis on forces and movement of cultivated particles in a rotating wall vessel bioreactor. *Biochemical Engineering Journal*, 2004; 18(2): 97-104.
160. Rodrigues AV, Fernandes TG, Diogo MM, et al. Stem cell cultivation in bioreactors. *Biotechnology Advances*, 2011; 29: 815-829.
161. Eagle H. Nutrition Needs of Mammalian Cells in Tissue Culture. *Science*, 1955; 122(3168): 501-514.
162. Meurant G. Physical Forces and the Mammalian Cell. *Nature*, 1993
163. Baker H, DeAngelis B & Frank O. Vitamins and other metabolites in various sera commonly used for cell culturing. *Experientia*, 1988; 44(11-22): 1007-1010.
164. Ozturk SS & Palsson BO. Examination of serum and bovine serum albumin as shear protective agents in agitated cultures of hybridoma cells. *Journal of Biotechnology*; 1991; 18: 13-28.
165. Mendicino M, Bailey AM, Wonnacott K, et al. MSC-based product characterization for clinical trials: an FDA perspective. *Cell Stem Cell*, 2014; 14: 141-145.
166. Siegel W & Foster L. Fetal Bovine Serum: The Impact of Geography. *BioProcessing Journal*, 2013; 12(3): 28-30.
167. Horwitz EM, Gordon PL, Koo WK, et al. Isolated allogeneic bone marrow-derived mesenchymal cells engraft and stimulate growth in children with osteogenesis imperfecta: implications for cell therapy of bone. *Proceedings of the National Academy of Sciences of the United States of America*, 2002; 99(13): 8932-8937.
168. Mackensen A, Dräger R, Schlesier M, et al. Presence of IgE antibodies to bovine serum albumin in a patient developing anaphylaxis after vaccination with human peptide-pulsed dendritic cells. *Cancer Immunology, Immunotherapy*; 2000; 49(3): 152-156.

169. Cho KS, Park HK, Park HY, et al. IFATS collection: immunomodulatory effects of adipose tissue-derived stem cells in an allergic rhinitis mouse model. *Stem Cells*, 2009; 27(1): 259–265.
170. Dessels C, Potgieter M & Pepper MS. Making the Switch: Alternative Fetal Bovine Serum for Adipose-Derived Stromal Cell Expansion. *Frontiers in Cell and Developmental Biology*, 2016; 4: e00115.
171. Gstraunthaler G, Lindl T & van der Valk J. A plea to reduce or replace fetal bovine serum in cell culture media. *Cytotechnology*, 2013; 65: 791-793.
172. Kummalue T, Okada M, Hara T, et al. Fetal Bovine Serum Lot Selection for OP9 Cells Culture Induction System in Differentiation of Hematopoietic Stem Cells. *Siriraj Medical Journal*, 2010; 62: 228-230.
173. Zheng X, Baker H, Hancock WS, et al. Proteomic Analysis for the Assessment of Different Lots of Fetal Bovine Serum as a Raw Material for Cell Culture. Part IV. Application of Proteomics to the Manufacture of Biological Drugs. *Biotechnology Progress*. 2006; 22(5): 1294-1300.
174. dos Santos VTM, Mizukami A, Orellana MD, et al. Characterization of Human AB Serum for Mesenchymal Stromal Cell Expansion. *Transfusion Medicine and Hemotherapy*, 2017; 44: 11-21.
175. Idahmash A, Haack-Sorensen M, Al-Nbaheen M, et al. Human serum is as efficient as fetal bovine serum in supporting proliferation and differentiation of human multipotent stromal (mesenchymal) stem cells in vitro and in vivo. *Stem Cell Reviews*, 2011; 7(4): 860-868.
176. Mizuno M, Katano H, Otabe K, et al. Complete human serum maintains viability and chondrogenic potential of human synovial stem cells: suitable conditions for transplantation. *Stem Cell Research & Therapy*, 2017; 8: 144.
177. Strandberg G, Sellberg F, Sommar P, et al. Standardizing the freeze-thaw preparation of growth factors from platelet lysate. *Transfusion*, 2017; 57(4): 1058-1065.

178. Shih DTB & Burnouf T. Preparation, quality criteria and properties of human blood platelet lysate supplements for *ex vivo* stem cell expansion. *New Technology*, 2015; 32(1): 199-211.
179. Matthyssen S, Dhubhghaill SN, Gerwen VV, et al. Xeno-Free Cultivation of Mesenchymal Stem Cells From the Corneal Stroma. *Investigate Ophthalmology & Visual Science*, 2017; 58(5): 2659-2665.
180. Ohetfond J, Tawonsawatruk T, Seenprachawong K, et al. Re-using blood products as an alternative supplement in the optimisation of clinical-grade adipose-derived mesenchymal stem cell culture. *Bone & Joint Research*, 2017; 6(7): 414-422.
181. Søndergaard RH, Follin B, Lund LD, et al. Senescence and quiescence in adipose-derived stromal cells: Effects of human platelet lysate, fetal bovine serum and hypoxia. *Cytotherapy*, 2017; 19: 95-106.
182. Oikonomopoulos A, van Deen WK, Manansala AR, et al. Optimization of human mesenchymal stem cell manufacturing: the effects of animal/xeno-free media. *Scientific Reports*, 2015; 5: 16570.
183. Saeed MA, El-Rahman M, Helal ME, et al. Efficacy of Human Platelet Rich Fibrin Exudate vs Fetal Bovine Serum on Proliferation and Differentiation of Dental Pulp Stem Cells. *International Journal of Stem Cells*, 2017; 10(1): 38-47.
184. do Amaral RJFC, Matsiko A, Tomazette MRP, et al. Platelet-rich plasma releasate differently stimulates cellular commitment toward the chondrogenic lineage according to concentration. *Journal of Tissue Engineering*, 2015; 6: 1-14.
185. Glovinski PV, Herly M, Mathiasen AB, et al. Overcoming the bottleneck of platelet lysate supply in large-scale clinical expansion of adipose-derived stem cells: A comparison of fresh versus three types of platelet lysates from outdated buffy coat-derived platelet concentrates. *Cytotherapy*, 2017; 19: 222-234.
186. Lee J, Roh KB, Kim SC, et al. Soy peptides-induced stem cell proliferation: involvement of ERK and TFG- $\beta$ 1. *The Journal of Nutritional Biochemistry*, 2012; 23(10): 1341-1351.

187. Miwa H, Hashimoto Y, Tensho K, et al. Xeno-free proliferation of human bone marrow mesenchymal stem cells. *Cytotechnology*, 2012; 64: 301-308.
188. Gottipamula S, Muttigi MS, Kolkundkar U, et al. Serum-free media for the production of human mesenchymal stromal cells: a review. *Cell Proliferation*, 2013; 46(6): 608–627.
189. Rajala K, Lindroos B, Hussein SM, et al. A Defined and Xeno-Free Culture Method Enabling the Establishment of Clinical-Grade Human Embryonic, Induced Pluripotent and Adipose Stem Cells. *PLoS ONE*, 2010; 5(4): e10246.
190. Mimura S, Kimura N, Hirata N, et al. Growth factor defined culture medium for human mesenchymal stem cells. *International Journal of Developmental Biology*, 2011; 55(2): 181–187.
191. Liu CH, Wu ML & Hwang SM. Optimization of serum free medium for cord blood mesenchymal stem cells. *Biochemical Engineering Journal*, 2007; 33(1): 1-9.
192. Wu X, Kang H, Liu X, et al. Serum and xeno-free, chemically defined, no-plate-coating-based culture system for mesenchymal stromal cells from the umbilical cord. *Cell Proliferation*, 2016; 49: 579-588.
193. Jung S, Sen A, Rosenberg L, et al. Identification of growth and attachment factors for the serum-free isolation and expansion of human mesenchymal stromal cells. *Cytotherapy*, 2010; 12: 637-657.
194. Boa X, Lian X, Dunn KK, et al. Chemically-defined albumin-free differentiation of human pluripotent stem cells to endothelial progenitor cells. *Stem Cell Research*, 2015; 15: 122-129.
195. Yang D, Chen S, Gao C, et al. Chemically defined serum-free conditions for cartilage regeneration from human embryonic stem cells. *Life Sciences*, 2016; 164: 9-14.
196. López M, Bollag RJ, Yu JC, et al. Chemically Defined and Xeno-Free Cryopreservation of Human Adipose-Derived Stem Cells. *PLoS ONE*, 2016; 11(3): e0152161.

197. Feng J, Zhang W, Han L, et al. Statistical optimization of medium components to improve the antibiotic activity of *Streptomyces* sp. 19G-317. *African Journal of Agricultural Research*, 2011; 6(19): 4424-4431.
198. Cockshott AR & Sullivan GR. Improving the fermentation medium for Echinocandin B production. Part I: sequential statistical experimental design. *Process Biochemistry*, 2001; 36: 647-660.
199. Plackett RL & Burman JP. The Design of Optimum Multifactorial Experiments. *Biometrika*, 1946; 33(4): 305-325.
200. Muthuvelayudham R & Viruthagiri T. Application of Central Composite Design Based Response Surface Methodology in Parameter Optimization and on Cellulase Production Using Agricultural Waste. *International Journal of Chemical and Biological Engineering*. 2010; 3(2): 97-104.
201. Singh V, Haque S, Niwas R, et al. Strategies for Fermentation Medium Optimization: An In-Depth Review. *Frontiers in Microbiology*. 2016; 7: 2087.
202. Patil SV, Jayaraman VK & Kulkarni BD. Optimization of media by evolutionary algorithms for production of polyols. *Applied Biochemistry and Biotechnology*, 2002; 102-103(1-6): 119-128.
203. Camacho-Rodríguez J, Verón-García MC, Fernández-Sevilla FM, et al. Genetic algorithm for the medium optimization of the microalga *Nannochloropsis gaditana* cultures to aquaculture. *Bioresource Technology*, 2015; 177: 102-109.
204. Paladino FV, Peixoto-Cruz JS, Santacruz-Perez C, et al. Comparison between isolation protocols highlights intrinsic variability of human umbilical cord mesenchymal cells. *Cell and Tissue Banking*, 2016; 17(1): 123-136.
205. Vakhrushev IV, Vdovin AS, Strukova LA, et al. Variability of the Phenotype and Proliferation and Migration Characteristics of Human Mesenchymal Stromal Cells Derived from the Deciduous Teeth Pulp of Different Donors. *Bulletin of Experimental Biology and Medicine*, 2016; 160(4): 525-529.
206. CK-12 Foundation. 13.65: Fertilization, Blastocyst Diagram. Image accessed 12 September 2017, <<https://www.ck12.org/book/CK-12-Biology-Concepts/section/13.65/>>

207. Ackermann M, Liebhaber S, Klusmann JH et al. Lost in translation: pluripotent stem cell- derived hematopoiesis. *EMBO Molecular Medicine*, 2015; 7(11): 1388-1402.
208. Infors Benelux BV. Bench-Top Bioreactors, Labfors 5. Image accessed 12 September 2017, <<http://www.infors-ht.nl/en/category/bioreactors/>>
209. The Dish. Raising the bar for rocking bioreactors: Introducing the ReadyToProcess WAVE 25 system. 2013, Image accessed 12 September 2017, <<http://cellculturedish.com/2013/12/raising-bar-rocking-bioreactors-introducing-readytoprocess-wave-25-system/>>
210. Pittenger MF, Mackay AM, Beck SC, et al. Multilineage Potential of Adult Human Mesenchymal Stem Cells. *Science*, 1999; 284(5411): 143-147.
211. Mareschi K, Rustichelli D, Calabrese R, et al. Multipotent Mesenchymal Stromal Stem Cell Expansion by Plating Whole Bone Marrow at a Low Cellular Density: A More Advantageous Method for Clinical Use. *Stem Cells International*, 2012; 2012: 920581.
212. Wang H, Xie Z, Hou T, et al. MiR-125b Regulates the Osteogenic Differentiation of Human Mesenchymal Stem Cells by Targeting BMPR1b. *Cellular Physiology and Biochemistry: International Journal of Experimental Cellular Physiology, Biochemistry, and Pharmacology*, 2017; 41(2): 530-542.
213. Meretoja VV, Rahlin RL, Kasper FK, et al. Enhanced chondrogenesis in co-cultures with articular chondrocytes and mesenchymal stem cells. *Biomaterials*, 2012; 33(27): 6362-9.
214. Neubauer M, Fischbach C, Bauer-Kreisel P, et al. Basic fibroblast growth factor enhances PPARgamma ligand-induced adipogenesis of mesenchymal stem cells. *FEBS Letters*, 2004; 577(1-2): 277-283.
215. Yadav AR, Sriram R, Carter JA, et al. Comparative study of solution-phase and vapor-phase deposition of aminosilanes on silicon dioxide surfaces. *Materials Science & Engineering. C, Materials for Biological applications*, 2014; 35: 283-290.
216. Kato Y & Gospodarowicz D. Growth requirements of low-density rabbit costal chondrocyte cultures maintained in serum-free medium. *Journal of Cellular Physiology*, 1984; 120(3): 354-363.
217. Shrader CD, Bailey KM, Konat GW, et al. Insulin enhances proliferation and viability of human umbilical vein endothelial cells. *Archives of Dermatological Research*, 2009; 301(2): 159-166.
218. Chen G, Sato T, Tanaka J, et al. Preparation of a biphasic scaffold for osteochondral tissue engineering. *Materials Science and Engineering: C*, 2006; 26(1): 118-123.

219. Gneccchi M, He H, Liang OD, et al. Paracrine action accounts for marked protection of ischemic heart by Akt-modified mesenchymal stromal cells. *Nature Medicine*, 2005; 11(4): 367-368.
220. Yang CC, Shih YH, Ko MH, et al. Transplantation of human umbilical mesenchymal stromal cells from Wharton's jelly after complete transection of the rat spinal cord. *PLoS ONE*, 2008; 3(10): e3336.
221. Murphy JM, Dixon K, Beck S, et al. Reduced Chondrogenic and Adipogenic Activity of Mesenchymal Stem Cells From Patients With Advanced Osteoarthritis. *Arthritis & Rheumatism*, 2002; 46(3): 704-713.
222. Lanza F, Campioni D, Moretti S, et al. Aberrant expression of HLA-DR antigen by bone marrow-derived mesenchymal stromal cells from patients affected by acute lymphoproliferative disorders. *Leukemia*, 2007; 21: 378-381.
223. Bocelli-Tyndall FGF2 induces RANKL gene expression as well as IL1 regulated MHC class II in human bone marrow-derived mesenchymal progenitor stromal cells. 2013; 74(1): 260-266.
224. Sotiropoulou PA, Perez SA, Salagianni M, et al. Characterization of the Optimal Culture Conditions for Clinical Scale Production of Human Mesenchymal Stem Cells. *Stem Cells Technology Development*, 2006; 24: 462-471.
225. Shafaei H, Esmaeili A, Mardani M, et al. Effects of human placental serum on proliferation and morphology of human adipose tissue-derived stem cells. *Bone Marrow Transplantation*, 2011; 46: 1464-1471.
226. Alimperti S & Andreadis ST. CDH2 and CDH11 act as regulators of stem cell fate decisions. *Stem Cell Research*, 2015; 14(3): 270-282.
227. Yang L, Clinton JM, Blackburn ML, et al. Rab23 regulates differentiation of ATDC5 chondroprogenitor cells. *The Journal of Biological Chemistry*, 2008; 283(16): 10649-10657.
228. Ikeda Y, Sakaue M, Chijimatsu R, et al. IGF-1 Gene Transfer to Human Synovial MSCs Promote Their Chondrogenic Differentiation Potential without Induction of the Hypertrophic Phenotype. *Stem Cells International*, 2017; 2017: Article ID 5804147.
229. Baksh D, Boland GM & Tuan RS. Cross-talk between Wnt signaling pathways in human mesenchymal stem cells leads to functional antagonism during osteogenic differentiation. *Journal of Cellular Biochemistry*. 2007; 101(5): 1109-1124.
230. Jamal M, Chogle SM, Karam SM, et al. NOTCH3 is expressed in human apical papilla and in subpopulations of stem cells isolated from the tissue. *Genes & Disease*, 2015; 2: 261-267.

231. Lui CH, Wu ML & Hwang SM. Optimization of serum free medium for cord blood mesenchymal stem cells. *Biochemical Engineering*. 2007; 33: 1-9.
232. Chase LG, Lakshmipathy U, Solchaga LA, Rao MS & Vemuri MC. A novel serum-free medium for the expansion of human mesenchymal stem cells. *Stem Cell Research & Therapy*. 2010: 1-8.
233. Choi KM, Seo YK, Yoon HH, Song KY, Kwon SY, Lee HS & Park JK. Effect of ascorbic acid on bone marrow-derived mesenchymal stem cell proliferation and differentiation. *Journal of Bioscience and Bioengineering*. 2008; 105(6): 586-594.
234. Marquez-Curtis LA & Janowska-Wieczorek A. Enhancing the Migration Ability of Mesenchymal Stromal Cells by Targeting the SDF-1/CXCR4 Axis. *BioMed Research International*. 2013.
235. Pricola KL, Kuhn NZ, Haleem-Smith H, Song Y & Tuan RS. Interleukin-6 maintains bone marrow-derived mesenchymal stem cell stemness by an ERK1/2-dependent mechanism. *Journal of Cellular Biochemistry*. 2009; 108(3): 577-588.
236. Yang J, Watkins D, Chen CL, Bhushan B, Zhou Y & Besner GE. Heparin-binding epidermal growth factor-like growth factor and mesenchymal stem cells act synergistically to prevent experimental necrotizing enterocolitis. *Journal of the American College of Surgeons*. 2012; 215(4): 534-545.
237. Stewart A, Guan H & Yang K. BMP-3 promotes mesenchymal stem cell proliferation through the TGF-beta/activin signaling pathway. *Journal of Cellular Physiology*. 2010; 223(3): 658-666.
238. Zhang J, Xie SS, Han XX, Ren JT, Lv FR, Tang JM, Zheng F, Guo LY, Yang JY, Kong X, Zhang L, Huang YZ & Wan JN. Effect of vascular endothelial growth factor on bone marrow-derived mesenchymal stem cell proliferation and the signaling mechanism. *Nan Fang Yi Ke Da Xue Xue Bao*. 2011; 31(10): 1697-1700.
239. Nakamura K, Yoshimura A, Kaneko T, Sato K & Hara Y. ROCK inhibitor Y-27632 maintains the proliferation of confluent human mesenchymal stem cells. *Journal of Periodontal Research*. 2014; 49(3): 363-370.
240. Jeon BJ, Yang Y, Kyung Shim S, Yang HM, Cho D & Ik Bang S. Thymosin beta-4 promotes mesenchymal stem cell proliferation via an interleukin-8-dependent mechanism. *Experimental Cell Research*. 2013; 319(17): 2526-2534.
241. Ng F, Boucher S, Koh S, et al. PDGF, TGF- $\beta$ , and FGF signalling is important for differentiation and growth of mesenchymal stem cells (MSCs): transcriptional profiling can identify markers and signaling pathways important in differentiation of MSCs into adipogenic, chondrogenic, and osteogenic lineages. *Blood*, 2008; 112(2): 295-307.

242. Lee MS, Youn C, Lim JH, et al. Enhanced Cell Growth of Adipocyte-Derived Mesenchymal Stem Cells Using Chemically-Defined Serum-Free Media. *International Journal of Molecular Sciences*, 2017; 18(8): E1779.
243. Brohlin M, Kelk P, Wiberg M, et al. Effects of a defined xeno-free medium on the growth and neurotrophic and angiogenic properties of human adult stem cells. *Cytotherapy*, 2017; 19(5): 629:639.
244. Mark P, Kleinsorge M, Gaebel R, et al. Human Mesenchymal Stem Cells Display Reduced Expression of CD105 after Culture in Serum-Free Medium. *Stem Cell International*, 2013; 2013: Article ID 698076.
245. Anderson P, Carrillo-Gálvez AB, García-Pérez A, et al. CD105 (Endoglin)-Negative Murine Mesenchymal Stromal Cells Define a New Multipotent Subpopulation with Distinct Differentiation and Immunomodulatory Capacities. *PLoS ONE*, 2013; 8(10): e76979.
246. Lotz S, Goderie S, Tokas N, et al. Sustained Levels of FGF2 Maintain Undifferentiated Stem Cell Cultures with Biweekly Feeding. *PLoS ONE*, 2013; 8(2): e56289.
247. Docheva D, Popov C, Mutschler W, et al. Human mesenchymal stem cells in contact with their environment: surface characteristics and the integrin system. *Journal of cellular and Molecular Medicine*, 2007; 11(1): 21-38.
248. Kisiday J, Hale BW, Almodovar JL, et al. Expansion of mesenchymal stem cells on fibrinogen-rich protein surfaces derived from blood plasma. *Journal of Tissue Engineering and Regenerative Medicine*. 2010; 5(8): 600-611.
249. Geiger B & Yamada KM. Molecular Architecture and Function of Matrix Adhesions. *CSH Perspectives*. 2011.
250. Yadav AR, Sriram R, Carter JA, et al. Comparative study of solution-phase and vapor-phase deposition of aminosilanes on silicon dioxide surfaces, *Materials Science and Engineering. C, Materials for Biological Applications*, 2014; 35: 283-290.
251. Majumdar MK, Banks V, Peluso DP, et al. Isolation, Characterization, and Chondrogenic Potential of Human Bone Marrow-Derived Multipotential Stromal Cells. *Journal of Cellular Physiology*, 2000; 185(1): 98-106.
252. Ouyang G, El-Youssef M, Yen-Lieberman B, et al. Expression of HLA-DR antigens in inflammatory bowel disease mucosa: Role of intestinal lamina propria mononuclear cell-derived interferon  $\gamma$ . *Digestive Diseases and Sciences*. 1988; 33(12): 1528-1536.
253. Varricchi G, Loffredo S, Galdiero, et al. Innate effector cells in angiogenesis and lymphangiogenesis. *Current Opinions in Immunology*. 2018; 53: 152-160.

# Appendices

## Appendix A

Appendix A		
nCounter Gene List		
Official Symbol	Alias / Previous Symbol	Official Full Name
ABCG2		ATP-binding cassette, sub-family G (WHITE), member 2
ACTC1	ACTC	actin, alpha, cardiac muscle 1
ADAM17	TACE	ADAM metallopeptidase domain 17
ADAR	IFI4, G1P1	adenosine deaminase, RNA-specific
ALDH1A1	PUMB1, ALDH1	aldehyde dehydrogenase 1 family, member A1
ALDH2		aldehyde dehydrogenase 2 family (mitochondrial)
APC		adenomatous polyposis coli
APH1A		anterior pharynx defective 1 homolog A ( <i>C. elegans</i> )
ASCL2		achaete-scute complex homolog 2 ( <i>Drosophila</i> )
AXIN1		axin 1
BMP1	PCOLC	bone morphogenetic protein 1
BMP2	BMP2A	bone morphogenetic protein 2
BMP3		bone morphogenetic protein 3
BTRC		beta-transducin repeat containing
CCNA2	CCNA, CCN1	cyclin A2
CCND1	BCL1, D11S287E, PRAD1	cyclin D1
CCND2		cyclin D2
CCND3		cyclin D3
CCNE1	CCNE	cyclin E1
CD3D	T3D	CD3d molecule, delta (CD3-TCR complex)
CD4		CD4 molecule
CD44	MIC4, MDU2, MDU3	CD44 molecule (Indian blood group)
CD8A	CD8	CD8a molecule
CD8B	CD8B1	CD8b molecule
CDC2		cell division cycle 2, G1 to S and G2 to M
CDC42		cell division cycle 42 (GTP binding protein, 25kDa)
CDH1	UVO	cadherin 1, type 1, E-cadherin (epithelial)
CDH2	NCAD	cadherin 2, type 1, N-cadherin (neuronal)
CIR1		corepressor interacting with RBPJ, 1
COL1A1		collagen, type I, alpha 1
COL2A1	SEDC	collagen, type II, alpha 1
CREBBP	RSTS	CREB binding protein
CSNK1A1		casein kinase 1, alpha 1
CSNK1A1L		casein kinase 1, alpha 1-like

CSNK1D		casein kinase 1, delta
CSNK1E		casein kinase 1, epsilon
CSNK1G 1		casein kinase 1, gamma 1
CSNK1G 2		casein kinase 1, gamma 2
CSNK1G 3		casein kinase 1, gamma 3
CSNK2A 1		casein kinase 2, alpha 1 polypeptide
CTBP1		C-terminal binding protein 1
CTBP2		C-terminal binding protein 2
CTNNA1		catenin (cadherin-associated protein), alpha 1, 102kDa
CTNNB1	CTNNB	catenin (cadherin-associated protein), beta 1, 88kDa
CXCL12	SDF1A, SDF1B, SDF1	chemokine (C-X-C motif) ligand 12 (stromal cell-derived factor 1)
DHH		desert hedgehog homolog (Drosophila)
DLL1		delta-like 1 (Drosophila)
DLL3		delta-like 3 (Drosophila)
DLL4		delta-like 4 (Drosophila)
DTX1		deltex homolog 1 (Drosophila)
DTX2		deltex homolog 2 (Drosophila)
DTX3		deltex homolog 3 (Drosophila)
DTX3L		deltex 3-like (Drosophila)
DTX4		deltex homolog 4 (Drosophila)
DVL1		dishevelled, dsh homolog 1 (Drosophila)
DVL2		dishevelled, dsh homolog 2 (Drosophila)
DVL3		dishevelled, dsh homolog 3 (Drosophila)
EP300		E1A binding protein p300
FBXW11	FBXW1B	F-box and WD repeat domain containing 11
FBXW2		F-box and WD repeat domain containing 2
FGF1	FGFA	fibroblast growth factor 1 (acidic)
FGF2	FGFB	fibroblast growth factor 2 (basic)
FGF4	HSTF1	fibroblast growth factor 4
FGFR1	FLT2, KAL2	fibroblast growth factor receptor 1
FOSL1		FOS-like antigen 1
FOXA2	HNF3B	forkhead box A2
FRAT1		frequently rearranged in advanced T-cell lymphomas
FOXD3		forkhead box D3
FURIN	PCSK3, FUR, PACE	furin (paired basic amino acid cleaving enzyme)
FZD1		frizzled homolog 1 (Drosophila)
FZD10		frizzled homolog 10 (Drosophila)
FZD2		frizzled homolog 2 (Drosophila)
FZD3		frizzled homolog 3 (Drosophila)
FZD5		frizzled homolog 5 (Drosophila)
FZD6		frizzled homolog 6 (Drosophila)
FZD7		frizzled homolog 7 (Drosophila)

FZD8		frizzled homolog 8 (Drosophila)
FZD9		frizzled homolog 9 (Drosophila)
GAS1		growth arrest-specific 1
GDF3		growth differentiation factor 3
GJB1	CMTX1, CMTX	gap junction protein, beta 1, 32kDa
GLI1	GLI	GLI family zinc finger 1
GLI2		GLI family zinc finger 2
GLI3	GCPS, PHS	GLI family zinc finger 3
GSK3B		glycogen synthase kinase 3 beta
HDAC1	RPD3L1	histone deacetylase 1
HDAC2		histone deacetylase 2
HES1	HRY	hairy and enhancer of split 1, (Drosophila)
HHIP		hedgehog interacting protein
IGF1		insulin-like growth factor 1 (somatomedin C)
IHH		Indian hedgehog homolog (Drosophila)
ISL1		ISL LIM homeobox 1
JAG1	AGS, JAGL1	jagged 1 (Alagille syndrome)
JAG2		jagged 2
JUN		jun oncogene
KAT2A	GCN5L2	K(lysine) acetyltransferase 2A
KRT15		keratin 15
LDLR		low density lipoprotein receptor
LFNG		LFNG O-fucosylpeptide 3-beta-N-acetylglucosaminyltransferase
LOC400927		TPTE and PTEN homologous inositol lipid phosphatase pseudogene
LOC652788		PREDICTED: Homo sapiens similar to dishevelled 1 isoform a
LRP2		low density lipoprotein-related protein 2
MAML1		mastermind-like 1 (Drosophila)
MAML2		mastermind-like 2 (Drosophila)
MAML3	TNRC3	mastermind-like 3 (Drosophila)
MAP3K7	TAK1	mitogen-activated protein kinase kinase kinase 7
MAP3K7IP1		mitogen-activated protein kinase kinase kinase 7 interacting protein 1
MAPK10	PRKM1	mitogen-activated protein kinase 10
MAPK9	PRKM9	mitogen-activated protein kinase 9
MFNG		MFNG O-fucosylpeptide 3-beta-N-acetylglucosaminyltransferase
MME		membrane metallo-endopeptidase
MYC		v-myc myelocytomatosis viral oncogene homolog (avian)
MYOD1	MYF3	myogenic differentiation 1
NANOG		Nanog homeobox
NCAM1		neural cell adhesion molecule 1
NCOR2		nuclear receptor co-repressor 2
NCSTN		nicastatin
NLK		nemo-like kinase
NOTCH1	TAN1	Notch homolog 1, translocation-associated (Drosophila)

NOTCH2		Notch homolog 2 (Drosophila)
NOTCH3	CADASIL	Notch homolog 3 (Drosophila)
NOTCH4	INT3	Notch homolog 4 (Drosophila)
NUMB		numb homolog (Drosophila)
NUMBL		numb homolog (Drosophila)-like
PAFAH1B1	MDCR, MDS	platelet-activating factor acetylhydrolase, isoform Ib, subunit 1 (45kDa)
KAT2B	PCAF	K(lysine) acetyltransferase 2B
PDX1	IPF1	pancreatic and duodenal homeobox 1
PLAU		plasminogen activator, urokinase
POU5F1	OCT3, Oct4, MGC22487, OTF3	POU class 5 homeobox 1
PPARD		peroxisome proliferator-activated receptor delta
PPARG		peroxisome proliferator-activated receptor gamma
PPP2CA		protein phosphatase 2 (formerly 2A), catalytic subunit, alpha isoform
PPP2R5C		protein phosphatase 2, regulatory subunit B', gamma isoform
PPP2R5E		protein phosphatase 2, regulatory subunit B', epsilon isoform
PRKACA		protein kinase, cAMP-dependent, catalytic, alpha
PRKACB		protein kinase, cAMP-dependent, catalytic, beta
PRKACG		protein kinase, cAMP-dependent, catalytic, gamma
PRKCA	PKCA	protein kinase C, alpha
PRKCB	PRKCB2, PKCB, PRKCB1	protein kinase C, beta
PRKCD		protein kinase C, delta
PRKCE		protein kinase C, epsilon
PRKCG	PKCG, SCA14	protein kinase C, gamma
PRKCH	PRKCL	protein kinase C, eta
PRKCI	DXS1179E	protein kinase C, iota
PRKCQ		protein kinase C, theta
PRKCZ		protein kinase C, zeta
PRKD1	PRKCM	protein kinase D1
PRKX		protein kinase, X-linked
PRKY		protein kinase, Y-linked
PSEN1	AD3	presenilin 1
PSEN2	AD4	presenilin 2 (Alzheimer disease 4)
PSENE1		presenilin enhancer 2 homolog (C. elegans)
RAB23		RAB23, member RAS oncogene family
RAC1		ras-related C3 botulinum toxin substrate 1 (rho family, small GTP binding protein Rac1)
RB1	OSRC	retinoblastoma 1
RBPJ	IGKJRB1, RBPSUH	recombination signal binding protein for immunoglobulin kappa J region
RFNG		RFNG O-fucosylpeptide 3-beta-N-acetylglucosaminyltransferase
RHOA	ARH12, ARHA	ras homolog gene family, member A
S100B		S100 calcium binding protein B
SFRP4		secreted frizzled-related protein 4

SHH	HPE3, HLP3	sonic hedgehog homolog (Drosophila)
SMAD4	MADH4	SMAD family member 4
SMO	SMOH	smoothened homolog (Drosophila)
SNW1	SKIIP	SNW domain containing 1
SOX1		SRY (sex determining region Y)-box 1
SOX2		SRY (sex determining region Y)-box 2
STK36		serine/threonine kinase 36, fused homolog (Drosophila)
SUFU		suppressor of fused homolog (Drosophila)
T		T, brachyury homolog (mouse)
TCF7		transcription factor 7 (T-cell specific, HMG-box)
TERT		telomerase reverse transcriptase
TLE1		transducin-like enhancer of split 1 (E(sp1) homolog, Drosophila)
WIF1		WNT inhibitory factor 1
WNT1	INT1	wingless-type MMTV integration site family, member 1
WNT10A		wingless-type MMTV integration site family, member 10A
WNT10B		wingless-type MMTV integration site family, member 10B
WNT11		wingless-type MMTV integration site family, member 11
WNT16		wingless-type MMTV integration site family, member 16
WNT2	INT1L1	wingless-type MMTV integration site family member 2
WNT2B	WNT13	wingless-type MMTV integration site family, member 2B
WNT3	INT4	wingless-type MMTV integration site family, member 3
WNT3A		wingless-type MMTV integration site family, member 3A
WNT4		wingless-type MMTV integration site family, member 4
WNT5A		wingless-type MMTV integration site family, member 5A
WNT5B		wingless-type MMTV integration site family, member 5B
WNT6		wingless-type MMTV integration site family, member 6
WNT7A		wingless-type MMTV integration site family, member 7A
WNT7B		wingless-type MMTV integration site family, member 7B
WNT8A		wingless-type MMTV integration site family, member 8A
WNT8B		wingless-type MMTV integration site family, member 8B
WNT9A	WNT14	wingless-type MMTV integration site family, member 9A
WNT9B	WNT15	wingless-type MMTV integration site family, member 9B
ZIC2		Zic family member 2 (odd-paired homolog, Drosophila)
<b>Internal Reference Genes</b>		
CLTC	CLTCL2, Hc	clathrin, heavy chain (Hc)
GAPDH	GAPD,	glyceraldehyde-3-phosphate dehydrogenase
GUSB		glucuronidase, beta
HPRT1	HPRT, HGPRT	hypoxanthine phosphoribosyltransferase 1
PGK1		phosphoglycerate kinase 1
TUBB	OK/SW-cl.56, MGC16435, M4, Tubb5	tubulin, beta

## Appendix B

<b>MSD V-PLEX Human Biomarker 40-Plex Analytes List</b>			
IFN- $\gamma$	GM-CSF	Eotaxin	VEGF-C
IL-1 $\beta$	IL-1 $\alpha$	MIP-1 $\beta$	VEGF-D
IL-2	IL-5	Eotaxin-3	Tie-2
IL-4	IL-7	TARC	SAA
IL-6	IL-12/IL-23p40	IP-10	CRP
IL-8	IL-15	MIP-1 $\alpha$	VCAM-1
IL-10	IL-16	IL-8(HA)	ICAM-1
IL-12p70	IL-17A	MCP-1	Flt-1
IL-13	TNF- $\beta$	MDC	PIGFI
TNF- $\alpha$	VEGF-A	MCP-4	FGF (basic)